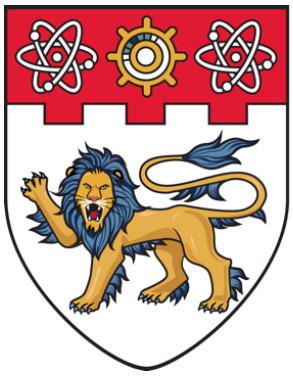

NANYANG TECHNOLOGICAL UNIVERSITY
SINGAPORE

Asymmetric synthesis of axially chiral biaryls and fluoroallenes through rhodium-catalyzed enantioselective transformations

NG JIA SHENG

SCHOOL OF PHYSICAL AND MATHEMATICAL SCIENCES

2020

Asymmetric synthesis of axially chiral biaryls and fluoroallenes through rhodium-catalyzed enantioselective transformations

NG JIA SHENG

SCHOOL OF PHYSICAL AND MATHEMATICAL SCIENCES

A thesis submitted to the Nanyang Technological University in partial fulfilment of the requirement for the degree of Doctor of Philosophy

2020

Statement of Originality

I hereby certify that the work embodied in this thesis is the result of original research done by me except where otherwise stated in this thesis. The thesis work has not been submitted for a degree or professional qualification to any other university or institution. I declare that this thesis is written by myself and is free of plagiarism and of sufficient grammatical clarity to be examined. I confirm that the investigations were conducted in accord with the ethics policies and integrity standards of Nanyang Technological University and that the research data are presented honestly and without prejudice.

09 July 2020

. . . . . .
Date

. . . . . .
Ng Jia Sheng

Supervisor Declaration Statement

I have reviewed the content and presentation style of this thesis and declare it of sufficient grammatical clarity to be examined. To the best of my knowledge, the thesis is free of plagiarism and the research and writing are those of the candidate's except as acknowledged in the Author Attribution Statement. I confirm that the investigations were conducted in accord with the ethics policies and integrity standards of Nanyang Technological University and that the research data are presented honestly and without prejudice.

09 July 2020

. . . . . .
Date

. . . . . .
Professor Chiba Shunsuke

Authorship Attribution Statement

Please select one of the following; *delete as appropriate:

*(A) This thesis **does not** contain any materials from papers published in peer-reviewed journals or from papers accepted at conferences in which I am listed as an author.

09 July 2020

. . . . . .
Date

. . . . . .
Ng Jia Sheng

Abstract

This thesis aims to explore the generation of axially chiral compounds through β-elimination reactions, building on the well-established rhodium-catalyzed conjugate addition protocol. Chapter one is an introduction that describes the definition of axial chirality and relevant terminologies. The history of axially chiral compounds was documented, along with their prevalence and importance. In addition, the β-elimination reactions are discussed in terms of their classification and mechanism. Furthermore, the foundation of classical rhodium-catalyzed asymmetric addition reactions is discussed in-depth, pertaining to its mechanistic and stereo-induction model. Chapter two uncovers a novel type of point-to-axial chirality transfer through β-alkoxide elimination, synthesizing axially chiral biaryls from enantioenriched rhodium-catalyzed hydroarylation products. Chapter three describes a novel type of rhodium-catalyzed reaction between organozinc reagent and alpha, alpha-difluoroalkynes to generate axially chiral fluoroallenes through enantioselective beta-fluoride elimination.

Acknowledgements

My Ph.D. journey hasn't always been smooth sailing. From the very beginning, I knew nothing; nothing that would allow me to weather the storm skillfully. Hence, I was very fortunate to have a supervisor who taught me without reservation. I would like to express my utmost gratitude to my Ph.D. supervisor, Professor Tamio Hayashi, for all the knowledge that he has imparted me. It has been an honor to be able to work with him and I am truly appreciative of it. His unique approach and insights have always managed to inspire me and will continue to be how I would approach other matters in the future. I would definitely say that I would not be who I am today without his kind guidance and patience.

I am also grateful to my supervisor Professor Chiba for all the support that he has given me.

I would also like to express my heartfelt thanks to my group of friends- (Sadeer, Ce qing, Wee shan) who have always been there, rain or shine, and have brought so much fun and joy throughout this arduous journey. They are incredibly smart and humorous people whom I look up to. They rock!

Last but not least, I would like to express my biggest thanks to my sweetest wife who truly has been there for me every single step of my Ph.D. The unwavering support and understanding that she has shown for me is what allowed me to focus on conquering the difficulties. Thank you for always believing in me. I am also very thankful to my parents for taking care of me.

Table of Contents

Chapter 1

Introduction

1.1. Chirality and its prevalence

Chirality refers to the geometric property that a rigid object possesses that endows it being non-superposable on its mirror image.[1] Such property is intrinsically linked to the array of both physical and biological characters that it may display. An illustration that can demonstrate this relation is fluticasone, a drug produced by GlaxoSmithKline for respiratory therapeutics (**Figure 1.1**).[2] It is often produced in a single enantiomer since the other enantiomer may have unwanted potent side effects. The significance of chirality further dwells into the fact that it exists as a crucial factor in drug design, particularly in the interaction with biomolecules. Other involvements include its impact on the less explored field in physiological processes; chiral nanoparticles regulating multiple biological events not limiting to cell adhesion, differentiation and DNA adsorption, and ultimately in molecular and supramolecular chirality.[3] It is therefore important to be able to control the enantioselectivity of a chemical drug during the synthetic pathway to enable the selective synthesis of the desired enantiomer.

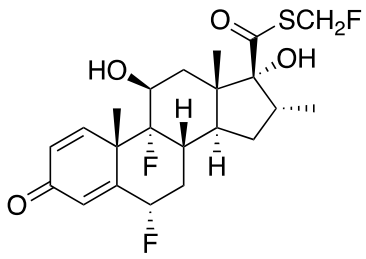

Fluticasone

Figure 1.1 Structure of fluticasone

First illustrated by Van't Hoff and Le Bel, majority of the studies on chirality hedges on the well-established central chirality, which refers to the stereochemistry that is created upon the presence of four distinct substituents attached to the central sp^3-carbon. It was not until 1922 that a new type of chirality was uncovered experimentally for the first time, by Christie and Kenner.[4] Fractional crystallization of 6,6'-dinitro-2,2' diphenic acid presented a unique and unseen type of chirality that revolves around a chiral axis (**Scheme 1.1**). This chiral axis exists due to the restricted movement, imposed by the bulky substituents around the C–C bond connecting the two phenyl rings. As a result, the interconversion between these two structures becomes impeded, and a significant barrier to rotation is then experienced. This phenomenon was termed atropisomerism by Richard Kuhn, describing a form of chirality that exists in molecules with a hindered rotation about a single bond.[5]

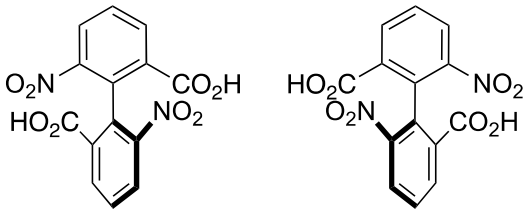

Enantiomers of 6,6'-dinitro-2,2'-diphenic acid

Scheme 1.1 The first example of atropisomeric molecules

1.2. Atropisomerism

1.2.1. Definition of atropisomerism

Atropisomerism came from the Greek word *atropos* (ατροπος), which means "without turn." In its original intent, the terminology was explicitly used for biaryl (**Scheme 1.2**). Atropisomeric biaryls are axially chiral. However, the converse is not true for the closely related axially chiral allenes and spiranes where they cannot be termed atropisomers. For the classification of atropisomers, it can be divided into different groupings based on the chiral axis and hybridization.[6] Apart from well-known biaryl atropisomers such as BINAP that revolves around the C–C chiral axis, styrenes and phenyl amides can also feature axial chirality. Others have also pointed to the possibility of incorporating atropisomerism along other axes. Chiral C–N, C–S, C–O and C–P axes were found to demonstrate such element of axial chirality, giving atropisomers shown in **Scheme 1.3**. For instance, Telenzepine, a drug used for the treatment of peptic ulcers and featuring a stereogenic non-traditional C–N axis, was found to have a racemization half life of 1000 years at 20 °C.[7-8]

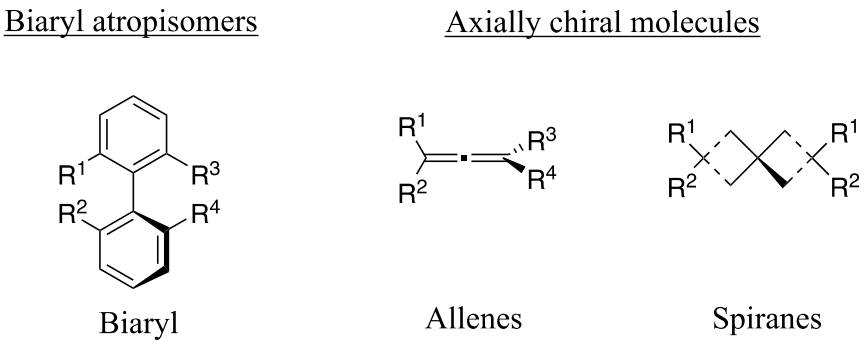

Scheme 1.2 Atropisomeric biaryls and non-atropisomeric allenes and spiranes

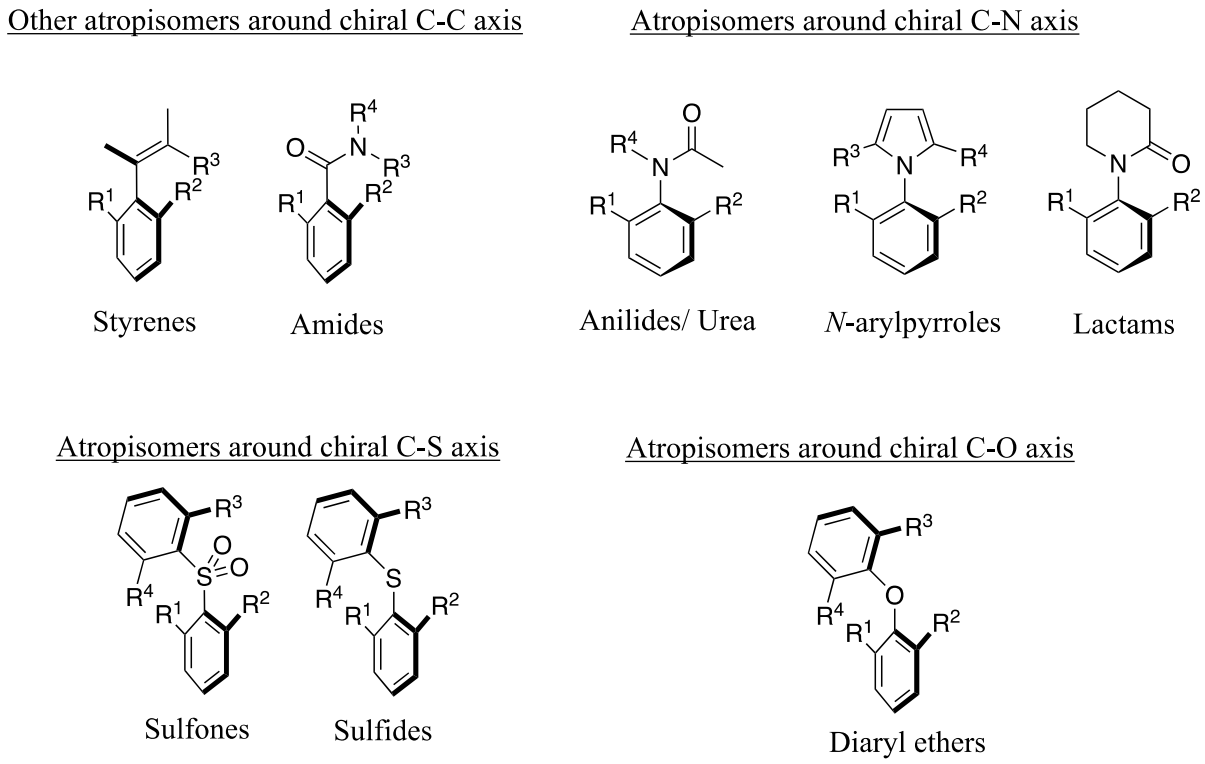

Scheme 1.3 Typical examples of atropisomers with chiral C–X axis

Where C–C chiral axis is concerned, it can also be subdivided into groupings based on the hybridization of the carbon atoms directly connected via the axis: sp^2–sp^2, sp^2–sp^3, sp^3–sp^3. Majority of the C–C chiral axis constitutes sp^2–sp^2 carbons, where BINAP and BINOL are some of the prominent examples. In the case of sp^2–sp^3 carbons, it is less common in nature. A pair of interesting diastereomeric natural products, cordypyridone A and cordypyridone B, contains such C(sp^2)–C(sp^3) chiral axis (**Scheme 1.4**). They are conformationally stable at room temperature and will only

interconvert upon prolonged heating. As for sp^3–sp^3 hybridized carbons, specially designed systems are in place to provide the necessary steric bulkiness and hindrance that are often found in triptycene systems.[9]

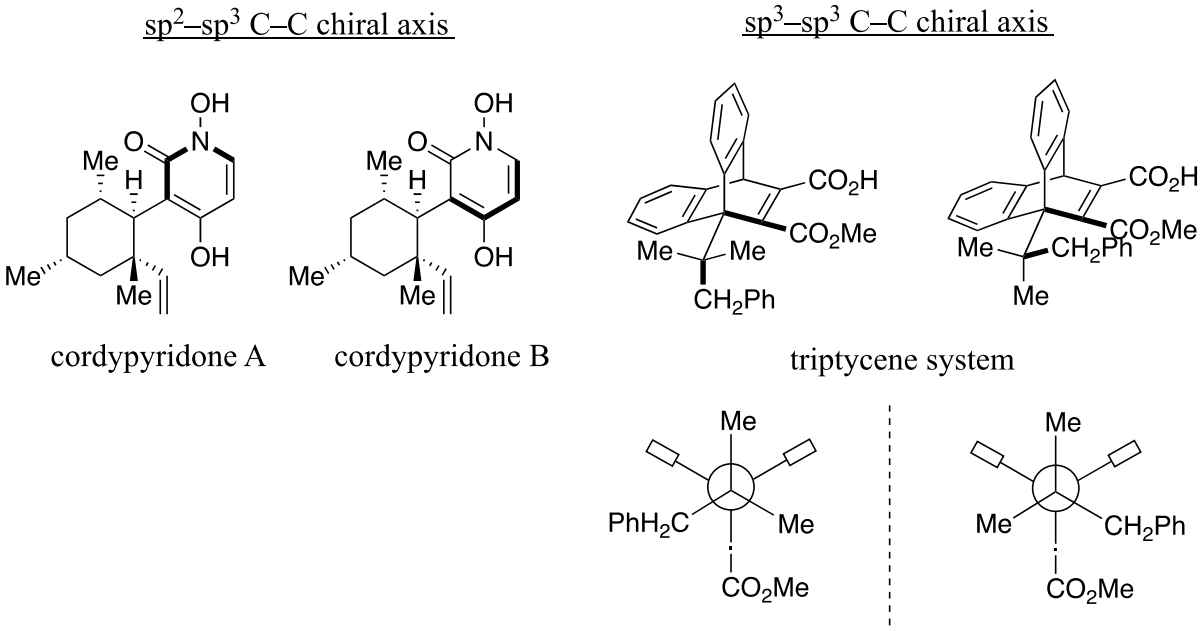

Scheme 1.4 Examples of sp^2–sp^3/sp^3–sp^3 C–C chiral axis

1.2.2. Conditions for maintaining atropisomerism

Specific criteria have to be met in order for atropisomers to retain the chirality that exists within themselves. As a prerequisite, the molecule should not contain an internal symmetry plane for it to display axial chirality. According to a study by Oki, the atropisomers should have at least a half-life time of 1000 s (16.7 min) in order for them to be separable.[10] In addition, the free rotation energy barrier, dependent on temperature, should also be minimally 61.5 kJ/ mol at –73 °C, 93.3 kJ/ mol at 27 °C, and 109.6 kJ/ mol at 77 °C. Generally, for sp^2–sp^2 hybridized carbons, tetra-*ortho*-substituted biaryls are considered conformationally stable and not prone to racemization, especially so if none of the substituents is fluorine or methoxy group. Tri-*ortho*-substituted biaryls, on the other hand, are relatively less conformationally stable but

stable enough if no small atom such as fluorine is involved. Others such as di-*ortho*-substituted biaryls are highly conformationally unstable and undergo racemization readily, and even more so at elevated temperature. A classic example would be 1,1'-binaphthyl that has a half-life of only 10 hours at 25 °C.[11]

1.2.3. Absolute configuration assignment for atropisomers

The absolute configuration of an atropisomer can be determined by the Cahn-Ingold-Prelog rules, using the R_a and S_a nomenclature (**Scheme 1.5**).[12] More often than not, they can also be represented by the helicity rules, with *P* (positive helix) and *M* (negative helix) nomenclature. In order to determine the absolute configuration of an atropisomer, the cross-section of a biaryl structure can be analyzed. By ensuring the highest priority group on the distal ring is at the top, the shortest 90° path, either left or right, is made to the highest priority group on the proximal ring. Should the 90° path follow an anti-clockwise direction, the absolute configuration would be S_a or *P*. If the 90° path follows a clockwise direction, the absolute configuration would be R_a or *M*.

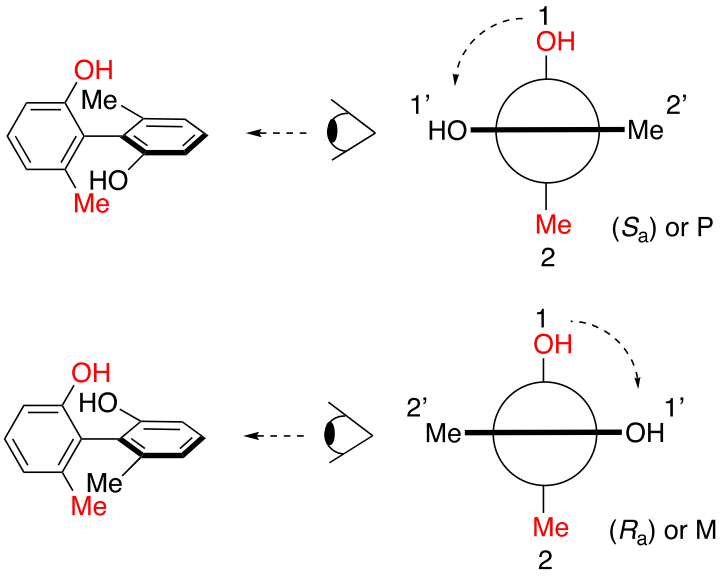

Scheme 1.5 Notation of absolute configuration of axially chiral compounds

1.2.4. Prevalence of atropisomerism

While central chirality pervaded the chemistry realm and has since become well-established, atropisomerism has also found its place in multiple areas such as natural product synthesis, pharmaceutical realms and asymmetric catalysis. Over the years, much attention has been garnered on the synthesis of natural products containing an element of axial chirality (**Scheme 1.6**). Vancomycin containing an element of axial chirality and first isolated by Eli Lilly in 1956, was demonstrated to be an effective antibiotic treating penicillin-resistant bacterial infection.[13-14] The *M* configuration of axially chiral Knipholone is another example that displays positive antimalarial and antitumor activities.[15] In the combat against the human-immunodeficiency virus, michellamine A and B are also highly active against the virus.[16-17] Apart from serving as effective measures against bacteria or viruses, axially chiral mastigophorene A is also capable of stimulating nerve growth.[18] In the case of asymmetric catalysis, axially chiral biaryl with a rigid framework, such as BINOL and BINAP, are excellent ligands for asymmetric Michael reaction and asymmetric isomerization reaction, respectively.[19-20] On this note, it can be seen that atropisomerism has contributed significantly in many ways similar to the more prominent central chirality. Henceforth, it may be worthwhile to venture into creating new methodologies for synthesizing compounds with axial chirality so that the application of these compounds can be better explored.

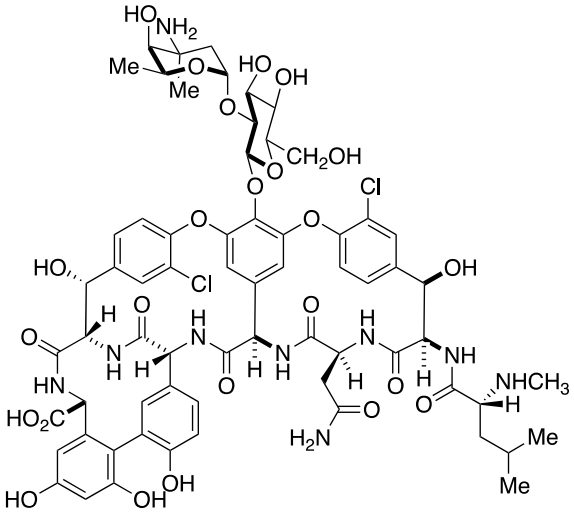

Vancomycin

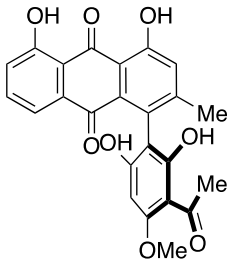

(M)-Knipholone

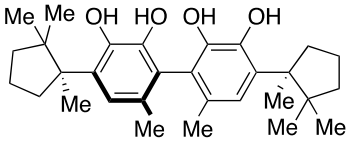

Mastigophorene A

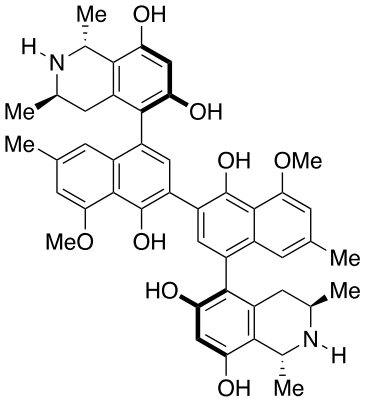

Michellamines A

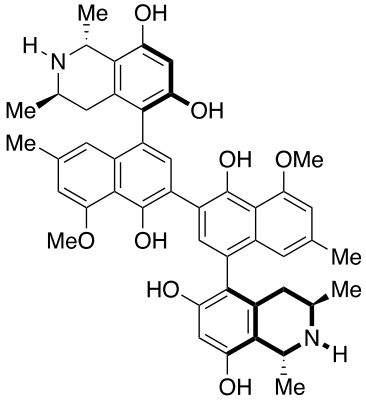

Michellamines B

Scheme 1.6 Structures of Vancomycin, (*M*)-Knipholone, Mastigophorene A, Michellamines A and Michellamines B

1.2.5. Chirality-conversion process in biaryl system

The chirality-conversion process was first explored by Berson and Brown in 1954 in their study of asymmetric induction, particularly in the conversion of chirality from a center of carbon atom asymmetry to the same center of biphenyl-type asymmetry. While most asymmetric inductions occur in the creation or destruction of a new carbon atom (chirality transfer), the asymmetric induction involving the same carbon atom where chirality conversion occurs was relatively unexplored then. In their study, a few requirements have to be met to fully explore the point-to-axial chirality transfer concept: 1) the starting material must be resolvable, 2) it should contain only one chiral center, 3) the starting material should be readily converted into only biphenyl asymmetric, 4) the product should have complete optical stability throughout the course of the reaction.

In their study, the use of circularly polarized ultraviolet lights resulted in the asymmetric decomposition of 4-aryl-1,4-dihydropyridine (R = NO_2) to 4-arylpyridine (R = NO), causing partial resolution of the 4-aryl-1,4-dihydropyridine (**Figure 1.2**). Subsequent oxidation of the recovered optically active 4-aryl-1,4-dihydropyridine with dichromate gave the racemic 4-arylpyridine product (R = NO_2) instead. It was presumably due to the starting material being only slightly optically active. Hence, an especially efficient chirality conversion is required to observe any traces of activity in the product.

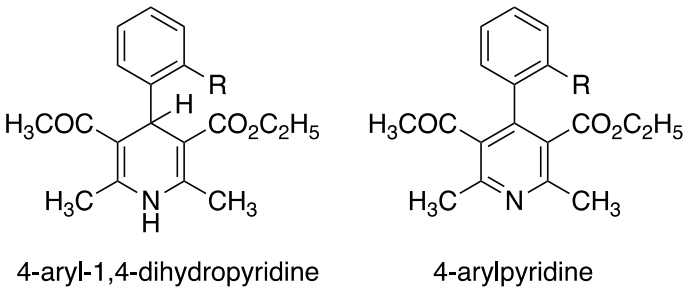

Figure 1.2 Structures of 4-aryl-1,4-dihydropyridine and 4-arylpyridine

Nevertheless, while the proof of such chirality conversion concept was not obtained, Berson and Brown proposed some possible mechanism for which such chirality conversion involving the aromatization of 4-aryl-1,4-dihydropyridine can take place (**Figure 1.3**).

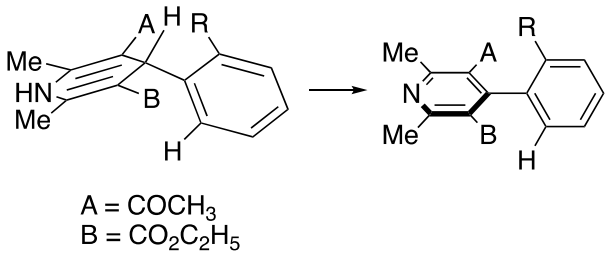

Figure 1.3 Proposed mechanism on chirality conversion of 4-aryl-1,4-dihydropyridine to 4-arylpyridine

Initially, there exists a stereogenic carbon in 4-aryl-1,4-dihydropyridine with an aryl group attached. Due to the tetrahedral nature of C_4, there is no interference between R and C_3 and C_5 substituents (A and B). However, as the reaction proceeds, it is likely to involve a transition state where the C_4–H bond is not completely broken and the heterocyclic ring approaches aromaticity concurrently, giving rise to two diastereomeric transition states (**Figure 1.4**).

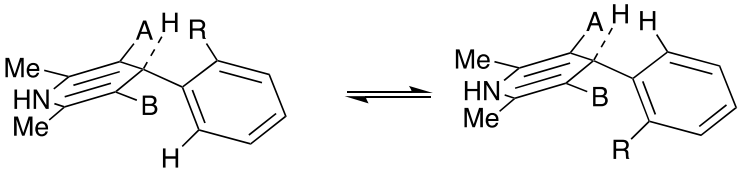

Figure 1.4 Proposed diastereomeric transition states for the aromatization of 4-aryl-1,4-dihydropyridine

As the reaction proceeds further, there will be some points in which there will be sufficient steric hindrance experienced between R and both A and B. This will result in an energetic preference for one rotational configuration of the phenyl ring over the other, leading to the selective formation of one enantiomer over the other eventually. Berson and Brown also proposed that the efficiency of the chirality conversion is dependent on the relative stabilities of the two diastereomeric transition states, which is in turn dependent on the bulk of both R and the C_3 and C_5 substituents.

1.3. Chiral allenes

1.3.1. Allenic structure and allenic axial chirality

Allenes are an important class of compounds that display axial chirality. They are often found as substructures of natural products, biomolecules, catalyst and even served as chiral building blocks in organic synthesis.[21-22] Their high reactivity sets them apart from related functional groups such as alkene and alkyne, where the former is able to partake in an array of reactions not limited to epoxidations, addition reactions, cyclizations and cycloaddition reactions.[22] The high reactivity of allenes is attributed to its unique structure, where it consists of two cumulated carbon–carbon double bond (**Figure 1.5**). It is also the arrangement of the two cumulated carbon–carbon double bond that allows the display of allenic axial chirality where $R^1 \neq R^2$ and $R^3 \neq R^4$. Allenes are also conformationally stable such that the enantiomers are separable under normal conditions. For instance, the rotation barrier of 1,3-dialkylallenes is approximately 46 kcal/mol.[23]

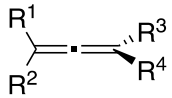

Figure 1.5 Structure of allene

The absolute configuration of axially chiral allenes can be determined according to the following **Figure 1.6**. By placing the more polarizable substituent in the vertical axis uppermost (i.e. **Y**), and the more polarizable substituent in the horizontal axis to the right (i.e. **A**), a clockwise screw pattern of polarizability will be obtained and the enantiomer should be dextrorotatory (+). Hence, a (*S*)-configuration can be assigned. Should the more polarizable substituent in the horizontal axis is to the left, an

anticlockwise screw pattern of polarizability will be obtained and the enantiomer should be laevorotatory (–). Hence, a (*R*)-configuration can be assigned.[24]

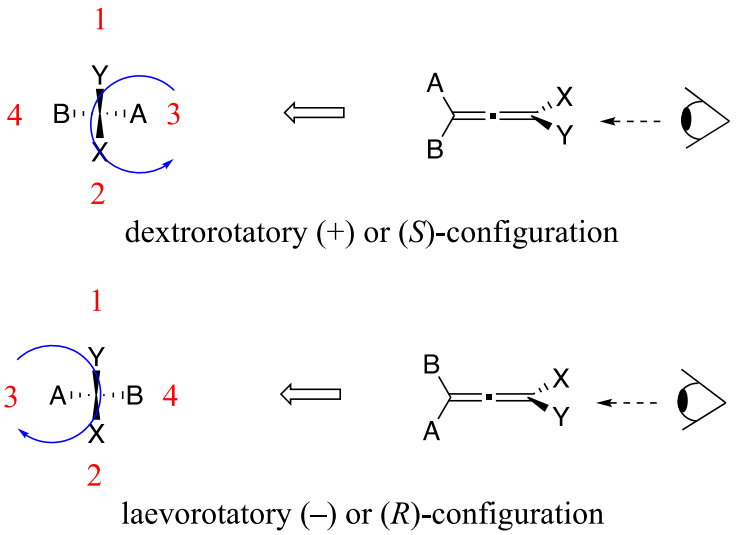

Figure 1.6 Notation of absolute configuration of axially chiral allene

Van't Hoff first predicted in 1875 the possibility that substituted allenes can exist as enantiomers. However, the experimental proof of this concept only came in much later in 1935, where Maitland and Mills reported the preparation of enantiomeric 1,3-di(α-naphthyl)-1,3-diphenylallene (**Scheme 1.7**). By using catalytic amount of camphorsulfonic acid, the asymmetric dehydration of the racemic allylalcohol afforded 1,3-di(α-naphthyl)-1,3-diphenylallene in approximately 5% ee. By way of recrystallization, either enantiopure form of the product could be obtained depending on *d*-camphorsulfonic acid or *l*-camphorsulfonic acid is used.

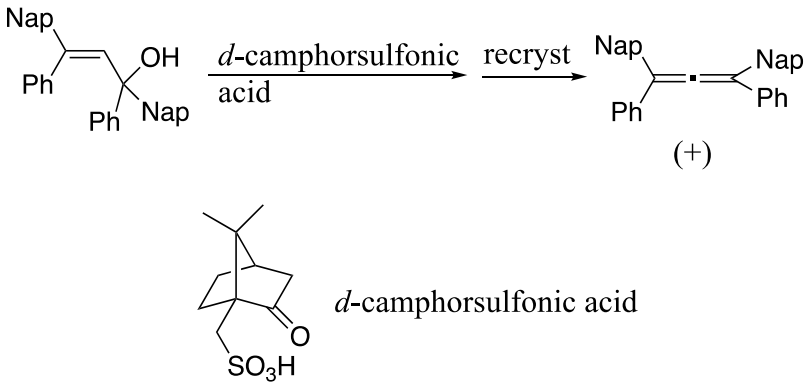

Scheme 1.7 Asymmetric dehydration of allylalcohol by camphorsulfonic acid

1.3.2. History of asymmetric synthesis of chiral allenes

Numerous methodologies are available for the synthesis of axially chiral allenes and can be broadly categorized into non-catalytic and catalytic asymmetric synthesis. The former involves the use of stoichiometric amount of chiral sources, with either enantioenriched substrates or reagents while the latter utilizes substoichiometric amount of chiral sources.[22, 25-27]

Typically, the asymmetric non-catalytic synthesis of chiral allenes involves the chirality transfer from enantioenriched propargyl derivatives. Since the pioneering work by Roma and Crabbe in 1968 involving the first example of organocopper-mediated synthesis of allene, a representative example of asymmetric synthesis of chiral allenes was then reported by Alexakis and co-workers (**Scheme 1.8**).[28-29] Starting with enantioenriched propargyl ether (37%–58% ee), the use of stoichiometric amount of organocopper reagent in the presence of Grignard reagent gave the desired chiral allene in 96% optical yield and high chemical yield. Other representative methods involving propargylic derivatives are S_Ni reaction of enantioenriched propargylic alcohol reported

by Smith,[30] and chirality transfer from central chirality at allylic position to axial chirality of allene reported by McGarvey.[31]

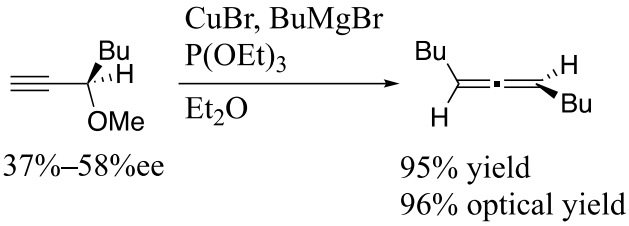

Scheme 1.8 Copper(I)-mediated reaction with enantioenriched propargyl ether

While non-catalytic asymmetric methodology of synthesizing chiral allenes remains robust and widely adopted, the catalytic asymmetric synthesis of chiral allenes are still in its infancy. In terms of atom-economic efficiency, reactions involving substoichiometric amount of chiral source are more attractive. In this aspect, chiral transition-metal-complexes are often employed in catalytic amount without the need for stoichiometric amount of chiral source. Hence, it is highly critical that more attention be focused on the development of catalytic asymmetric synthesis of chiral allenes, particularly one that is catalyzed by chiral transition-metal-complex.

The very first transition-metal-complex-catalyzed asymmetric synthesis of axially chiral allenes was pioneered by Elsevier in 1989 (**Scheme 1.9**).[32] In the presence of *n*-BuLi, selective lithiation at the terminal position of 4,4-dimethyl-1,2-pentadiene took place. This was followed by the addition of zinc chloride to generate the allenylzinc species, which undergoes cross-coupling reaction with iodobenzene in the presence of 1 mol% of $PdCl_2$[(*R*,*R*)-diop] complex to afford the desired axially chiral allene in 26% ee.

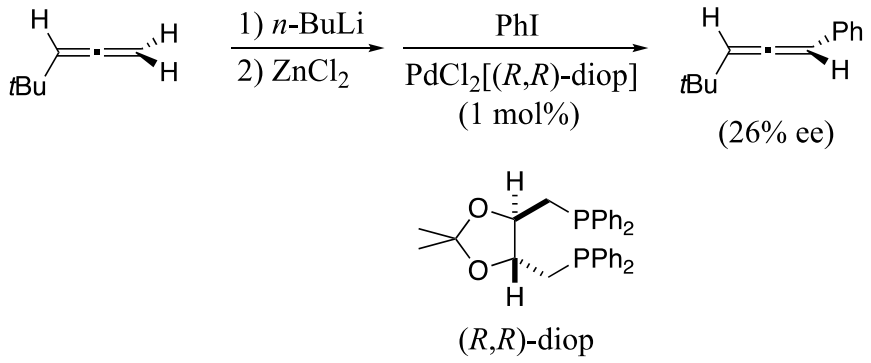

Scheme 1.9 Palladium-catalyzed cross-coupling allenylzinc species

Following the pioneering report by Elsevier on the transition-metal-catalyzed asymmetric synthesis of axially chiral allenes, several closely related classical syntheses of chiral allenes by way of substitution are also reported. In 2000, Hayashi and co-worker reported the use palladium/bisphosphine complex in the synthesis of chiral tri-substituted allenes from 2-bromo-1,3-butadiene derivatives with soft nucleophiles in yields up to 91% and enantioselectivity up to 89% ee (**Scheme 1.10**).[33]

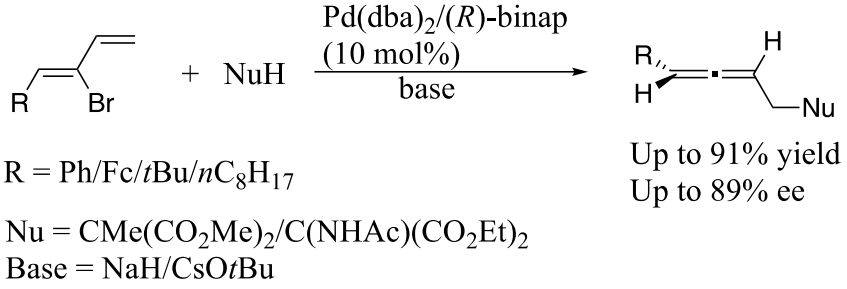

Scheme 1.10 Palladium-catalyzed nucleophilic substitution of 2-bromo-1,3-dienes

On the other hand, the asymmetric synthesis of chiral allenes by way of addition reactions was also made possible through different transition-metal catalysis. Well known addition reactions to give chiral allenes involved reactions such as asymmetric hydrosilylation, hydroboration and conjugate addition of aryltitanates. In 2000, Tillack

and co-workers reported a [RhCl(cod)]$_2$/(2*S*,4*S*)-(–)-PPM catalyzed double hydrosilylation of 1,3-butadiyne derivative to give axially chiral disilyllated allenes in up to 27% ee. (**Scheme 1.11**).[34]

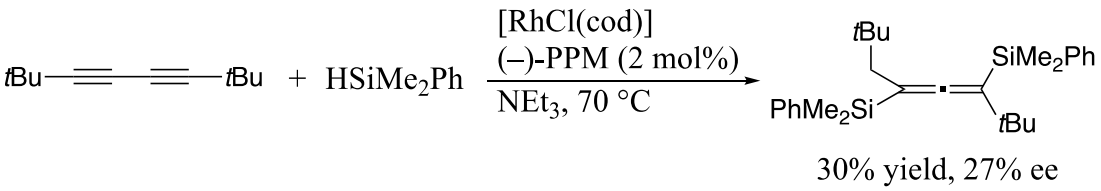

Scheme 1.11 Rhodium-catalyzed asymmetric double hydrosilylation of 1,3-butadiyne

Using different substrates, Hayashi and co-workers also reported a palladium-catalyzed asymmetric hydrosilylation of 4-substituted-but-1-en-3-ynes with trichlorosilane in 2001 (**Scheme 1.12**).[35] Despite the limited scope that requires bulky substitutent at the 4-position in but-1-en-3-ynes derivatives to achieve selective hydropalladation of alkene, the use of (*S*)-(*R*)-PPFOMe based ligands afforded axially chiral silylated allenes in up to 94% yield and up to 90% ee.

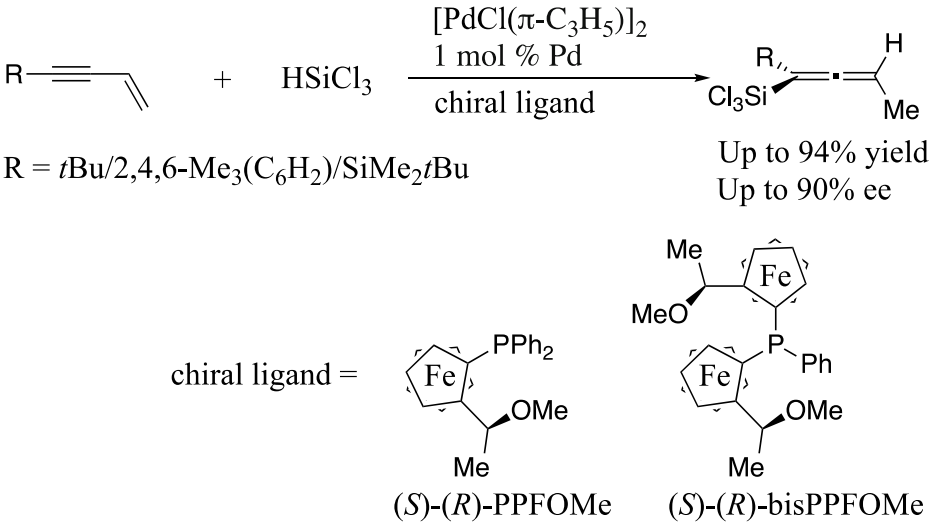

Scheme 1.12 Palladium-catalyzed asymmetric hydrosilylation of but-1-en-3-ynes derivatives

Complementary to hydrosilylation, report of hydroboration of but-1-en-3-ynes catalyzed by Pd/(*S*)-(–)-MeO-MOP complex to give axially chiral borylated allenes in up to more than 61% ee, was also documented by Hayashi in 1993 (**Scheme 1.13**).[36]

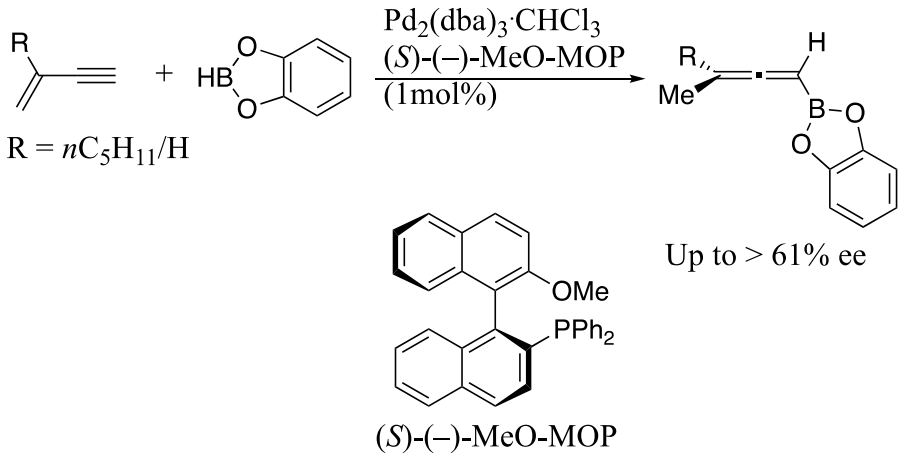

Scheme 1.13 Palladium-catalyzed asymmetric hydroboration of but-1-en-3-ynes derivatives

More recently, the enantioselective synthesis of axially chiral allenes catalyzed by copper complex was realized by Hoveyda and co-worker in 2018 (**Scheme 1.14**). The use of HBPin in the presence of copper/(*R*,*R*)-phenyl-bpe complex allowed hydroboration of 1,3-enynes to give the desired axially chiral tri-substituted allenyl boronates in up to 80% yield and 96% ee for the first time.[37] The use of the same chiral Cu/-phenyl-bpe complex and strategy were also explored by Ge and co-workers in 2018, in the synthesis of quinolinyl-substituted axially chiral allenes in up to 95% yield and 99% ee.[38] Other further utilization of the same strategy of Cu–H addition to afford axially chiral di-substituted allenes in the presence of trialkylsilane was subsequently reported by Buchwald in 2019.[39]

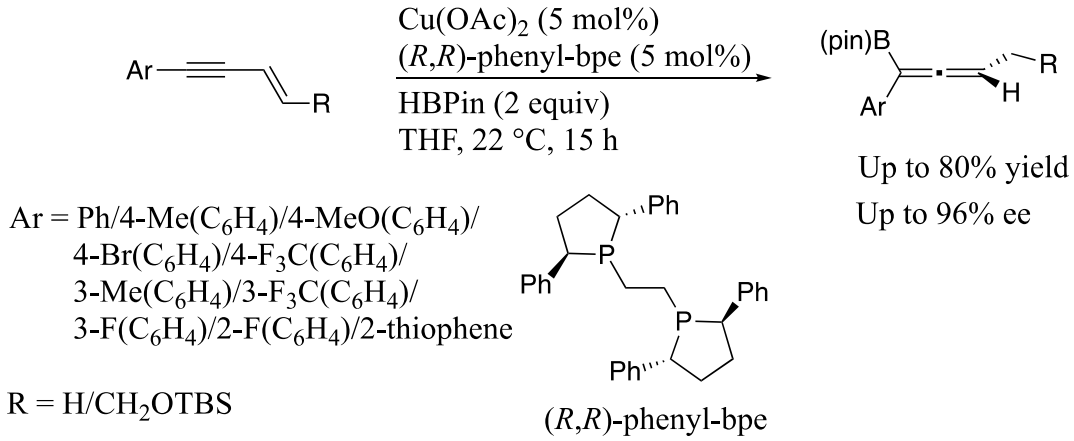

Scheme 1.14 Cu/(*R*,*R*)-phenyl-bpe-catalyzed asymmetric hydroboration of 1,3-enynes

Other asymmetric addition reactions catalyzed by transition metal complex also include the work by Hayashi and co-workers in 2003 where aryltitanate reagents were added onto 3-alkynyl-2-en-1-ones in the presence of chlorotrimethylsilane and a rhodium-(*R*)-segphos complex (**Scheme 1.15**).[40] The addition of various aryl groups took place in a 1,6-addition fashion, followed by trapping with chlorotrimethylsilane. In the presence of methyllithium, the silyl enol ethers were then converted to the desired enol pivalate esters in yields up to 91% and enantioselectivities up to 93% ee. It is also noteworthy to mention that the synthesis of axially chiral tetra-substituted allenes are rare and there are no general approaches for its synthesis.

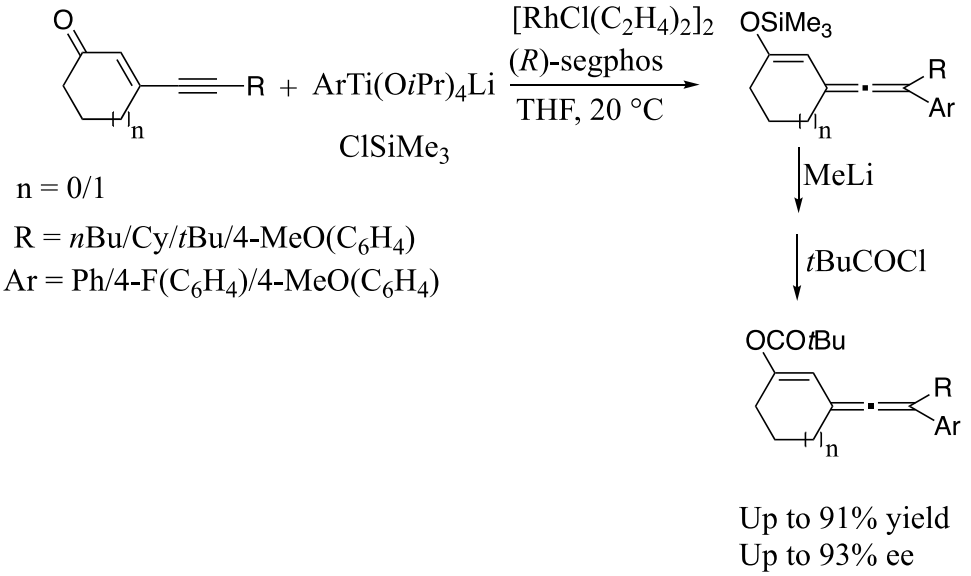

Scheme 1.15 Rh-(*R*)-segphos-complex-catalyzed 1,6-addition onto 3-alkynyl-2-en-1-ones with aryltitanate reagents in the presence of chlorotrimethylsilane

Up until recently, the asymmetric synthesis of axially chiral allenes by the way of 1,3-substitution on prochiral propargylic substrates catalyzed by copper salt and chiral ligand was finally realized by Alexakis and co-worker in 2012 (**Scheme 1.16**).[41] High enantioselectivity of up to 93% ee was observed when the modified SimplePhos ligand was employed with the optimized conditions. Interestingly, the reaction failed to afford the desired product when bulky *t*Bu group as R^2 was introduced as Grignard reagent.

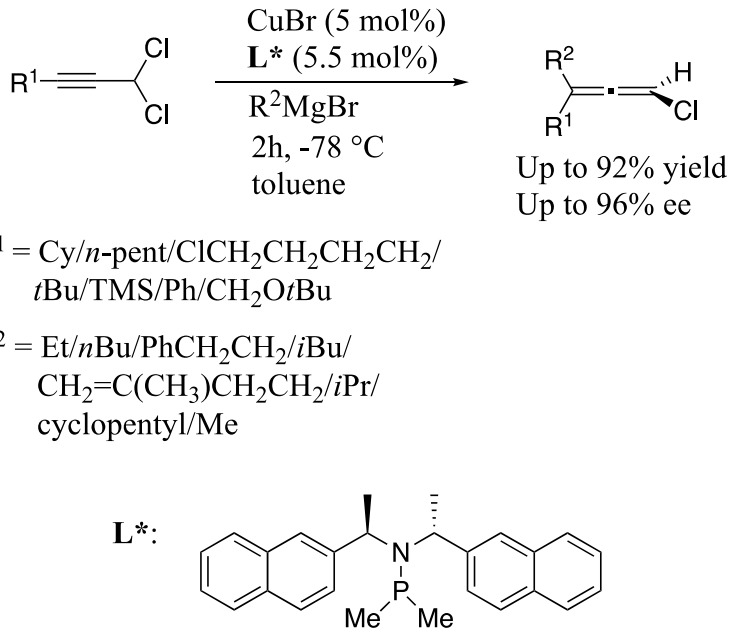

Scheme 1.16 Copper-catalyzed enantioselective synthesis of axially chiral allene by Alexakis in 2012

Focusing on a new direction not involving the traditional substitution or addition reaction pathway, Frantz reported a new strategy by way of β-H elimination to generate axially chiral allenes in 2013 (**Scheme 1.17**).[42] From (*E*)-enol triflates, the use of **L1** or **L2** phosphite ligands afforded the desired axially chiral 2,3-allenoates in up to 96% ee. The low reaction temperature was required for the inhibition of further hydropalldation of the desired allenes, as well as preventing racemization of the product. A limitation of the reaction, however, is that only di-substituted allenes can be produced using this methodology since fully substituted enol triflates was only converted to the desired tri-substituted allenes in very poor yields.

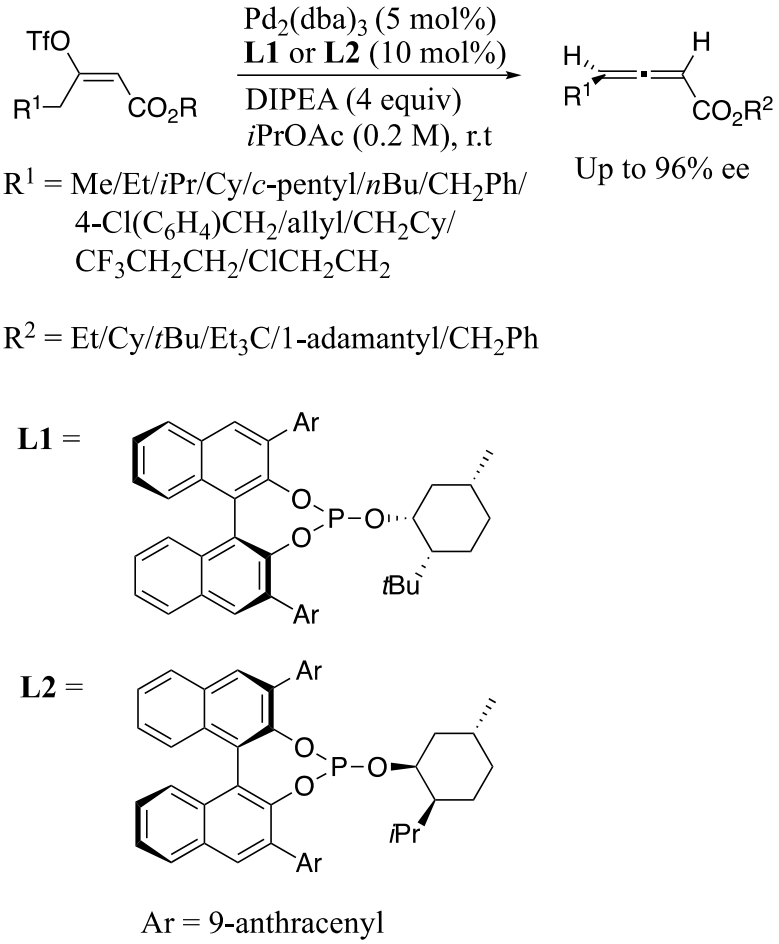

Scheme 1.17 Asymmetric palladium-catalyzed β-H elimination to generate di-substituted axially chiral 2,3-allenoates

In addition to the strategies mentioned above, Liu, Feng and co-workers also reported the first catalytic asymmetric coupling α-diazoesters for the synthesis of axially chiral allenoates in 2015 (**Scheme 1.18**).[43] The use of chiral cationic guanidinium salt along with Cu(I) complex enabled the synthesis of axially chiral allenoates in yields up to 99% and 98% ee. Despite the significant breakthrough in expanding the methods for catalytic asymmetric synthesis of allenes, the potential of the methodology was limited to the use of α-diazoesters. This was then subsequently overcame by Wang and co-worker who were able to utilize diazoalkanes as the coupling partner to furnish axially chiral tri-substituted allenes in up to 96% yield and 98% ee.[44]

Further expansion of the substrate scope was also observed in the catalytic asymmetric synthesis of allenes, through the coupling of flow-generated diazo compounds and propargylated amines, reported by Ley and co-workers in 2017.[45]

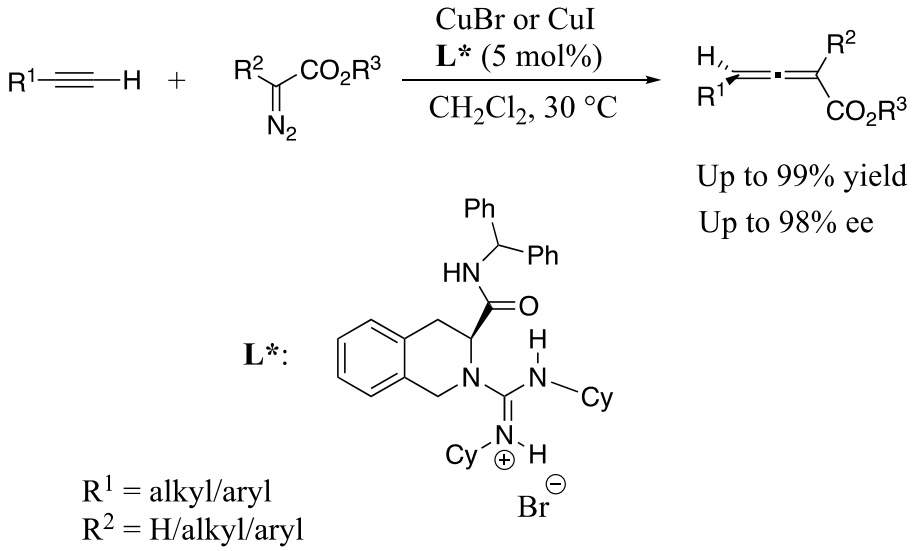

Scheme 1.18 Asymmetric copper-catalyzed coupling of α-diazoesters with terminal acetylene to afford chiral allenoates

As it can be seen, there are myriad amount of strategies for the catalytic asymmetric synthesis of di-substituted and tri-substituted axially allenes. However, the reports for catalytic asymmetric synthesis of tetra-substituted allenes are few and far between. The first catalytic asymmetric synthesis of tetra-substituted allenes was reported by Hayashi and co-workers back in 2003 with the use of Rh/(*R*)-segphos complex (**Scheme 1.15**). However, it was not until 2013 when Maruoka and co-workers reported the asymmetric synthesis of chiral allenes through organocatalysis (**Scheme 1.19**).[46] In the presence of phase transfer catalyst **4c**, cumulenoate was generated from 1-alkylallene-1,3-dicarboxylate under the phase transfer conditions. With the addition of electrophiles, in this case *N*-tosyl imine derivatives, the cumulenotes were trapped

to give the desired alkylated chiral allenes in up to 98% yield, 96% and diastereoselecitivity ratio of up to 97:3. Taking inspiration from Maruoka's work, reports with modified protocols and substrates have since surfaced, with Miller and co-workers reporting a catalytic asymmetric synthesis of chiral allenes from allenic esters in the presence of pyridylalanine-based peptide.[47] Guo and co-workers also reported an asymmetric allylation of Morita-Baylis-Hillman carbonate with allene ketones catalyzed by cinchona-derived tertiary amine in 2020.[48]

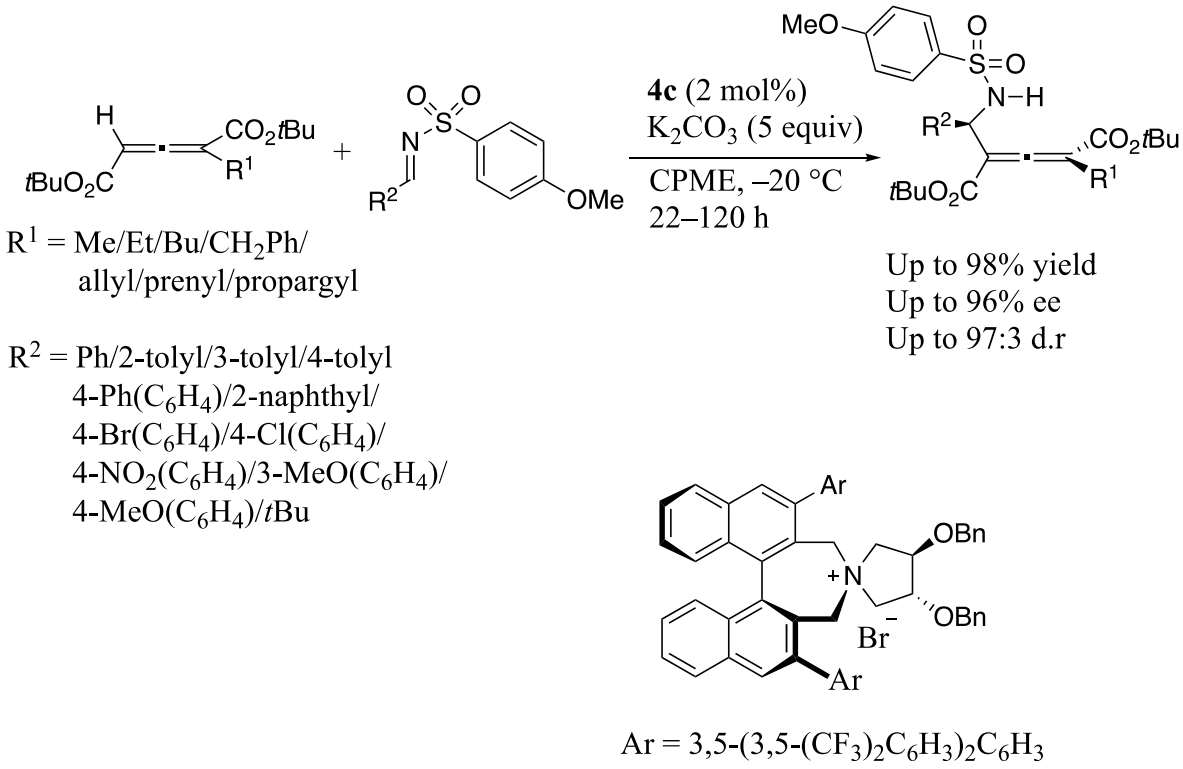

Scheme 1.19 Asymmetric organocatalzyed of 1-alkylallene-1,3-dicarboxylate with *N*-tosylimine to give axially chiral tetrasubstituted allenes

Apart from the strategy that Maruoka introduced, List and co-workers utitlized their chiral silylated disulfonimide lewis acid to catalyze the alkynlogous Mukaiyama aldol reaction between silyl alkynyl ketene acetals and aldehyde, affording the

corresponding tetra-substituted allenes (**Scheme 1.20**).[49] Up to 92% yield of the targeted allenes was achieved in this transformation, giving enantioselectivity as high as 96% ee, along with high diastereoselectivity of up to 27:1.

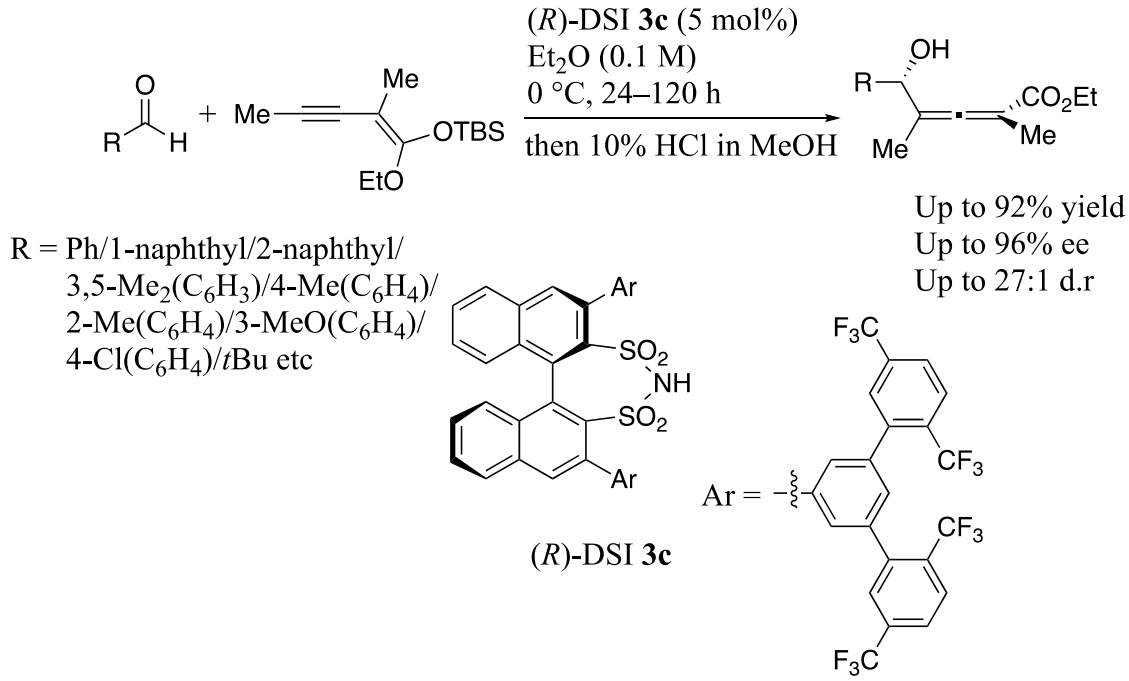

Scheme 1.20 Asymmetric alkynlogous Mukaiayama aldol reaction catalyzed by silylated disulfonimide lewis acid in 2016

On the other hand, Sun and Wang adopted a different strategy toward the synthesis of axially chiral α-amino allenoates through a dearomative γ-addition of indoles to β,γ-alkynyl-α-imino ester.[50] The use of chiral phosphoric acid enabled a double activation mode through hydrogen bonding, eventually affording the desired tetra-substituted allenes in good yields and enantioselectivity (**Scheme 1.21**).

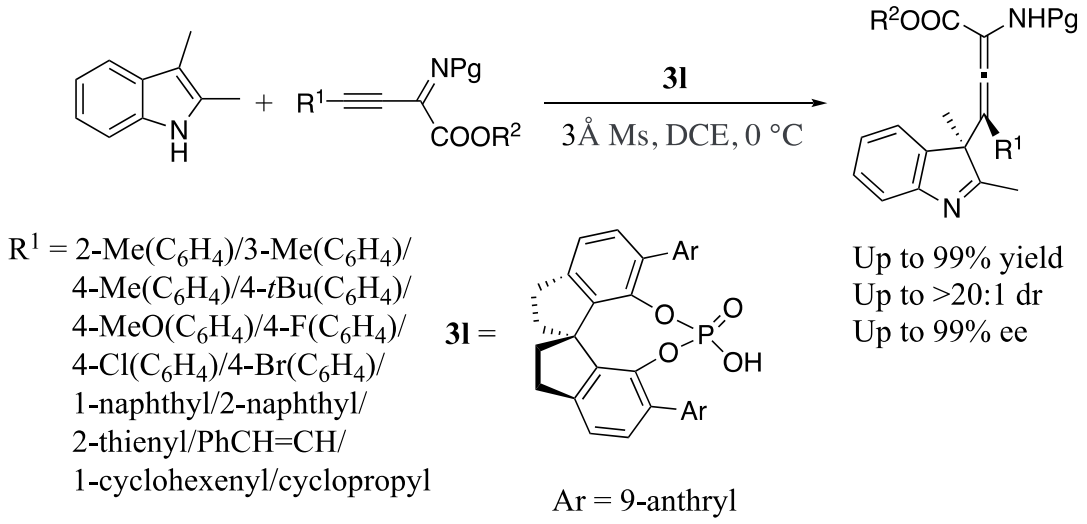

Scheme 1.21 Chiral phosphoric acid catalyzed asymmetric synthesis of tetra-substituted allenes through γ-addition of indoles to β,γ-alkynyl-α-imino ester

Of all the above methodologies pertaining to the catalytic asymmetric synthesis of tetra-substituted allenes, only one example involved the use of transition-metal to catalyze the transformation. Majority of the asymmetric synthesis of chiral tetra-substituted allenes are still dominated by the use of organocatalysts. In fact, it was only until recently that the synergic cooperation between copper and palladium complexes was reported by Liao and co-worker in 2020, in the synthesis of tri and tetra-substituted allenes (**Scheme 1.22**).[51] With CuBr/Sulfoxide phosphine complex, the copper-boration takes place and formation of allenylcopper species follows suit. By the introduction of $PdCl_2$(dppf) and aryl iodide, transmetallation followed by reductive elimination affords a myriad of desired allenes in up to 70% yield and 90% ee. This showcases an example where further functionalization is possible through the use of transition metal. Hence, the use of transition metal in the catalytic asymmetric synthesis of tetra-substituted allenes remains an attractive option.

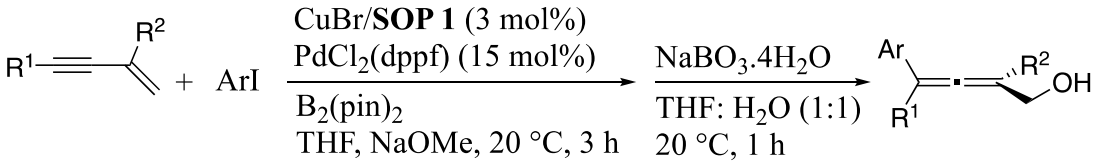

R^1 = 4-MeO(C_6H_4)/CH_2CH_2Ph/
$CH_2CH_2CH_2Cl$

R^2 = Ph/4-Ph(C_6H_4)/4-MeO(C_6H_4)

Ar = Ph/3-Me(C_6H_4)/4-Me(C_6H_4)/
3,5-Me_2(C_6H_4)/3,4-Me_2(C_6H_4)
4-OEt(C_6H_4)/4-Ph(C_6H_4)/
4-*t*Bu(C_6H_4) etc.

Up to 70% yield
Up to 90% ee

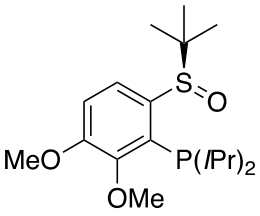

SOP 1

Scheme 1.22 Enantioselective synthesis of tri- and tetra-substituted allenes through a synergic cooperation of Cu/Pd catalysis via arylboration of 1,3-enynes

1.4. β-Elimination

β-Elimination, or 1,2-elimination, is referred to as a process that involves the loss of 2 groups called eliminands that are from 2 different centers.[52] This leads to the formation of a new π bond (**Scheme 1.23**). β-Elimination can be generally sub-divided into E_1 or E_2 type elimination.

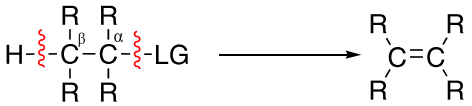

Scheme 1.23 Cleavage of bonds in an elimination reaction

In E_1 type elimination, the reaction is characterized by the initial formation of a carbocation that may be catalyzed by acid (**Scheme 1.24**). The C–H then collapses to form the π bond. Due to this mechanistic sequence, an E_1 type elimination occurs more favorably and readily with substrates that form 3° carbocation, followed by those

forming 2° and 1° cations. As such, an E_1 elimination is a unimolecular process where the rate is solely dependent on the concentration of the substrate.

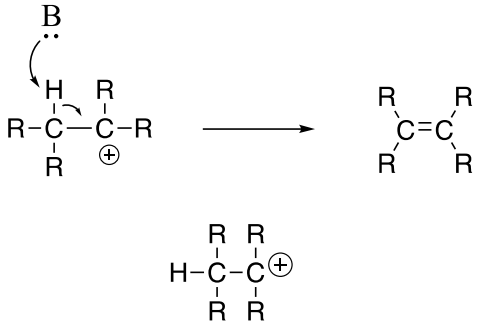

stability: 3° > 2° > 1°

Scheme 1.24 Reaction profile of E_1 elimination and the relative stability of carbocation generated

In an E_2 type elimination, the reaction is favored by the usage of a strong base. This allows for the abstraction of a hydrogen atom in the β-position relative to the carbon with the leaving group (**Scheme 1.25**). Concomitantly, a π-bond is generated with the leaving group being kicked out. The whole process is concerted and happens in an anti-periplanar fashion. The E_2 elimination is bimolecular, indicating that the rate is governed by both the concentration of the base and the substrate involved.

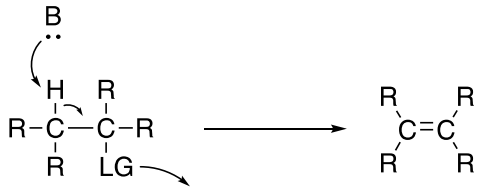

Scheme 1.25 Mechanism of E_2 type elimination

In stark contrast, other eliminations such as E_1cb and E_i also exist despite being not as common. The E_1cb proceeds in a different manner where the acidic proton is first extracted by a weak base. The prerequisite is that the anion formed can be stabilized by

an electron-withdrawing group at the same carbon. Thereafter, the elimination of a poor leaving group generates a new π bond. On the other hand, E_i involves an intramolecular E_2 elimination, often in the presence of a tertiary amine oxide. A *syn* periplanar conformation of the leaving group with the β-hydrogen is required for this elimination, otherwise known as Cope elimination.[53]

While the aforementioned β-eliminations are prevalent in many organic transformations, there exists an alternate type of β-elimination in metal catalyzed reactions that rely on a different set of criteria. β-Eliminations in transition metal–catalyzed reactions involve the transition metal positioning itself in a coplanar manner with the "leaving group", in a M–C–C–LG sequence. As in the case of β-H elimination, the transition metal often has to have a vacant site for such elimination to occur to give a new π bond.[54] Besides hydrogen, other heteroatoms are also known to participate in beta-eliminations.[55] In the classical palladium-catalyzed Heck reaction to form stilbene, alkyl palladium species underwent a β-OAc elimination to afford stilbene (**Scheme 1.26**).[56] β-Cl elimination was also observed in the termination of polymerization reaction with vinyl chloride and palladium(II) olefin catalyst (**Scheme 1.27**).[57]

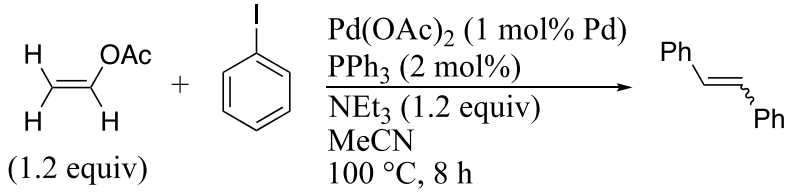

Scheme 1.26 Formation of stilbene through β-OAc elimination

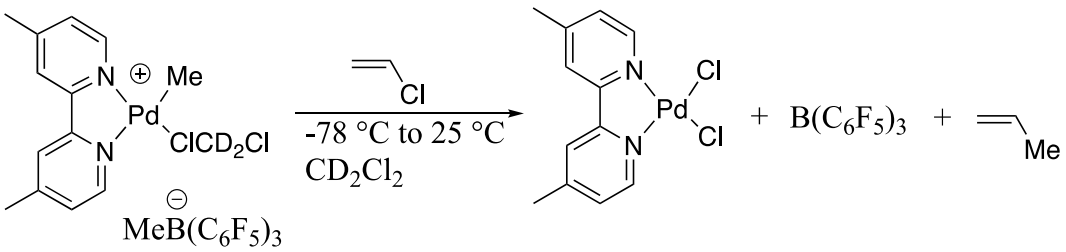

Scheme 1.27 Formation of propylene through β-Cl elimination

The relative rates of β-eliminations are not always easy to discern. A recent theoretical study by Lin reveals that β-halide elimination (Cl, Br, I) may be much easier than β-X elimination (X = OMe, OH, F).[55] The former is an exothermic reaction pathway while the latter is an endothermic reaction pathway. Moreover, the β-X eliminations for (X = F, OH, OMe) also face higher reaction barrier, compared to those of X = Cl/Br/I. It follows that the barriers to overcome increases from F (14.0 kcal/mol) to OH (24.0 kcal/mol), and OMe (36.3 kcal/mol) for Pd-X elimination.[55] This trend may change on a case-to-case basis depending on the transition metal involved. However, the general consensus for β-elimination of F/OH/OMe is that it still is quite difficult, especially for those involving late transition-metal. Hence, it would be vital to drive research in that area and study those reaction pathways in detail.

1.5. History of rhodium-catalyzed asymmetric addition

In 1997, the first report of rhodium-catalyzed addition of aryl and alkenyl boronic acids onto enones was made by Miyaura (**Scheme 1.28**). The combination of $Rh(acac)(CO)_2$ and 1,4-bis(diphenylphosphino)butane allowed the addition of aryl and alkenyl groups onto the α,β-unsaturated enones in generally high yields.[58]

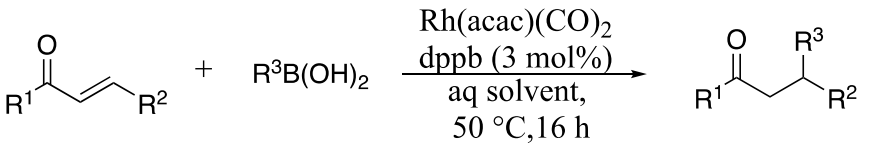

R^1 = H, CH_3, C_4H_9, Ph
R^2 = H, CH_3, Ph, $–CH_2CH_2CH_2–$
R^3 = Ph, 4-Br(C_6H_4), 4-MeO(C_6H_4)
2-MeO(C_6H_4), 4-CH_3CO(C_6H_4)
2,4,6-$(CH_3)_3$(C_6H_4)

up to 99% yield

Scheme 1.28 First rhodium-catalyzed 1,4-addition reaction of organoboronic acids

While the majority of the additions took place with the use of β-unsubstituted enones, particularly methyl vinyl ketone, examples of β-substituted enones were scarce and limited to chalcone type. The latter often proceeded with modest yield, indicating the need for further exploration. In spite of that, this remarkable report has shown the great utility of the relatively unreactive boronic acid. Compared to other organometallic reagents as such organomagnesium and organozinc reagents, the use of benchtop-stable organoboron reagents proved to be far more attractive. Miyaura and Hayashi then reported the use of Rh(acac)$(C_2H_4)_2$/(*S*)-Binap complex in the addition of phenylboronic acid to cyclohexenone, giving enantioenriched (*S*)-3-phenylcyclohexanone in 93% yield and 97% ee (**Scheme 1.29**).[59]

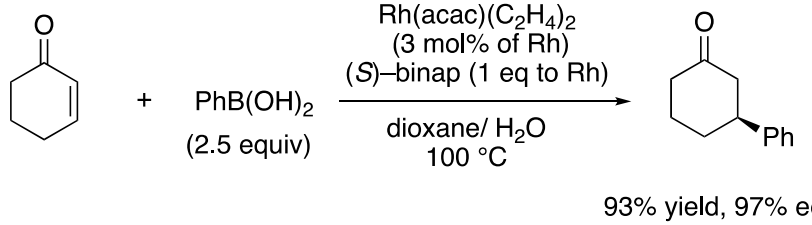

93% yield, 97% ee

Scheme 1.29 Asymmetric addition of $PhB(OH)_2$ onto cyclohexenone

This representative example is the first instance of rhodium-catalyzed asymmetric addition reaction. Other cyclic and acyclic substrates also performed well

with a variety of aryl and alkenyl boronic acid. However, it should be noted that a high temperature of 100 °C was required to ensure smooth conversion of 2-cyclohexen-1-one to furnish the product. The reaction at a lower temperature of 80 °C gave the product only in 42% yield and 97% ee. Should the reaction be carried out at a much lower temperature such as 60 °C or 40 °C, the reaction was sluggish and gave almost no product.

In a mechanistic study, Hayashi showed that a high temperature of 80 °C was essential to facilitate the otherwise slow transmetallation between [Rh]–acac species and $PhB(OH)_2$ to generate [Rh]–Ph species (**Scheme 1.30**).[60]

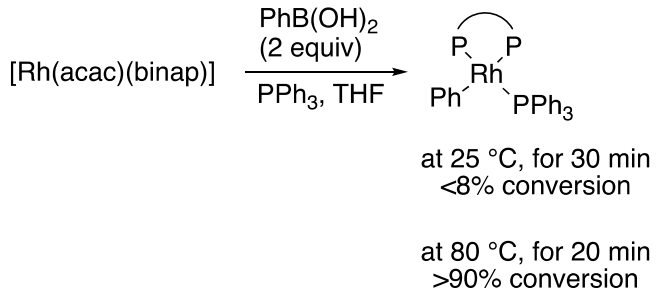

Scheme 1.30 Effects of temperature on rate of conversion of Rh–acac to Rh–Ph

Hayashi and co-workers also subsequently showed that the triphenylphosphine stabilized rhodium(acac)–Ph species is likely the key species that adds onto 2-cyclohexen-1-one to furnish the corresponding product in 64% yield and 98.8% ee (**Scheme 1.31**).

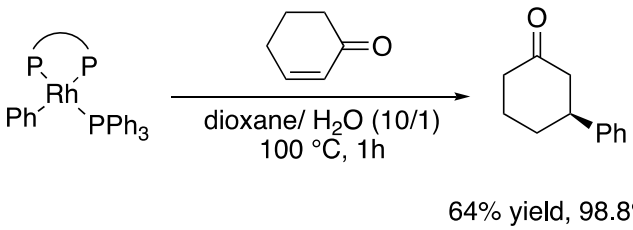

Scheme 1.31 Indicative evidence of active catalytic Rh–Ph species

In the same study, Hayashi also demonstrated that the reaction, at ambient temperature, was plagued by the easy replacement of the hydroxorhodium complex with acetylacetone to give back the Rh(acac)binap species (**Scheme 1.32**).

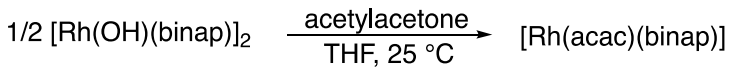

Scheme 1.32 Fast ligand replacement of Rh–OH by acac

The essence of the discovery and proposed catalytic cycle can be illustrated below in **Scheme 1.33**. In pathway a, the transmetallation from [Rh]–acac with $PhB(OH)_2$ to give [Rh]–Ph is slow. Upon addition onto cyclohexenone, the oxa-π-allylrhodium complex is generated. In the presence of water, this complex undergoes hydrolysis to give hydroxorhodium species that is immediately converted into [Rh]–acac complex by reaction with the acetylacetone generated at the prior transmetallation step. Compared to pathway a, the exclusion of acetylacetone by use of [Rh]–OH complex enabled smooth reaction even at 35 °C. Hence, this significantly circumvents the issue of high temperature by eliminating the slow transmetalation associated with [Rh]–acac complex.

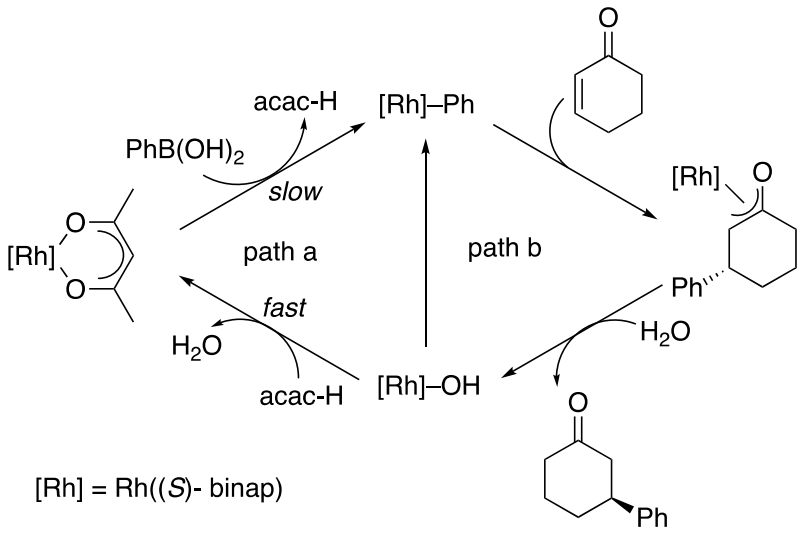

Scheme 1.33 Competing pathways a and b

The outstanding performance of hydroxorhodium binap as catalyst was subsequently found to give rise to different addition products in up to 98% yield and 99% ee , at a much lower temperature of 35 °C (**Scheme 1.34**). The more catalytically active rhodium species marks an important milestone in rhodium-catalyzed conjugate-addition reaction.

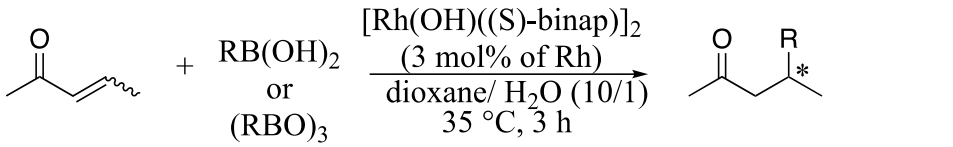

up to 98% yield, 99% ee

R = Ph, 4-F(C_6H_4), 4-MeO(C_6H_4), 4-CF_3(C_6H_4)

Scheme 1.34 Successful rhodium-catalyzed asymmetric addition at ambient temperature

In 2003, Miyaura and co-workers reported the use of cyclooctadiene(cod), in place of the usual phosphine based ligands, for the conjugate addition of arylboronic

acid onto conjugated enone.[61] The use of cod, together with potassium hydroxide, significantly promoted the reaction, driving it to completion within 2 hours.

In the same year, Hayashi and co-worker also pioneered the synthesis and use of the first C_2 symmetric chiral benzylic norbornadiene (nbd), for the rhodium-catalyzed 1,4-conjugate addition (**Scheme 1.35**).[62] This was shortly followed by the synthesis of chiral bicyclo[2.2.2]octadiene (Bod*) in 2004, which is inherently more stable compared to the norbornadiene backbone.[63] Meanwhile, Carreira also reported a similar chiral bicyclo[2.2.2]octadiene ligand.[64] Further exploration by Hayashi and his co-workers expanded the backbone of chiral dienes to bicyclo-[3.3.1]nona-2,6-diene (Bnd*),[65] bicyclo[3.3.2]deca-2,6-diene (Bdd*).[66] These sparked the interest, and uprising trend for the creation and usage of novel dienes in asymmetric catalysis, namely by Lin,[67,68] Laschat,[69] Corey,[70] Carnell,[71] Lam,[72] Wu.[73] Most of these creations were based predominantly on either the nbd or the Bod backbone, which provided a rigid structure excellent for inducing high enantioselectivity. However, the coordinating ability of these dienes may still be an issue. In 2008, Hayashi and co-workers reported another inspiring backbone, namely the chiral tetrafluorobenzobarrelenes (tfb).[74-75] This tfb backbone introduces a stronger coordination, possibly enhancing the protection of the integrity of the catalyst during a reaction.

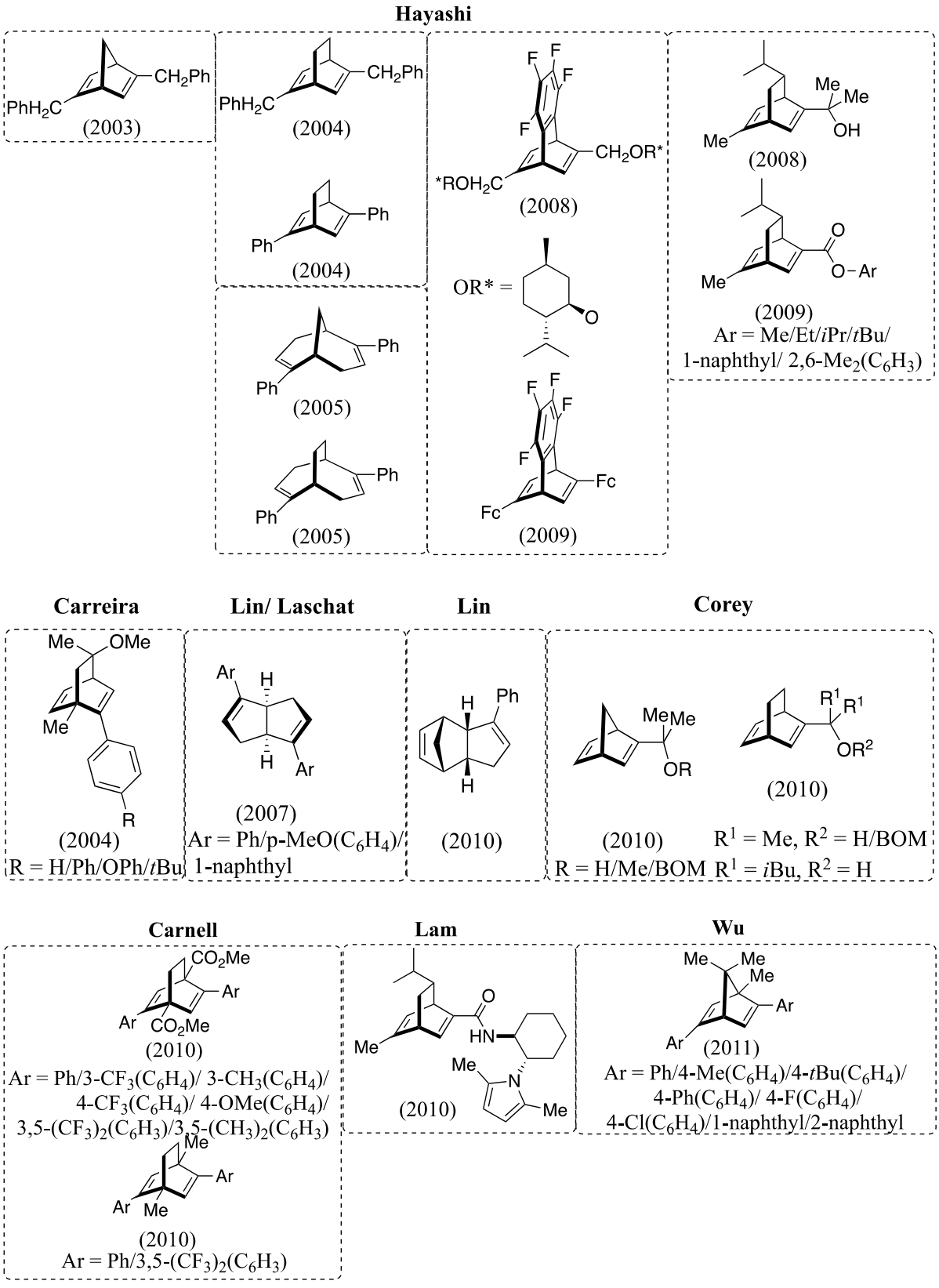

Scheme 1.35 Different diene-based ligands

In the mentioned catalytic cycle proposed by Hayashi, the stereochemistry is decided at the migratory insertion step and can be explained by the stereochemical induction model proposed by Hayashi (**Scheme 1.36** & **Scheme 1.37**).[62] With (*R*, *R*)-Bn-nbd as the chiral ligand, the 1st and the 4th quadrant provides the steric hindrance via the two benzyl functional groups. Should the cyclohexanone coordinate to the rhodium via its *Si*-face (in the 1st quadrant), steric repulsion will be experienced. As such, the coordination of the cyclohexanone proceeds via its re-face. Subsequently, the product is released upon hydrolysis, giving (*R*)-3-phenylcyclohexan-1-one.

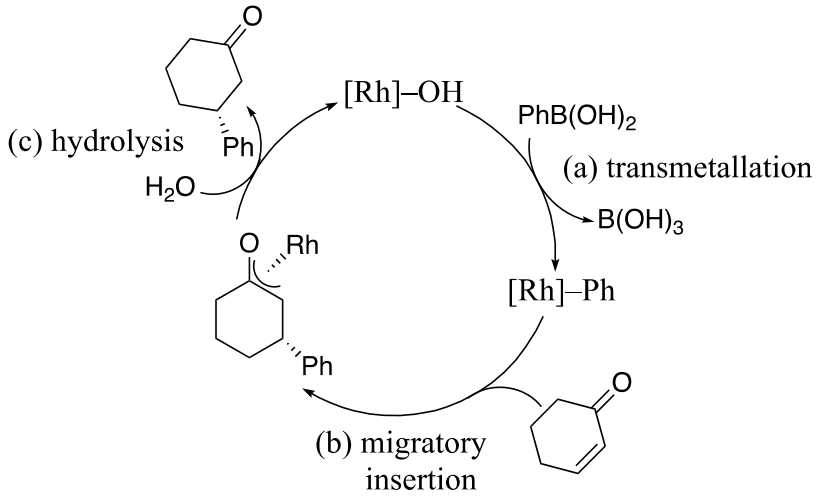

[Rh] = Rh(binap)

Scheme 1.36 Catalytic cycle of [Rh]-binap catalyzed asymmetric addition reactions

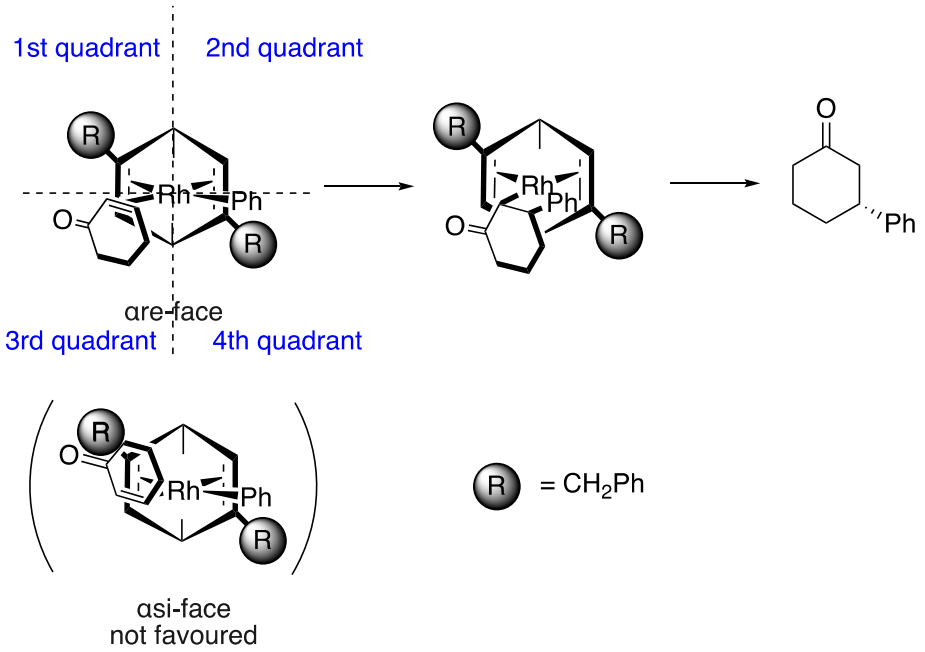

Scheme 1.37 Stereoinduction model of chiral diene

1.6. Conclusion

Since the initial report by Hayashi on the synthesis of novel chiral dienes and their application in asymmetric rhodium-catalyzed conjugate addition reaction, different types of conjugated substrates have been explored for the creation of stereogenic carbon centers. Such chiral carbon centered motif was hardly further utilized for the creation of other types of chirality. Furthermore, conjugate addition reactions are also rarely used for the direct synthesis of a different type of chirality other than central chirality. Hence, the incorporation of β-elimination as a strategy along with either a point-to-axial chirality conversion or asymmetric transition-metal catalyzed addition reaction, would be a rewarding and exciting venture.

1.7. References

1. Moss, G. P. *Pure and Applied Chemistry* **1996**, *68*, 2193–2222.
2. Daniel, K. G.; Brooks, W. H.; Guida, W. C. *Curr. Top. Med. Chem.* **2011**, *11*, 760–770.
3. Dou, X.; Wu, B.; Liu, J.; Zhao, C.; Qin, M.; Wang, Z.; Schonherr, H.; Feng, C. *ACS Appl Mater Interfaces* **2019**, *11*, 38568–38577.
4. Kenner, J.; Christie, G. H. *J. Chem. Soc., Trans.* **1922**, *121*, 614–620.
5. Richard, K., *<Molekulare asymmetrie. Stereochemie (Kark Freudenberg, Ed.). Leipzig-Wien:Franz-Deutike>*. 1933.
6. Kumarasamy, E.; Raghunathan, R.; Sibi, M. P.; Sivaguru, J. *Chem Rev* **2015**, *115*, 11239–11300.
7. Clayden, J.; Moran, W. J.; Edwards, P. J.; LaPlante, S. R. *Angew. Chem. Int. Ed.* **2009**, *48*, 6398–6401.
8. Clayden, J. *Angew. Chem. Int. Ed.* **1997**, *36*, 949–951.
9. Ōki, M. *Angew. Chem. Int. Ed.* **1976**, *15*, 87–93.
10. Oki, M. *Proc. Jpn. Acad. Ser. B Phys. Biol. Sci.* **2010**, *86*, 867–883.
11. Wilson, K. R.; Pincock, R. E. *J. Am. Chem. Soc.* **1975**, *97*, 1474–1478.
12. Prelog, V.; Helmchen, G. *Angew. Chem. Int. Ed.* **1982**, *21*, 567–583.
13. McCormick, M. H.; McGuire, J. M.; Pittenger, G. E.; Pittenger, R. C.; Stark, W. M. *Antibiot Annu* **1955**, *3*, 606–611.
14. Mehreen Farooq; Wasam liaqat Tarar; Fatima Amin; Mahmood, K. T. *Int. J. Pharma. Sci. Res.* **2011**, *3*, 1599–1603.
15. Wyk, B.-E. V.; Yenesew, A.; Dagne, E. *Biochem. Syst. Ecol.* **1995**, *23*, 277–281.
16. Supko, J. G.; Malspeis, L. *Antimicrob. Agents Chemother.* **1995**, *39*, 9–14.
17. Bringmann, G.; Steinert, C.; Feineis, D.; Mudogo, V.; Betzin, J.; Scheller, C. *Phytochemistry* **2016**, *128*, 71–81.
18. Fukuyama, Y.; Asakawa, Y. *J. Chem. Soc., Perkin Trans. 1* **1991**, 2737–2741.
19. Chen, Y.; Yekta, S.; Yudin, A. K. *Chem. Rev.* **2003**, *103*, 3155–3212.
20. Kočovský, P.; Vyskočil, Š.; Smrčina, M. *Chem. Rev.* **2003**, *103*, 3213–3246.
21. Krause, N.; Hashmi A. S. K., *Modern Allene Chemistry*. Wiley: 2004.
22. Yu, S.; Ma, S. *Angew. Chem. Int. Ed.* **2012**, *51*, 3074–3112.

23. Roth, W. R.; Ruf, G.; Ford, P. W. *Chem. Ber.* **1974**, *107*, 48–52.
24. Lowe, G. *Chemical Communications (London)* **1965**, 411–413.
25. Neff, R. K.; Frantz, D. E. *ACS Catalysis* **2014**, *4*, 519–528.
26. Ye, J.; Ma, S. *Organic Chemistry Frontiers* **2014**, *1*, 1210–1224.
27. Ogasawara, M. *Tetrahedron: Asymmetry.* **2009**, *20*, 259–271.
28. Rona, P.; Crabbe, P. *J. Am. Chem. Soc.* **1968**, *90*, 4733–4734.
29. Marek, I.; Mangeney, P.; Alexakis, A.; Normant, J. F. *Tetrahedron Lett.* **1986**, *27*, 5499–5502.
30. Evans, R. J. D.; Landor, S. R.; Smith, R. T. *Journal of the Chemical Society (Resumed)* **1963**, 1506–1511.
31. Torres, E.; Larson, G. L.; McGarvey, G. J. *Tetrahedron Lett.* **1988**, *29*, 1355–1358.
32. de Graaf, W.; Boersma, J.; van Koten, G.; Elsevier, C. J. *J. Organomet. Chem.* **1989**, *378*, 115–124.
33. Ogasawara, M.; Ikeda, H.; Hayashi, T. *Angew. Chem. Int. Ed.* **2000**, *39*, 1042–1044.
34. Tillack, A.; Koy, C.; Michalik, D.; Fischer, C. *J. Organomet. Chem.* **2000**, *603*, 116–121.
35. Han, J. W.; Tokunaga, N.; Hayashi, T. *J. Am. Chem. Soc.* **2001**, *123*, 12915–12916.
36. Matsumoto, Y.; Naito, M.; Uozumi, Y.; Hayashi, T. *J. Chem. Soc., Chem. Commun.* **1993**, 1468–1469.
37. Huang, Y.; del Pozo, J.; Torker, S.; Hoveyda, A. H. *J. Am. Chem. Soc.* **2018**, *140*, 2643–2655.
38. Yu, S.; Sang, H. L.; Zhang, S.-Q.; Hong, X.; Ge, S. *Communications Chemistry* **2018**, *1*, 64–73.
39. Bayeh-Romero, L.; Buchwald, S. L. *J. Am. Chem. Soc.* **2019**, *141*, 13788–13794.
40. Hayashi, T.; Tokunaga, N.; Inoue, K. *Org. Lett.* **2004**, *6*, 305–307.
41. Li, H.; Müller, D.; Guénée, L.; Alexakis, A. *Org. Lett.* **2012**, *14*, 5880–5883.
42. Crouch, I. T.; Neff, R. K.; Frantz, D. E. *J. Am. Chem. Soc.* **2013**, *135*, 4970–4973.
43. Tang, Y.; Chen, Q.; Liu, X.; Wang, G.; Lin, L.; Feng, X. *Angew. Chem. Int. Ed.* **2015**, *54*, 9512–9516.

44. Chu, W.-D.; Zhang, L.; Zhang, Z.; Zhou, Q.; Mo, F.; Zhang, Y.; Wang, J. *J. Am. Chem. Soc.* **2016**, *138*, 14558–14561.
45. Poh, J.-S.; Makai, S.; von Keutz, T.; Tran, D. N.; Battilocchio, C.; Pasau, P.; Ley, S. V. *Angew. Chem. Int. Ed.* **2017**, *56*, 1864–1868.
46. Hashimoto, T.; Sakata, K.; Tamakuni, F.; Dutton, M. J.; Maruoka, K. *Nat. Chem.* **2013**, *5*, 240–244.
47. Mbofana, C. T.; Miller, S. J. *J. Am. Chem. Soc.* **2014**, *136*, 3285–3292.
48. Hu, Y.; Shi, W.; Zheng, B.; Liao, J.; Wang, W.; Wu, Y.; Guo, H. *Angew. Chem. Int. Ed.* **2020**, *59*, 19820–19824.
49. Tap, A.; Blond, A.; Wakchaure, V. N.; List, B. *Angew. Chem. Int. Ed.* **2016**, *55*, 8962–8965.
50. Yang, J.; Wang, Z.; He, Z.; Li, G.; Hong, L.; Sun, W.; Wang, R. *Angew. Chem. Int. Ed.* **2020**, *59*, 642–647.
51. Liao, Y.; Yin, X.; Wang, X.; Yu, W.; Fang, D.; Hu, L.; Wang, M.; Liao, J. *Angew. Chem. Int. Ed.* **2020**, *59*, 1176–1180.
52. Muller, P. *Pure and Applied Chemistry* **1994**, *66*, 1077–1184.
53. Astles, P. C.; Mortlock, S. V.; Thomas, E. J., 5.3 - The Cope Elimination, Sulfoxide Elimination and Related Thermal Reactions. In *Comprehensive Organic Synthesis*, Trost, B. M.; Fleming, I., Eds. Pergamon: Oxford, 1991; pp 1011–1039.
54. Abbott, J. K. C.; Smith, B. A.; Cook, T. M.; Xue, Z. L., Chapter 10 - Synthesis of Organometallic Compounds. In *Modern Inorganic Synthetic Chemistry (Second Edition)*, Xu, R.; Xu, Y., Eds. Elsevier: Amsterdam, 2017; pp 247–277.
55. Zhao, H.; Ariafard, A.; Lin, Z. *Organometallics* **2006**, *25*, 812–819.
56. Akira, K.; Taeko, I.; Naoki, F. *Bull. Chem. Soc. Jpn.* **1977**, *50*, 551–552.
57. Foley, S. R.; Stockland, R. A.; Shen, H.; Jordan, R. F. *J. Am. Chem. Soc.* **2003**, *125*, 4350–4361.
58. Sakai, M.; Hayashi, H.; Miyaura, N. *Organometallics* **1997**, *16*, 4229–4231.
59. Takaya, Y.; Ogasawara, M.; Hayashi, T.; Sakai, M.; Miyaura, N. *J. Am. Chem. Soc.* **1998**, *120*, 5579–5580.
60. Hayashi, T.; Takahashi, M.; Takaya, Y.; Ogasawara, M. *J. Am. Chem. Soc.* **2002**, *124*, 5052–5058.
61. Itooka, R.; Iguchi, Y.; Miyaura, N. *J. Org. Chem.* **2003**, *68*, 6000–6004.

62. Hayashi, T.; Ueyama, K.; Tokunaga, N.; Yoshida, K. *J. Am. Chem. Soc.* **2003**, *125*, 11508–11509.
63. Tokunaga, N.; Otomaru, Y.; Okamoto, K.; Ueyama, K.; Shintani, R.; Hayashi, T. *J. Am. Chem. Soc.* **2004**, *126*, 13584–13585.
64. Fischer, C.; Defieber, C.; Suzuki, T.; Carreira, E. M. *J. Am. Chem. Soc.* **2004**, *126*, 1628–1629.
65. Otomaru, Y.; Tokunaga, N.; Shintani, R.; Hayashi, T. *Org. Lett.* **2005**, *7*, 307–310.
66. Otomaru, Y.; Kina, A.; Shintani, R.; Hayashi, T. *Tetrahedron: Asymmetry*. **2005**, *16*, 1673–1679.
67. Wang, Z.-Q.; Feng, C.-G.; Xu, M.-H.; Lin, G.-Q. *J. Am. Chem. Soc.* **2007**, *129*, 5336–5337.
68. Shao, C.; Yu, H.-J.; Wu, N.-Y.; Feng, C.-G.; Lin, G.-Q. *Org. Lett.* **2010**, *12*, 3820–3823.
69. Helbig, S.; Sauer, S.; Cramer, N.; Laschat, S.; Baro, A.; Frey, W. *Adv. Synth. Catal.* **2007**, *349*, 2331–2337.
70. Brown, M. K.; Corey, E. J. *Org. Lett.* **2010**, *12*, 172–175.
71. Luo, Y.; Carnell, A. J. *Angew. Chem. Int. Ed.* **2010**, *49*, 2750–2754.
72. Pattison, G.; Piraux, G.; Lam, H. W. *J. Am. Chem. Soc.* **2010**, *132*, 14373–14375.
73. Wei, W.-T.; Yeh, J.-Y.; Kuo, T.-S.; Wu, H.-L. *Chem. Eur. J.* **2011**, *17*, 11405–11409.
74. Nishimura, T.; Nagaosa, M.; Hayashi, T. *Chem. Lett.* **2008**, *37*, 860–861.
75. Nishimura, T.; Kumamoto, H.; Nagaosa, M.; Hayashi, T. *Chem. Commun.* **2009**, 5713–5715.

Chapter 2

Point-to-axial chirality conversion of aryltetralone monoketal to give axially chiral arylnaphthalene

2.1. Introduction to the synthesis of biaryl

Since the discovery and resolution of tartaric acid by Louis Pasteur, the synthesis of compounds with stereogenic chiral centers has garnered much attention.[1] Such attention has led to the development of many astounding and excellent enantioselective procedures that allow the synthesis of chiral center containing compounds relatively easier. In comparison to stereogenic center creation, the formation of axial chirality remains less explored. The mainstream approaches for the synthesis of axially chiral biaryl can be summarized according to the type of reactions 1) cross-coupling of two aromatic groups, 2) desymmetrization of preformed biaryl, and 3) construction of aromatic rings through cycloaddition reaction.[2]

In general, the cross-coupling reactions for axially chiral biaryl synthesis can be categorized into diastereoselective and enantioselective cross-couplings. For the latter, the pioneering report by Wilson and Cram elegantly demonstrated the use of (*R*)-menthol as a good leaving group with high chiral induction in the reaction with Grignard reagents (**Scheme 2.1**).[3] This methodology allows the synthesis of axially chiral biaryls with yields up to 88% and 95 % ee, albeit requiring a stoichiometric amount of chiral leaving group. Other methods involving catalytic cross-coupling reactions have been also reported, with Suzuki/Negishi/and Kumuda cross-coupling being some of the popular choices.[4-6]

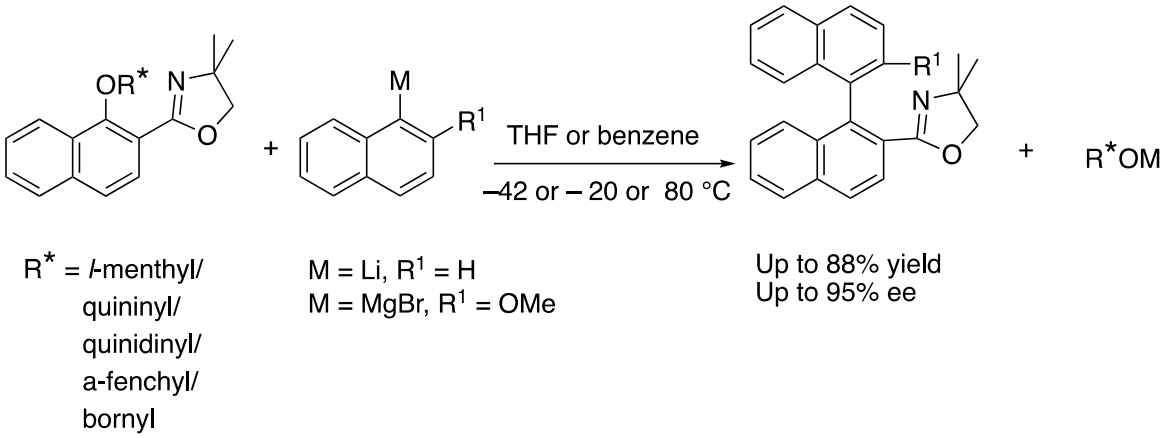

Scheme 2.1 First example of asymmetric induction by chiral leaving group in nucleophilic aromatic substitution by Wilson and Cram.

The desymmetrization of achiral biaryls usually involves the conversion of one of the prochiral *ortho*-substituents into another functional group. An example by Hayashi involves transforming one of the two *ortho*-triflate groups in a prochiral biaryl into another functional group through palladium catalyzed-coupling reaction (**Scheme 2.2**).[7] While the scope of the Grignard reagent is limited, high yields of up to 87% and good enantioselectivity of up to 93% ee were observed. The work also presented a possibility where axial chirality is not generated at the coupling of two aryl units but through the desymmetrization reaction of pro-chiral biaryl ditriflate motif.

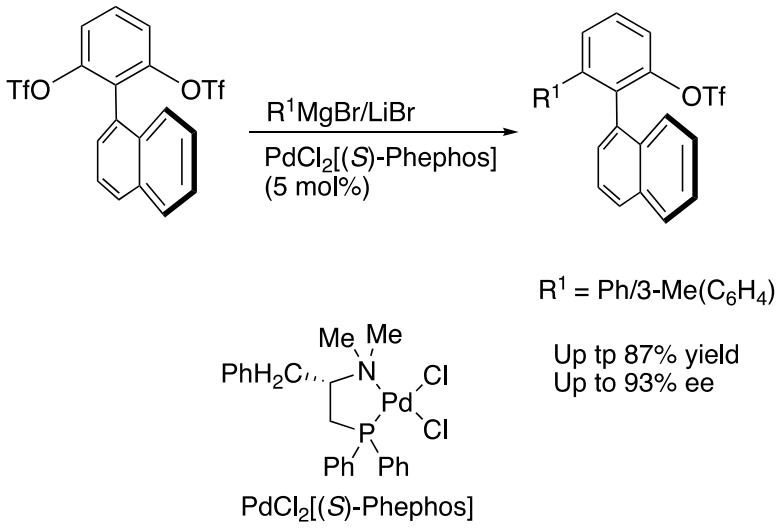

Scheme 2.2 Elegant display of palladium-catalyzed enantioposition-selective desymmetrization of biaryl ditriflate by Hayashi

Compared to coupling and desymmetrization reactions, the construction of aromatic rings through cycloadditions is also an alternative method to synthesize axially chiral biaryls. The [2+2+2] atroposelective formation of axially chiral 2-arylpyridines in up to 93% ee, catalyzed by a chiral cobalt complex, was reported by Gutnov and Heller (**Scheme 2.3**).[8]

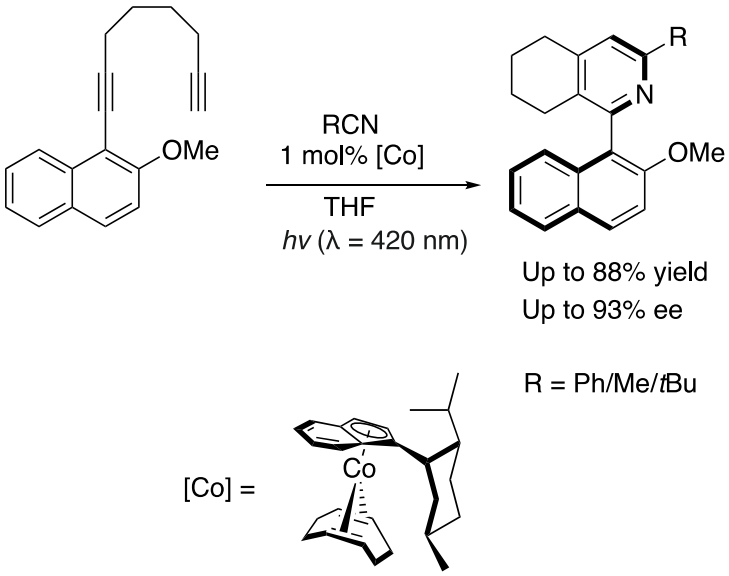

Scheme 2.3 [2+2+2] Cycloaddition of Alkynes and Nitriles by Gutnov and Heller to give 2-arylpyridines

On the other hand, Shibata revealed the formation of a two-fold teraryls catalyzed by a chiral iridium complex (**Scheme 2.4**).[9] The cycloaddition of such α,ω-diynes and monoalkynes afforded the corresponding axially chiral teraryl compounds in up to 97% yield and 99.8% ee.

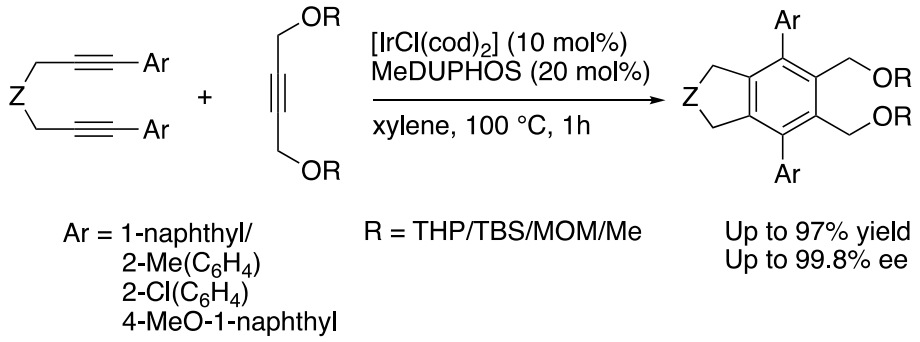

Scheme 2.4 Asymmetric intermolecular cyclization of diynes and monoalkyne to give teraryl axially chiral compounds.

Using a chiral cationic [Rh{(*S*)-H8-binap}]BF_4 complex, Tanaka was also able to efficiently synthesize axially chiral phthalides through cyclotrimerization of 1,6-diynes with monoynes, in high yield of up to 73% and excellent enantioselectivity up to 99% ee (**Scheme 2.5**).[10]

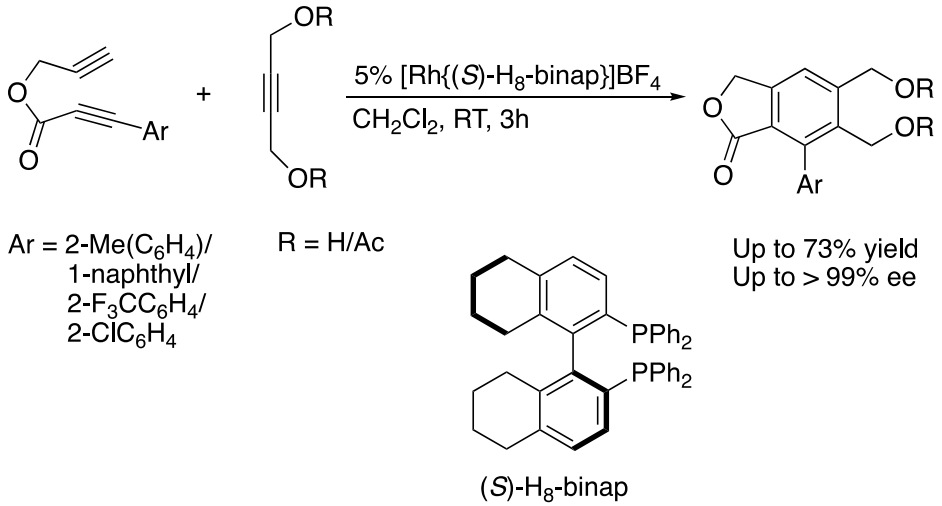

Scheme 2.5 Enantioselective cross alkyne cyclotrimerization of 1,6-diynes with monoynes

On the contrary, point-to-axial chirality transfer or conversion is less explored compared to the above-mentioned methodologies, yet it remains one of the uprising strategies for the synthesis of atropisomers. Since compounds containing stereogenic

centers can be easily obtained in excellent enantioselectivity, efficient point-to-axial chirality transfer or conversion will then give the corresponding product in much higher enantiopurity. Some preliminary examples of this type of transformation have been reported prior to date.

2.2. Background of point-to-axial chirality transfer and conversion

The general scheme for point-to-axial chirality conversion is outlined in **Scheme 2.6** shown below. Point-to-axial chirality transfer involves the installation of axial chirality in the final product, from the original proximal central chirality in the substrate.

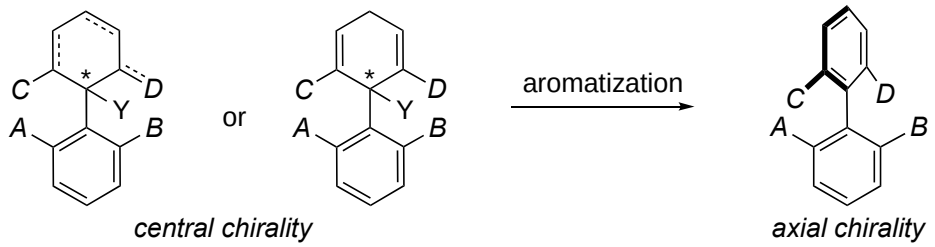

Scheme 2.6 Point-to-axial chirality conversion

In 2004, the report by Tanabe and co-workers first documented such benzannulation transformation (**Scheme 2.7**).[11] The chirality transfer went from a neighboring sp^3 central chirality in the optically active aryl(aryl')-2,2-dichlorocyclopropylmethanols, to chiral biaryls as the product. By using stoichiometric amount of $TiCl_4$, the $TiCl_4$ promoted elimination of the OH group then generates the cationic intermediate. This cationic intermediate is stabilized by its conjugation with the neighboring benzene ring system, thus preventing the bond rotation of the C (sp^3)–C (sp^2) bond. The "memory effect" of the chiral sp^3 carbon then served as the chiral source for the subsequent induction of axial chirality in the final product, with a yield of up to 96% ee and high chirality conservation .[12]

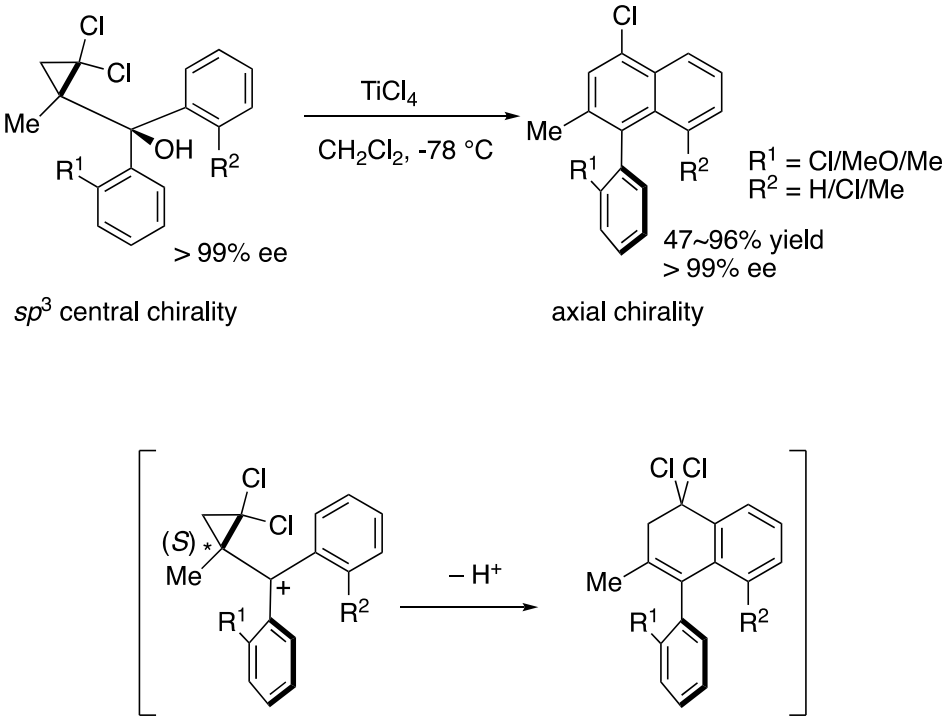

Scheme 2.7 Tanabe's benzannulation, 2004

In 2011, Thomson demonstrated the atroposelective synthesis of biphenol through oxidative dimerization of chiral 1,4-diketone, followed by a point-to-axial chirality transfer approach (**Scheme 2.8**).[13] The use of $BF_3.OEt_2$ in large excess allowed the synthesis of axially chiral biphenol in up to 89% yield and 98% ee. The high chirality transfer may be due to the remote stereogenic element providing some assistance in controlling the transfer of chirality during the course of transformation from bicyclohexenone to axially chiral biphenol.

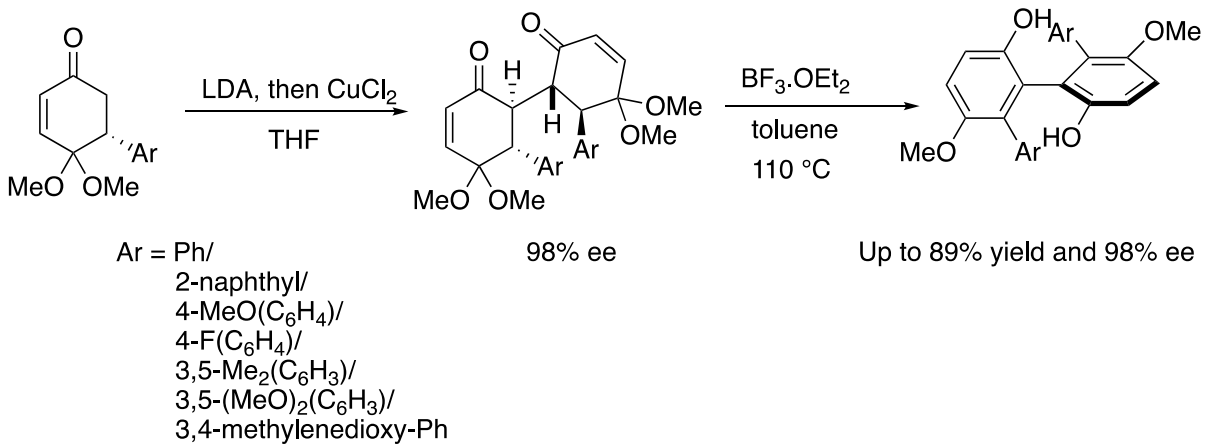

Scheme 2.8 Thomson's oxidative dimerization to give axially chiral biphenol

In 2016, Rodriguez and co-workers reported the synthesis of axially chiral aryl-pyridine product (**Scheme 2.9**). In the presence of MnO_2, the atroposelective oxidation of substituted 1,4-dihydropyridine gave the corresponding product in high yield, albeit with modest chirality conversion.[14] Furthermore, it would appear that under such oxidative condition, low yields and low functional group compatibility are expected. The synthesis of 1,4-dihydropyridines with high enantioselectivity may also be problematic, making it harder to obtain 4-arylpyridines in high enantiomeric excess after the point-to-axial chirality conversion. However, it is critical to note that this report further proves that the loss of stereogenic center was accompanied by the concomitant formation of the axial chirality without any remote chirality control.

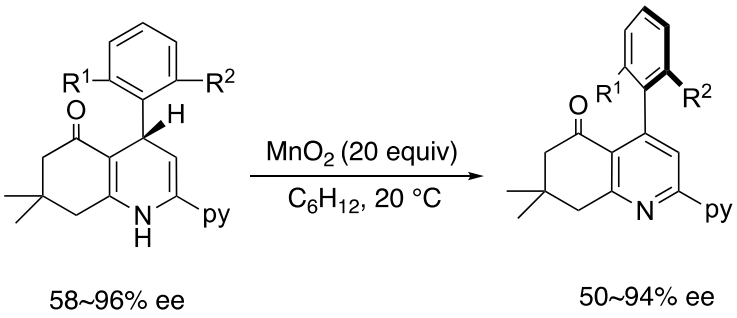

Scheme 2.9 Rodriguez's oxidation of 1,4–dihydropyridine

In 2018, Sparr and co-worker reported a reductive aromatization of 1,4-bisalkoxide to generate axially chiral biaryl silane (**Scheme 2.10**).[15] The Ti(O-*i*Pr)$_4$ promoted in situ reduction of the bis- metal alkoxide that is formed from the diastereoselective cyclization of the ketone , allowed for the aromatization to give a naphthyl-aryl motif with high atroposelectivity. In any case, the efficiency of atroposelectivity is heavily dependent on the remote stereogenic center that is simultaneously destroyed during the course of reduction.

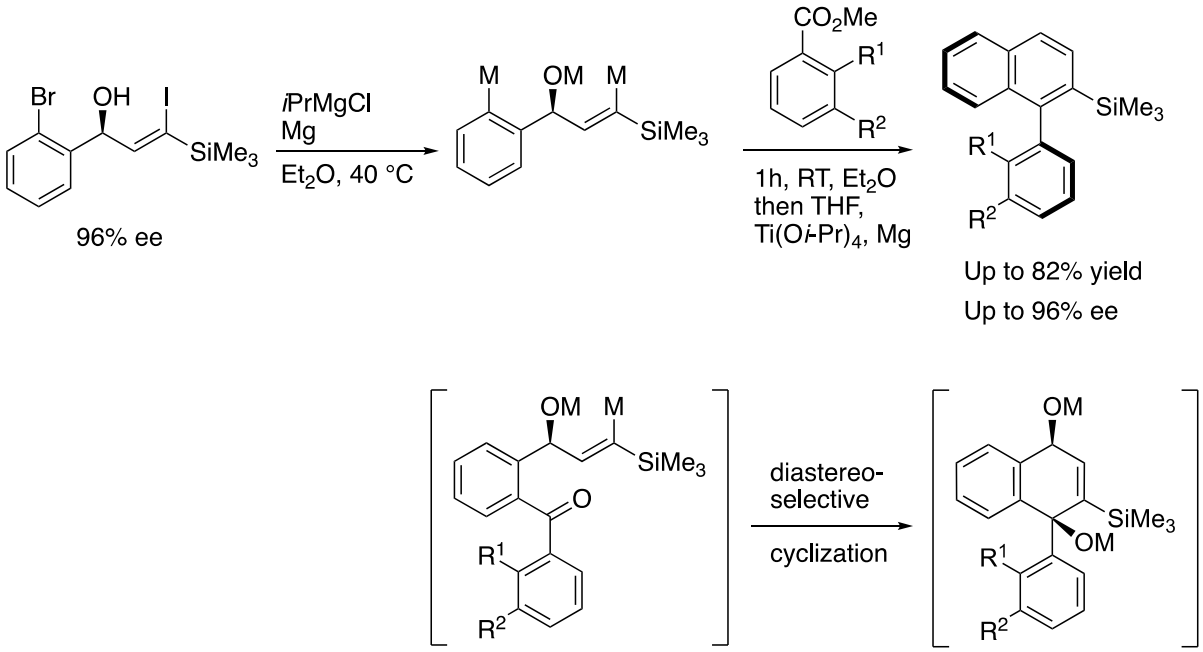

Scheme 2.10 Sparr's generation of chiral biaryl silane

Given the above reports, it can be seen that the concepts entailing point-to-axial chirality transfer often require the stereoinduction by a proximal stereogenic center that is simultaneously destroyed along with the formation of a new chiral axis. Reports of point-to-axial chirality conversion involving translation of central chirality to axial chirality at the same carbon, however, are rarely documented.[16] Non-redox neutral conditions are also often involved. In addition, these reactions also often require

stoichiometric amount of reagents to induce the point-to-axial chirality transfer or conversion. Hence, we report herein a novel strategy involving: 1) rhodium-catalyzed asymmetric arylation of naphthoquinone monoketal to provide enantioenriched aryltetralone, 2) in situ *C,O*-dialkylation of aryltetralone through the use of sodium hydride, followed by aromatization through deprotection of ketal group to give axially chiral arylnaphthalenes (**Scheme 2.11**).

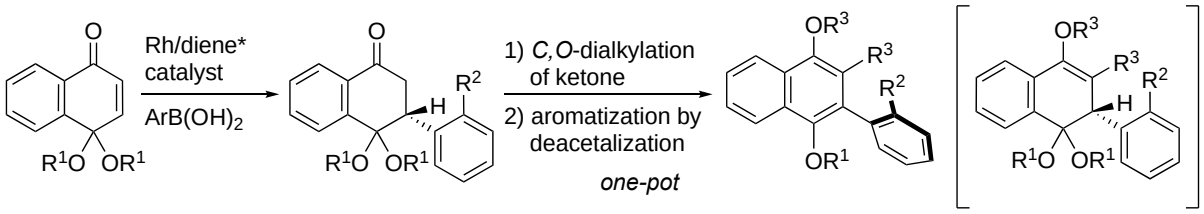

Scheme 2.11 Overall reaction scheme of rhodium catalysis and point-to-axial chirality transfer

2.3. Results and discussion

Relying on the methodologies established by Hayashi and co-workers, (*R*)-2-(1-naphthyl)-2,3-dihydro-4H-spiro[naphthalene-1,2'-[1,3]dioxolan]-4-one, (*R*)-**3aa** was synthesized in high yield of 90% and enantioselectivity of 99% ee (**Scheme 2.12**).[17]

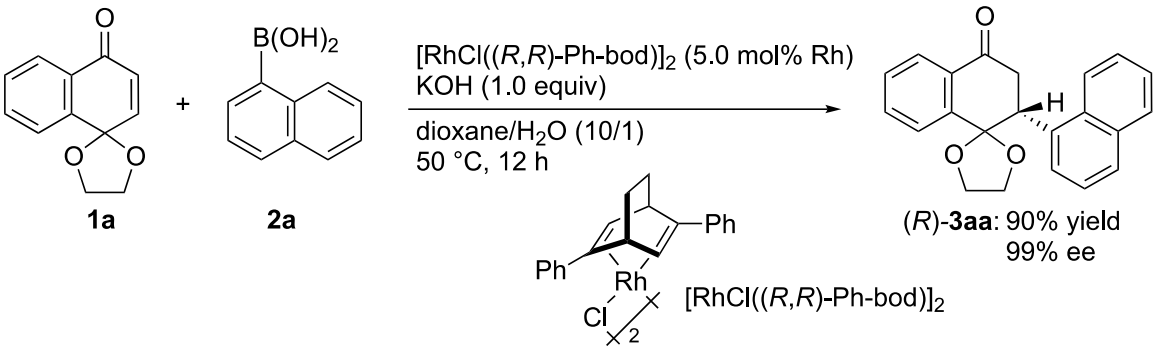

Scheme 2.12 Addition of 1-naphthylboronic acid onto **1a**

Our initial design follows that the α-position relative to the ketone functionality is essential in providing enough steric hindrance and barrier to inhibit the rotation of the atropisomers formed (**Scheme 2.13**). As such, it would be vital to replace the acidic hydrogen with a suitable alkyl group through the formation of an enolate.

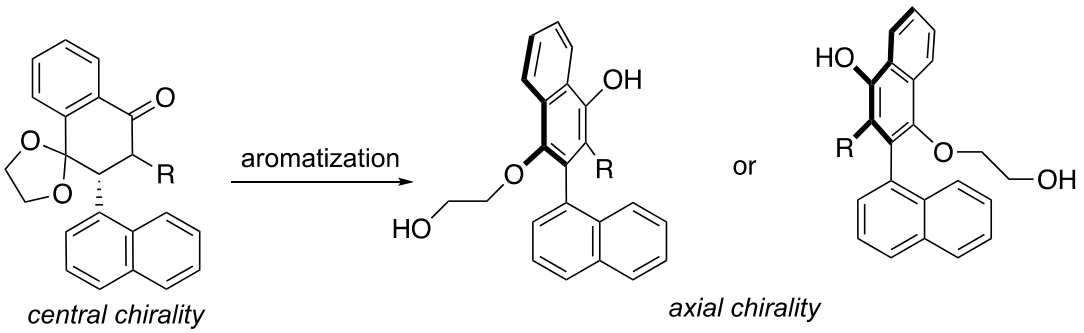

Scheme 2.13 Our design of point-to-axial chirality conversion

With the usage of lithium bis(trimethylsilyl)amide as the base, a benzylic group could be introduced onto (*R*)-**3aa** in good yield of 66% (**Scheme 2.14**). Expectedly, the high enantioselectivity of 99% ee was also retained in mono-benzylated tetralone monoketal **4'** obtained as a mixture of diastereomers.

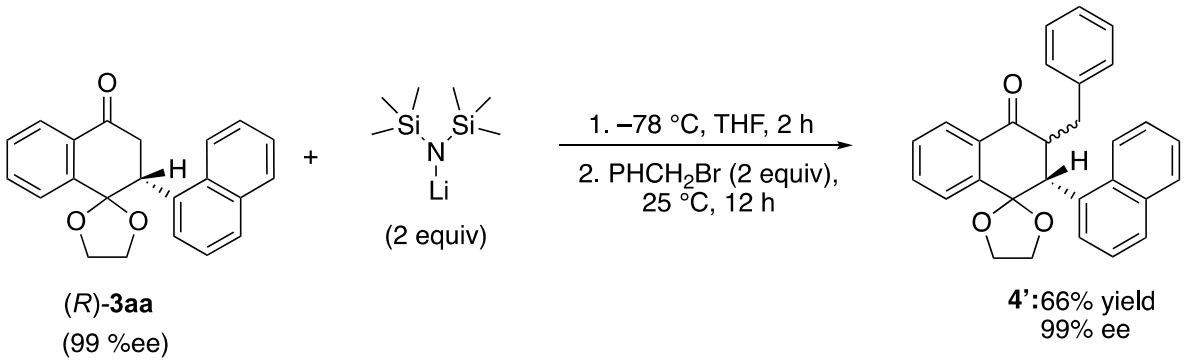

(*R*)-**3aa**
(99 %ee)

4':66% yield
99% ee

Scheme 2.14 Monobenzylation of **3aa** with LHMDS

When the benzylated product **4'** was subjected to concentrated hydrochloric acid, a naphthoquinone derivative **5'** was generated in 75% yield instead (**Scheme 2.15**). The targeted biaryl **5''** could only be obtained in poor yield of 11% yield. It was also discovered that **5'** racemizes overtime and thus implying that the rotational barrier is low. The ketone functional group may not provide enough steric hindrance to prevent rotation of the naphthyl motif in compound **5'**. In hindsight, the formation of **5'** also indicates that anhydrous condition is essential to inhibit side reaction, such as water acting as nucleophile and attacking the acid-activated ketal group.

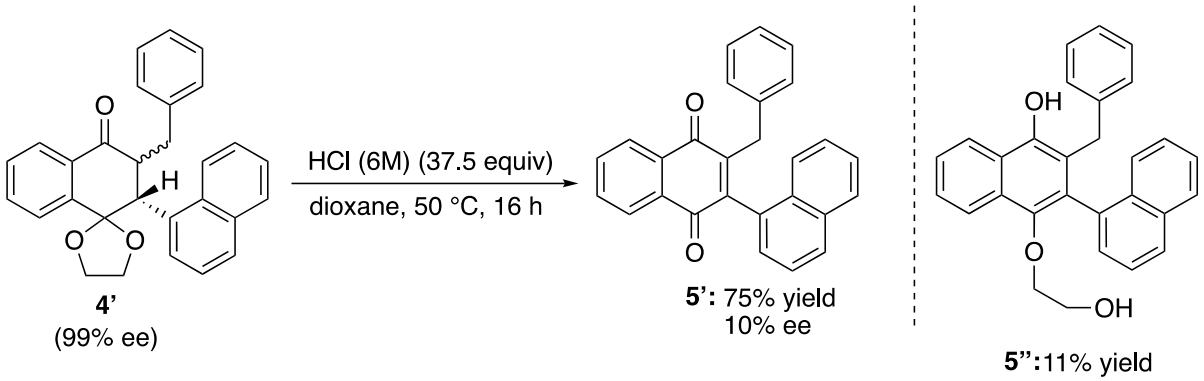

Scheme 2.15 Attempted aromatization of **4'** under acidic condition

Given the above problem, we devised an alternative strategy to obtain a biaryl product with conformationally stable chirality in a better yield. The targeted biaryl could be formed by a 2-steps reaction: 1) formation of enolate, 2) deketalization with the concomitant aromatization to generate the axially chiral binaphthyl motif (**Scheme 2.16**). Hence, this strategy eliminates the equilibrium of the enolate formation and thereby lowers the energy of the intermediate through increased conjugation.

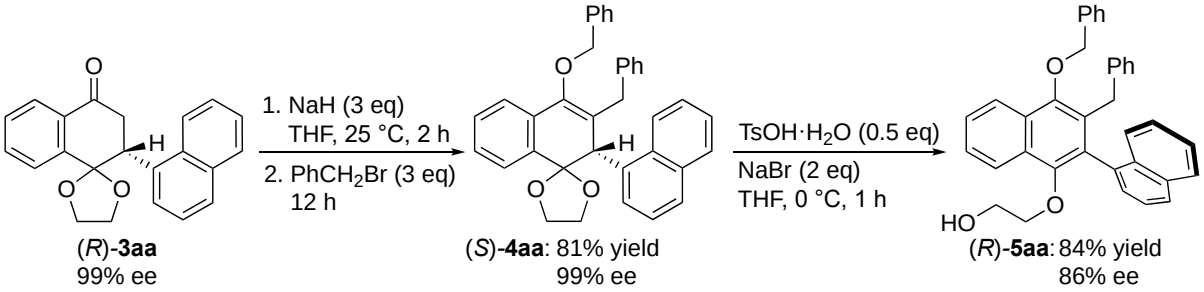

Scheme 2.16 Stepwise benzylation/aromatization

When (*R*)-**3aa** was subjected to a large excess of sodium hydride as the base and benzyl bromide as the electrophile, the corresponding *O,C*-dibenzylated styrene product **4**aa was isolated in 81% yield and 99% ee. The absolute configuration of the product **4aa** was determined to be (*S*) by its X-ray crystallographic analysis. The deketalization/aromatization of (*S*)-**4aa** was then carried out. The combination of

catalytic amount of TsOH•H_2O, along with NaBr, proved to be ideal for activating the ketal group, leading to aromatization. In the absence of NaBr, the reaction was sluggish. With this combination, we could move on to controlling the efficiency of the point-to-axial chirality conversion.

To explore the effect of the ketal group on the point-to-axial chirality conversion process, we synthesized the napthyltetralone derivatives (*R*)-**3ba** and (*R*)-**3ca** in high yield and high enantioselectivity of 99% ee (**Scheme 2.17**).

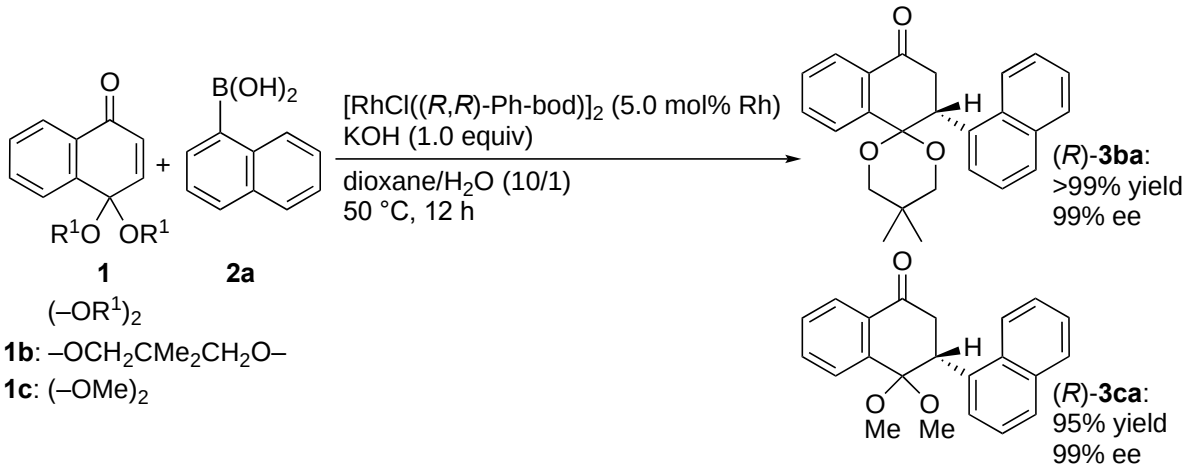

Scheme 2.17 Addition of 1-naphthylboronic acid onto **1b**/**1c**

When (*R*)-**3aa**, (*R*)-**3ba** and (*R*)-**3ca** were subject to the dibenzylation reaction condition, the corresponding *O*,*C*-dibenzylated product could be seen in the crude NMR. However, the isolation of dibenzylated (*R*)-**3ba** and (*R*)-**3ca** was difficult, possibly due to the instability of the ketal groups with acidic silica gel column purification. In spite of this, the greater instability of the ketal group meant that it is easier to achieve aromatization of the dibenzylated **3ba** and **3ca**. Following that notion, we proceeded to uncover a one-pot reaction of (*R*)-**3aa**, by combining the dibenzylation and aromatization reactions (**Scheme 2.18**).

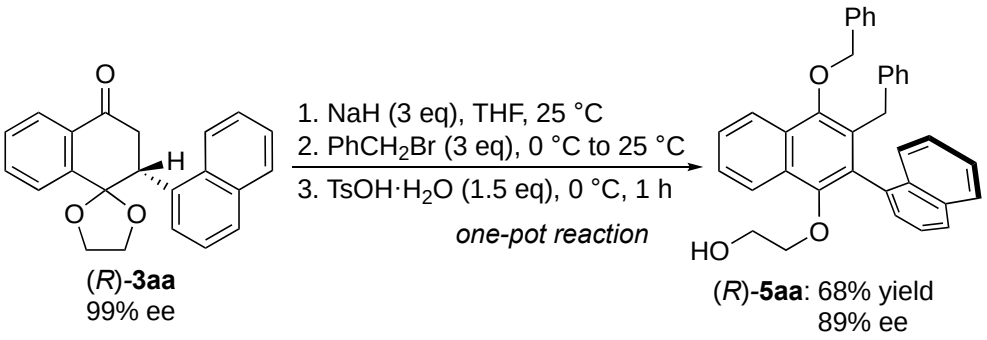

Scheme 2.18 *O*,*C*-dibenzylation of (*R*)-**3aa** to give (*R*)-**5aa**

Much to our delight, the in-situ generation of (*R*)-**5aa** proceeded with similar overall isolated yield of 68%, and an even higher chirality conversion of 89% ee. This proves to be an extremely versatile protocol that is easy to operate and eliminates any aromatization that occurs outside of the experimental condition. Expectedly, both (*R*)-**3ba** and (*R*)-**3ca** underwent the one-pot transformation to give (*R*)-**5ba** and (*R*)-**5ca** in high yield and enantioselectivity respectively (**Scheme 2.19**).

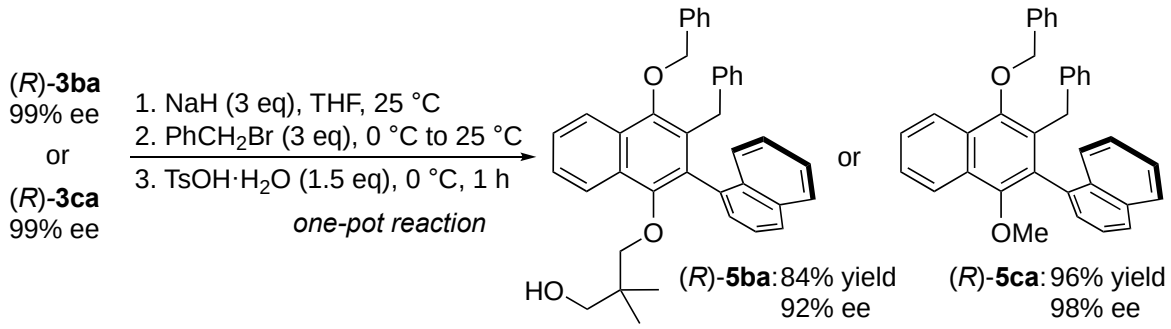

Scheme 2.19 *O*,*C*-dibenzylation of **3ba**/**3ca** to give **5ba**/**5ca**

Interestingly, the efficiency of the point-to-axial chirality conversion was higher in the acyclic ketal substrate. To investigate this phenomenon, we performed further substrate screening (**Scheme 2.20**).

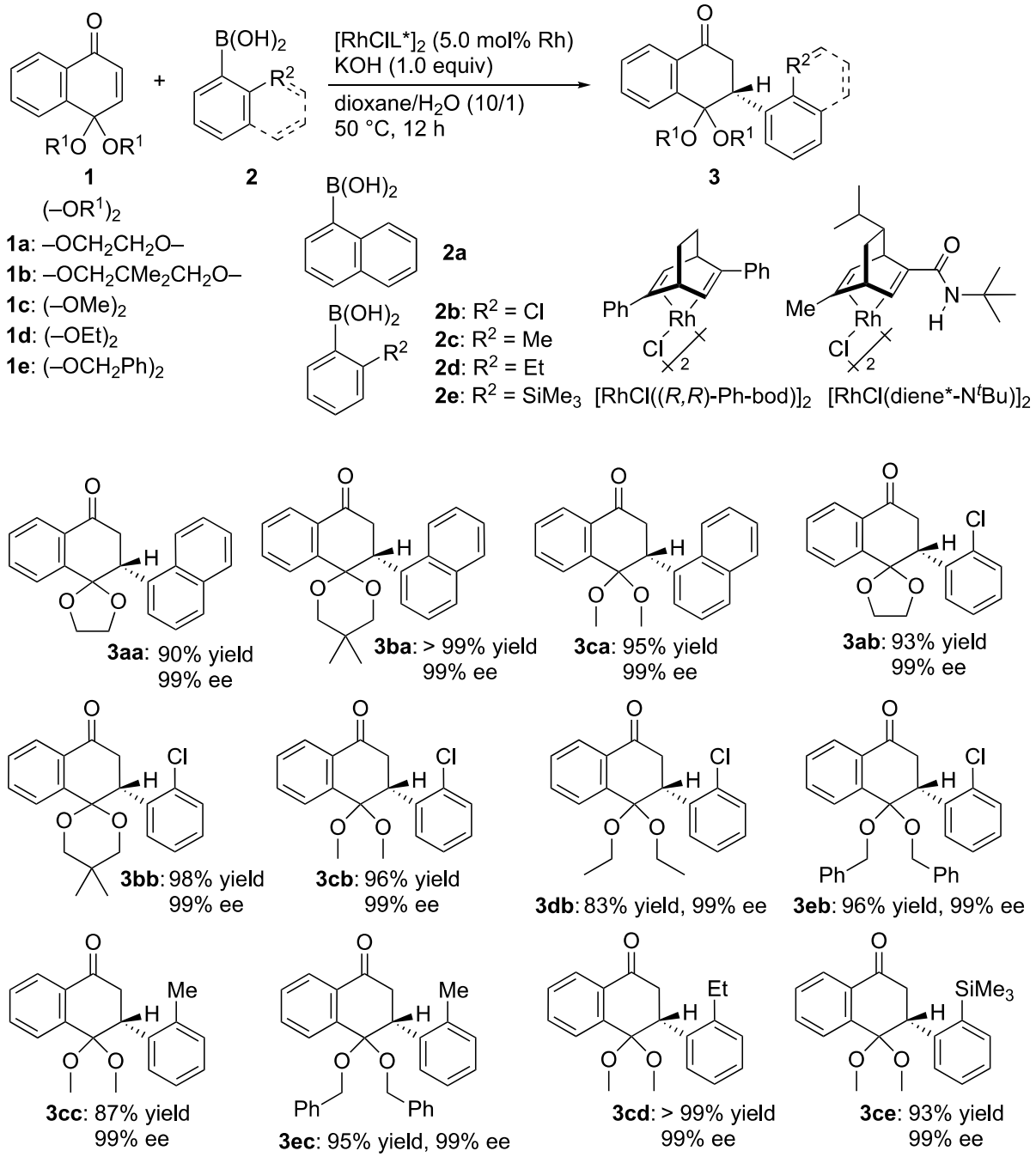

Scheme 2.20 Summary of asymmetric rhodium–catalyzed conjugate addition of **1**

With [RhCl(*R*,*R*)-Ph-bod]$_2$ catalyst, **3cc**, **3ec**, **3cd**, and **3ce** were synthesized in high yield and high enantioselectivity of 99% ee. The addition of 2-Cl(C_6H_4)B(OH)$_2$, however, did not proceed well with [RhCl(*R*,*R*)-Ph-bod]$_2$ catalyst; the reaction was

sluggish. In turn, the use of [RhCl(diene*-N*t*Bu)]$_2$ as catalyst gave smooth conversion of the substrate **1a**–**1e** to afford the corresponding **3ab**, **3bb**, **3cb**, **3db** and **3eb**. The absolute configuration of the product **3ce** was determined to be (*S*) by its X-ray crystallographic analysis. All its analogous counterparts are assumed to have the same absolute configuration.

From the previous results, we have established that the reactions ran smoothly to afford the desired biaryls **5aa**–**5ca**. In terms of chirality conversion, bulkier ketal group such as the one derived from neopentyl glycol was more efficient than the one derived from 1,2-ethanediol. In the case of dimethoxy ketal group, the % ee was even higher at 98%. It is perplexing to see that a smaller methoxy group was more efficient in maintaining the point-to-axial chirality transfer. Hence, we seek to verify if the higher chirality conversion was due to other factors, such as the ease of hydrolysis of the ketal groups. When aryltetralone **3ab** was subjected to the dibenzylation/aromatization protocol, the biaryl derivative **5ab** was only obtained in 14% yield and 40% ee (**Scheme 2.21**).

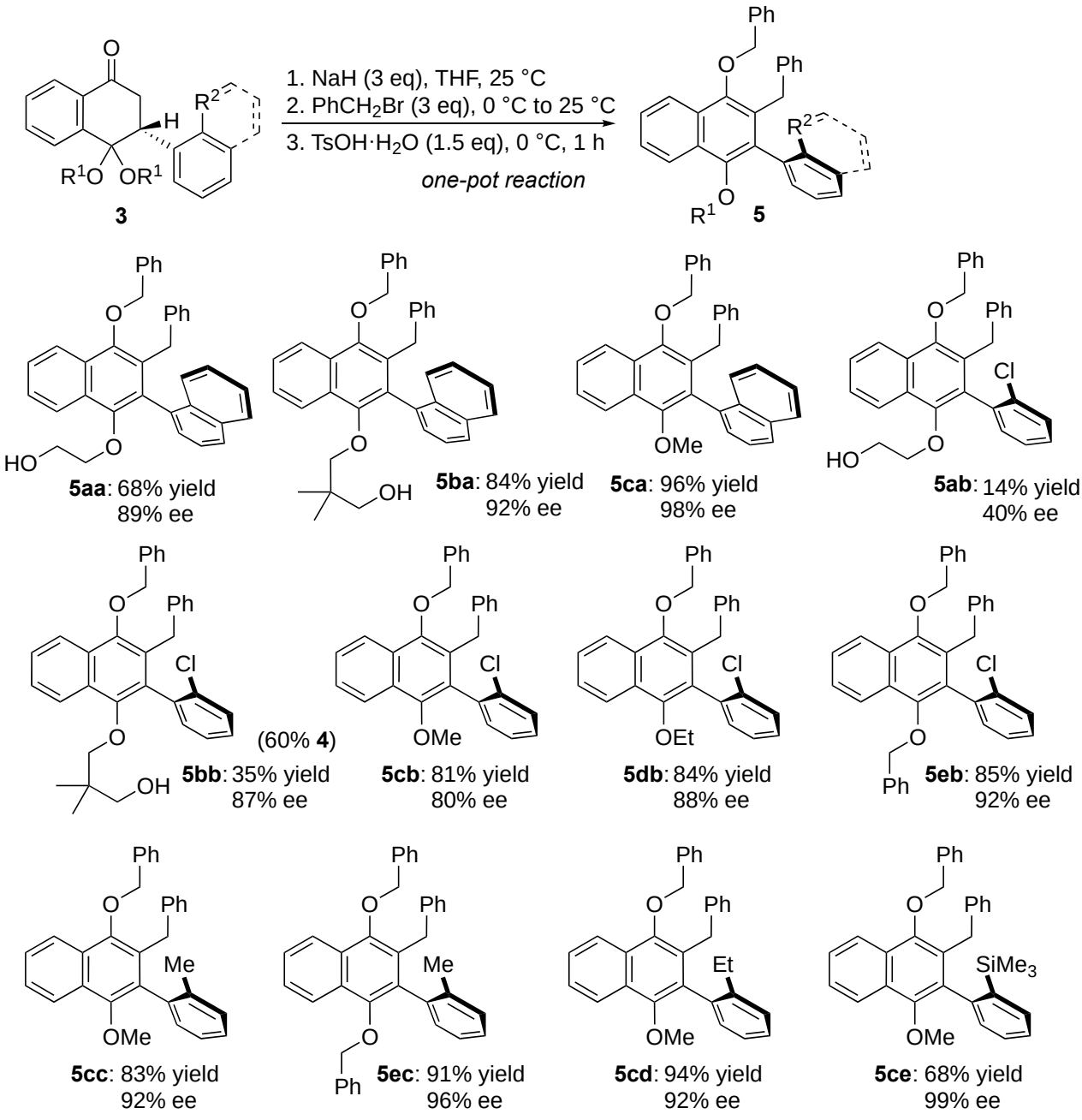

Scheme 2.21 One-pot *O*,*C*-dibenzylation of **3** following aromatization to give biaryl **5**

The low yield of **5ab** was a result of the difficulty faced in the aromatization of the *O*,*C*-dibenzylation intermediate that was formed in 80% yield. When the 1,2-ethanediol protecting group was replaced by neopentyl glycol protecting group, the dibenzylation/aromatization afforded biaryl **5bb** in slightly higher 35% yield and 87% ee. The low yield was again due to the low conversion of the *O*,*C*-dibenzylation

intermediate into the aromatized product. For dibenzylated **3ab** and **3bb** containing cyclic ketal, the reversibility of the ketal group leaving upon activation and returning may serve to impede the following aromatization. On this note, it is also important to realize that when the aromatization proceed in a relatively slow rate, the reaction is more susceptible to the rotation of 2-Cl(C_6H_4) group. As such, it would generally lead to lower % ee, should a bulky group be not in place to provide the steric hindrance needed to inhibit such rotation.

In the case of dimethoxy ketal group with 2-Cl(C_6H_4), the reaction proceeded smoothly to give biaryl **5cb** in 81% yield and relatively high 80% ee despite it being a small ketal group. This shows that the easier hydrolysis of dimethoxy ketal is likely a more prominent factor in maintaining the conversion of chirality.

The steric effect of the alkoxy groups was also observed with the introduction of slightly larger ethoxy group and benzyloxy group, giving **5db** and **5eb** in 88 and 92% ee. Other products such as **5cc**, **5ec** and **5cd** could also be synthesized in high yields and up to 96% ee. Not surprisingly, the incorporation of a bulky trimethylsilyl group to the *ortho* position pushed the chirality transfer to its maximum potential, giving **5ce** of 99% ee. The absolute configuration of **5ce** was determined to be (*R*) by its X-ray crystal structure analysis.

In general, the aromatization reaction tends to proceed fast to completion for substrate with acyclic ketal protecting group where the ease of hydrolysis is higher . As such, the point-to-axial chirality conversion also tends to be more efficient without experiencing much rotation of the *ortho*-substituted aryl group. For substrate with cyclic ketal protecting group, steric hindrance by the incorporation of bulky group in the *ortho* position has to be in place to achieve high point-to-axial chirality conversion.

Using 3-$NO_2(C_6H_4)CH_2Br$ as the electrophile instead of benzyl bromide, (*R*)-**3ca** was efficiently converted to the corresponding biaryl product **5cf** high yield with stereochemical fidelity (**Scheme 2.22**). The absolute configuration of **5cf** was determined to be (*R*) by X-ray crystallographic analysis. On the basis of this observation, all the rest of the biaryl products were assumed to have the (*R*) configuration.

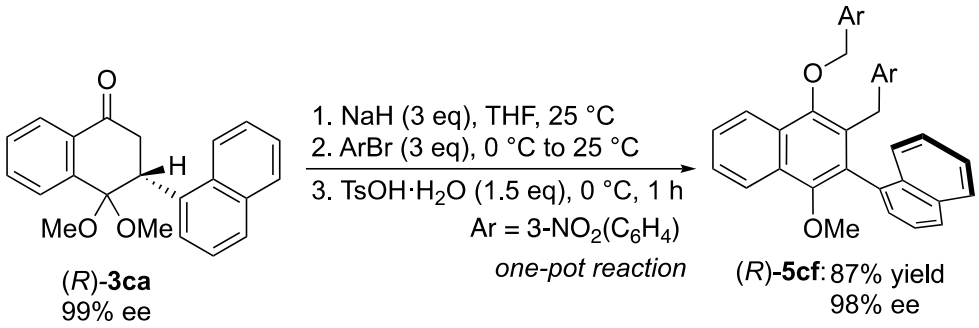

Scheme 2.22 *O*,*C*-dibenzylation of **3ca** following aromatization to give **5cf**

Other than benzylic bromides, allyl and methallyl bromides can also be introduced as electrophile. Upon the one-pot aromatization, the corresponding products **6a** and **6b** were synthesized in similar fashion as **5ca** in high yield of 84% and 81% respectively **(Scheme 2.23**).

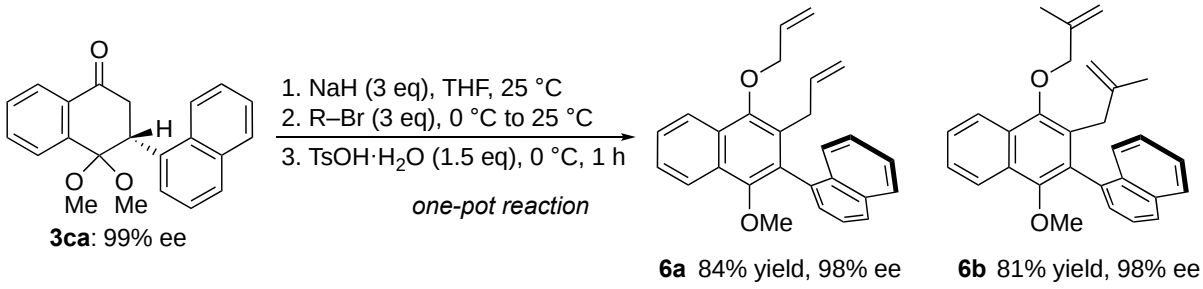

Scheme 2.23 *O*,*C*-Diallylation/dimethallylation of **3ca** following aromatization to give **6a**/**6b**

Furthermore, different substitution patterns can be introduced first through selective *C*-benzylation to generate a single diastereomer **7** in 55% yield and 99% ee, followed by *O*-alkylation of different electrophiles. The one-pot protocol again can be applied with a tweak of the reaction condition to afford the products **8a**, **8b**, **8c** of up to 99% ee (**Scheme 2.24**).

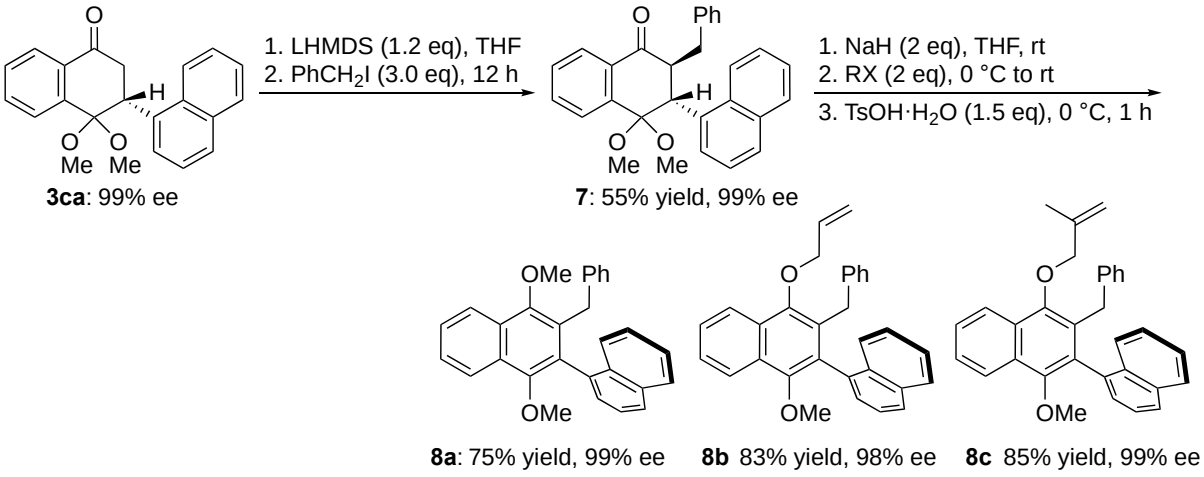

Scheme 2.24 Stepwise *C*-benzylation and *O*-alkylation of **3ca**, followed by aromatization to give **8a**, **8b** and **8c**

Prior to aromatization, there are two conformations that the *O*,*C*-dibenzylated intermediate can adopt. They are namely the *exo*-conformation and *endo*-conformation that exist in an equilibrium (**Scheme 2.25).**

.

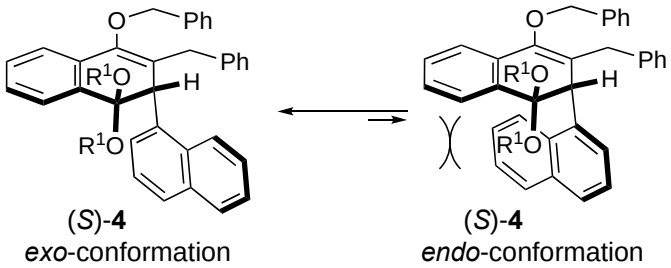

Scheme 2.25 Possible conformation prior to aromatization

With the *exo*-conformation, the outer ring of the 1-naphthyl moiety faces away from the main body of the dihydronaphthalene motif. With the *endo*-conformation, the outer ring of the 1-naphthyl moiety resides under the π-conjugated dihydronaphthalene system. As such, the equilibrium should lie on the left since adopting the *endo*-conformation will lead to significant repulsion between the naphthyl and the dihydronaphthalene motifs. The *exo*-conformation of **4** was further confirmed by the X-ray crystal structure analysis of **4ca** and **4ce** (**Scheme 2.26** & **Scheme 2.27**).

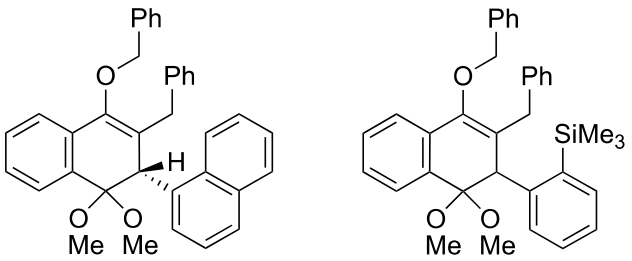

(*S*)-**4ca** *rac*-**4ce**

Scheme 2.26 Structures of **4ca** and **4ce**

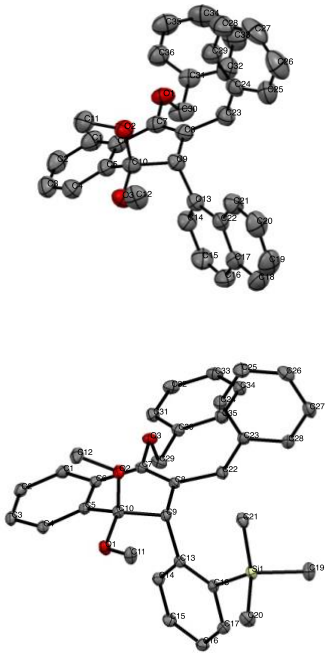

Scheme 2.27 ORTEP diagrams of **4ca** and **4ce**

The proposed mechanism can be as follows (**Scheme 2.28**). Due to the steric repulsion by the dihydronaphthalene motif, the *O*,*C*-dibenzylated intermediate adopts the favored *exo*-conformation. In the presence of TsOH•H_2O and NaBr, the oxygen atom of the ketal group is activated by H^+. In an E1 elimination fashion, the alkoxy group leaves as its corresponding alcohol, and an oxonium cation is generated. Subsequent loss of alpha-proton leads to the formation of the double bond, generating axially chiral (*R*)-**5**. In the same manner, the disfavored *endo*-conformation would lead to (*S*)-**5**.

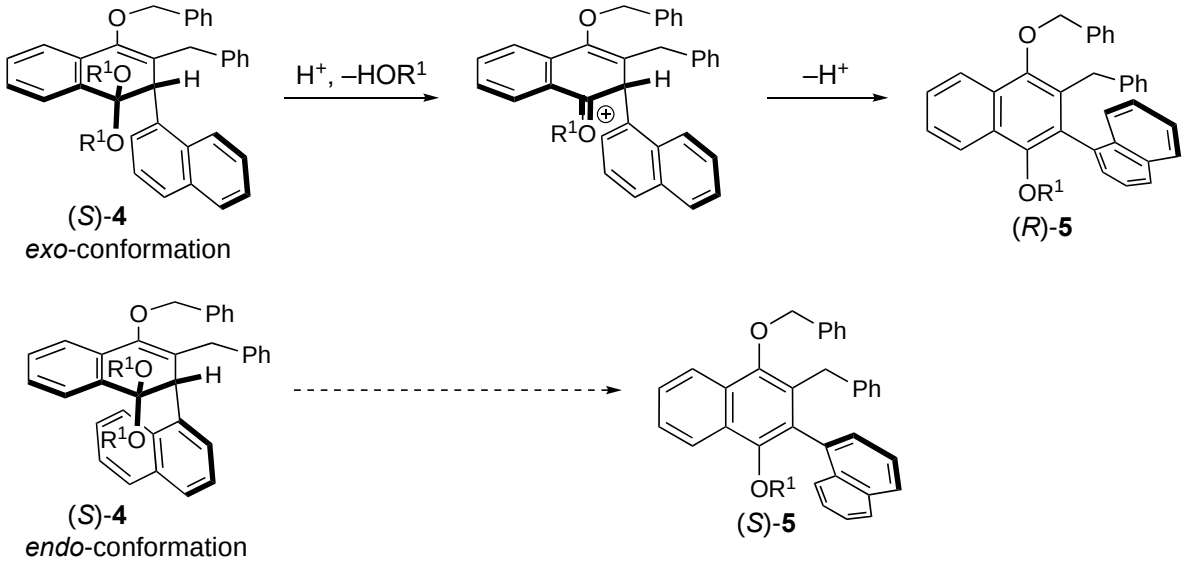

Scheme 2.28 Mechanistic proposal

2.4. Conclusion

In conclusion, we have demonstrated that the rhodium-catalyzed enantioselective 1,4-addition, when combined with an efficient point-to-axial chirality conversion process, allows highly atroposelective synthesis of biaryl compounds. The efficiency of the point-to-axial chirality conversion was found to be heavily dependent

on the ketal protecting group and the *ortho* substituent on the aryl group attached via the rhodium-catalyzed conjugate addition.

2.5. Experimental

2.4.1. General method

All anaerobic and moisture-sensitive manipulations were carried out with standard Schlenk techniques under inert gas. NMR spectra were recorded on a Bruker AV 400, QNP probe (400 MHz for ^{1}H, 100 MHz for ^{13}C), or Bruker AVIII 400 MHz NMR, BBFO Probe (400 MHz for ^{1}H, 100 MHz for ^{13}C). Chemical shifts are reported in δ (ppm) referenced to the residual peaks of $CDCl_3$ (δ 7.26) for ^{1}H NMR and $CDCl_3$ (δ 77.00) for ^{13}C NMR. The following abbreviations are used; s: singlet, d: doublet, t: triplet, q: quartet, sext: sextet, m: multiplet. High resolution mass spectra (HRMS) were obtained on a Waters Q-Tof Premier mass spectrometer. For thin layer chromatography (TLC), Merck pre-coated TLC plates (Merck 60 F254) were used, and compounds were visualized with a UV light at 254 nm. Further visualization was achieved by basic aqueous $KMnO_4$ solution stain. Flash column chromatography was performed with Silica gel 60 (Merck). Optical rotations were recorded on an Anton Paar MCP 150 machine. Enantiomeric excesses (ee) were determined by HPLC analysis on Shimadzu HPLC with Daicel chiral columns.

2.4.2. Materials

All commercially available reagents listed below were used as received for the reactions without further purification: degassed anhydrous 1,4-dioxane (Sigma Aldrich), 1-naphthylboronic acid (**2a**) (Alfa Aesar), 2-chlorophenylboronic acid (**2b**) (Alfa

Aesar), 2-methylphenylboronic acid (**2c**) (Alfa Aesar), 2-ethylphenylboronic acid (**2d**) (Fluorochem), benzyl bromide (Sigma aldrich), sodium hydride (TCI), sodium bromide (Sigma aldrich), potassium hydroxide (GCE laboratory chemicals), and LHMDS (Sigma aldrich). Dry tetrahydrofuran was obtained via a solvent purification system (PS-400-5, innovative technology Inc.). Deionized water was degassed prior to usage. Benzyl iodide (Sigma aldrich) was crystallized prior to usage. 2-Trimethylsilylphenylboronic acid (**2e**),[18] [RhCl((*R*,*R*)-Ph-bod)]$_2$,[19] and [RhCl(diene*-N*t*Bu)]$_2$[20-21] were prepared according to the reported procedures.

2.4.3. Preparation of starting materials

4*H*-Spiro[naphthalene-1,2'-[1,3]dioxolan]-4-one (**1a**),[22] 5',5'-dimethyl-4*H*-spiro[naphthalene-1,2'-[1,3]dioxan]-4-one (**1b**),[23] 4,4-dimethoxynaphthalen-1(4*H*)-one (**1c**),[24] and 4-benzyloxynaphthalen-1-ol[25] were prepared according to reported procedures.

4,4-Diethoxynaphthalen-1(4H)-one (**1d**)

An oven-dried 2-neck rbf (round bottom flask) was charged with 1,4-dihydroxynaphthalene (1.14 g, 10.0 mmol) under N_2 gas. Ethanol (50 mL) was added and the solution was stirred for 10 min. Thereafter, HCl (g), generated from the slow addition of 37% HCl (10 mL) in a dropping funnel to $CaCl_2$ (10 g, 12 mmol) in another 2-neck rbf with stirring, was introduced to the solution. The resulting mixture was stirred for a duration of 1 h to give 4-ethoxynaphthalen-1-ol, which was used without further purification.

An oven-dried 2-neck rbf was charged with 4-ethoxynaphthalen-1-ol (0.94 g, 5.0 mmol) under N_2 gas. Ethanol (10 mL) was added and the solution was stirred at 0 °C for 10 min. $PhI(OAc)_2$ (1.99 g, 6.0 mmol) was added in portions over a period of

15 min at 0 °C, and the solution was warmed to room temperature. After stirring for 1 h, saturated aqueous $NaHCO_3$ was added slowly until orange-yellow solution was observed. The precipitates formed were filtered off and the filtrate was extracted with diethyl ether (10 mL x 2). The combined organic layer was washed with brine (10 mL), dried over $MgSO_4$, filtered. Removal of solvent on a rotary evaporator and silica gel chromatography of the residue with hexane/dichloromethane (2/1), followed by hexane/diethyl ether (10/1) to give 4,4-diethoxynaphthalen-1(4*H*)-one (363 mg, 30% yield).

4-Bis(benzyloxy)naphthalen-1(4H)-one (**1e**)

An oven-dried 2-neck rbf was charged with 4-benzyloxynaphthalen-1-ol (2.00 g, 10.0 mmol) under N_2 gas. Benzyl alcohol (50 mL) was added and the solution was stirred at 0 °C for 10 min. To the solution was added K_2CO_3 (5.18 g, 90 mmol) and the mixture was stirred for 10 min. $PhI(OAc)_2$ (1.4 g, 11 mmol) was added in portions over a duration of 15 min at 0 °C. The mixture was then stirred for 5 min at 0 °C before warming to room temperature and stirred for 1 h. The reaction mixture was diluted with diethyl ether (30 mL) and filtered to remove any visible solids. The filtrate was distilled under reduced pressure (92 °C/2 mmHg) to remove most of the benzyl alcohol. The residue was diluted with diethyl ether (30 mL) and filtered to remove the blackish solids. Silica gel column chromatography with hexane/ethyl acetate (5/1) gave 4,4-dibenzyloxynaphthalen-1(4*H*)-one (1.29 g, 45% yield).

2.4.4. Characterization of the starting materials

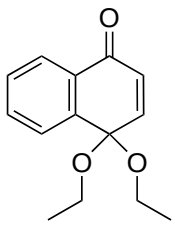

1d

Compound 1d (pale yellow liquid). ^{1}H NMR (400 MHz, $CDCl_3$) δ 1.16 (t, *J* = 7.0 Hz, 6H), 3.17 (dq, *J* = 8.8 Hz, 7.0 Hz, 2H), 3.45 (dq, *J* = 8.8 Hz, 7.0 Hz, 2H), 6.56 (d, *J* = 10.5 Hz, 1H), 6.91 (d, *J* = 10.4 Hz, 1H), 7.49 (td, *J* = 7.8 Hz, 1.3 Hz, 1H), 7.65 (td, *J* = 7.8 Hz, 1.4 Hz, 1H), 7.78 (dd, *J* = 7.8 Hz, 0.8 Hz, 1H), 8.07 (dd, *J* = 7.8 Hz, 0.9 Hz, 1H). ^{13}C NMR ($CDCl_3$) δ 15.4, 59.1, 94.6, 126.2, 126.7, 129.1, 131.6, 132.1, 133.5, 140.8, 145.8, 184.0. HRMS (ESI) calcd for $C_{14}H_{17}O_3$ $[M+H]^+$ 233.1178, found 233.1183.

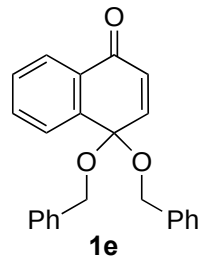

1e

Compound 1e (blueish liquid). ^{1}H NMR (400 MHz, $CDCl_3$) δ 4.40 (d, *J* = 11.3 Hz, 2H), 4.62 (d, *J* = 11.3 Hz, 2H), 6.59 (d, *J* = 10.5 Hz,1 H), 7.09 (d, *J* = 10.5 Hz, 1H), 7.24 – 7.36 (m, 10H), 7.53 (td, *J* = 7.6 Hz, 1.2 Hz, 1H), 7.68 (td, *J* = 7.5 Hz, 1.4 Hz, 1H), 7.91 (dd, *J* = 7.8 Hz, 0.8 Hz, 1H), 8.13 (dd, *J* = 7.8 Hz, 1.1 Hz, 1H). ^{13}C NMR ($CDCl_3$) δ 65.8, 94.9, 126.3, 127.1, 127.5, 127.7, 128.3, 129.4, 131.3, 131.9, 133.6, 137.6, 140.4, 144.4, 183.9. HRMS (ESI) calcd for $C_{24}H_{21}O_3$ $[M+H]^+$ 357.1491, found 357.1498.

2.4.5. Procedures for rhodium-catalyzed hydroarylation of 1a–1e

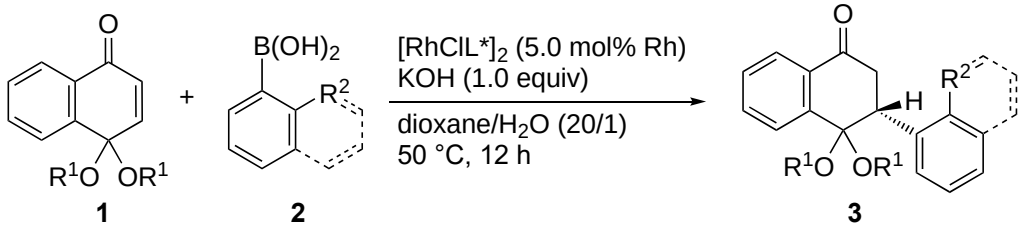

A schlenk tube was charged with naphthoquinone monoketal **1** (0.15 mmol), chiral rhodium catalyst (5 mol% of Rh), and arylboronic acid **2** (0.30 mmol, 2 equiv) under N_2 atmosphere. To the tube were added dioxane (1.0 mL) and 1.5 M KOH (0.15 mmol, 0.10 mL H_2O). The mixture was kept stirring at 50 °C for 12 h, before it was diluted with ethyl acetate and passed through a short silica pad for crude NMR analysis. Silica gel column chromatography with hexane/ether or ethyl acetate as eluent afforded the hydroarylation product **3**.

2.4.6. Characterization of hydroarylation product 3

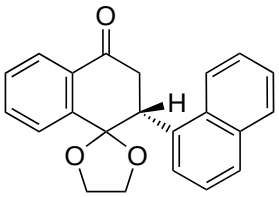

3aa

Compound 3aa (white flakes, 90% yield, 99% ee). The ee was measured by HPLC (Chiralpak IB column, 1.0 mL/min, hexane/2-propanol = 95/5, 280 nm, t_{major} = 18.3 min (*R*), t_{minor} = 44.9 min (*S*)); $[\alpha]^{25}_D$ –143 (*c* 0.513, $CHCl_3$) for 99% ee. ^{1}H NMR (400 MHz, $CDCl_3$) δ 2.78 (q, *J* = 7.6 Hz, 1H), 3.00 (dd, *J* = 16.9 Hz, 3.7 Hz, 1Hz), 3.70 (td, *J* = 7.5 Hz, 3.6 Hz, 1H), 3.76 (dd, *J* = 16.9 Hz, 13.0 Hz, 1H), 3.83 (q, *J* = 7.8 Hz, 1H), 3.90 (td, *J* = 7.2 Hz, 3.6 Hz, 1H), 4.75 (dd, *J* = 12.8 Hz, 3.7 Hz, 1H), 7.45–7.50 (m, 2H), 7.51 (d, *J* = 8.7 Hz, 1H), 7.53–7.58 (m, 1H), 7.59–7.71 (m, 3H), 7.84 (d, *J* = 8.2 Hz, 1H), 7.86–7.91 (m, 1H), 8.18 (d, *J* = 7.9 Hz, 1H), 8.21 (d, *J* = 6.4 Hz, 1H). ^{13}C NMR ($CDCl_3$) δ 42.5, 43.1, 64.8, 66.7, 107.9, 124.0, 124.9, 125.0, 125.3,

125.8, 126.3, 127.0, 127.9, 128.4, 129.0, 131.5, 132.8, 133.6, 133.9, 134.4, 144.2, 197.2. HRMS (ESI) calcd for $C_{22}H_{19}O_3$ $[M+H]^+$ 331.1334, found 331.1339.

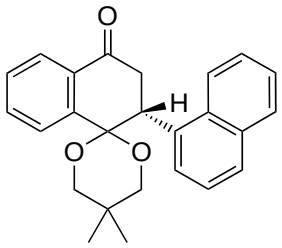

3ba

Compound 3ba (pale yellowish flakes, > 99% yield, 99% ee). The ee was measured by HPLC (Chiralpak IB column, 1.0 mL/min, hexane/2-propanol = 95/5, 280 nm, t_{major} = 9.90 min (R), t_{minor} = 21.0 min (S)); $[\alpha]^{25}_D$ +18.3 (c 0.655, $CHCl_3$) for 99% ee. ^{1}H NMR ($CDCl_3$) δ 0.76 (s, 3H), 1.20 (s, 3H), 3.27 (d, *J* = 4.6 Hz, 2H), 3.32 (dd, *J* = 9.3 Hz, 1H), 3.41–3.48 (m, 2H), 3.54 (d, *J* = 9.2 Hz, 1H), 5.18 (t, *J* = 4.6 Hz, 1H), 7.13 (d, *J* = 5.8 Hz, 1H), 7.23 (t, *J* = 6.1 Hz, 1H), 7.50 (t, *J* = 6.0 Hz, 0.6 Hz, 1H), 7.53–7.56 (m, 1H), 7.56–7.59 (m, 1H), 7.71 (d, *J* = 6.5 Hz, 1H), 7.75 (td, *J* = 6.0 Hz, 1.1 Hz, 1H), 7.86 (d, *J* = 6.2 Hz, 1H), 8.06 (td, *J* = 5.9 Hz, 0.9 Hz, 2H), 8.15 (d, *J* = 6.9 Hz, 1H). ^{13}C NMR ($CDCl_3$) δ 23.4, 23.9, 30.9, 42.1, 70.1, 71.7, 97.6, 122.6, 125.1, 125.4, 126.1, 126.3, 126.6, 127.0, 127.7, 129.2, 129.3, 132.16, 132.17, 133.98, 133.99, 134.00, 143.3, 196.6. HRMS (ESI) calcd for $C_{25}H_{25}O_3$ $[M+H]^+$ 373.1804, found 373.1808.

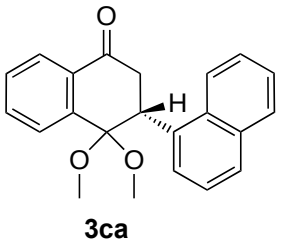

3ca

Compound 3ca (white blueish flakes, 95% yield, 99% ee). The ee was measured by HPLC (Chiralpak IB column, 1.0 mL/min, hexane/2-propanol = 95/5, 280 nm, t_{minor} = 7.7 min (*S*), t_{major} = 9.2 min (*R*)); $[\alpha]^{25}_D$ +200 (*c* 0.079, $CHCl_3$) for 99% ee. ^{1}H NMR (400 MHz, $CDCl_3$) δ 3.03 (s, 3H), 3.09 (dd, *J* = 17.6 Hz, 3.8 Hz, 1H), 3.13 (s, 3H), 3.50 (dd, *J* = 17.6 Hz, 6.4 Hz 3H), 4.76 (dd, *J* = 6.3 Hz, 3.8 Hz, 1H), 7.03 (d, *J* = 7.2 Hz, 1H), 7.14 (t, *J* = 7.6 Hz, 1H), 7.49 (td, *J* = 8.0 Hz, 1.0 Hz, 1H), 7.52 – 7.59

(m, 2H), 7.66 (d, J = 8.2 Hz, 1H), 7.73 (td, J = 7.5 Hz, 1.4 Hz, 1H), 7.85 (d, J = 8.1 Hz, 1H), 7.98 (d, J = 7.8 Hz, 1H), 8.06 (dd, J = 6.2 Hz, 1.3 Hz, 1H), 8.08 (d, J = 5.6 Hz, 1H). ^{13}C NMR ($CDCl_3$) δ 42.1, 43.0, 48.5, 49.1, 98.9, 122.4, 125.1, 125.4, 125.7, 126.4, 127.1, 127.39, 127.44, 129.0, 129.3, 131.3, 131.9, 133.2, 134.1, 134.4, 141.0, 196.5. HRMS (ESI) calcd for $C_{22}H_{21}O_3$ $[M+H]^+$ 333.1491, found 333.1498.

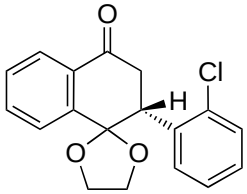

3ab

Compound 3ab (white flakes, 93% yield, 99% ee). The ee was measured by HPLC (Chiralpak IB column, 1.0 mL/min, hexane/2-propanol = 95/5, 280 nm, t_{major} = 9.3 min (*R*), t_{minor} = 11.2 min (*S*)); $[\alpha]^{25}_D$ –58.3 (*c* 0.642, $CHCl_3$) for 99% ee. ^{1}H NMR (400 MHz, $CDCl_3$) δ 2.94 (dd, J = 17.2 Hz, 4.4 Hz, 1H), 3.23 (q, J = 7.5 Hz, 1H), 3.44 (dd, J = 17.2 Hz, 12.2 Hz, 1H), 3.84–3.92 (m, 2H), 4.16 (ddd, J = 7.6 Hz, 5.8 Hz, 4.0 Hz, 1H), 4.49 (dd, J = 12.2 Hz, 4.4 Hz, 1H), 7.19–7.26 (m, 2H), 7.39–7.45 (m, 1H), 7.46–7.49 (m, 1H), 7.52 (td, J = 7.7 Hz, 1.4 Hz, 1H), 7.58 (dd, J = 7.7 Hz, 1.0 Hz, 1H), 7.64 (td, J = 7.8 Hz, 1.3 Hz, 1H), 8.09 (dd, J = 7.8 Hz, 0.9 Hz, 1H). ^{13}C NMR ($CDCl_3$) δ 41.7, 44.4, 64.6, 67.0, 107.5, 124.8, 126.4, 127.2, 128.4, 129.1, 129.5, 129.8, 131.5, 134.0, 135.5, 135.8, 143.6, 196.7. HRMS (ESI) calcd for $C_{18}H_{16}ClO_3$ $[M+H]^+$ 315.0788, found 315.0793.

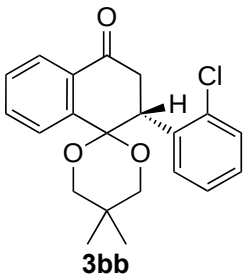

3bb

Compound 3bb (white flakes, 98% yield, 99% ee). The ee was measured by HPLC (Chiralpak IB column, 1.0 mL/min, hexane/2-propanol = 98/2, 280 nm, t_{minor} = 6.1 min (*S*), t_{major} = 6.8 min (*R*)); $[\alpha]^{25}_D$ +25.4 (*c* 0.696, $CHCl_3$) for 99% ee. ^{1}H NMR (400 MHz, $CDCl_3$) δ 0.84 (s, 3H), 1.29 (s, 3H), 2.96 (dd, J = 17.2 Hz, 4.0 Hz, 1H), 3.23 (dd, J = 17.2 Hz, 6.2 Hz, 1H), 3.35 (dd. J = 11.6 Hz, 1.8 Hz, 1H), 3.56 (d, J = 12.1 Hz,

1H), 3.59 (dd, *J* = 11.6 Hz, 1.8 Hz, 1H), 3.84 (d, *J* = 11.6 Hz, 1H), 5.02 (dd, *J* = 6.0 Hz, 4.0 Hz, 1H), 6.79 (dd, *J* = 8.0 Hz, 1.4 Hz, 1H), 6.93 (td, *J* = 7.9 Hz, 1.2 Hz, 1H), 7.10 (td, *J* = 7.5 Hz, 1.6 Hz, 1H), 7.38 (dd, *J* = 8.0 Hz, 1.2 Hz, 1H), 7.54 (td, *J* = 7.6 Hz, 1.2 Hz, 1H), 7.74 (td, *J* = 7.5 Hz, 1.3 Hz, 1H), 8.02 (dd, *J* = 4.0 Hz, 1.1 Hz, 1H), 8.04 (dd, *J* = 4.4 Hz, 1.4 Hz, 1H). ^{13}C NMR ($CDCl_3$) δ 22.9, 23.6, 30.3, 38.1, 41.1, 70.2, 71.7, 96.9, 126.2, 126.5, 126.7, 128.2, 129.3, 129.7, 129.8, 132.2, 134.4, 134.7, 136.2, 143.0, 196.1. HRMS (ESI) calcd for $C_{21}H_{22}ClO_3$ $[M+H]^+$ 357.1257, found 357.1259

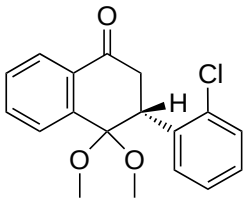

3cb

Compound 3cb (white blueish flakes, 96% yield, 99% ee). The ee was measured by HPLC (Chiralpak IB column, 1.0 mL/min, hexane/2-propanol = 95/5, 280 nm, t_{minor} = 4.6 min (*S*), t_{major} = 4.9 min (*R*)); $[\alpha]^{25}_D$ +106.2 (*c* 1.410, $CHCl_3$) for 99% ee. ^{1}H NMR (400 MHz, $CDCl_3$) δ 2.96 (dd, *J* = 17.9 Hz, 4.2 Hz, 1H), 3.04 (s, 3H), 3.17 (s, 3H), 3.33 (dd, *J* = 17.9 Hz, 6.4 Hz, 1H), 4.47 (dd, *J* = 6.3 Hz, 4.2 Hz, 1H), 6.88 (d, *J* = 7.3 Hz, 1H), 6.93 (td, *J* = 7.2 Hz, 1.0 Hz, 1H), 7.10 (td, *J* = 8.0 Hz, 1.9 Hz, 1H), 7.36 (dd, *J* = 8.0 Hz, 1.1 Hz, 1H), 7.53 (td, *J* = 7.7 Hz, 1.2 Hz, 1H), 7.69 (td, *J* = 7.7 Hz, 1.4 Hz, 1H), 7.88 (dd, *J* = 7.8 Hz, 0.8 Hz, 1H), 8.07 (dd, *J* = 7.7 Hz, 1.3 Hz, 1H). ^{13}C NMR ($CDCl_3$) δ 42.0, 43.4, 48.5, 49.3, 98.7, 126.6, 127.1, 127.3, 128.0, 129.1, 129.3, 129.9, 132.1, 133.2, 134.2, 136.8, 140.5, 196.4. HRMS (ESI) calcd for $C_{18}H_{18}ClO_3$ $[M+H]^+$ 317.0944, found 317.0946.

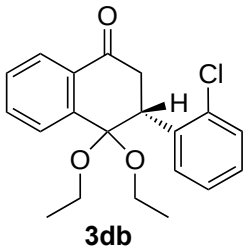

3db

Compound 3db (white blueish flakes, 83% yield, 99% ee). The ee was measured by HPLC (Chiralpak IC column, 1.0 mL/min, hexane/2-propanol = 98/2, 280 nm, t_{minor} = 7.9 min (*S*), t_{major} = 8.4 min (*R*)); $[\alpha]^{25}_{D}$ +15×10 (*c* 0.015, $CHCl_3$) for 99% ee. ^{1}H NMR (400 MHz, $CDCl_3$) δ 1.07 (t, *J* = 7.0 Hz,1 H), 2.98 (dd, *J* = 17.9 Hz, 4.6 Hz, 1H), 3.05 (dq, *J* = 9.0 Hz, 7.0 Hz, 1H), 3.31 (dq, *J* = 8.8 Hz, 7.0 Hz, 1H), 3.34 (dd, *J* = 17.9 Hz, 6.2 Hz, 1H), 3.43 (dq, *J* = 9.0 Hz, 7.1 Hz, 1H), 3.52 (dq, *J* = 8.8 Hz, 7.1 Hz, 1H), 4.45 (dd, *J* = 6.2 Hz, 4.6 Hz, 1H), 6.93 (t, *J* = 7.1 Hz, 1H), 6.97 (d, *J* = 7.2 Hz, 1H), 7.08 (td, *J* = 7.0 Hz, 1.9 Hz, 1H), 7.35 (dd, *J* = 7.8 Hz, 0.9 Hz, 1H), 7.51 (td, *J* = 7.6 Hz, 1.2 Hz, 1H), 7.68 (td, *J* = 7.5 Hz, 1.4 Hz, 1H), 7.92 (dd, *J* = 7.8 Hz, 1H), 8.05 (dd, *J* = 7.8 Hz, 1.2 Hz, 1H). ^{13}C NMR ($CDCl_3$) δ 14.9, 15.1, 42.2, 44.2, 56.3, 57.2, 98.3, 126.5, 127.0, 127.2, 127.9, 128.8, 129.6, 129.8, 132.0, 133.2, 134.2, 137.1, 141.7, 196.7. HRMS (ESI) calcd for $C_{20}H_{22}ClO_3$ $[M+H]^+$ 345.1257, found 345.1263.

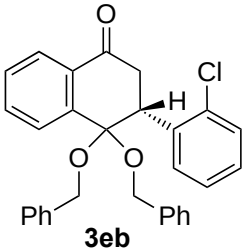

3eb

Compound 3eb (white blueish flakes, 96% yield, 99% ee). The ee was measured by HPLC (Chiralpak IB column, 1.0 mL/min, hexane/2-propanol = 98/2, 280 nm, t_{minor} = 5.9 min (*S*), t_{major} = 6.4 min (*R*)); $[\alpha]^{25}_{D}$ +12×10 (*c* 0.093, $CHCl_3$) for 99% ee. ^{1}H NMR (400 MHz, $CDCl_3$) δ 3.06 (dd, *J* = 18.0 Hz, 3.9 Hz, 1H), 3.49 (dd, *J* = 18.0 Hz, 6.4 Hz, 1H), 4.12 (d, *J* = 11.1 Hz, 1H), 4.35 (d, *J* = 11.0 Hz, 1H), 4.51 (d, *J* = 11. 2Hz, 1H), 4.64 (d, *J* = 11.0 Hz, 1H), 4.68 (dd, *J* = 6.4 Hz, 3.9 Hz, 1H), 6.93 (t, *J* = 8.1 Hz, 1H), 6.99 (d, *J* = 7.6 Hz, 1H), 7.10 (td, 7.2 Hz, 1.8 Hz, 1H), 7.14 (dd, *J* = 7.8, 2.0 Hz, 2H), 7.19 (dd, *J* = 8.0 Hz, 1.6 Hz, 2H), 7.22–7.33 (m, 6H), 7.36 (dd, *J* = 8.0 Hz, 1.1 Hz, 1H), 7.54 (td, *J* = 7.6 Hz, 1.2 Hz, 1H), 7.71 (td, *J* = 7.5 Hz, 1.4 Hz, 1H), 8.06 (dd, *J* = 8.0 Hz, 0.8 Hz, 1H), 8.09 (dd, *J* = 7.8 Hz, 1.2 Hz, 1H). ^{13}C NMR ($CDCl_3$) δ 42.1,

44.3, 63.2, 64.2, 99.1, 126.6, 127.2, 127.46, 127.53, 127.55, 127.59, 128.2, 128.3, 128.4, 129.3, 129.5, 129.9, 132.1, 133.5, 134.3, 136.6, 137.5, 137.7, 140.8, 196.2. HRMS (ESI) calcd for $C_{30}H_{26}ClO_3$ $[M+H]^+$ 469.1570, found 469.1571.

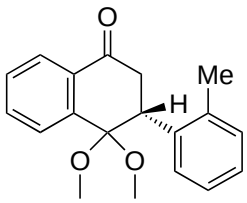

3cc

Compound 3cc (white blueish flakes, 87% yield, 99% ee). The ee was measured by HPLC (Chiralpak IC column, 1.0 mL/min, hexane/2-propanol = 97/3, 254 nm, t_{minor} = 9.3 min (*S*), t_{major} = 12.1 min (*R*)); $[\alpha]^{25}_D$ +66.3 (*c* 0.935, $CHCl_3$) for 99% ee. ^{1}H NMR (400 MHz, $CDCl_3$) δ 2.38 (s, 3H), 2.93 (dd, *J* = 17.7 Hz, 5.2 Hz, 1H), 3.00 (s, 3H), 3.11 (s, 3H), 3.23 (dd, *J* = 17.7 Hz, 6.1 Hz, 1H), 4.11 (t, *J* = 5.7 Hz, 1H), 6.88 (d, *J* = 8.2 Hz, 1H), 6.90 (t, *J* = 7.4 Hz, 1H), 7.06 (td, *J* = 7.2 Hz, 1.8 Hz, 1H), 7.14 (d, *J* = 7.5 Hz, 1H), 7.52 (td, *J* = 7.6 Hz, 1.2 Hz, 1H), 7.68 (td, *J* = 7.5 Hz, 1.4 Hz, 1H), 7.89 (dd, *J* = 7.8 Hz, 0.8 Hz, 1H), 8.06 (dd, *J* = 7.8 Hz, 1.0 Hz, 1H); ^{13}C NMR ($CDCl_3$) δ 19.9, 42.6, 43.6, 48.7, 49.4, 99.0, 125.9, 126.7, 127.1, 127.2, 127.7, 128.9, 130.7, 132.0, 133.1, 135.8, 137.7, 141.3, 196.9. HRMS (ESI) calcd for $C_{19}H_{21}O_3$ $[M+H]^+$ 297.1491, found 297.1485.

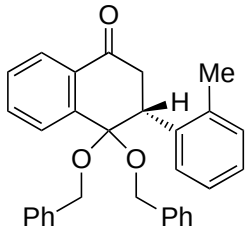

3ec

Compound 3ec (white blueish flakes, 95% yield, 99% ee). The ee was measured by HPLC (Chiralpak IB column, 1.0 mL/min, hexane/2-propanol = 99/1, 230 nm, t_{minor} = 8.2 min (*S*), t_{major} = 8.7 min (*R*)); $[\alpha]^{25}_D$ +50.7 (*c* 0.647, $CHCl_3$) for 99% ee. ^{1}H NMR (400 MHz, $CDCl_3$) δ 2.38 (s, 3H), 3.03 (dd, *J* = 17.8 Hz, 5.1 Hz, 1H), 3.37 (dd, *J* = 17.8 Hz, 6.1 Hz, 1H), 4.13 (d, *J* = 11.3 Hz, 1H), 4.29 (d, *J* = 11.2 Hz, 1H), 4.31 (t, *J* = 5.6 Hz, 1H), 4.37 (d, *J* = 11.3 Hz, 1H), 4.51 (d, *J* = 10.9 Hz, 1H), 6.92 (t, *J* = 7.4 Hz, 1H), 7.02 (d, *J* = 7.6 Hz, 1H), 7.08 (t, *J* = 7.5 Hz, 1H), 7.10–7.15 (m, 3H), 7.18 (d, *J* =

6.6 Hz, 2H), 7.20–7.32 (m, 6H), 7.53 (td, *J* = 7.8 Hz, 1.0 Hz, 1H), 7.69 (td, *J* = 7.6 Hz, 1.2 Hz, 1H), 8.07 (d, *J* = 7.2 Hz, 1H), 8.09 (d, *J* = 7.4 Hz, 1H). ^{13}C NMR ($CDCl_3$) δ 20.0, 42.7, 44.4, 63.5, 64.3, 99.5, 125.9, 126.9, 127.1, 127.4, 127.49, 127.51, 127.52, 127.6, 128.0, 128.28, 128.34, 129.1, 130.8, 132.0, 133.4, 136.0, 137.5, 137.6, 138.1, 141.6, 196.7. HRMS (ESI) calcd for $C_{31}H_{29}O_3$ $[M+H]^+$ 449.2117, found 449.2113.

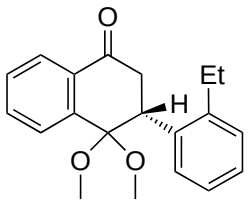

3cd

Compound 3cd (white blueish flakes, > 99% yield, 99% ee). The ee was measured by HPLC (Chiralpak IB column, 1.0 mL/min, hexane/2-propanol = 98/2, 280 nm, t_{minor} = 5.1 min (*S*), t_{major} = 5.5 min (*R*)); $[\alpha]^{25}_D$ +42 (*c* 0.580, $CHCl_3$) for 99% ee. ^{1}H NMR (400 MHz, $CDCl_3$) δ 1.25 (t, *J* = 7.6 Hz, 3H), 2.65–2.80 (m, 2H), 2.97 (s, 3H), 3.00 (dd, *J* = 17.8 Hz, 6.1 Hz, 1H), 3.11 (s, 3H), 3.20 (dd, *J* = 17.8 Hz, 6.0 Hz), 4.13 (t, *J* = 6.0 Hz, 1H), 6.93 (td, *J* = 7.6 Hz, 1.3 Hz, 1H), 7.01 (d, *J* = 7.7 Hz, 1H), 7.12 (td, *J* = 7.2 Hz, 1.3 Hz, 1H), 7.17 (dd, *J* = 7.5 Hz, 1.0 Hz, 1H), 7.52 (td, *J* = 7.6 Hz, 1.2 Hz, 1H), 7.67 (td, *J* = 7.5 Hz, 1.4 Hz, 1H), 7.89 (dd, *J* = 7.8 Hz, 0.7 Hz, 1H), 8.07 (dd, *J* = 7.8 Hz, 1.0 Hz, 1H). ^{13}C NMR ($CDCl_3$) δ 15.4, 25.9, 43.3, 43.6, 49.0, 49.7, 99.0, 125.7, 127.0, 127.1, 127.2, 128.0, 128.9, 129.0, 132.0, 133.1, 137.1, 141.6, 141.9, 197.0. HRMS (ESI) calcd for $C_{20}H_{23}O_3$ $[M+H]^+$ 311.1647, found 311.1643.

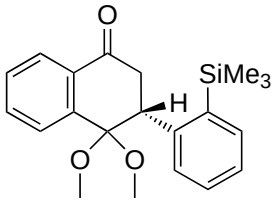

3ce

Compound 3ce (white blueish flakes, 93% yield, 99% ee). The ee was measured by HPLC (Chiralpak IC column, 1.0 mL/min, hexane/2-propanol = 98/2, 280 nm, t_{minor} = 5.9 min (*S*), t_{major} = 6.4 min (*R*)); $[\alpha]^{25}_D$ +14.3 (*c* 0.814, $CHCl_3$) for 99% ee. ^{1}H NMR (400 MHz, $CDCl_3$) δ 0.31 (s, 9H), 2.86 (s, 3H), 3.00 (dd, *J* = 18.0 Hz, 5.6 Hz, 1H), 3.04 (s, 3H), 3.15 (dd, *J* = 18.1 Hz, 8.6 Hz, 1H), 4.02 (dd, *J* = 8.6 Hz, 5.6 Hz, 1H),

7.18–7.23 (m, 2H), 7.37–7.44 (m, 1H), 7.47–7.55 (m, 2H), 7.65 (td, *J* = 7.6 Hz, 1.5 Hz, 1H), 7.88 (dd, *J* = 7.8 Hz, 0.8 Hz, 1H), 8.07 (dd, *J* = 7.7 Hz, 1.2 Hz, 1H). ^{13}C NMR ($CDCl_3$) δ 0.68, 44.9, 49.2, 49.6, 50.3, 99.1, 126.3, 127.1, 127.2, 128.4, 128.7, 129.0, 131.6, 132.9, 135.1, 139.0, 142.3, 145.8, 197.0. HRMS (ESI) calcd for $C_{21}H_{27}SiO_3$ $[M+H]^+$ 355.1729, found 355.1731.

2.4.7. Procedures for stepwise dibenzylation/aromatization of 3aa to 4aa to 5aa

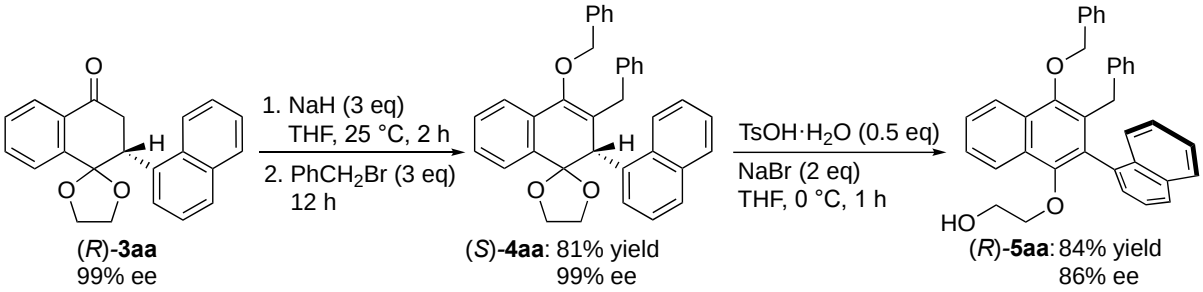

(*R*)-**3aa**
99% ee

(*S*)-**4aa**: 81% yield
99% ee

(*R*)-**5aa**: 84% yield
86% ee

A schlenk tube was charged with (*R*)-**3aa** (33.0 mg, 0.10 mmol) under N_2 atmosphere. Three vacuum/refill cycles were performed before THF (2.0 mL) was added. The solution was stirred for 5 min before NaH (60% in mineral oil, 12 mg, 0.30 mmol) was introduced in one portion. The reaction mixture was stirred at room temperature for 2 h and cooled to 0 °C. Benzyl bromide (51.3 mg, 0.30 mmol) was added and the reaction mixture was allowed to warm to room temperature before being stirred for 12 h. The mixture was cooled to 0 °C and quenched with H_2O (0.2 mL). It was returned to room temperature before being diluted with dichloromethane. Filtration through a short silica gel pad followed by purification on silica gel column chromatography with hexane/ethyl acetate as the eluent afforded (*S*)-**4aa** (41.3 mg, 81% yield).

A schlenk tube was charged with (*S*)-**4aa** (51.0 mg, 0.10 mmol) under N_2 atmosphere. Three vacuum/refill cycles were performed before THF (2.0 mL) was added. The mixture was cooled to 0 °C . To the tube was added NaBr (20.6 mg, 0.20 mmol) and TsOH•H_2O (9.51 mg, 0.05 mmol). The mixture was kept stirring for 1 h. The mixture was quenched with saturated $NaHCO_3$ (0.2 mL) and allowed to return to room temperature before being diluted with dichloromethane. Flitration through a short silica gel pad followed by purification on silica gel column chromatography with hexane/ether or hexane/ethyl acetate as the eluent afforded (*R*)-**5aa**.

2.4.8. Characterization of dialkylated intermediate 4

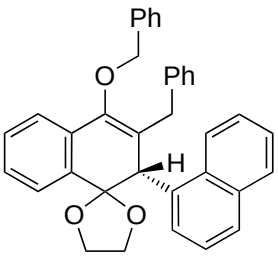

4aa

Compound 4aa (yellowish flakes, 81% yield, 99% ee). The ee was measured by HPLC (Chiralpak IE column, 1.0 mL/min, hexane/2-propanol = 97/3, 280 nm, t_{major} = 5.6 min (*S*), t_{minor} = 6.2 min (*R*)); $[\alpha]^{25}_D$ +158.7 (*c* 1.313, $CHCl_3$) for 99% ee. ^1H NMR (400 MHz, $CDCl_3$) δ 2.89 (d, *J* = 15.6 Hz, 1H), 3.96–4.06 (m, 4H), 4.18 (d, *J* = 15.6 Hz, 1H), 4.56 (s, 1H), 4.86 (d, *J* = 11.2 Hz, 1H), 5.10 (d, *J* = 11.2 Hz, 1H), 7.05 (dd, *J* = 7.3 Hz, 0.8 Hz, 1H), 7.08–7.14 (m, 2H), 7.14–7.25 (m, 4H), 7.27–7.31 (m, 2H), 7.31–7.47 (m, 6H), 7.50 (m, 2H), 7.67 (t, *J* = 7.5 Hz., 2H), 7.77–7.82 (m, 2H). ^{13}C NMR ($CDCl_3$) δ 34.2, 46.1, 63.8, 66.8, 74.0, 109.1, 122.3, 123.5, 124.8, 124.9, 125.2, 125.3, 125.4, 125.9, 127.6, 127.7, 127.8, 127.9, 128.0, 128.2, 128.5, 128.9, 129.07, 129.12, 131.9, 132.0, 133.5, 134.0, 135.3, 137.4, 139.8, 148.5. HRMS (ESI) calcd for $C_{36}H_{31}O_3$ $[M+H]^+$ 511.2273, found 511.2271.

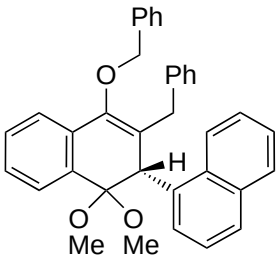

4ca

Compound 4ca (colorless crystalline). ^{1}H NMR (400 MHz, $CDCl_3$) δ 2.88 (d, *J* = 16.0 Hz, 1H), 2.98 (s, 3H), 3.01 (s, 3H), 4.08 (d, *J* = 16.1 Hz, 1H), 4.71 (s, 1H), 4.74 (d, *J* = 11.3 Hz, 1H), 4.93 (d, *J* = 11.2 Hz, 1H), 6.97 (d, *J* = 7.4 Hz, 1H), 7.11 (t, *J* = 7.6 Hz, 1H), 7.19–7.25 (m, 3H), 7.26–7.36 (m, 6H), 7.36–7.43 (m, 4H), 7.47 (td, *J* = 7.5 Hz, 1.2 Hz, 1H), 7.62–7.67 (m, 2H), 7.74 (d, *J* = 7.5 Hz, 1H), 7.75–7.82 (m, 2H).

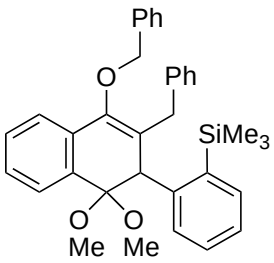

rac-**4ce**

Compound 4ce (colorless crystalline). ^{1}H NMR (400 MHz, $CDCl_3$) δ 0.14 (s, 9H), 3.01 (s, 3H), 3.03 (d, *J* = 16.4 Hz, 1H), 3.25 (s, 3H), 4.09 (d, *J* = 16.4 Hz, 1H), 4.27 (s, 1H), 4.50 (d, *J* = 11.1 Hz, 1H), 4.78 (d, *J* = 11.0 Hz, 1H), 6.76 (d, *J* = 8.0 Hz, 1H), 6.94 (td, *J* = 8.1 Hz, 1.4 Hz, 1H), 7.12 (td, *J* = 7.3 Hz,1.1 Hz, 1H), 7.18 (d, *J* = 6.8 Hz, 1H), 7.26–7.44 (m, 12H), 7.56 (d, *J* = 7.8 Hz, 1H), 7.73 (d, *J* = 7.8 Hz, 1H). ^{13}C NMR ($CDCl_3$) δ 1.8, 33.3, 49.4, 49.5, 51.8, 73.5, 101.2, 122.0, 125.7, 126.3, 126.8, 127.5, 127.70, 127.74, 127.8, 128.32, 128.33, 128.6, 128.66, 128.70, 128.8, 131.6, 134.1, 135.2, 137.5, 140.1, 140.4, 143.0, 147.5. HRMS (ESI) calcd for $C_{35}H_{39}O_3Si$ $[M+H]^+$ 535.2668, found 535.2664.

2.4.9. Procedures for one–pot dibenzylation/aromatization of 3 to 5

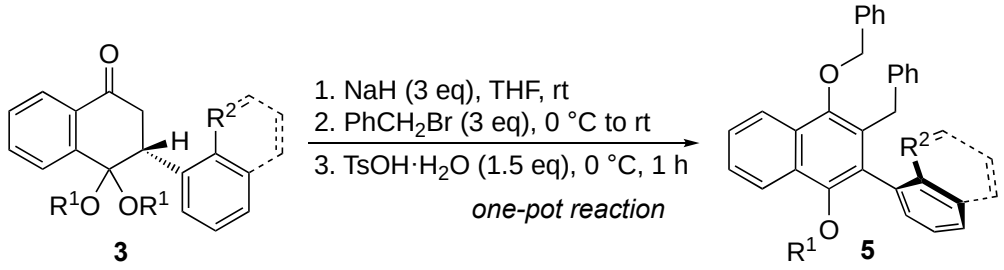

A schlenk tube was charged with **3** (0.10 mmol) under N_2 atmosphere. Three vacuum/refill cycles were performed before THF (2.0 mL) was added. The solution was stirred for 5 min before NaH (60% in mineral oil, 12 mg, 0.30 mmol) was introduced in one portion. The reaction mixture was stirred at room temperature for 2 h and cooled to 0 °C. Benzyl bromide (51.3 mg, 0.30 mmol) was added and the reaction mixture was allowed to warm to room temperature before being stirred for 12 h. The mixture was cooled to 0 °C and TsOH•H_2O (28.5 mg, 0.15 mmol) was added and stirred for 1 h. The mixture was quenched with saturated $NaHCO_3$ (0.2 mL) and allowed to return to room temperature before being diluted with dichloromethane. Filtration through a short silica gel pad followed by purification on silica gel column chromatography with hexane/ether or hexane/ethyl acetate as the eluent afforded **5**.

2.4.10. Characterization of *O,C*-dialkylated product 5

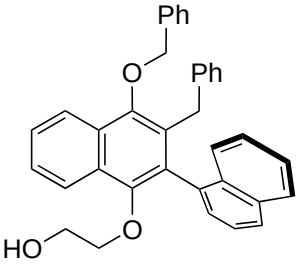

5aa

Compound 5aa (colorless oil, 68% yield, 89% ee). The ee was measured by HPLC (Chiralpak IE column, 1.0 mL/min, hexane/2-propanol = 93/7, 280 nm, t_{major} = 9.9 min (*R*), t_{minor} = 12.0 min (*S*)); $[\alpha]^{25}_{D}$ –33.5 (*c* 0.710, $CHCl_3$) for 89% ee. ^1H NMR (400 MHz, $CDCl_3$) δ 1.12 (brs, 1H), 3.35 (brs, 2H), 3.61 (d, *J* = 14.8 Hz, 1H), 3.68 (dt, *J* = 9.8 Hz, 4.6 Hz, 1H), 3.75 (dt, *J* = 6.2 Hz, 4.4 Hz, 1H), 4.14 (d, *J* = 14.8 Hz, 1H), 5.08 (d, *J* = 11.3 Hz, 1H), 5.11 (d, *J* = 11.3 Hz, 1H), 6.62 (m, 2H), 6.93 (m, 3H), 7.15 (dd, *J* = 7.0 Hz, 1.1 Hz, 1H), 7.29 (dd, *J* = 6.4 Hz, 1.2 Hz, 1H), 7.32 (d, *J* = 7.7 Hz, 1H), 7.34–7.48 (m, 3H), 7.41 (d, *J* = 7.2 Hz, 2H), 7.48–7.54 (m, 2H), 7.54–7.66 (m, 2H), 7.87 (d, *J* = 3.9 Hz, 1H), 7.89 (d, *J* = 3.9 Hz, 1H). 8.21 (d, *J* = 7.2 Hz, 1.3 Hz, 1H), 8.29 (d, *J* = 7.3 Hz, 1.2 Hz, 1H). δ ^{13}C NMR ($CDCl_3$) δ 33.6, 61.8, 75.4, 76.4, 122.8, 122.9, 125.0, 125.3, 125.5, 125.7, 126.1, 126.2, 126.6, 127.66, 127.74, 128.0, 128.1, 128.2, 128.3, 128.38, 128.42, 128.5, 128.8, 130.6, 131.0, 132.3, 133.4, 134.1, 137.3, 140.7, 149.1, 149.4. HRMS (ESI) calcd for $C_{36}H_{31}O_3$ $[M+H]^+$ 511.2273, found 511.2281.

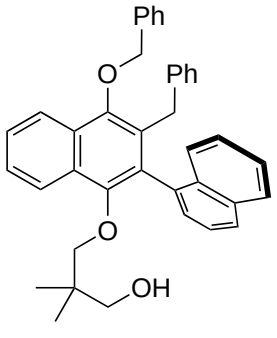

5ba

Compound 5ba (colorless oil, 84% yield, 92% ee). The ee was measured by HPLC (Chiralpak IB column, 1.0 mL/min, hexane/2-propanol = 97/3, 230 nm, t_{minor} = 12.0 min (*S*), t_{major} = 14.8 min (*R*); $[\alpha]^{25}_{D}$ –27.8 (*c* 1.088, $CHCl_3$) for 92% ee. ^1H NMR (AV400, $CDCl_3$) δ 0.57 (s, 3H), 0.60 (s, 3H), 0.90 (bs, 1H), 2.79 (dd, *J* = 10.7 Hz, 3.3 Hz. 1H), 2.85 (dd, *J* = 10.8 Hz, 3.3 Hz, 1H), 3.36 (d, *J* = 8.5 Hz, 1H), 3.45 (d, *J* = 8.4 Hz, 1H), 3.61 (d, *J* = 14.8 Hz, 1H), 4.11 (d, *J* = 14.8 Hz,

1H), 5.08 (d, *J* = 11.3 Hz, 1H), 5.10 (d, *J* = 11.4 Hz, 1H), 6.59–6.66 (m, 2H), 6.88–6.94 (m, 3H), 7.14 (d, *J* = 7.0 Hz, 1H), 7.27 (t, *J* = 7.4 Hz, 1H), 7.31 (d, *J* = 7.4 Hz, 1H), 7.33–7.47 (m, 5H), 7.50 (d, *J* = 6.9 Hz, 2H), 7.55 – 7.64 (m, 2H), 7.88 (d, *J* = 8.2 Hz, 2H), 8.17 (dd, *J* = 7.0 Hz, 1.7 Hz, 1H), 8.28 (dd, *J* = 7.1 Hz, 1.7 Hz, 1H). ^{13}C NMR ($CDCl_3$) δ 21.1, 21.2, 33.6, 36.3, 69.8, 76.4, 81.2, 122.7, 122.8, 124.9, 125.3, 125.6, 125.8, 126.1, 126.2, 126.5, 127.65, 127.74, 128.0, 128.06, 128.13, 128.27, 128.29, 128.34, 128.5, 128.9, 130.6, 131.3, 132.3, 133.3, 134.2, 137.3, 140.7, 148.9, 149.4. HRMS (ESI) calcd for $C_{39}H_{37}O_3$ $[M+H]^+$ 553.2743, found 553.2749.

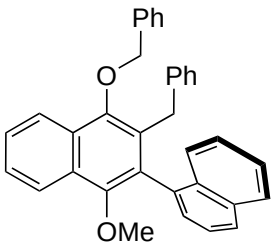

5ca

Compound 5ca (colorless oil, 96% yield, 98% ee). The ee was measured by HPLC (Chiralpak IE column, 1.0 mL/min, hexane/2-propanol = 98/2, 280 nm, t_{major} = 7.1 min (*R*), t_{minor} = 9.2 min (*S*)); $[\alpha]^{25}_D$ –20.7 (*c* 0.188, $CHCl_3$) for 98% ee. ^{1}H NMR (400 MHz, $CDCl_3$) δ 3.42 (s, 3H), 3.51 (d, *J* = 14.8 Hz, 1H), 4.09 (d, *J* = 14.8 Hz, 1H), 5.05 (d, *J* = 11.3 Hz, 1H), 5.09 (d, *J* = 11.3 Hz, 1H), 6.57–6.64 (m, 2H), 6.88–6.96 (m, 3H), 7.11 (d, *J* = 6.8 Hz, 1H), 7.23–7.28 (m, 1H), 7.31 (d, *J* = 7.7 Hz, 1H), 7.32–7.46 (m, 5H), 7.49 (d, *J* = 6.9 Hz, 2H), 7.53–7.64 (m, 2H), 7.86 (t, *J* = 8.8 Hz, 2H), 8.18 (dd, *J* = 7.3 Hz, 1.6 Hz, 1H), 8.26 (dd, *J* = 7.3 Hz, 1.8 Hz, 1H). ^{13}C NMR ($CDCl_3$) δ 33.6, 61.9, 76.4, 122.7, 123.1, 125.0, 125.3, 125.5, 125.6, 126.0, 126.4, 127.6, 127.7, 128.0, 128.1, 128.26, 128.32, 128.34, 128.5, 128.8, 130.6, 130.9, 132.5, 133.4, 134.3, 137.4, 140.9, 149.1, 150.8. HRMS (ESI) calcd for $C_{35}H_{29}O_2$ $[M+H]^+$ 481.2168, found 481.2164.

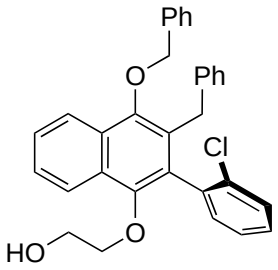

5ab

Compound 5ab (colorless oil, 14% yield, 40% ee). The ee was measured by HPLC (Chiralpak IE column, 1.0 mL/min, hexane/2-propanol = 98/2, 280 nm, t_{major} = 19.9 min (*R*), t_{minor} = 22.1 min (*S*)); $[\alpha]^{25}_{D}$ –9.95 (*c* 0.714, $CHCl_3$) for 40% ee. ^{1}H NMR (400 MHz, $CDCl_3$) δ 1.62 (bs, 1H), 3.55 (ddd, *J* = 8.6 Hz, 5.8 Hz, 2.8 Hz, 1H), 3.64 (ddd, *J* = 9.0 Hz, 6.3 Hz, 2.7 Hz, 1H), 3.71 (d, *J* = 15.1 Hz, 1H), 3.80 (ddd, *J* = 9.2 Hz, 6.3 Hz, 2.8 Hz, 1H), 3.93 (ddd, *J* = 8.7 Hz, 5.8 Hz, 2.8 Hz, 1H), 4.33 (d, *J* = 15.1 Hz, 1H), 5.07 (s, 2H), 6.72–6.78 (m, 2H), 6.93 (dd, *J* = 7.6 Hz, 1.6 Hz, 1H), 7.00–7.05 (m, 3H), 7.12 (td, *J* = 7.6 Hz, 1.2, 1H), 7.30 (td, *J* = 7.5 Hz, 1.6 Hz, 1H), 7.34–7.44 (m, 3H), 7.48 (dd, *J* = 8.1 Hz, 1.0 Hz, 1H), 7.51 (d, *J* = 6.7 Hz, 1H), 7.53–7.63 (m, 2H), 8.19 (dd, *J* = 6.9 Hz, 1.6 Hz, 1H), 8.24 (dd, *J* = 7.0 Hz, 1.5 Hz, 1H). ^{13}C NMR ($CDCl_3$) δ 33.4, 62.0, 75.2, 76.5, 122.8, 125.5, 126.1, 126.2, 126.7, 127.7, 127.8, 128.1, 128.2, 128.4, 128.6, 128.9, 129.1, 129.4, 129.8, 130.4, 132.7, 134.0, 135.6, 137.3, 140.5, 148.6, 149.4. HRMS (ESI) calcd for $C_{32}H_{28}ClO_3$ $[M+H]^+$ 495.1727, found 495.1733.

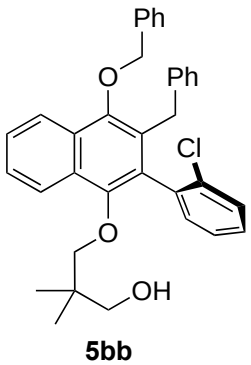

5bb

Compound 5bb (colorless oil, 35% yield, 87% ee). The ee was measured by HPLC (Chiralpak IB column, 1.0 mL/min, hexane/2-propanol = 99/1, 230 nm, t_{major} = 20.9 min (*R*), t_{minor} = 22.6 min (*S*)); $[\alpha]^{25}_{D}$ –40.9 (*c* 0.602, $CHCl_3$) for 87% ee. ^{1}H NMR (400 MHz, $CDCl_3$) δ 0.76 (s, 3H), 0.82 (s, 3H), 1.49 (bs, 1H), 3.20 (d, *J* = 14.0 Hz, 1H), 3.21 (d, *J* = 14.0 Hz, 1H), 3.51 (d, *J* = 8.6 Hz, 1H), 3.54 (d, *J* = 8.6 Hz, 1H), 3.69 (d, *J* = 15.1 Hz, 1H), 4.27 (d, *J* = 15.0 Hz, 1H), 5.05 (d, *J* = 11.6 Hz, 1H), 5.06 (d, *J* = 11.6 Hz, 1H), 6.67–6.77 (m, 2H), 6.93 (dd, *J* = 7.6 Hz, 1.4 Hz, 1H), 6.98–7.05 (m, 3H), 7.12 (td, *J* = 7.5 Hz, 0.9 Hz, 1H),

7.29 (td, J = 7.8 Hz, 1.5 Hz, 1H), 7.33–7.44 (m, 3H), 7.44–7.52 (m, 3H), 7.52–7.60 (m, 2H), 8.14 (dd, J = 6.2 Hz, 2.0 Hz, 1H), 8.22 (dd, J = 6.4 Hz, 2.0 Hz, 1H). δ ^{13}C NMR ($CDCl_3$) δ 21.3, 21.4, 33.3, 36.5, 70.2, 76.5, 81.0, 122.7, 122.8, 125.5, 126.1, 126.2, 126.6, 127.7, 127.8, 128.1, 128.2, 128.4, 128.6, 129.0, 129.3, 129.7, 130.6, 132.8, 134.3, 135.8, 137.3, 140.5, 148.4, 149.4. HRMS (ESI) calcd for $C_{35}H_{34}ClO_3$ $[M+H]^+$ 537.2196, found 537.2191.

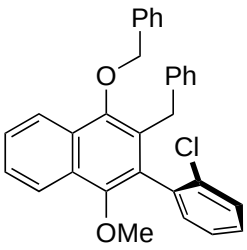

5cb

Compound 5cb (colorless oil, 81% yield, 80% ee). The ee was measured by HPLC (Chiralpak IE column, 1.0 mL/min, hexane/2-propanol = 98/2, 280 nm, t_{major} = 6.1 min (*R*), t_{minor} = 7.7 min (*S*)); $[\alpha]^{25}_D$ –86.0 (*c* 0.547, $CHCl_3$) for 80% ee. ^{1}H NMR (400 MHz, $CDCl_3$) δ 3.61 (s, 3H), 3.69 (d, J = 15.0 Hz, 1H), 4.32 (d, J = 15.0 Hz, 1H), 5.07 (s, 2H), 6.75–6.81 (m, 2H), 6.92 (dd, J = 7.6 Hz, 1.6 Hz, 1H), 7.02–7.07 (m, 3H), 7.12 (td, J = 7.6 Hz, 1.2 Hz, 1H), 7.29 (td, J = 7.6 Hz, 1.6 Hz, 1H), 7.34–7.45 (m, 3H), 7.48 (dd, J = 8.0 Hz, 1.0 Hz, 1Hz), 7.52 (d, J = 6.8 Hz, 2H), 7.54–7.62 (m, 2H), 8.19 (dd, J = 6.4 Hz, 2.0 Hz, 1H), 8.24 (dd, J = 6.6 Hz, 2.0 Hz, 1H). ^{13}C NMR ($CDCl_3$) δ 33.3, 61.5, 76.5, 122.7, 123.0, 125.5, 125.9, 126.2, 126.6, 127.7, 127.8, 128.0, 128.1, 128.4, 128.5, 128.8, 128.9, 129.1, 129.8, 130.2, 132.6, 134.0, 135.8, 137.4, 140.6, 149.2, 150.2. HRMS (ESI) calcd for $C_{31}H_{26}ClO_2$ $[M+H]^+$ 465.1621, found 465.1618.

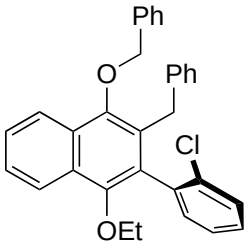

5db

Compound 5db (colorless oil, 84% yield, 88% ee). The ee was measured by HPLC (Chiralpak IE column, 1.0 mL/min, hexane/2-propanol = 98/2, 280 nm, t_{major} = 5.0 min (*R*), t_{minor} = 6.0 min (*S*)); $[\alpha]^{25}_{D}$ –67.7 (*c* 2.109, $CHCl_3$) for 88% ee. ^{1}H NMR (400 MHz, $CDCl_3$) δ 1.09 (t, *J* = 7.0 Hz, 1H), 3.70 (d, *J* = 14.6 Hz, 1H), 3.72 (dq, *J* = 9.1 Hz, 6.8 Hz, 1H), 3.79 (dq, *J* = 9.2 Hz, 6.7 Hz, 1H), 4.33 (d, *J* = 15.1 Hz, 1H), 5.07 (s, 2H), 6.74–6.81 (m, 2H), 6.94 (dd, *J* = 7.6 Hz, 1.6 Hz, 1H), 7.02–7.06 (m, 3H), 7.11 (td, *J* = 7.6 Hz, 1.0 Hz, 1H), 7.27 (td, *J* = 7.6 Hz, 1.6 Hz, 1H), 7.34–7.45 (m, 3H), 7.46 (dd, *J* = 8.0 Hz, 0.9 Hz, 1H), 7.51 (d, *J* = 7.6 Hz, 2H), 7.53–7.62 (m, 2H), 8.20 (dd, *J* = 7.0 Hz, 1.7 Hz, 1H), 8.23 (dd, *J* = 7.2 Hz, 1.7 Hz, 1H). ^{13}C NMR ($CDCl_3$) δ 15.6, 33.4, 69.9, 76.4, 122.6, 123.2, 125.4, 125.8, 126.1, 126.5, 127.7, 127.8, 128.0, 128.4, 128.5, 128.7, 128.8, 129.0, 129.8, 130.2, 132.8, 134.0, 136.0, 137.4, 140.7, 149.0, 149.7. HRMS (ESI) calcd for $C_{32}H_{28}ClO_2$ $[M+H]^+$ 479.1778, found 479.1776.

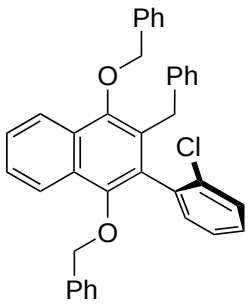

5eb

Compound 5eb (colorless oil, 85% yield, 92% ee). The ee was measured by HPLC (Chiralpak IE column, 1.0 mL/min, hexane/2-propanol = 98/2, 280 nm, t_{major} = 6.0 min (*R*), t_{minor} = 8.6 min (*S*)); $[\alpha]^{25}_{D}$ –53.2 (*c* 1.130, $CHCl_3$) for 92% ee. ^{1}H NMR (400 MHz, $CDCl_3$) δ 3.72 (d, *J* = 151. Hz, 1H), 4.35 (d, *J* = 15.1 Hz, 1H), 4.65 (d, *J* = 10.6 Hz, 1H), 4.72 (d, *J* = 10.7 Hz, 1H), 5.07 (s, 2H), 6.72–6.81 (m, 2H), 6.92–7.06 (m, 6H), 7.10 (td, *J* = 7.6 Hz, 1.1 Hz, 1H), 7.21–7.26 (m, 3H), 7.29 (td, *J* = 7.8 Hz, 1.6 Hz, 1H), 7.33–7.45 (m, 3H), 7.47 (dd, *J* = 8.0 Hz, 0.9 Hz, 1H), 7.51 (d, *J* = 7.0 Hz, 2H), 7.54 (dd, *J* = 8.3 Hz, 1.4 Hz, 1H), 7.55–7.61 (m, 1H), 8.19 (d, *J* = 8.0 Hz, 1H), 8.23 (d, *J* = 7.8 Hz, 1H). ^{13}C NMR ($CDCl_3$) δ 33.4, 75.9, 76.5, 122.7,

123.1, 125.5, 126.0, 126.3, 126.6, 127.7, 127.8, 127.9, 127.9, 128.0, 128.3, 128.4, 128.5, 128.6, 128.8, 128.9, 129.2, 129.9, 130.7, 133.1, 134.1, 135.9, 137.1, 137.4, 140.6, 149.2, 149.3. HRMS (ESI) calcd for $C_{37}H_{30}ClO_2$ $[M+H]^+$ 541.1934, found 541.1940.

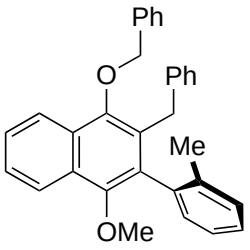

5cc

Compound 5cc (colorless oil, 83% yield, 92% ee). The ee was measured by HPLC (Chiralpak IE column, 1.0 mL/min, hexane/2-propanol = 97/3, 230 nm, t_{major} = 4.5 min (*R*), t_{minor} = 4.9 min (*S*)); $[\alpha]^{25}_D$ +53.5 (*c* 1.689, $CHCl_3$) for 92% ee. ^{1}H NMR (400 MHz, $CDCl_3$) δ 1.74 (s, 3H), 3.54 (s, 3H), 3.93 (d, *J* = 14.5 Hz, 1H), 3.97 (d, *J* = 14.5 Hz, 1H), 5.05 (d, *J* = 11.4 Hz, 1H), 5.12 (d, *J* = 11.4 Hz, 1H), 6.72–6.81 (m, 2H), 7.00–7.08 (m, 4H), 7.17 (t, *J* = 7.8 Hz, 1H), 7.18 (d, *J* = 7.8 Hz, 1H), 7.28 (t, *J* = 8.0 Hz, 1H), 7.35–7.45 (m, 3H), 7.52 (d, *J* = 6.8 Hz, 2H), 7.55–7.61 (m, 2H), 8.17 (dd, *J* = 6.1 Hz, 2.0 Hz, 1H), 8.24 (dd, *J* = 6.1 Hz, 2.0 Hz, 1H). ^{13}C NMR ($CDCl_3$) δ 19.6, 33.3, 61.3, 76.4, 122.6, 122.9, 125.0, 125.5, 125.8, 126.2, 127.4, 127.70, 127.72, 128.0, 128.2, 128.51, 128.54, 128.7, 129.7, 130.0, 130.3, 132.1, 136.2, 137.4, 137.5, 140.5, 149.0, 149.8. HRMS (ESI) calcd for $C_{32}H_{29}O_2$ $[M+H]^+$ 445.2168, found 445.2162.

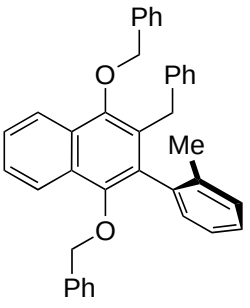

5ec

Compound 5ec (colorless oil, 91% yield, 96% ee). The ee was measured by HPLC (Chiralpak IE column, 1.0 mL/min, hexane/dichloromethane = 85/15, 280 nm, t_{major} = 8.3 min (*R*), t_{minor} = 12.8 min (*S*); $[\alpha]^{25}_D$ +54 (*c* 0.050, $CHCl_3$) for 96% ee. ^{1}H NMR (400 MHz, $CDCl_3$) δ 1.74 (s, 3H), 3.99 (d, *J* =15.1 Hz, 1H), 3.99 (d, *J* = 15.1 Hz, 1H), 4.56 (d, *J* = 10.2 Hz, 1H), 4.65 (d, *J* = 10.3 Hz, 1H),

5.06 (d, *J* = 11.4 Hz, 1H), 5.13 (d, *J* = 11.4 Hz, 1H), 6.71–6.80 (m, 2H), 6.90–6.99 (m, 2H), 6.99–7.07 (m, 3H), 7.11 (d, *J* = 7.7 Hz, 1H), 7.18 (t, *J* = 7.6 Hz, 1H), 7.19 (d, *J* = 7.7 Hz, 1H), 7.22–7.26 (m, 3H), 7.26–7.31 (m, 1H), 7.33–7.46 (m, 3H), 7.49–7.61 (m, 4H), 8.19 (d, *J* = 8.2 Hz, 1H), 8.24 (d, *J* = 8.2 Hz, 1H). ^{13}C NMR ($CDCl_3$) δ 19.6, 33.4, 75.8, 76.4, 122.6, 123.0, 125.2, 125.5, 125.9, 126.3, 127.6, 127.71, 127.74, 127.8, 128.0, 128.1, 128.2, 128.4, 128.5, 128.6, 128.7, 129.8, 130.1, 130.4, 132.6, 136.3, 137.3, 137.5, 137.9, 140.5, 148.8, 149.2. HRMS (ESI) calcd for $C_{38}H_{33}O_2$ $[M+H]^+$ 521.2481, found 521.2474.

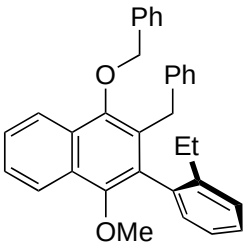

5cd

Compound 5cd (colorless oil, 94% yield, 92% ee). The ee was measured by HPLC (Chiralpak IE column, 1.0 mL/min, hexane/2-propanol = 97/3, 280 nm, t_{major} = 4.0 min (*R*), t_{minor} = 4.3 min (*S*)); $[\alpha]^{25}_D$ +83.0 (*c* 0.200, $CHCl_3$) for 92% ee. ^{1}H NMR (400 MHz, $CDCl_3$) δ 0.99 (t, *J* = 7.6 Hz, 3H), 1.99 (dq, *J* = 15.2 Hz, 7.6 Hz), 2.27 (dq, *J* = 15.1 Hz, 7.5 Hz, 1H), 3.58 (s, 3H), 3.86 (d, *J* = 14.6 Hz, 1H), 4.05 (d, *J* = 14.6 Hz, 1H), 5.07 (d, *J* = 11.4 Hz, 1H), 5.13 (d, *J* = 11.4 Hz, 1H), 6.77–6.87 (m, 2H), 7.03 (d, *J* = 7.4 Hz, 1H), 7.05–7.12 (m, 3H), 7.17 (t, *J* = 7.4 Hz, 1H), 7.31 (d, *J* = 7.1 Hz, 1H), 7.31 (d, *J* = 7.8 Hz, 1H), 7.38–7.47 (m, 3H), 7.53 (d, *J* = 7.0 Hz, 2H), 7.55–7.63 (m, 2H), 8.21 (dd, *J* = 5.9 Hz, 2.2 Hz, 1H), 8.27 (d, *J* = 6.0 Hz, 2.2, 1H). ^{13}C NMR ($CDCl_3$) δ 13.7, 25.5, 33.6, 61.5, 76.3, 122.6, 123.0, 124.9, 125.4, 125.8, 126.2, 127.4, 127.6, 127.7, 127.8, 128.0, 128.2, 128.48, 128.51, 128.7, 130.0, 130.4, 132.1, 135.7, 137.4, 140.6, 142.8, 149.0, 150.0. HRMS (ESI) calcd for $C_{33}H_{31}O_2$ $[M+H]^+$ 459.2324, found 459.2320.

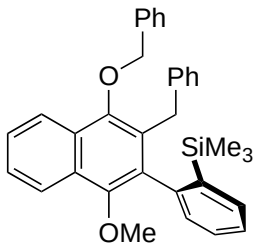

5ce

Compound 5ce (colorless crystalline, 68% yield, 99% ee). The ee was measured by HPLC (Chiralpak IE column, 1.0 mL/min, hexane/dichloromethane = 92/8, 280 nm, t_{major} = 6.6 min (*R*), t_{minor} = 9.6 min (*S*)); $[\alpha]^{25}_D$ –6.0 (*c* 0.797, $CHCl_3$) for 99% ee. ^{1}H NMR (400 MHz, $CDCl_3$) δ –0.10 (s, 9H), 3.56 (s, 3H), 3.64 (d, *J* = 14.6 Hz, 1H), 4.28 (d, *J* = 14.6 Hz, 1H), 5.01 (d, *J* = 11.3 Hz, 1H), 5.07 (d, *J* = 11.3 Hz, 1H), 6.84–6.93 (m, 3H), 7.06–7.14 (m, 3H), 7.21 (td, *J* = 7.6 Hz, 1.4 Hz, 1H), 7.32–7.45 (m, 4H), 7.52 (d, *J* = 7.1 Hz, 2H), 7.54–7.60 (m, 2H), 7.67 (dd, *J* = 7.5 Hz, 1.1 Hz, 1H), 8.15–8.20 (m, 1H), 8.20–8.25 (m, 1H). ^{13}C NMR ($CDCl_3$) δ –0.2, 34.0, 61.3, 76.0, 122.6, 123.1, 125.5, 125.9, 126.2, 126.4, 127.6, 127.75, 127.84, 128.0, 128.2, 128.5, 128.6, 128.9, 130.2, 130.7, 134.3, 134.6, 137.5, 139.9, 140.8, 142.0, 149.0, 150.3. HRMS (ESI) calcd for $C_{34}H_{35}SiO_2$ $[M+H]^+$ 503.2406, found 503.2405.

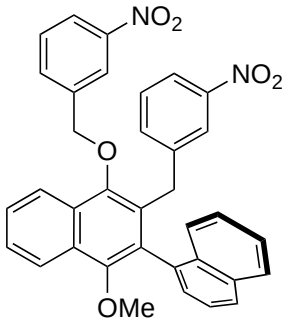

5cf

Compound 5cf (colorless crystalline, 87% yield, 98% ee). The ee was measured by HPLC (Chiralpak IE column, 1.0 mL/min, hexane/2-propanol = 92/8, 280 nm, t_{major} = 45.5 min (*R*), t_{minor} = 49.8 min (*S*)); $[\alpha]^{25}_D$ +20.4 (*c* 0.500, $CHCl_3$) for 98% ee. ^{1}H NMR (400 MHz, $CDCl_3$) δ 3.46 (s, 3H), 3.82 (d, *J* = 15.2 Hz, 1H), 3.98 (d, *J* = 14.9 Hz, 1H), 5.21 (d, *J* = 12.3 Hz, 1H), 5.26 (d, *J* = 12.3 Hz, 1H), 6.94 (d, *J* = 7.8 Hz, 1H), 7.02 (t, *J* = 7.8 Hz, 1H), 7.14–7.21 (m, 4H), 7.38 (ddd, *J* = 8.1 Hz, 5.3 Hz, 2.8 Hz, 1H), 7.43 (dd, *J* = 8.2 Hz, 7.0 Hz, 1H), 7.60 (d, *J* = 8.0 Hz, 1H), 7.61–7.67 (m, 2H), 7.70 (m, 1H), 7.84 (d, *J* = 8.5 Hz, 1H), 7.85–7.89 (m, 2H), 8.15–8.25 (m, 3H), 8.36 (brs, 1H). ^{13}C NMR ($CDCl_3$) δ 33.2, 62.0, 74.9, 120.6, 122.0, 122.2, 123.06, 123.13, 123.3, 125.0, 125.2, 125.8, 126.1, 126.6, 127.1, 127.9, 128.2, 128.3, 128.41, 128.44, 128.6, 129.1, 129.7, 130.3, 132.2, 133.1, 133.4, 133.9,

134.4, 139.2, 142.2, 147.5, 148.4, 148.6, 151.4. HRMS (ESI) calcd for $C_{35}H_{27}N_2O_6$ $[M+H]^+$ 571.1869, found 571.1862.

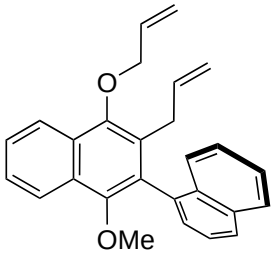

6a

Compound 6a (colorless oil, 84% yield, 98% ee). The ee was measured by HPLC (Chiralpak IE column, 1.0 mL/min, hexane/2-propanol = 97/3, 280 nm, t_{major} = 5.6 min (*R*), t_{minor} = 6.7 min (*S*); $[\alpha]^{25}_D$ –111 (*c* 0.737, $CHCl_3$) for 98% ee. ^{1}H NMR (400 MHz, $CDCl_3$) δ 2.96 (dd, *J* = 14.9 Hz, 6.2 Hz, 1H), 3.42 (s, 3H), 3.48 (dd, *J* = 15.0 Hz, 6.2 Hz, 1H), 4.52–4.60 (m, 2H), 4.63 (dd, *J* = 12.6 Hz, 5.3 Hz, 1H), 4.71 (dd, *J* = 10.1 Hz, 1.5 Hz, 1H), 5.34 (dd, *J* = 10.5 Hz, 1.3 Hz, 1H), 5.56 (dd, *J* = 17.2 Hz, 1.6 Hz, 1H), 5.62 (ddt, *J* = 17.1 Hz, 10.2 Hz, 6.2 Hz, 1H), 6.23 (ddt, *J* = 17.2 Hz, 10.6 Hz, 5.3 Hz, 1H), 7.34 (t, *J* = 7.2 Hz, 1H), 7.41 (d, *J* = 8.3 Hz. 1H), 7.45 (d, *J* = 6.9 Hz, 1H), 7.47 (t, *J* = 7.4 Hz, 1H), 7.50–7.62 (m, 3H), 7.92 (d, *J* = 8.2 Hz, 2H), 8.15 (dd, *J* = 8.5 Hz, 1.3 Hz, 1H), 8.18 (dd, *J* = 8.6 Hz, 1.3 Hz, 1H). ^{13}C NMR ($CDCl_3$) δ 32.3, 61.9, 75.3, 115.0, 117.1, 122.5, 122.9, 125.1, 125.7, 125.8, 125.9, 126.1, 126.3, 127.90, 127.94, 128.2, 128.3, 129.0, 129.2, 130.7, 132.6, 133.5, 134.0, 134.5, 137.0, 149.4, 150.5. HRMS (ESI) calcd for $C_{27}H_{25}O_2$ $[M+H]^+$ 381.1855, found 381.1860.

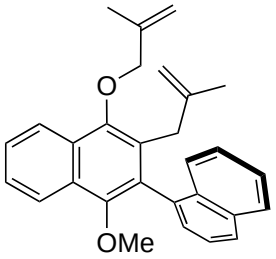

6b

Compound 6b (colorless oil, 81% yield, 98% ee). The ee was measured by HPLC (Chiralpak IE column, 1.0 mL/min, hexane/dichloromethane = 95/5, 230 nm, t_{major} = 24.3 min (*R*), t_{minor} = 33.7 min (*S*); $[\alpha]^{25}_{D}$ –111 (*c* 0.737, $CHCl_3$) for 98% ee. ^{1}H NMR (400 MHz, $CDCl_3$) δ 1.40 (s, 3H), 1.94 (s, 3H), 2.77 (d, *J* = 15.9 Hz, 1H), 3.42 (s, 3H), 3.48 (d, *J* = 16.0 Hz, 1H), 4.12 (s, 1H), 4.41 (d, *J* = 12.2 Hz, 1H), 4.51 (s, 1H), 4.52 (d, *J* = 11.8 Hz, 1H), 5.05 (s, 1H), 5.30 (s, 1H), 7.32 (ddd, *J* = 8.0 Hz, 6.6 Hz, 1.1 Hz, 1H), 7.40 (d, *J* = 8.2 Hz, 1H), 7.44 (dd, *J* = 6.9 Hz, 1.2 Hz, 1H), 7.46 (ddd, *J* = 8.0 Hz, 6.8 Hz, 1.2 Hz, 1H), 7.50–7.62 (m, 3H), 7.90 (d, *J* = 8.0 Hz, 2H), 8.17 (dd, *J* = 6.4 Hz, 1.6 Hz, 1H), 8.19 (dd, *J* = 7.2 Hz, 1.6 Hz, 1H). ^{13}C NMR ($CDCl_3$) δ 19.7, 23.1, 35.5, 61.9, 78.0, 110.9, 112.0, 122.6, 122.9, 125.0, 125.6, 125.75, 125.81, 126.0, 126.3, 127.7, 128.0, 128.2, 128.3, 128.9, 129.3, 130.9, 132.6, 133.4, 134.4, 141.7, 145.0, 149.6, 150.5. HRMS (ESI) calcd for $C_{29}H_{29}O_2$ $[M+H]^+$ 409.2168, found 409.2164.

2.4.11. Characterization of *C*-benzylated product 7 & *O*-alkylated/aromatized product 8a–8c

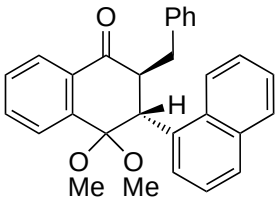

7

Compound 7 (colorless oil, 55% yield, 99% ee). The ee was measured by HPLC (Chiralpak IE column, 1.0 mL/min, hexane/2-propanol = 97/3, 280 nm, t_{major} = 8.6 min (*R*, *S*), t_{minor} = 9.7 min (*S*, *R*); $[\alpha]^{25}_{D}$ +35.7 (*c* 0.515, $CHCl_3$) for 99% ee. ^1H NMR (400 MHz, $CDCl_3$) δ 2.98 (s, 3H), 2.99 (s, 3H), 3.08 (dd, *J* = 13.0 Hz, 4.8 Hz, 1H), 3.27 (dt, *J* = 9.5 Hz, 4.7 Hz, 1H), 3.47 (dd, *J* = 13.0 Hz, 9.5 Hz, 1H), 4.54 (d, *J* = 4.2 Hz, 1H), 6.98 (d, *J* = 8.6 Hz, 1H), 7.08 (d, *J* = 7.2 Hz, 1H), 7.13 (t, *J* = 7.6 Hz, 1H), 7.18 (t, *J* = 7.6 Hz, 1H), 7.26–7.29 (m, 2H), 7.29–7.35 (m, 3H), 7.38 (t, *J* = 7.3 Hz, 1H), 7.58 (td, *J* = 7.6 Hz, 1.2 Hz, 1H), 7.66 (d, *J* = 8.1 Hz, 1H), 7.72 (td, *J* = 7.5 Hz, 1.4 Hz, 1H), 7.77 (d, *J* = 8.0 Hz, 1H), 7.93 (dd, *J* = 7.8 Hz, 0.8 Hz, 1H), 8.17 (dd, *J* = 7.8 Hz, 1.1 Hz, 1H). ^{13}C NMR ($CDCl_3$) δ 38.2, 43.3, 48.9, 49.0, 55.0, 99.4, 122.6, 125.1, 125.2, 125.8, 126.1, 126.4, 127.0, 127.4, 127.9, 128.4, 128.8, 129.1, 130.4, 131.7, 131.8, 133.1, 134.0, 135.6, 139.7, 141.2, 199.4. HRMS (ESI) calcd for $C_{29}H_{27}O_3$ $[M+H]^+$ 423.1960, found 423.1963.

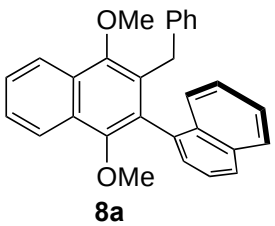

8a

Compound 8a (colorless oil, 75% yield, 99% ee). The ee was measured by HPLC (Chiralpak IE column, 1.0 mL/min, hexane/2-propanol = 97/3, 280 nm, t_{major} = 6.1 min (*R*), t_{minor} = 10.0 min (*S*); $[\alpha]^{25}_{D}$ –72.4 (*c* 1.843, $CHCl_3$) for 99% ee.^1H NMR (400 MHz, $CDCl_3$) δ 3.42 (s, 3H), 3.57 (d, *J* = 14.9 Hz, 1H), 3.94 (s, 3H), 4.11 (d, *J* = 14.9 Hz,1 H), 6.62–6.69 (m, 2H), 6.91–6.99 (m, 3H), 7.14 (dd, *J* = 7.0 Hz, 1.0 Hz, 1H), 7.26 (td, *J* = 7.6 Hz, 1.1 Hz, 1H), 7.33 (d, *J* = 8.3 Hz, 1H), 7.38 (dd, *J* = 8.1

Hz, 7.1 Hz, 1H), 7.43 (td, *J* = 6.9 Hz, 1.2 Hz, 1H), 7.57 (ddd, *J* = 8.3 Hz, 6.8 Hz, 1.4 Hz, 1H), 7.62 (ddd, *J* = 8.1 Hz, 6.8 Hz, 1.3 Hz, 1H) 7.85 (d, *J* = 8.4 Hz, 1H), 7.88 (d, *J* = 8.7 Hz, 1H), 8.18 (d, *J* = 8.4 Hz, 1H), 8.23 (d, *J* = 8.3 Hz, 1H). ^{13}C NMR ($CDCl_3$) δ 33.4, 61.9, 62.2, 122.6, 123.0, 125.0, 125.3, 125.5, 125.6, 125.9, 126.0, 126.3, 127.66, 127.73, 128.1, 128.2, 128.3, 128.7, 130.0, 130.9, 132.5, 133.4, 134.3, 140.9, 150.6. HRMS (ESI) calcd for $C_{29}H_{25}O_2$ $[M+H]^+$ 405.1855, found 405.1852.

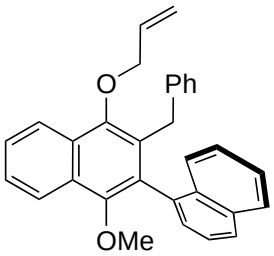

8b

Compound 8b (colorless oil, 83% yield, 98% ee). The ee was measured by HPLC (Chiralpak IE column, 1.0 mL/min, hexane/2-propanol = 98/2, 280 nm, t_{major} = 5.2 min (*R*), t_{minor} = 6.5 min (*S*); $[\alpha]^{25}_D$ –67.3 (*c* 2.528, $CHCl_3$) for 98% ee. ^{1}H NMR (400 MHz, $CDCl_3$) δ 3.41 (s, 3H), 3.55 (d, *J* = 14.8 Hz, 1H), 4.12 (d, *J* = 14.8 Hz, 1H), 4.51 (dd, *J* = 12.5 Hz, 5.4 Hz, 1H) , 4.56 (dd, *J* = 12.6 Hz, 5.4 Hz, 1H), 5.30 (d, *J* = 10.3 Hz, 1H), 5.49 (d, *J* = 17.2 Hz, 1H), 6.17 (ddt, *J* = 17.2 Hz, 10.6 Hz, 5.3 Hz, 1H), 6.58–6.66 (m, 2H), 6.88–6.98 (m, 3H), 7.11 (d, *J* = 6.8 Hz, 1H), 7.25 (t, *J* = 9.0 Hz, 1H), 7.31 (d, *J* = 8.2 Hz, 1H), 7.37 (t, *J* = 7.4 Hz, 1H), 7.42 (t, *J* = 7.0 Hz, 1H), 7.52–7.64 (m, 2H), 7.85 (d, *J* = 8.9 Hz, 1H), 7.87 (d, *J* = 8.8 Hz, 1H), 8.17 (d, *J* = 7.8 Hz, 1H), 8.21 (d, *J* = 8.0 Hz, 1H). ^{13}C NMR ($CDCl_3$) δ 33.6, 61.9, 75.4, 117.3, 122.7, 123.0, 125.0, 125.3, 125.5, 125.6, 125.94, 125.95, 126.4, 127.6, 127.7, 128.1, 128.2, 128.30, 128.33, 128.9, 130.4, 130.9, 132.5, 133.4, 133.9, 134.3, 140.9, 149.4, 150.7. HRMS (ESI) calcd for $C_{31}H_{27}O_2$ $[M+H]^+$ 431.2011, found 431.2004.

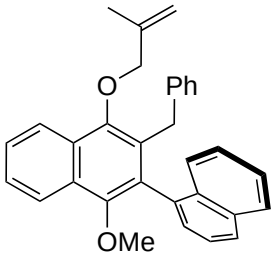

8c

Compound 8c (colorless oil, 85% yield, 99% ee). The ee was measured by HPLC (Chiralpak IF column, 1.0 mL/min, hexane/2-propanol = 98/2, 280 nm, t_{major} = 4.1 min (*R*), t_{minor} = 4.4 min (*S*); $[\alpha]^{25}_{D}$ –69.7 (*c* 2.645, $CHCl_3$) for 99% ee.^{1}H NMR (400 MHz, $CDCl_3$) δ 1.90 (s, 3H), 3.42 (s, 3H), 3.57 (d, *J* = 14.8 Hz, 1H), 4.13 (d, *J* = 14.8 Hz, 1H), 4.40 (d, *J* = 12.2 Hz, 1H), 4.43 (d, *J* = 12.2 Hz, 1H), 5.03 (s, 1H), 5.27 (s, 1H), 6.60–6.66 (m, 2H), 6.89–6.97 (m, 3H), 7.13 (d, *J* = 6.8 Hz, 1H), 7.26 (dd, *J* = 7.2 Hz, 4.3 Hz, 1H), 7.32 (d, *J* = 8.3 Hz, 1H), 7.38 (t, *J* = 7.9 Hz, 1H), 7.43 (t, *J* = 7.9 Hz, 1H), 7.53–7.64 (m, 2H), 7.86 (d, *J* = 8.3 Hz, 1H), 7.88 (d, *J* = 8.3 Hz, 1H), 8.18 (d, *J* = 7.7 Hz, 1H), 8.23 (d, *J* = 7.8 Hz, 1H). ^{13}C NMR ($CDCl_3$) δ 19.7, 33.5, 61.9, 78.0, 112.1, 122.6, 123.0, 125.0, 125.2, 125.5, 125.6, 125.9, 126.0, 126.4, 127.6, 127.7, 128.1, 128.2, 128.3, 128.4, 128.9, 130.4, 130.9, 132.5, 133.4, 134.3, 140.9, 141.5, 149.5, 150.7. HRMS (ESI) calcd for $C_{32}H_{29}O_2$ $[M+H]^+$ 445.2168, found 445.2173.

2.4.12. Data for X–ray crystal structures

Crystals of **4aa** suitable for X-ray crystallographic analysis were obtained by recrystallization from hexane/diethyl ether. The ORTEP drawing of **4aa** is shown in Figure S1. The absolute configuration of **4aa** was determined to be (*R*).

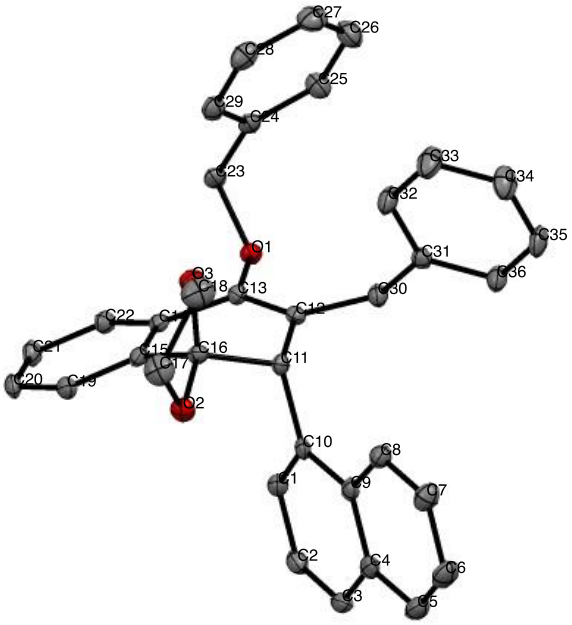

Figure S1. ORTEP illustration of compound (*R*)-**4aa**.

Table S1. Sample and crystal data for (*R*)-**4aa**

Chemical formula	$C_{36}H_{30}O_3$	
Formula weight	510.60 g/mol	
Temperature	103(2) K	
Wavelength	1.54178 Å	
Crystal size	0.120 x 0.220 x 0.320 mm	
Crystal habit	colorless block	
Crystal system	monoclinic	
Space group	P 1 21 1	
Unit cell dimensions	a = 8.51940(10) Å	α = 90°
	b = 18.4481(3) Å	β = 103.5451(7)°
	c = 8.68110(10) Å	γ = 90°
Volume	1326.43(3) $Å^3$	
Z	2	
Density (calculated)	1.278 g/cm^3	
Absorption coefficient	0.628 mm^{-1}	

F(000)	540

Table S2. Data collection and structure refinement for (*R*)-**4aa**

Theta range for data collection	4.79 to 66.87°	
Index ranges	-10<=h<=10, -21<=k<=21, -9<=l<=10	
Reflections collected	14012	
Independent reflections	4642 [R(int) = 0.0508]	
Coverage of independent reflections	99.6%	
Absorption correction	Multi-Scan	
Max. and min. transmission	0.9280 and 0.8240	
Structure solution technique	direct methods	
Structure solution program	SHELXT 2014/5 (Sheldrick, 2014)	
Refinement method	Full-matrix least-squares on F^2	
Refinement program	SHELXL-2016/6 (Sheldrick, 2016)	
Function minimized	$\Sigma\, w(F_o^2 - F_c^2)^2$	
Data / restraints / parameters	4642 / 1 / 353	
Goodness-of-fit on F^2	1.045	
Final R indices	4570 data; I>2σ(I)	R1 = 0.0397, wR2 = 0.1038
	all data	R1 = 0.0401, wR2 = 0.1044
Weighting scheme	$w=1/[\sigma^2(F_o^2)+(0.0713P)^2+0.0970P]$ where $P=(F_o^2+2F_c^2)/3$	
Absolute structure parameter	0.08(9)	
Extinction coefficient	0.0146(16)	
Largest diff. peak and hole	0.477 and -0.294 eÅ^{-3}	
R.M.S. deviation from mean	0.076 eÅ^{-3}	

Crystals of **4ca** suitable for X-ray crystallographic analysis were obtained by recrystallization from hexane/diethyl ether. The ORTEP drawing of **4ca** is shown in Figure S2. The absolute configuration of **4ca** was determined to be (*S*).

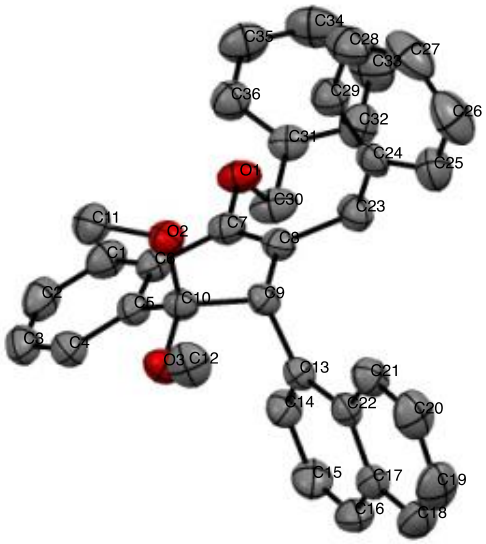

Figure S2. ORTEP illustration of compound (*S*)-**4ca**.

Table S3. Sample and crystal data for (*S*)-**4ca**

Chemical formula	$C_{36}H_{32}O_3$	
Formula weight	512.61 g/mol	
Temperature	296(2) K	
Wavelength	1.54178 Å	
Crystal size	0.160 x 0.200 x 0.220 mm	
Crystal habit	colorless block	
Crystal system	orthorhombic	
Space group	P 21 21 21	
Unit cell dimensions	a = 11.2404(9) Å	α = 90°
	b = 12.7233(10) Å	β = 90°
	c = 19.0214(14) Å	γ = 90°
Volume	2720.3(4) $Å^3$	
Z	4	
Density (calculated)	1.252 g/cm^3	
Absorption coefficient	0.613 mm^{-1}	
F(000)	1088	

Table S4. Data collection and structure refinement for (*S*)-**4ca**

Theta range for data collection	4.18 to 68.04°	
Index ranges	-13<=h<=13, -13<=k<=15, -22<=l<=22	
Reflections collected	29141	
Independent reflections	4903 [R(int) = 0.0505]	
Coverage of independent reflections	98.9%	
Absorption correction	Multi-Scan	
Max. and min. transmission	0.9080 and 0.8770	
Structure solution technique	direct methods	
Structure solution program	XT, VERSION 2014/5	
Refinement method	Full-matrix least-squares on F^2	
Refinement program	SHELXL-2016/6 (Sheldrick, 2016)	
Function minimized	$\Sigma\, w(F_o^2 - F_c^2)^2$	
Data / restraints / parameters	4903 / 0 / 354	
Goodness-of-fit on F2	1.037	
Δ/σmax	0.010	
Final R indices	4652 data; I>2σ(I)	R1 = 0.0339, wR2 = 0.0907
	all data	R1 = 0.0361, wR2 = 0.0941
Weighting scheme	$w=1/[\sigma^2(F_o^2)+(0.0575P)^2+0.2095P]$ where $P=(F_o^2+2F_c^2)/3$	
Absolute structure parameter	-0.02(7)	
Largest diff. peak and hole	0.121 and -0.171 eÅ^{-3}	
R.M.S. deviation from mean	0.032 eÅ^{-3}	

Crystals of **4ce** suitable for X-ray crystallographic analysis were obtained by recrystallization from methanol. The ORTEP drawing of **4ce** is shown in Figure S3.

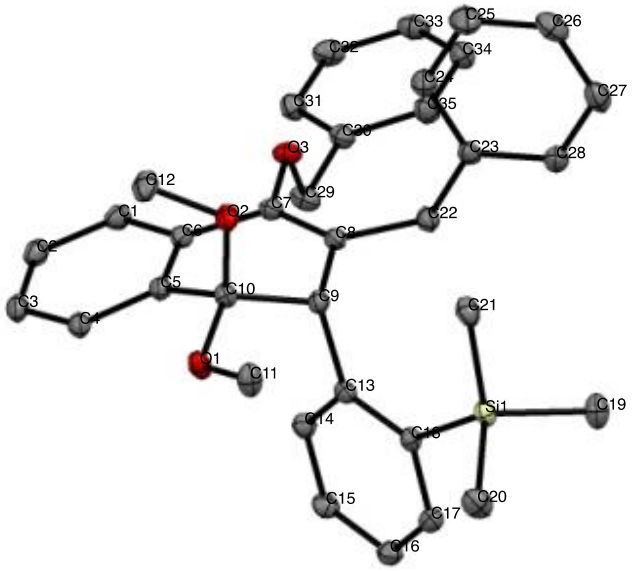

Figure S3. ORTEP illustration of compound rac-**4ce**.

Table S5. Sample and crystal data for rac-**4ce**

Chemical formula	$C_{35}H_{38}O_3Si$	
Formula weight	534.74 g/mol	
Temperature	100(2) K	
Wavelength	0.71073 Å	
Crystal size	0.200 x 0.220 x 0.240 mm	
Crystal habit	colorless block	
Crystal system	monoclinic	
Space group	P 1 21/n 1	
Unit cell dimensions	a = 11.3190(3) Å	α = 90°
	b = 13.9462(5) Å	β = 94.3230(10)°
	c = 18.2946(6) Å	γ = 90°
Volume	2879.72(16) $Å^3$	
Z	4	
Density (calculated)	1.233 g/cm^3	
Absorption coefficient	0.116 mm^{-1}	
F(000)	1144	

Table S6. Data collection and structure refinement for rac-**4ce**

Theta range for data collection	2.52 to 34.34°	
Index ranges	-14<=h<=17, -22<=k<=22, -29<=l<=29	
Reflections collected	53639	
Independent reflections	11952 [R(int) = 0.0599]	
Coverage of independent reflections	99.1%	
Absorption correction	Multi-Scan	
Max. and min. transmission	0.9770 and 0.9730	
Structure solution technique	direct methods	
Structure solution program	XT, VERSION 2014/5	
Refinement method	Full-matrix least-squares on F^2	
Refinement program	SHELXL-2017/1 (Sheldrick, 2017)	
Function minimized	$\Sigma\, w(F_o^2 - F_c^2)^2$	
Data / restraints / parameters	11952 / 0 / 357	
Goodness-of-fit on F2	1.025	
Δ/σmax	0.001	
Final R indices	8595 data; I>2σ(I)	R1 = 0.0506, wR2 = 0.1077
	all data	R1 = 0.0819, wR2 = 0.1238
Weighting scheme	$w=1/[\sigma^2(F_o^2)+(0.0441P)^2+1.1484P]$ where $P=(F_o^2+2F_c^2)/3$	
Largest diff. peak and hole	0.446 and -0.320 eÅ^{-3}	
R.M.S. deviation from mean	0.062 eÅ^{-3}	

Crystals of **3ce** suitable for X-ray crystallographic analysis were obtained by recrystallization from pentane/dichloromethane. The ORTEP drawing of **3ce** is shown in Figure S4. The absolute configuration of **3ce** was determined to be (*R*).

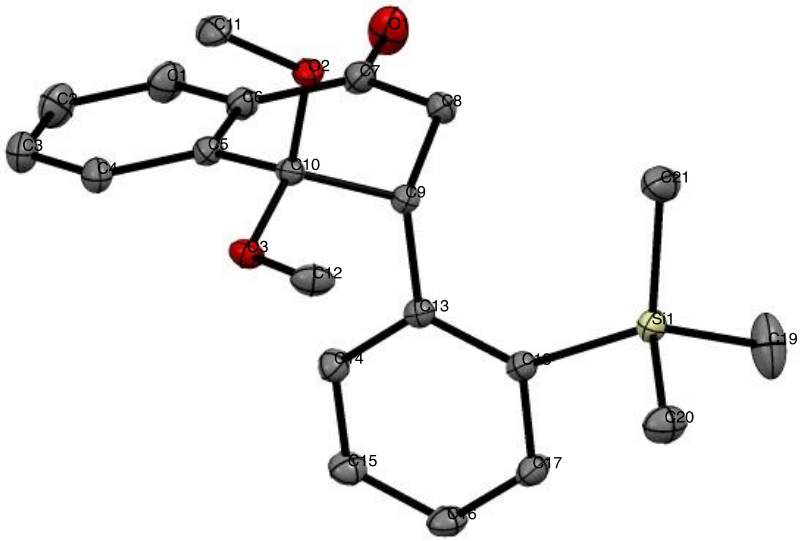

Figure S4. ORTEP illustration of compound (*R*)-**3ce**.

Table S7. Sample and crystal data for (*R*)-**3ce**

Chemical formula	$C_{21}H_{26}O_3Si$	
Formula weight	354.51 g/mol	
Temperature	100(2) K	
Wavelength	0.71073 Å	
Crystal size	0.200 x 0.240 x 0.280 mm	
Crystal habit	colorless block	
Crystal system	orthorhombic	
Space group	P 21 21 21	
Unit cell dimensions	a = 8.3776(2) Å	α = 90°
	b = 12.5633(3) Å	β = 90°
	c = 17.8956(5) Å	γ = 90°
Volume	1883.52(8) $Å^3$	
Z	4	
Density (calculated)	1.250 g/cm^3	
Absorption coefficient	0.141 mm^{-1}	
F(000)	760	

Table S8. Data collection and structure refinement for (*R*)-**3ce**

Theta range for data collection	2.28 to 35.64°	
Index ranges	-12<=h<=13, -20<=k<=19, -25<=l<=29	
Reflections collected	22184	
Independent reflections	8623 [R(int) = 0.0389]	
Coverage of independent reflections	99.2%	
Absorption correction	Multi-Scan	
Max. and min. transmission	0.9720 and 0.9620	
Structure solution technique	direct methods	
Structure solution program	XT, VERSION 2014/5	
Refinement method	Full-matrix least-squares on F^2	
Refinement program	SHELXL-2017/1 (Sheldrick, 2017)	
Function minimized	$\Sigma\, w(F_o^2 - F_c^2)^2$	
Data / restraints / parameters	8623 / 0 / 231	
Goodness-of-fit on F^2	1.022	
Δ/σ_{max}	0.001	
Final R indices	7193 data; I>2σ(I)	R1 = 0.0443, wR2 = 0.1015
	all data	R1 = 0.0597, wR2 = 0.1114
Weighting scheme	$w=1/[\sigma^2(F_o^2)+(0.0555P)^2+0.0853P]$ where $P=(F_o^2+2F_c^2)/3$	
Absolute structure parameter	0.00(4)	
Largest diff. peak and hole	0.342 and -0.332 eÅ^{-3}	
R.M.S. deviation from mean	0.053 eÅ^{-3}	

Crystals of **5ce** suitable for X-ray crystallographic analysis were obtained by recrystallization from hexane/ethanol. The ORTEP drawing of **5ce** is shown in Figure S5. The absolute configuration of **5ce** was determined to be (*R*).

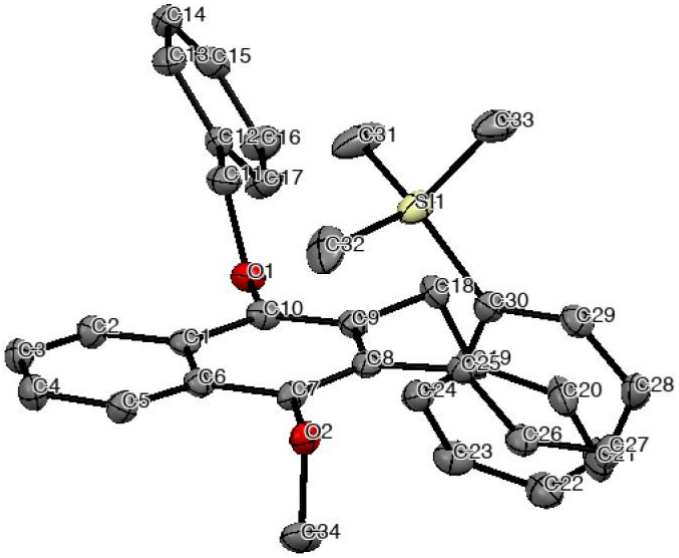

Figure S5. ORTEP illustration of compound (*R*)-**5ce**

Table S9. Sample and crystal data for (*R*)-**5ce**

Chemical formula	$C_{34}H_{34}O_2Si$	
Formula weight	502.70 g/mol	
Temperature	93(2) K	
Wavelength	0.71073 Å	
Crystal size	0.140 x 0.180 x 0.200 mm	
Crystal habit	colorless block	
Crystal system	monoclinic	
Space group	P 1 21 1	
Unit cell dimensions	a = 11.9795(4) Å	α = 90°
	b = 12.4617(5) Å	β = 105.7907(11)°
	c = 19.0603(8) Å	γ = 90°
Volume	2738.04(18) $Å^3$	
Z	4	
Density (calculated)	1.219 g/cm^3	
Absorption coefficient	0.115 mm^{-1}	
F(000)	1072	

Table S10. Data collection and structure refinement for (*R*)-**5ce**

Theta range for data collection	2.33 to 31.01°	
Index ranges	-15<=h<=17, -18<=k<=17, -27<=l<=25	
Reflections collected	59034	
Independent reflections	17367 [R(int) = 0.1023]	
Coverage of independent reflections	99.8%	
Absorption correction	Multi-Scan	
Max. and min. transmission	0.9840 and 0.9770	
Structure solution technique	direct methods	
Structure solution program	XT, VERSION 2014/5	
Refinement method	Full-matrix least-squares on F^2	
Refinement program	SHELXL-2017/1 (Sheldrick, 2017)	
Function minimized	$\Sigma\, w(F_o^2 - F_c^2)^2$	
Data / restraints / parameters	17367 / 1 / 675	
Goodness-of-fit on F^2	1.017	
Δ/σ_{max}	0.001	
Final R indices	10710 data; I>2σ(I)	R1 = 0.0596, wR2 = 0.0943
	all data	R1 = 0.1287, wR2 = 0.1177
Weighting scheme	$w=1/[\sigma^2(F_o^2)+(0.0372P)^2+0.0250P]$ where $P=(F_o^2+2F_c^2)/3$	
Absolute structure parameter	-0.06(7)	
Largest diff. peak and hole	0.262 and -0.331 eÅ^{-3}	
R.M.S. deviation from mean	0.064 eÅ^{-3}	

Crystals of rac-**5ca** suitable for X-ray crystallographic analysis were obtained by recrystallization from acetone/isopropyl alcohol. The ORTEP drawing of rac-**5ca** is shown in Figure S6.

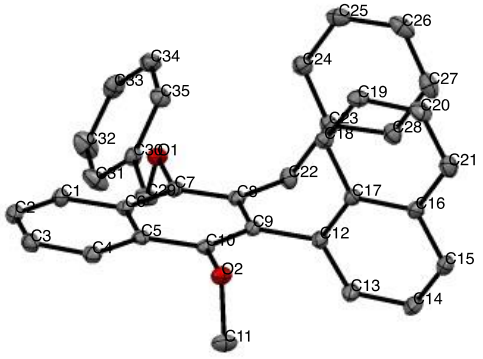

Figure S6. ORTEP illustration of compound rac-**5ca**

Table S11. Sample and crystal data for rac-**5ca**

Chemical formula	$C_{35}H_{28}O_2$	
Formula weight	480.57 g/mol	
Temperature	100(2) K	
Wavelength	0.71073 Å	
Crystal size	0.120 x 0.160 x 0.200 mm	
Crystal habit	colorless block	
Crystal system	triclinic	
Space group	P -1	
Unit cell dimensions	a = 10.1893(5) Å	α = 114.2495(16)°
	b = 12.0980(6) Å	β = 95.0262(18)°
	c = 12.6934(6) Å	γ = 113.6768(19)°
Volume	1245.38(11) $Å^3$	
Z	2	
Density (calculated)	1.282 g/cm^3	
Absorption coefficient	0.078 mm^{-1}	
F(000)	508	

Table S12. Data collection and structure refinement for rac-**5ca**

Theta range for data collection	2.24 to 32.61°	
Index ranges	-15<=h<=15, -18<=k<=18, -19<=l<=15	
Reflections collected	18795	
Independent reflections	8985 [R(int) = 0.0674]	
Coverage of independent reflections	98.6%	
Absorption correction	Multi-Scan	
Max. and min. transmission	0.9910 and 0.9850	
Structure solution technique	direct methods	
Structure solution program	XT, VERSION 2014/5	
Refinement method	Full-matrix least-squares on F^2	
Refinement program	SHELXL-2017/1 (Sheldrick, 2017)	
Function minimized	$\Sigma\, w(F_o^2 - F_c^2)^2$	
Data / restraints / parameters	8985 / 0 / 335	
Goodness-of-fit on F^2	1.028	
Final R indices	5256 data; I>2σ(I)	R1 = 0.0676, wR2 = 0.1390
	all data	R1 = 0.1277, wR2 = 0.1737

Weighting scheme	$w=1/[\sigma^2(F_o^2)+(0.0600P)^2+0.2364P]$ where $P=(F_o^2+2F_c^2)/3$
Largest diff. peak and hole	0.405 and -0.344 eÅ^{-3}
R.M.S. deviation from mean	0.072 eÅ^{-3}

Crystals of **5cf** suitable for X-ray crystallographic analysis were obtained by recrystallization from dichloromethane/ethanol/diethyl ether. The ORTEP drawing of **5cf** is shown in Figure S7. The absolute configuration of **5cf** was determined to be (*R*).

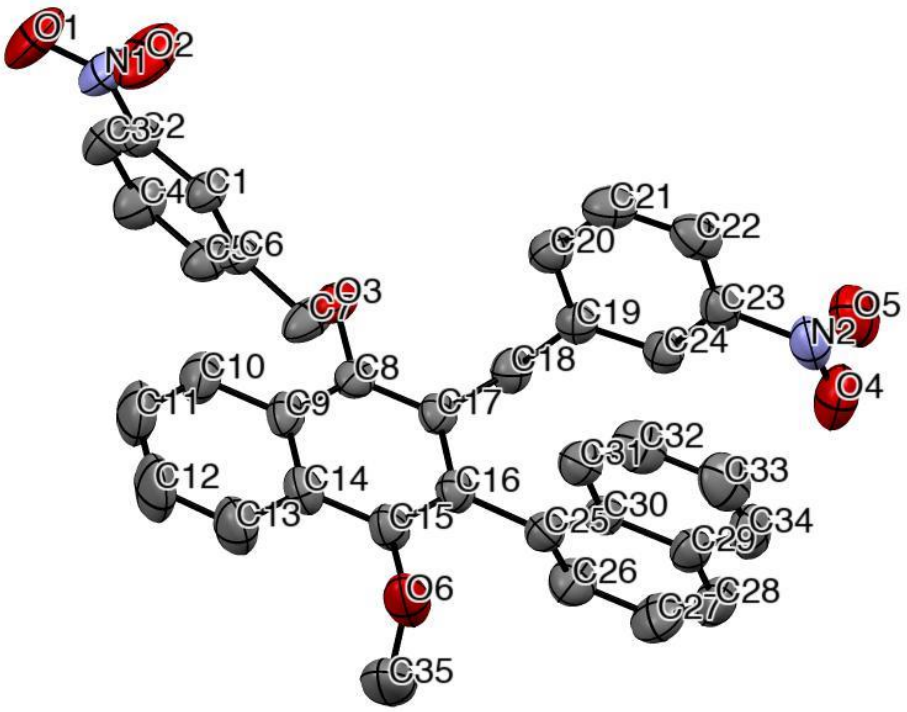

Figure S7. ORTEP illustration of compound (*R*)-**5cf**

Table S13. Sample and crystal data for (*R*)-**5cf**

Chemical formula	$C_{35}H_{26}N_2O_6$	
Formula weight	570.58 g/mol	
Temperature	296(2) K	
Wavelength	1.54178 Å	
Crystal size	0.020 x 0.100 x 0.220 mm	
Crystal habit	colorless plate	
Crystal system	monoclinic	
Space group	P 1 21 1	
Unit cell dimensions	a = 10.8455(6) Å	α = 90°
	b = 8.2734(5)Å	β = 91.602(3)°
	c = 15.9613(9) Å	γ = 90°
Volume	1431.63(14) $Å^3$	
Z	2	
Density (calculated)	1.324 g/cm^3	
Absorption coefficient	0.745mm^{-1}	
F(000)	596	

Table S14. Data collection and structure refinement for (*R*)-**5cf**

Theta range for data collection	2.77 to 66.61°	
Index ranges	-12<=h<=12, -9<=k<=9, -18<=l<=18	
Reflections collected	44437	
Independent reflections	5035 [R(int) = 0.0610]	
Coverage of independent reflections	100.0%	
Absorption correction	Multi-Scan	
Max. and min. transmission	0.9850 and 0.8530	
Structure solution technique	direct methods	
Structure solution program	XT, VERSION 2014/5	
Refinement method	Full-matrix least-squares on F^2	
Refinement program	SHELXL-2018/3 (Sheldrick, 2018)	
Function minimized	$\Sigma\, w(F_o^2 - F_c^2)^2$	
Data / restraints / parameters	5035 / 1 / 389	
Goodness-of-fit on F^2	1.050	
Final R indices	4680 data; I>2σ(I)	R1 = 0.0318, wR2 = 0.0810
	all data	R1 = 0.0353, wR2 = 0.0849

Weighting scheme	$w=1/[\sigma^2(F_o^2)+(0.0431P)^2+0.1538P]$ where $P=(F_o^2+2F_c^2)/3$
Absolute structure parameter	0.01(8)
Largest diff. peak and hole	0.134 and -0.170 $eÅ^{-3}$
R.M.S. deviation from mean	0.029 $eÅ^{-3}$

2.6. References

1. Kauffman, G. B.; Myers, R. D. *J. Chem. Educ.* **1975**, *52*, 777–781.
2. Bringmann, G.; Price Mortimer, A. J.; Keller, P. A.; Gresser, M. J.; Garner, J.; Breuning, M. *Angew. Chem. Int. Ed.* **2005**, *44*, 5384–5427.
3. Wilson, J. M.; Cram, D. J. *J. Am. Chem. Soc.* **1982**, *104*, 881–884.
4. Yin, J.; Buchwald, S. L. *J. Am. Chem. Soc.* **2000**, *122*, 12051–12052.
5. Hayashi, T.; Hayashizaki, K.; Kiyoi, T.; Ito, Y. *J. Am. Chem. Soc.* **1988**, *110*, 8153–8156.
6. Genov, M.; Fuentes, B.; Espinet, P.; Pelaz, B. *Tetrahedron: Asymmetry.* **2006**, *17*, 2593–2595.
7. Hayashi, T.; Niizuma, S.; Kamikawa, T.; Suzuki, N.; Uozumi, Y. *J. Am. Chem. Soc.* **1995**, *117*, 9101–9102.
8. Gutnov, A.; Heller, B.; Fischer, C.; Drexler, H.-J.; Spannenberg, A.; Sundermann, B.; Sundermann, C. *Angew. Chem. Int. Ed.* **2004**, *43*, 3795–3797.
9. Shibata, T.; Fujimoto, T.; Yokota, K.; Takagi, K. *J. Am. Chem. Soc.* **2004**, *126*, 8382–8383.
10. Tanaka, K.; Nishida, G.; Wada, A.; Noguchi, K. *Angew. Chem. Int. Ed.* **2004**, *43*, 6510–6512.
11. Nishii, Y.; Wakasugi, K.; Koga, K.; Tanabe, Y. *J. Am. Chem. Soc.* **2004**, *126*, 5358–5359.
12. Kawabata, T.; Yahiro, K.; Fuji, K. *J. Am. Chem. Soc.* **1991**, *113*, 9694–9696.
13. Guo, F.; Konkol, L. C.; Thomson, R. J. *J. Am. Chem. Soc.* **2011**, *133*, 18–20.
14. Quinonero, O.; Jean, M.; Vanthuyne, N.; Roussel, C.; Bonne, D.; Constantieux, T.; Bressy, C.; Bugaut, X.; Rodriguez, J. *Angew. Chem. Int. Ed.* **2016**, *55*, 1401–1405.
15. Link, A.; Sparr, C. *Angew. Chem. Int. Ed.* **2018**, *57*, 7136–7139.
16. Chapter 6 Asymmetric Synthesis with Stereodynamic Compounds: Introduction, Conversion and Transfer of Chirality. In *Dynamic Stereochemistry of Chiral Compounds: Principles and Applications*, The Royal Society of Chemistry: 2008; pp 233–271.
17. Tokunaga, N.; Hayashi, T. *Adv. Synth. Catal.* **2007**, *349*, 513–516.

18. Tobisu, M.; Onoe, M.; Kita, Y.; Chatani, N. *J. Am. Chem. Soc.* **2009**, *131*, 7506–7507.
19. Otomaru, Y.; Kina, A.; Shintani, R.; Hayashi, T. *Tetrahedron: Asymmetry.* **2005**, *16*, 1673–1679.
20. Hatano, M.; Nishimura, T. *Angew. Chem. Int. Ed.* **2015**, *54*, 10949–10952.
21. Miyamura, H.; Nishino, K.; Yasukawa, T.; Kobayashi, S. *Chem. Sci.* **2017**, *8*, 8362–8372.
22. Farina, F.; Paredes, M. C.; Soto, J. J. *An. Quim.* **1995**, *91*, 50–55.
23. Henderson, D. A.; Collier, P. N.; Pavé, G.; Rzepa, P.; White, A. J. P.; Burrows, J. N.; Barrett, A. G. M. *J. Org. Chem.* **2006**, *71*, 2434–2444.
24. Yanai, H.; Sasaki, Y.; Yamamoto, Y.; Matsumoto, T. *Synlett.* **2015**, *26*, 2457–2461.
25. Kumamoto, T.; Aoyama, N.; Nakano, S.; Ishikawa, T.; Narimatsu, S. *Tetrahedron: Asymmetry.* **2001**, *12*, 791–795.

Chapter 3

Asymmetric rhodium-catalyzed alkylation and β-F elimination to generate tetra-substituted fluoroallenes

3.1. Introduction

The importance of fluorine atom cannot be overemphasized with it playing a significant role in areas such as medicinal chemistry,[1] agrochemicals,[2-3] and material science.[4] It can be seen from the prevalence of fluorine incorporated molecules occupying as much as 30–40% of the agrochemicals and even 20% of the pharmaceuticals in the market.[5] Furthermore, ^{19}F atom can be used as a tag in a probe molecule for the exploration of biological processes. One such occurrence is the NMR analysis of ^{19}F nuclei that allows for in vivo magnetic resonance imaging.[6]

Various methods have been developed for the synthesis of fluoroalkanes and fluoroarenes. For instance, fluorine atom can be incorporated into alkyl chains and aromatic rings through nucleophilic fluorination using an array of nucleophilic reagents developed over the centuries.[7-8] With such advancement, nucleophilic fluorination methodology has flourished and become well adopted. On a similar ground, the electrophilic fluorination of aliphatic and aromatic compounds have also been extensively developed.[9] In spite of these advances, the synthesis of fluoroallenes has been scarce.

In 1982, Dolbier reported the synthesis of 1,1-difluoropropadiene and monofluoropropadiene in good yields and purity (**Scheme 3.1**).[10]

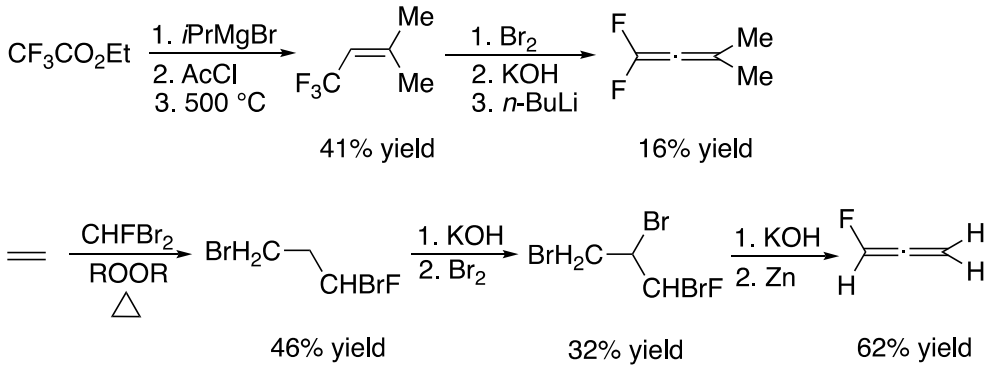

Scheme 3.1 Synthesis of difluoropropadiene and monofluoropropadiene

Despite the progress, it was not until 1987 that variation of the substitution pattern for monofluoroallene was reported by Krantz (**Scheme 3.2**).[11] Although an overall low yield of 17% was obtained for the synthesis of fluoroallenyl amino acid, it was able incorporate different functional groups in the desired fluoroallene, particularly amino acid functionality.

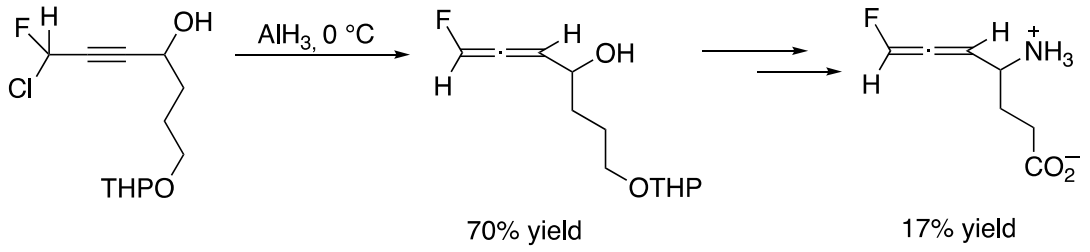

Scheme 3.2 Synthesis of substituted monofluoropropadiene

Later in 1989, Xu also reported the efficient synthesis of alkyl-substituted 1,1-difluoropropadiene through Shapiro reaction, giving 1,1-difluoroallene in up to 72%

yield (**Scheme 3.3**).[12] It was also discovered that for 1,1-difluoroallene with phenyl substituent, it was not stable enough for isolation due to it undergoing oligomerization.

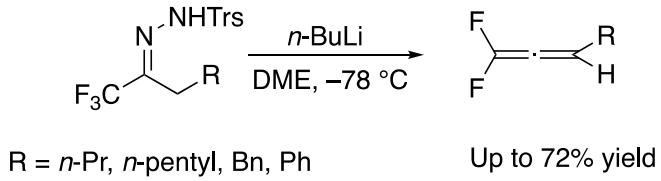

Scheme 3.3 Synthesis of substituted 1,1-difluoropropadiene

Interestingly in 2000, Hammond demonstrated the use of a novel isolable indium allenyl intermediate in the synthesis of substituted 1,1-difluoroallene (**Scheme 3.4**).[13] In the presence of electrophiles such as aldehyde or H^+, the reaction with the indium complex gave the corresponding substituted 1,1.-difluoroallenes in up to 100% yield.

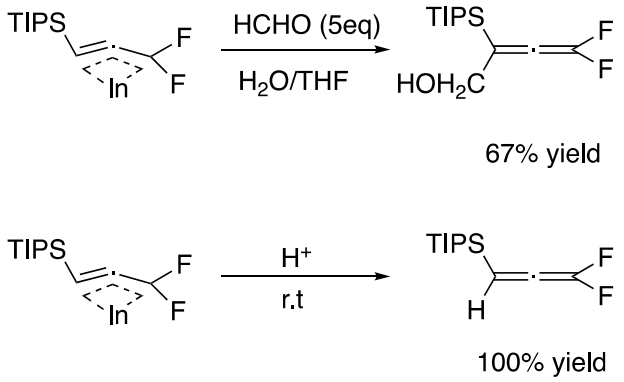

Scheme 3.4 Conversion of allenylindium to difluoroallene

On the other hand, the use of transition metal for the synthesis of fluorinated allenes has no precedence until 2006, where Hammond proceeded to expand the methodologies for the synthesis of both difluoroallene and monofluoroallene. A stoichiometric amount of organocopper reagent prepared from copper(I) halide and alkyl Grignard reagent underwent a S_N2' alkylation of alpha, alpha-difluoropropargyl

bromide to afford substituted difluoroallene in up to 91% yield **(Scheme 3.5).**[14] Further transformation of difluoroallene to monofluoroallene, giving a yield of up to 65%, was performed in the presence of stoichiometric amount of copper(I) source and Grignard reagents under slightly different reaction conditions.

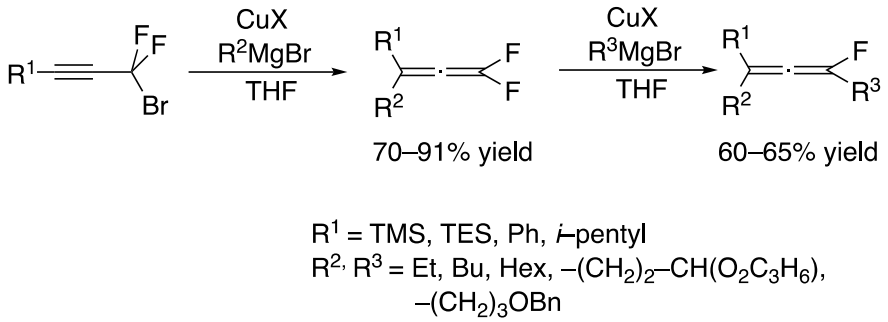

Scheme 3.5 Copper mediated S_N2' alkylation of alpha, alpha-difluoropropargyl bromide

The use of organocatalyst for the formation of fluorinated allenes was rarely documented. In 2016, Wang and co-workers reported the first NHC organocatalyzed C_{sp2}–F bond formation to generate α-fluoroallenoate in high yield of up to 98% (**Scheme 3.6**).[15]

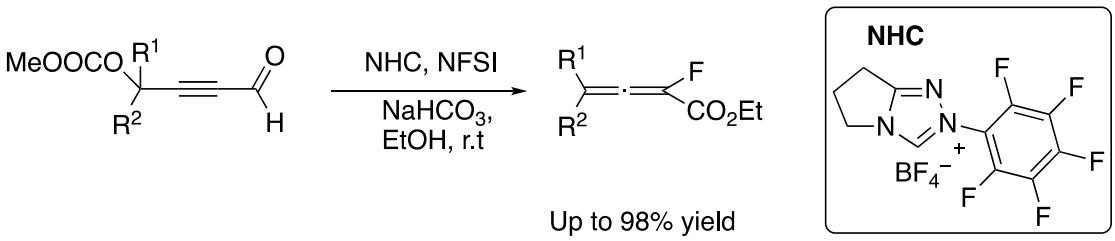

Scheme 3.6 Synthesis of fluoroallene via NHC organocatalysis

Up until then, the use of either transition metal or organocatalyst to effect the transformation to give fluorinated allenes have been few and far between. The inherent

instability of fluorinated allenes, coupled with the difficulty in finding a suitable catalytic system to catalyze such reactions, may have contributed to the slow progress in this field.[12] Furthermore, there has also not been any report of the asymmetric synthesis of fluorinated allenes of any kind.

In 2018, Wang and co-authors reported the asymmetric synthesis of alkynyl and monofluoroalkenyl isoindolinones through a CpRh(III)-catalyzed C–H activation/[4+1] annulation reaction between benzamide derivatives and alpha, alpha-difluoroalkynes (**Scheme 3.7**).[16] The reaction is proposed to proceed through amide-directed C–H activation, insertion of the alkyne into the Rh–C bond, and β-fluorine elimination, resulting in the installation of a fluoroallenyl group to the *ortho* position. This would be followed by the insertion of the allenic C=C bond into the Rh–N bond and second β-F elimination to furnish the [4+1] product (**Scheme 3.8**). When a bulky group such as *tert*-butyl was present at the alpha position of the alkyne, the reaction gave the desired product only in 11% yield along with a significant amount (45%) of the allene derivative with 60% ee, presumably due to the sluggishness of the allene insertion step.

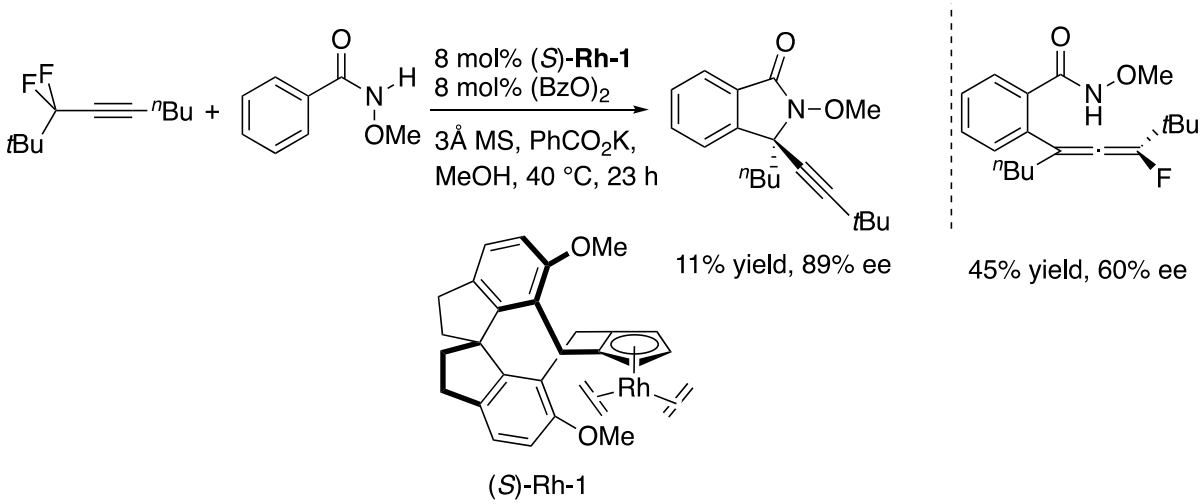

Scheme 3.7 Enantioselective [4+1] annulation via Rh(III)-catalyzed C–H cleavage

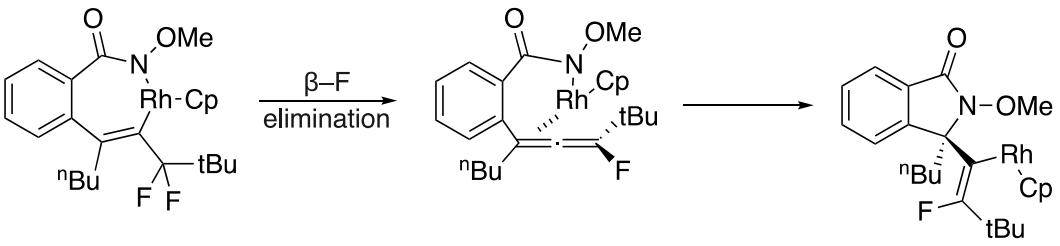

Scheme 3.8 Proposed allenylrhodium intermediate

On this note, it is important to realize that prior to this, the β-F elimination for such sp^2-Rh(III) intermediate has yet to be realized. Hence, this indicates the possibility of adopting the strategy of β-F elimination of sp^2-Rh intermediate to generate axially chiral fluorinated allene. We seek to explore the possibility of incorporating the rhodium-fluoride elimination step in our well-established rhodium arylation of internal alkyne for the synthesis of axially chiral fluoroallene.

In our conventional arylrhodation of internal alkyne, the [Rh]–Ph species first adds onto the triple bond in a *syn*-fashion (**Scheme 3.9**). This concomitant formation of C–C bond and C–Rh bond gives the alkenylrhodium intermediate, which is in constant equilibration with the arylrhodium intermediate through a 1,4-shift C–H activation process. Depending on the electrophile, the trapping of alkenyl species with an electrophile is usually one of the possible applications of this alkenyl rhodium intermediate.

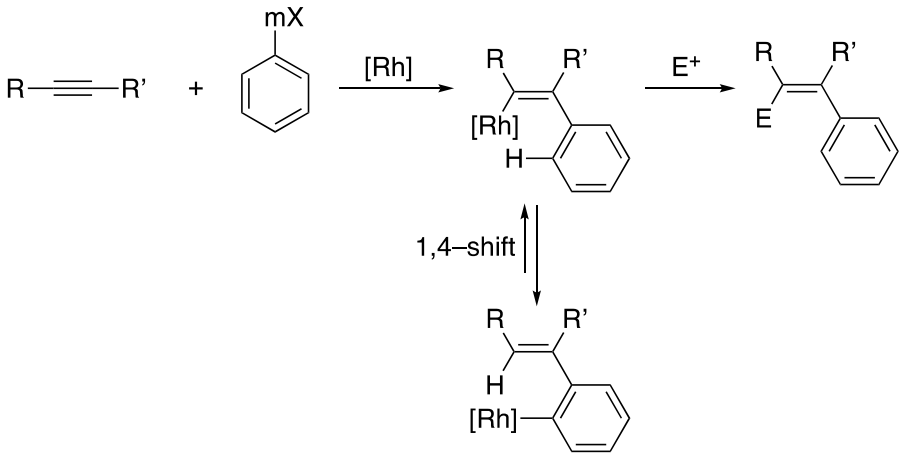

Scheme 3.9 Reaction pathway of alkenyl rhodium intermediate

An earlier publication by Hayashi and co-workers in 2016 has demonstrated the β-F elimination of an alkyl-Rh intermediate, generated by the arylrhodation of trifluoromethyl substituted alkene, give highly enantioenriched 1,1,-difluoroalkenes in yields up to 95% (**Scheme 3.10**).[17]

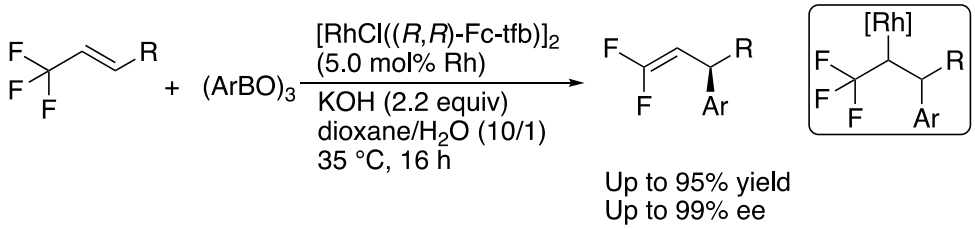

Scheme 3.10 Rhodium-catalyzed addition of boronic acid onto trifluoromethyl alkene

Henceforth, the incorporation of β-F elimination, as an alternate pathway for the alkenylrhodium intermediate, in the synthesis of allenes appears to be promising. We herein report the asymmetric synthesis of chiral fluoroallenes through a rhodium-catalyzed addition of alkylzinc reagents with alpha, alpha-difluoroalkynes, followed by enantioselective defluorination of allylic difluorides (**Scheme 3.11**).

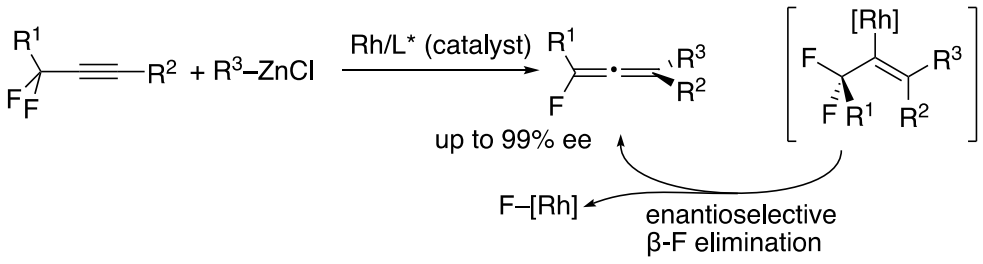

Scheme 3.11 Current work involving rhodium-catalyzed enantioselective alkylation/defluorination of propargyl difluorides with alkylzincs

3.2. Results and Discussion

As a start, we have employed an aprotic anhydrous condition involving 2,2-difluorodec-3-yne as the substrate, along with the use of organozinc halide and $[RhCl(cod)]_2$ as the catalyst (**Scheme 3.12**).

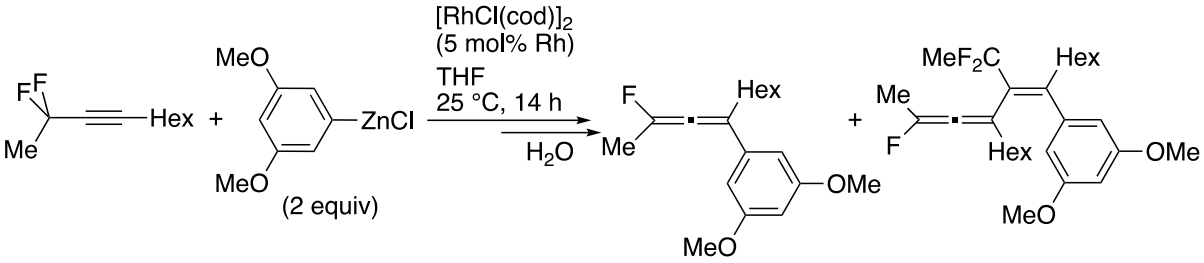

No additive:	13%	20%
$ZnCl_2$: (2 equiv)	22%	78%
ZnF_2: (2 equiv)	13%	39%
LiCl: (2 equiv)	50%	0%

[a]Ratio of ArZnCl: (ArBr: n-BuLi: $ZnCl_2$ = 1.1: 1.0 : 1.3)

Scheme 3.12 Rhodium-catalyzed addition of aromatic zinc chloride onto difluoroalkyne

In the absence of additive, the aromatic zinc reagent in the presence of $[RhCl(cod)]_2$ catalyst gave the expected fluoroallene product only in 13% yield as determined by NMR. The conversion was low at 33%, with a major side product arising from the intermolecular reaction of the alkenylrhodium intermediate with another molecule of the substrate, followed by β-F elimination of the alkenylrhodium species (**Scheme 3.13**). The addition of $ZnCl_2$ (2 equiv) to the reaction system led to full conversion of the starting material, affording the arylative dimerization product as the major product (78%) along with the desired product (22%). The use of ZnF_2 instead of

$ZnCl_2$ led to similar observation, albeit a smaller increment of side product was observed. The preference for the dimerization product may be due to the higher reactivity of the alkenylrhodium species over the arylrhodium species. The addition of zinc halide may facilitate the equilibration between alkenylrhodium and alkenylzinc, which in turn may promote the alkenylrhodation. Interestingly, when LiCl additive was employed, the target product was obtained in a much higher yield of 50% without the arylative dimerization product.

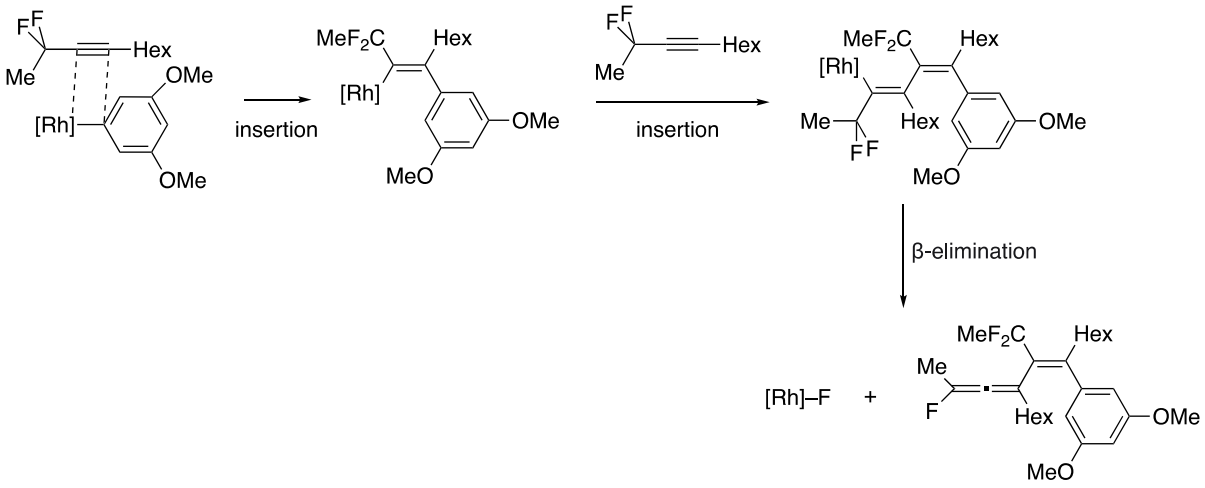

Scheme 3.13 Proposed formation of arylative dimerization side product through addition of alkenylrhodium species with another alpha,alpha-difluoroalkyne

With a change of substrate incorporating a bulkier isopropyl group, the β-F elimination proceeded even more efficiently to generate the targeted allene in much higher yield of 92% (NMR) (**Scheme 3.14**). On a similar observation, no arylative dimerization product was formed in the presence of LiCl. The screening of other metal salts such a LiBr and KCl revealed little difference, while the latter gave slightly higher NMR yield of 94%.

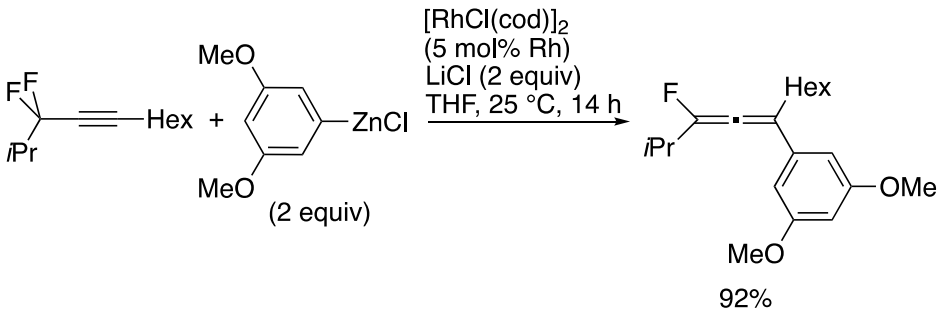

Scheme 3.14 Rhodium-catalyzed addition of 3,5-MeO(C_6H_3)ZnCl onto alpha,alpha-difluoroalkyne with isopropyl group

For the enantioselective-variant of the reaction, [RhCl(*R*,*R*)-Ph-bod]$_2$ was employed as the chiral catalyst under the optimized reaction conditions (**Scheme 3.15**). Not surprisingly, the conversion was much lower at 49% while the target allene was obtained in 44% NMR yield. However, we realized that the allene formed was racemic. Similarly, when [RhCl(diene*-N*t*Bu)]$_2$ was used, the allene formed was also racemic. Importantly, the allene product was accompanied by the hydroarylation product, which points to the possibility of competing background β-F elimination of alkenylzinc intermediate to give racemic product. On this note, we understand that similar phenomenon was also observed in the 1,2-addition of aryl aldehyde, where the present of LiCl gave either racemic product or caused a huge decrease in enantioselectivity.[18] Hence, there is a possibility that LiCl may promote the β-F elimination of alkenylzinc species, giving racemic product. The switch of chiral diene ligand to phosphine ligand such as (*S*)-binap together with KCl (2 equiv) failed to give an appreciable yield of the intended allene.

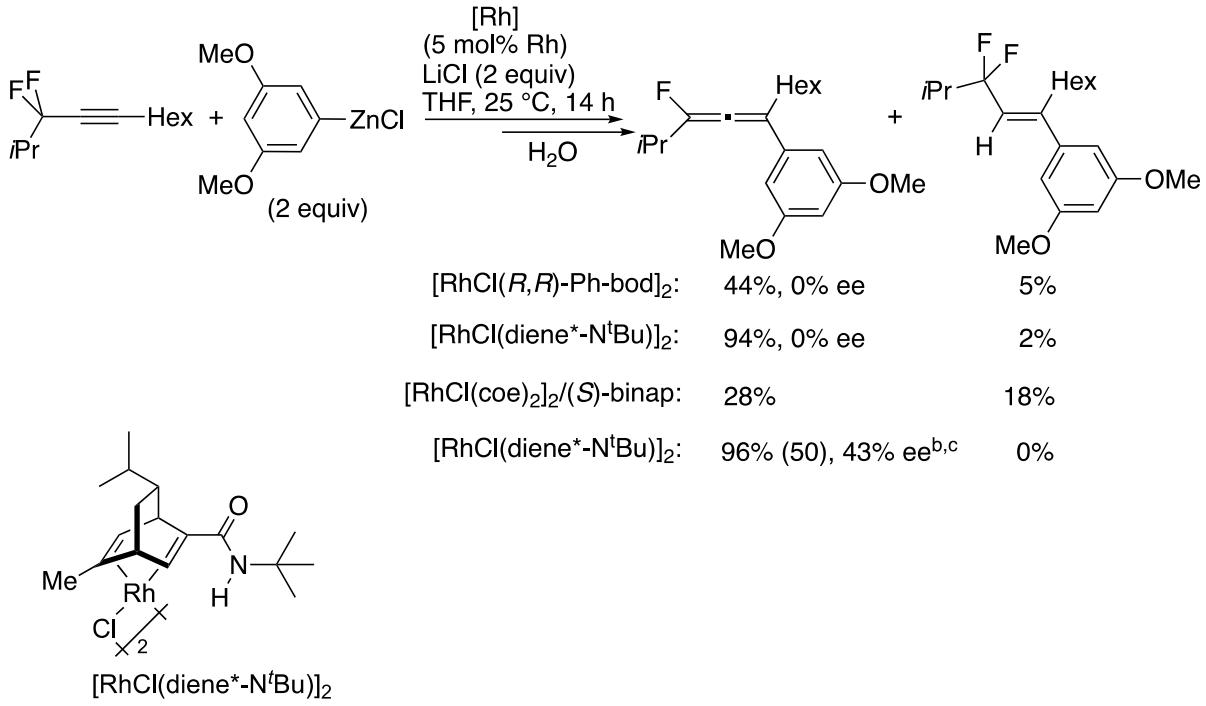

[a]Ratio of ArZnCl: (ArBr: *n*-BuLi: $ZnCl_2$ = 1.1: 1.0 : 1.3)
[b]Ratio of ArZnCl: (ArMgBr: $ZnCl_2$ = 1.0: 2.0)
[c]No addition of LiCl

Scheme 3.15 Screening of chiral rhodium-diene catalyst system

To examine the effect of LiCl on the enantioselectivity, we proceeded to examine a different preparative method for arylzinc reagent. Thus, we tested the reaction using an arylzinc reagent prepared from the corresponding Grignard reagent and $ZnCl_2$ (2 equiv) in the absence of LiCl. Much to our surprise, an equally high NMR yield of 96% was observed. Upon isolating the compound by silica gel column chromatography and gel permeation chromatography (GPC), the product was obtained in 50% yield and 43% ee. In this case, while magnesium salt MgX_2 is generated during the preparation of arylzinc reagent from RMgX and $ZnCl_2$, it may have been inhibited from acting like LiCl salt due to the formation of magnesium halozincate $[\{Mg(thf)_6\}^{2+}\{Zn_2Br_xCl_{6-x}\}^{2-}]$.[19] Magnesium halozincate complex are also known to have low solubility, which may prevent it from participating in the reaction medium

upon precipitation. The unique phenomenon observed may serve as evidence that main group metal salt can have an exceptional influence on the pathway of product formation.

In an attempt to identify the reason for the low enantioselectivity and shed some light on the reaction mechanism, we tested a substrate bearing a bulky tert-butyl group (**Scheme 3.16**). Much to our delight, the *tert*-butyl group proved to have an immensely positive effect on both the reactivity and the enantioselectivity. The corresponding chiral allene was produced in >99% NMR yield and 91% ee upon isolation by GPC. However, before we could work on the optimization of the reaction condition, we realized that the product was relatively unstable and underwent decomposition to blackish oil after some time. This observation was similar to those made by Hammond, where phenyl substituted fluoroallene are highly unstable.[14] Attempt to stabilize the fluorinated allene by adjusting both the substitution pattern and electronic properties of the aryl group also gave no positive encouragement. Aromatic groups such as 3,5-$Me_2(C_6H_3)$ gave the targeted allene solely, only to decompose about isolation on even triethylamine treated silica gel. Other *p*-substituted aryl groups such as 4-MeO(C_6H_4), 4-Me(C_6H_4) and even electronically neutral phenyl group gave more unstable allenes. Furthermore, they are often plagued with bimolecular side product, arising from the 1,4-shift of Rh-alkenyl species to Rh-aryl. Hence, the rhodium arylation protocol of such alkyne may be quite limited by the scope of the nucleophile, and the stability of the fluoroallenes formed.

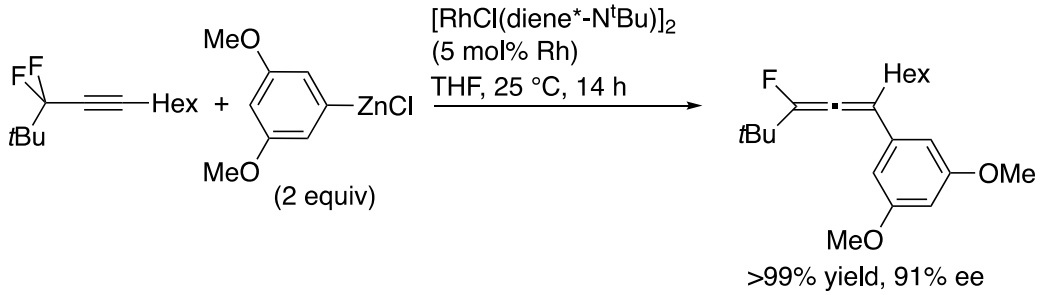

[a]Ratio of ArZnCl: (ArMgBr: $ZnCl_2$ = 1.0: 2.0)

Scheme 3.16 Rhodium-catalyzed addition of arylzinc chloride onto tert-butyl difluoroalkyne

In 2009, Lam and co-workers reported the alkylation and arylation of ynamides via rhodium-catalyzed addition of organozinc reagents (**Scheme 3.17**).[20] Although the driving force of the reaction was attributed to the stability of the oxygen coordinated alkenylzinc intermediate, it has demonstrated that alkylrhodation of alkyne is possible under a specially designed system. Thus, we sought to examine the generality of such rhodium-catalyzed alkylation on the basis of our preliminary results, as well as the electronic effect of alkyl groups on the stability of fluoroallenes.

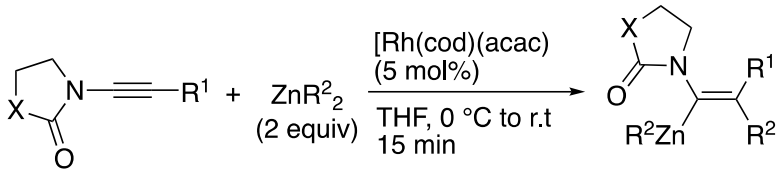

X = C/O/N
R^1 = Ph/Alkyl
R^2 = Bn/Ar/Het-Ar/alkenyl

Scheme 3.17 Rhodium-catalyzed addition of alkylzinc chloride onto ynamide

Fortunately, the rhodium-catalyzed benzylation of 3,3-difluoro-2,2-dimethylundec-4-yne with a 3-methoxybenzylzinc reagent proceeded smoothly to

afford the corresponding racemic fluorinated allene in excellent 98% NMR yield (**Scheme 3.18**). The trialkyl-substituted fluoroallene proved to be much more stable than its aryl-substituted fluoroallene counterpart.

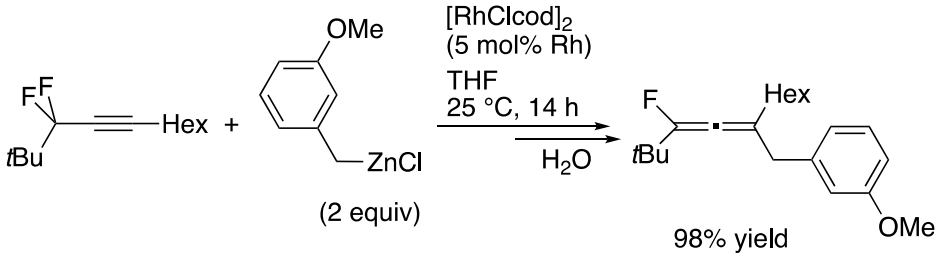

Scheme 3.18 Rhodium-catalyzed addition of 3-OMe(C_6H_4)CH_2ZnCl onto tert-butyl difluoroalkyne

Optimization of the reaction conditions, including the chiral catalyst, solvent, temperature, organozinc reagents was performed. Using [RhCl-(diene*-N*t*Bu)]$_2$, under the standard reaction condition, **3aa** was afforded in good isolated yield of 69% and 91% ee (entry 1) (**Table 3.1**). Increasing the temperature of the reaction gave similar conversion and yield (entry 2). Although increasing the catalyst loading to 10 mol% Rh increased the yield of **3aa**, the increment was not substantial (entry 3). Interestingly, the change of solvent from THF to diethyl ether caused a huge decline in the enantioselectivity of **3aa** to 8% ee (entry 4). Perhaps, the background side reaction of β-F elimination of alkenyl zinc intermediate is comparatively faster than the β-F elimination of alkenylrhodium intermediate in diethyl ether. The use of dibenzylic zinc reagent led to poorer yield and conversion (entry 5). Similarly, benzylzinc bromide prepared from RMgBr and $ZnBr_2$, gave lower isolated yield despite the similar conversion (entry 6). However, the enantioselectivity was essentially the same, indicating that the halide ions have little to no effects on the enantioselectivity.

Furthermore, increasing the amount of $ZnCl_2$ for the preparation of RZnCl led to a decline in the conversion and thus the isolated yield (entries 7 and 8). Fortunately, the enantioselectivity remained the same, showing that the concentration of zinc chloride does not affect the rate of the background reaction. On the other hand, the use of other organometallic reagents such as 3-MeO(C_6H_4)CH_2SnBu_3 gave recovery of starting material.

Table 3.1 Optimization of reaction conditions

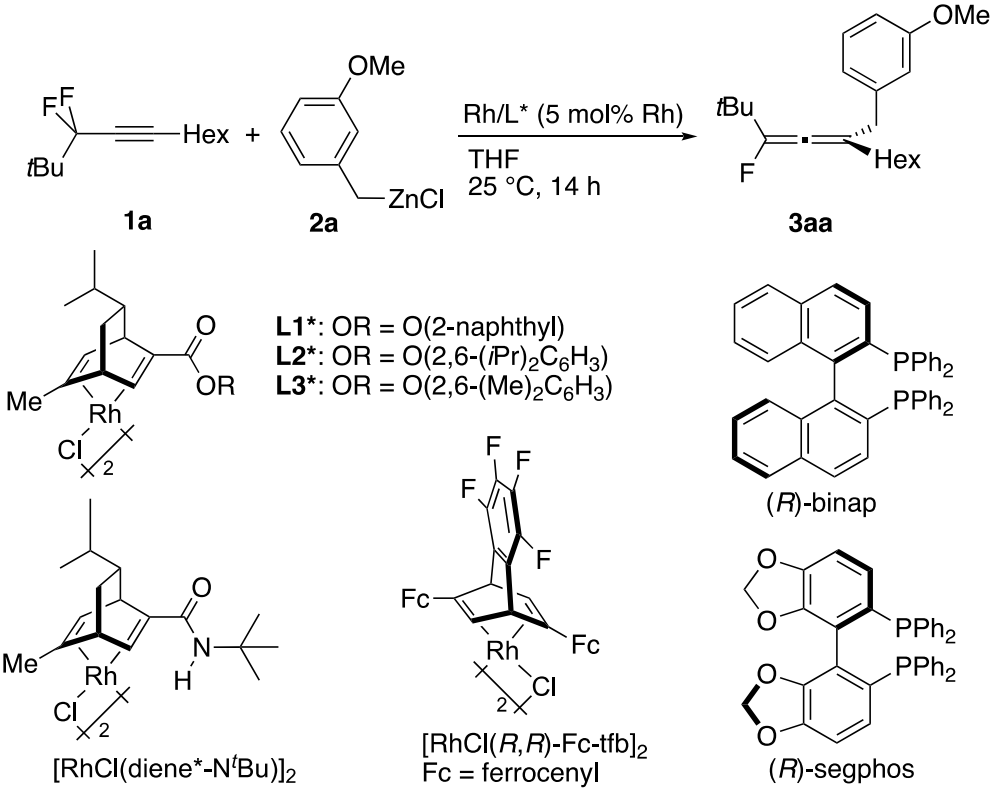

Entry	Rh/L*	Variation from standard Condition	Conv. [%][b] of **1a**	Yield [%][c] of **3aa**	*ee* [%] of **3aa**[d]
1	[RhCl(diene*-N*t*Bu)]$_2$	—	72	69	91 (*R*)
2	[RhCl(diene*-N*t*Bu)]$_2$	40 °C	73	70[b]	—
3	[RhCl(diene*-N*t*Bu)]$_2$	10 mol% Rh	87	77	93 (*R*)
4	[RhCl(diene*-N*t*Bu)]$_2$	Et_2O	73	55	8
5	[RhCl(diene*-N*t*Bu)]$_2$	(R_2Zn)	41	41[b]	—
6	[RhCl(diene*-N*t*Bu)]$_2$	RZnBr	71	55	90 (*R*)

7	[RhCl(diene*****-N*t*Bu)]$_2$	RZnCl[e]	60	47	90 (*R*)
8	[RhCl(diene*****-N*t*Bu)]$_2$	RZnCl[f]	43	24	91 (*R*)
9	[RhCl(diene*****-N*t*Bu)]$_2$	RSnBu$_3$[g]	recovery	—	—
10	Rh-L1*****	—	98	74	92 (*R*)
11	Rh-L2*****	—	92	60	97 (*R*)
12	Rh-L3*****	—	94	61	96 (*R*)
13	[RhCl(*R*,*R*)-Fc-tfb]$_2$	—	96	75	98 (*S*)
14	(*R*)-binap[h]	—	recovery	—	—
15	(*R*)-segphos[i]	—	recovery	—	—

[a] Reaction condition: **1a** (0.15 mmol), **2a** (0.30 mmol), 5 mol% of Rh, THF (0.8 mL), 25 °C, 14 h. **2a** (0.2 M) prepared from RMgBr (1.0 equiv) + $ZnCl_2$ (2.2 equiv). [b] Determined by ^{19}F NMR of the reaction mixture. [c] Isolated yield. [d] The *ee* value was determined by HPLC using a chiral stationary phase column. [e] $ArCH_2MgBr$ (1.0 equiv) + $ZnCl_2$ (3.0 equiv) [f] $ArCH_2MgBr$ (1.0 equiv) + $ZnCl_2$ (5.0 equiv) [g] Conducted in dioxane (1 mL), NaOMe (20 mol%), 25 °C, 14 h. [h] binap = 2,2′-bis(diphenylphosphino)-1,1′-binaphthyl. [Rh] = $[RhCl(coe)_2]_2$ (5 mol% Rh)/ L* (5.5 mol%) [i] segphos = 5,5′-bis(diphenylphosphino)-4,4′-bi-1,3-benzodioxole. [Rh] = $[RhCl(coe)_2]_2$ (5 mol% Rh)/ L* (5.5 mol%). THF = tetrahydrofuran

Upon screening other diene-based catalysts, we realized that the C_1-symmetric ester diene **L1*** gave better yield and slightly higher enantioselectivity (entry 10). In addition, the use of analogous catalysts bearing bulkier 2,6-(*i*Pr)$_2C_6H_3$ group or 2,6-(Me)$_2C_6H_3$ led to even better enantioselectivity of 97% ee and 96% ee respectively (entries 11 & 12). However, this was also accompanied by a modest yield of 60–61% yield. Thus, we arrived at [RhCl(*R*,*R*)-Fc-tfb]$_2$ that gave the best combination of high yield and excellent enantioselectivity (entry 13). Diphosphine ligands such as (*R*)-binap or (*R*)-segphos were ineffective in this transformation (entries 14 and 15).

The alpha, alpha-difluoroalkynes bearing different substituents at the propargylic (**R^1**) and acetylenic (**R^2**) positions were subjected to the reaction with 3-methoxybenzylzinc reagent under the optimized conditions, affording the corresponding fluoroallenes **3aa**–**3ha** in good yields and enantioselectivity (**Table 3.2**). The substrate bearing a phenethyl group as R^2 (**1b**) gave the desired product **3ba** in 85% yield and 96% ee. Interestingly, a methoxymethyl group as R^2 (**1c**) caused slight decrease in the enantioselectivity to 86% ee (see **3ca**). With a tosylethyl group as R^2

(**1e**), similarly high enantioselectivity of 94% ee was obtained. Other substrates featuring bulkier R^2 group such cyclohexylmethyl group (**1d**) gave the desired fluoroallene **3da** in excellent enantioselectivity of 98% ee. By incorporating a bulkier group at the propargylic (R^1) position, substrates bearing a 1-adamantyl (**1f**), 1-methylcyclohexane (**1g**), and 1-methylethylbenzene groups all gave excellent enantioselectivity induction, giving the targeted fluoroallenes **3fa**, **3ga**, **3ha** in 99% ee.

Table 3.2 Asymmetric benzylation of **1a**–**1h** to give **3aa**–**3ha**

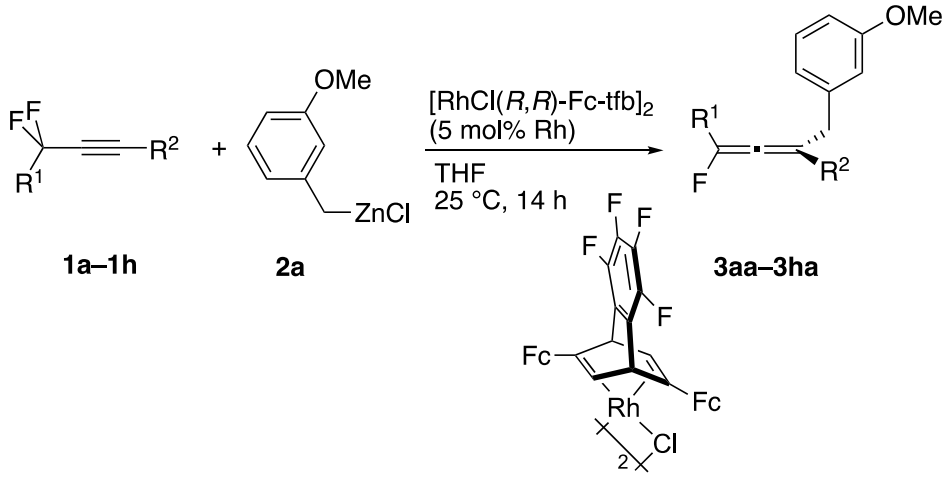

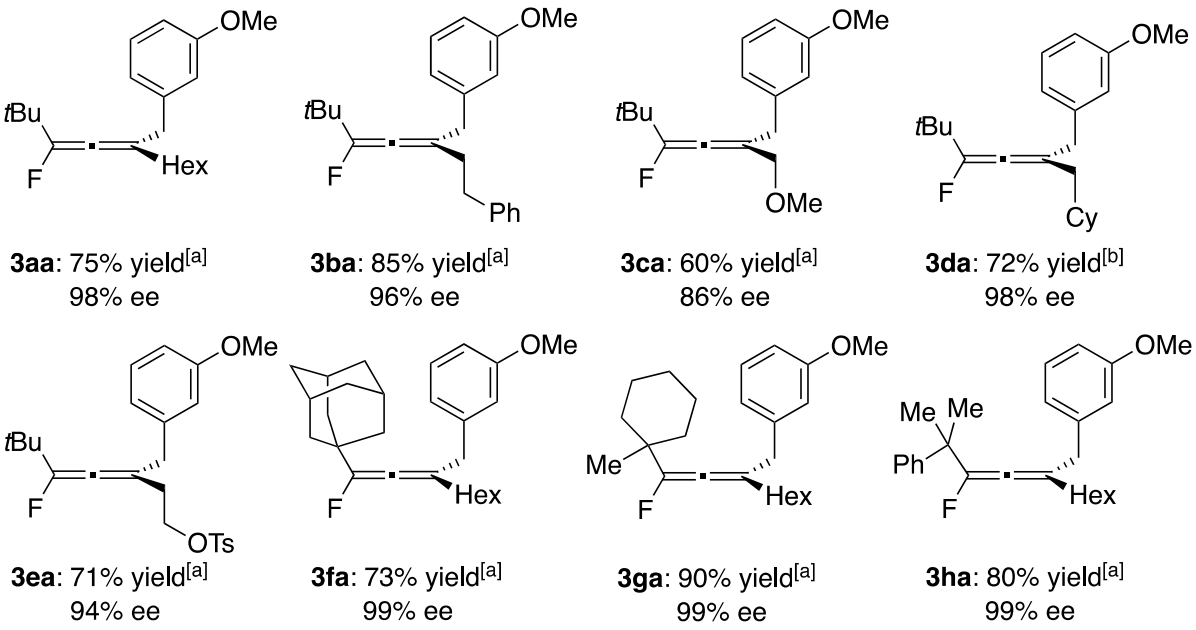

3aa: 75% yield[a] 98% ee

3ba: 85% yield[a] 96% ee

3ca: 60% yield[a] 86% ee

3da: 72% yield[b] 98% ee

3ea: 71% yield[a] 94% ee

3fa: 73% yield[a] 99% ee

3ga: 90% yield[a] 99% ee

3ha: 80% yield[a] 99% ee

[a] Reaction condition: **1a**–**1h** (0.15 mmol), **2a** (0.30 mmol), 5 mol% of Rh, THF (0.8 mL), 25 °C, 14 h. **2a** (0.2 M) prepared from RMgBr (1.0 equiv) + $ZnCl_2$ (2.2 equiv). [b] RZnCl = RMgBr (1.0 equiv) + $ZnCl_2$ (2.8 equiv)

The present reaction proved to tolerate a series of benzylzinc reagents, as demonstrated by their reactions with the alkyne substrate **1e** (**Table 3.3**). For instance, the unsubstituted benzyl group of the zinc reagent **2b** was introduced with an isolated yield of 47% and 96% ee. The low yield was due to the difficulty in isolation from the unconverted substrate. Prolonged isolation on silica gel, in addition to the inherent instability of the product, led to a diminished yield. When 3-methylbenzylzinc chloride was employed, the corresponding fluoroallene **3ec** was obtained in a yield of 51% and 93% ee, due to the low conversion of the substrate. Interestingly, the attempt to increase the conversion by increasing temperature (50 °C) did not improve the yield and yet led to an erosion of enantioselectivity, giving **3ec** of 76% ee.

Table 3.3 Asymmetric alkylation of **1e** to give **3ea**–**3eh**

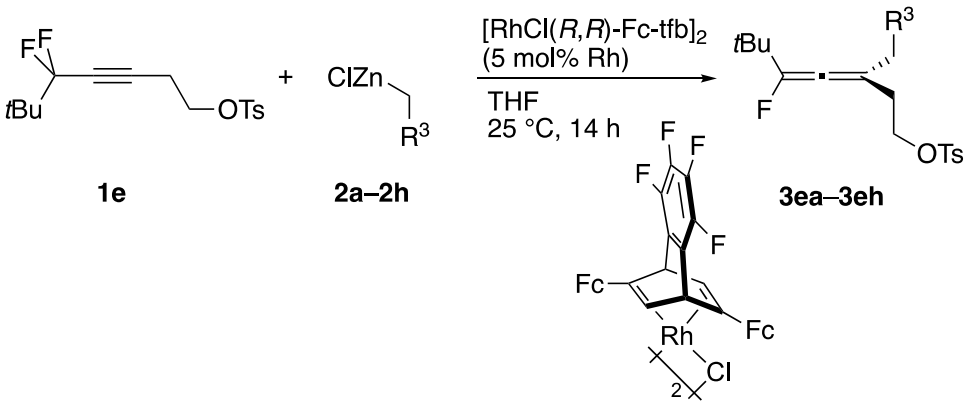

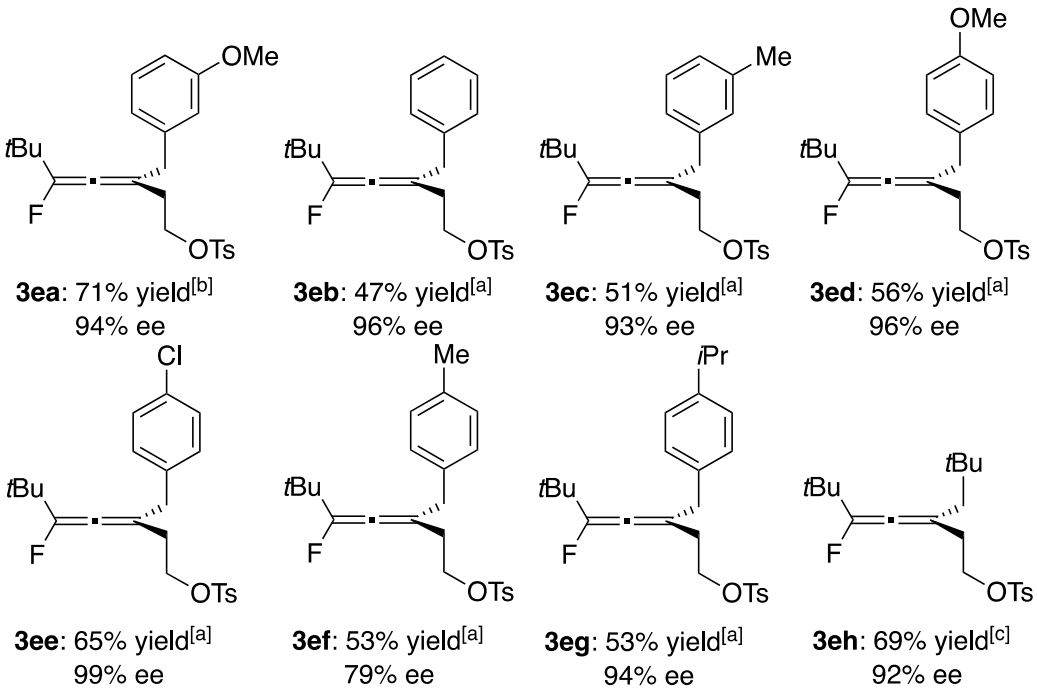

[a] Reaction condition: **1e** (0.15 mmol), **2a**–**2h** (0.30 mmol), 5 mol% of Rh, THF (0.8 mL), 25 °C, 14 h. RZnCl = RMgCl (1.0 equiv) + $ZnCl_2$ (2.2 equiv). [b] RZnCl = RMgBr (1.0 equiv) + $ZnCl_2$ (2.2 equiv). [c] RZnCl = RMgBr (1.0 equiv) + $ZnCl_2$ (2.0 equiv)

Generally, the use of para-substituted benzylzinc chloride was successful in the case of fluoroallene **3ed** and **3ee**, with 4-methoxybenzyl and 4-chlorobenzyl group being incorporated to give **3ed** and **3ee** in 96% ee and 99% ee respectively. It is noteworthy to realize that the highest enantioselectivity was achieved with 4-$Cl(C_6H_4)CH_2$ group. Furthermore, it was also interesting to note that electronically

similar 4-Me(C_6H_4)CH_2 (**3ef**) and 4-*i*Pr(C_6H_4)CH_2 (**3eg**) group contributed stark difference to the final enantioselectivity of the product. Axially chiral fluoroallene **3ef** with 4-methylphenyl group as R^3 was isolated in only 79% ee while fluoroallene **3eg** with 4-isopropylphenyl group as R^3 was obtained in much higher 94% ee. Electron-withdrawing group such as 4-F(C_6H_4)CH_2 led to complex mixture. Given these observations, the role of the electronic and steric nature of the benzyl group in the present reaction remain unclear.

Besides the benzylzinc reagents, neopentylzinc chloride also afforded the corresponding fluoroallene **3eh** in good yield of 69% and 92% ee. In the case of other alkyl zinc reagent such as EtZnCl/*i*PrZnCl/*i*PrCH_2ZnCl, the reaction either gave recovery of the substrate or very poor conversion, possibly due to the availability of β-hydrogen.

Based on our previous understanding of unstable electron-rich aryl-substituted fluoroallene, we figured that electron-withdrawing groups may aid in stabilizing the targeted fluoroallene. In the presence of [RhCl(*R,R*)-Fc-tfb]$_2$ catalyst, the addition of 4-chlorobenzylzinc chloride **2e** onto alpha, alpha-difluoroalkyne containing 3,5-difluorophenyl group **1i** gave **3ie** in good yield of 73% and 89% ee (**Scheme 3.19**). Despite the lower enantioselectivity, we hope that this may serve as a preliminary indication for the future development of stable aryl-substituted fluoroallenes. Furthermore, by preparative HPLC purification with the use of a chiral stationary phase column (Chiralpak IB), we were able to obtain enantiopure (*R*)-**3ie** as the major enantiomer. The absolute configuration of **3ie** was determined to be (*R*) by X-ray crystallographic analysis. All other analogous fluoroallenes were assumed to have the same absolute configuration.

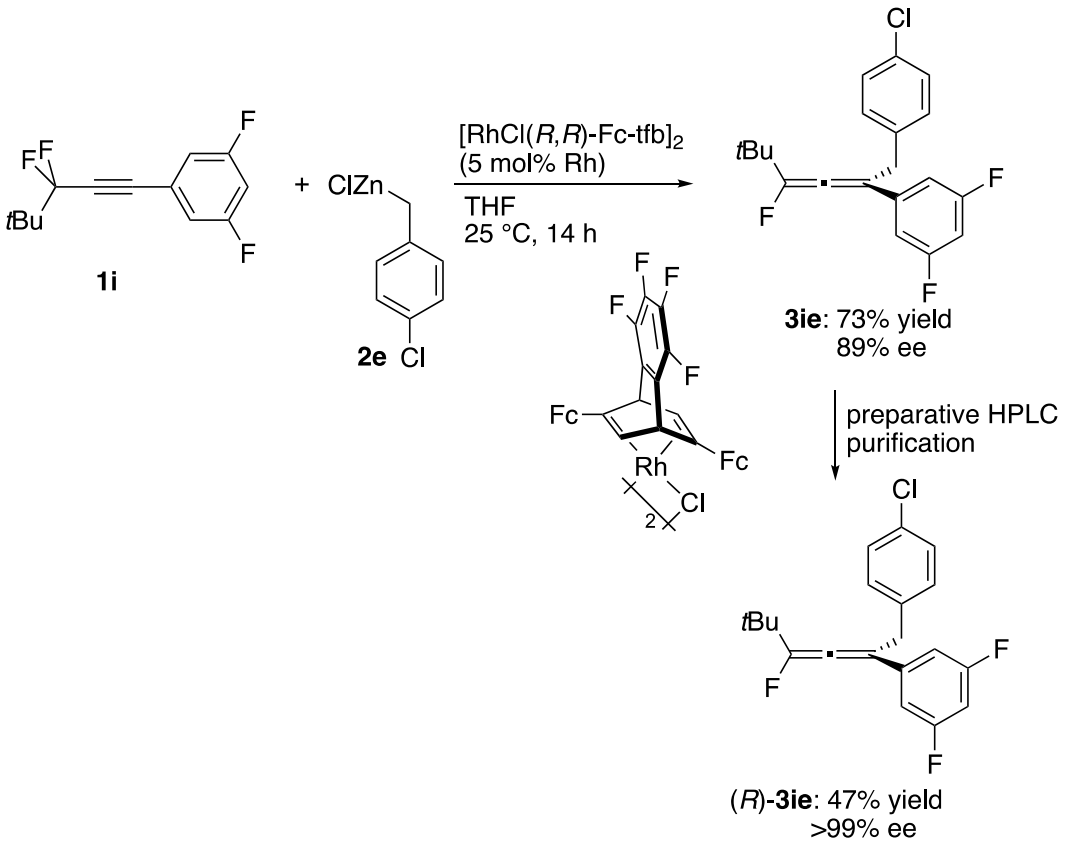

Scheme 3.19 Asymmetric addition of zinc reagent **2e** onto aryl substituted **1i**

A catalytic cycle of the present alkylation of the alkyne/β-fluoride elimination is proposed in **Scheme 3.20**. First, the [Rh]–Cl species (**A**) undergoes transmetalation with alkylzinc chloride **2** to generate alkylrhodium intermediate [Rh]–R^3, (**B**). The intermediate **B** then adds onto the alpha,alpha-difluoroalkyne **1** via alkylrhodation in a *syn*-fashion, giving alkenylrhodium intermediate **C**. The intermediate **C**, with its neighboring fluoride atom positioned in a Rh–C_{sp2}–C_{sp3}–F co-planar spatial arrangement, then proceeds to undergo *syn* β-fluoride elimination. Alternatively, the intermediate **C** can also transmetalate with zinc chloride to give the alkenylzinc intermediate. The β-fluoride elimination of the Rh intermediate **C** affords the target fluoroallene, giving [Rh]–F as intermediate **D**. **D** can either undergo a halide exchange to regenerate [Rh]–Cl species **A**, or a direct transmetallation with alkylzinc chloride **2** to regenerate **B**.

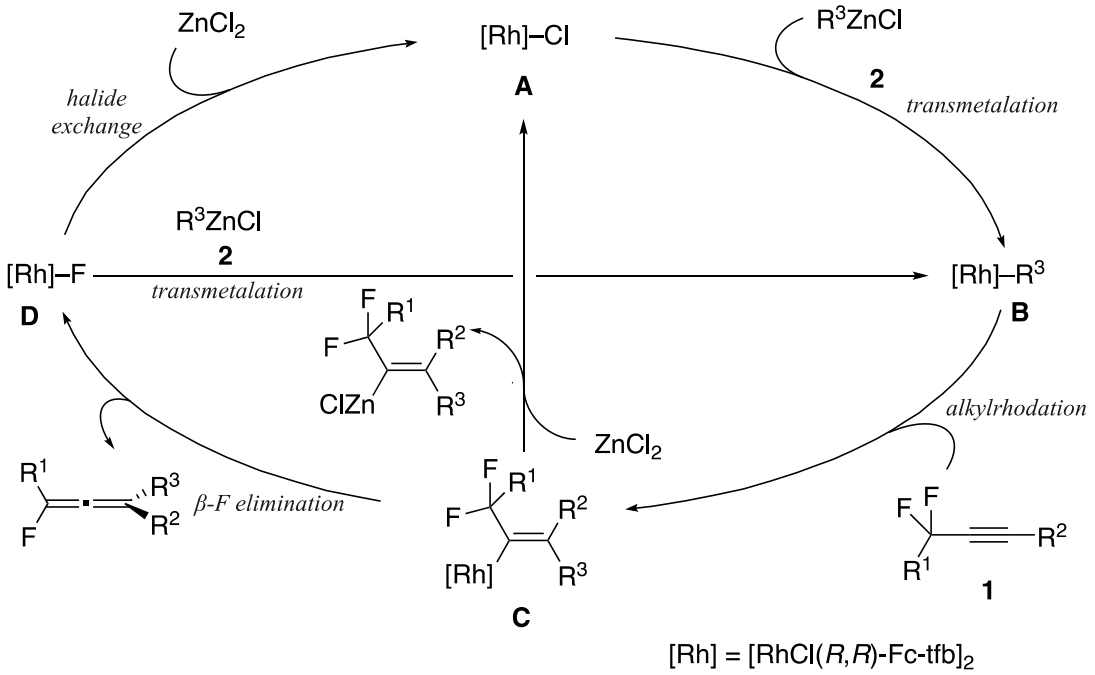

Scheme 3.20 Proposed catalytic cycle

On a side note, the background reaction stems from the ability of the alkenylzinc intermediate to undergo β-fluoride elimination to afford the racemic allene. We speculate that the step from **C** to **D** is likely the rate-determining step. Should this step be slow, the formation of the stable alkenylzinc reagent would be favored and result in a lowering of the enantioselectivity.

A stereoinduction model was also proposed for the control of the enantioselectivity by the [RhCl(*R*,*R*)-Fc-tfb]$_2$ catalyst (**Scheme 3.21**). First, the alkyne substrate coordinates to the rhodium in a position parallel to Rh–CH_2 bond. This then allows for the *syn* addition of the Rh–CH_2Ar bond onto the triple bond. The alkenylrhodium intermediate formed exists in an equilibrium as proposed, with it favoring the *tert*-butyl group pointing away from the ferrocenyl group. The massive difference between the steric bulkiness of the *tert*-butyl group and the fluoride group

thus allows for excellent chirality induction. Upon *syn* β-fluoride elimination, it will give the target fluoroallene in the (*R*)-configuration.

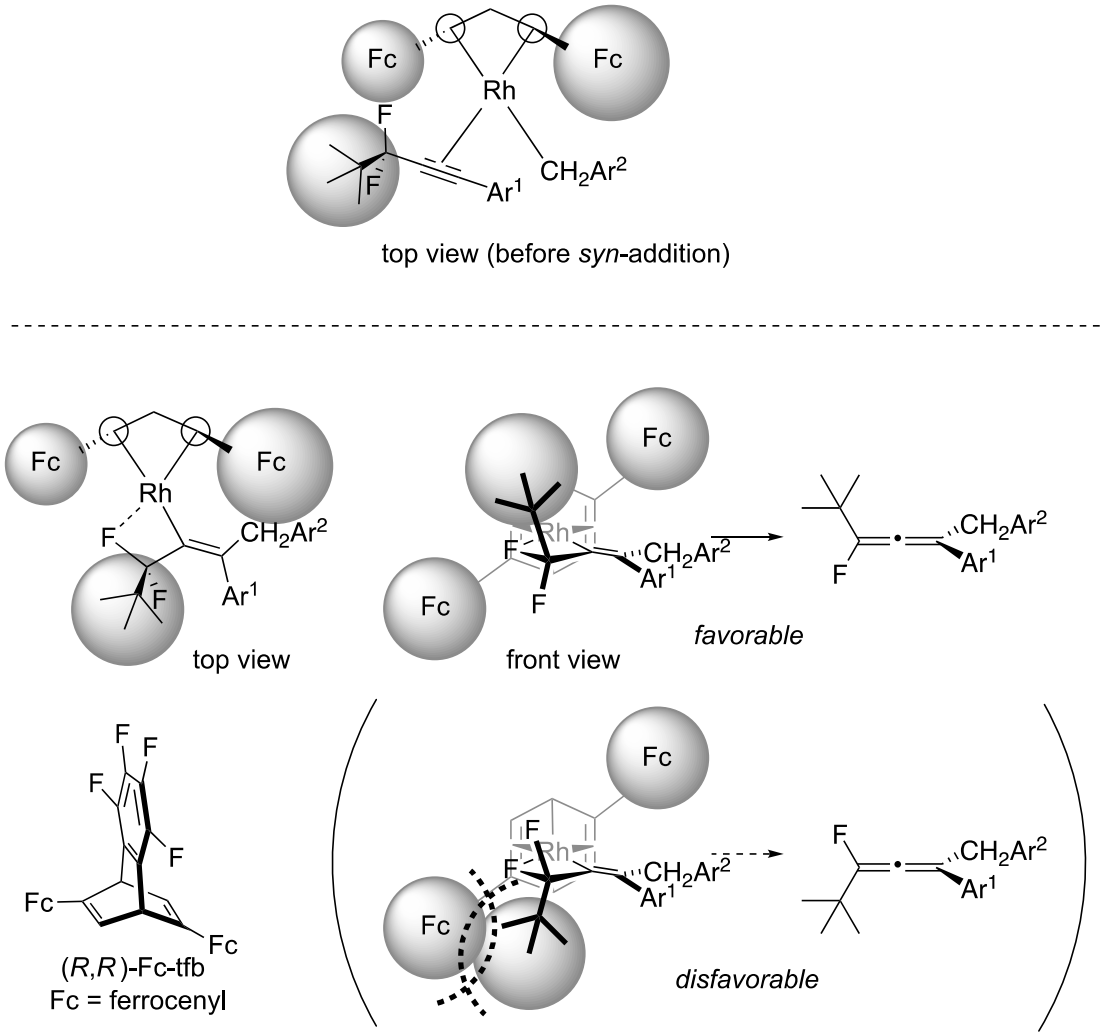

Scheme 3.21 Proposed stereoinduction model

In an attempt to further elucidate the reaction pathway, the addition of benzylzinc chloride **2b** onto alpha,alpha-difluoroalkyne **1i** bearing 3,5-difluorophenyl group proceeded smoothly to give the corresponding fluoroallene (*R*)-**3ib** in excellent 94% yield and good enantioselectivity of 83% ee (**Scheme 3.22**).

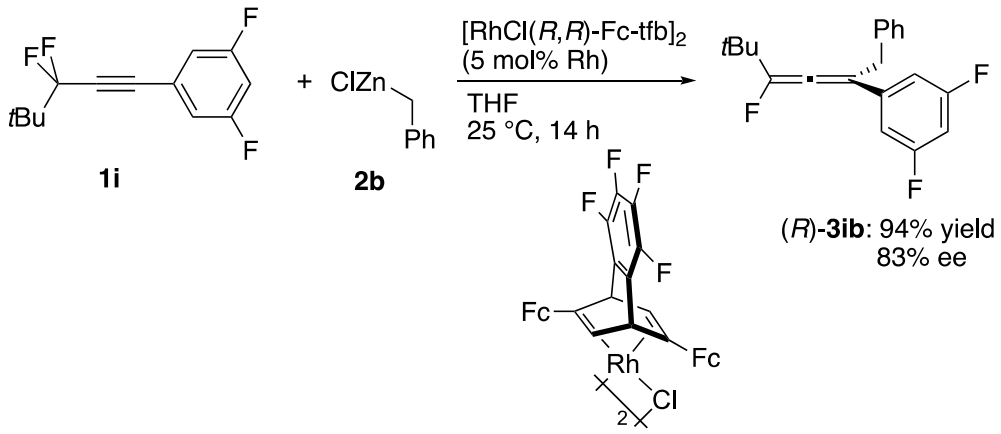

Scheme 3.22 Rhodium-catalyzed benzylic addition onto alpha, alpha-difluoroalkyne **1i** to give (*R*)-**3ib**

On this note, we notice that **3ib** can also be synthesized with an inverse combination of substrate and arylzinc reagent. The aryl-addition of 3,5-difluorophenylzinc chloride **2i** was performed with alpha, alpha-difluoroalkyne **1j** bearing benzyl group as the substrate to give fluoroallene (*S*)-**3ib** (**Scheme 3.23**). With the use of RhCl(*R*,*R*)-Fc-tfb complex as the catalyst, **3ib** was obtained in 67% yield and a much higher 93% ee. More importantly, it must be highlighted that the product **3ib** obtained in **Scheme 3.22** and **Scheme 3.23** are of opposite configuration based on HPLC analysis. The underlying importance of this discovery cannot be overemphasized that opposite enantiomers of an axially chiral fluoroallene were synthesized with the same chiral catalyst configuration. This interesting phenomenon can be explained closely by the prior stereo-induction model proposed (**Scheme 3.24**).

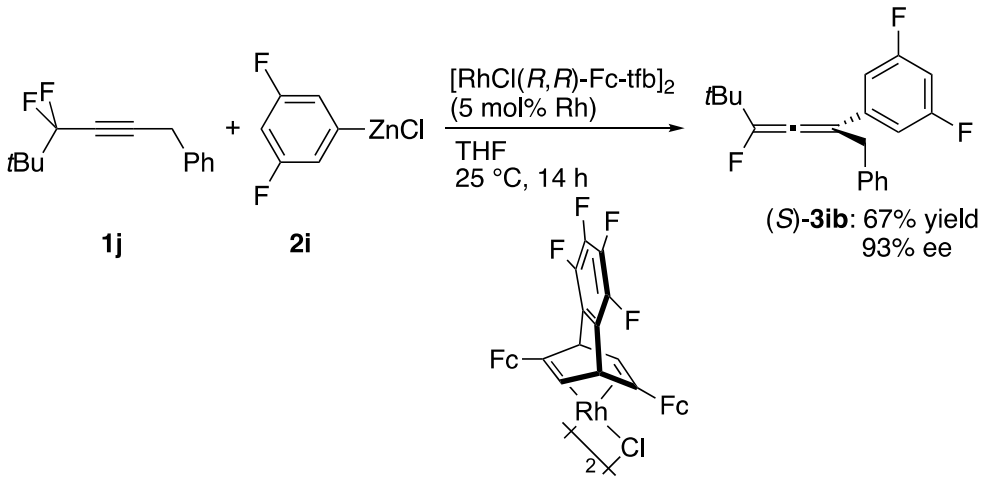

Scheme 3.23 Rhodium-catalyzed aryl addition of 3,5-difluorophenylzinc chloride onto **1j** to give fluoroallene (*S*)-**3ib**

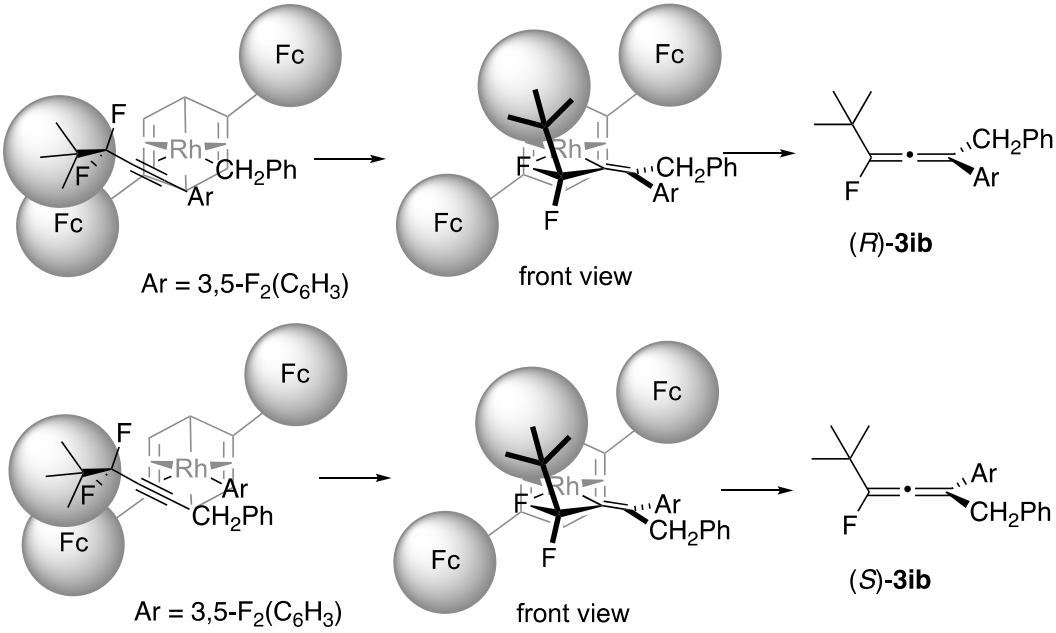

Scheme 3.24 Proposed stereo-induction model for inversed combination

In both cases, the benzyl and aryl addition take place in the same *syn*-addition fashion onto the difluoroalkyne. This gives a diastereomeric alkenylrhodium intermediate, with the former having the benzyl group *cis* to rhodium and the latter having the benzyl group *trans* to rhodium. As the position of the ferrocenyl groups on

the diene ultimately decides which enantiotopic fluorine atoms eliminate, both rhodium intermediates should undergo a *syn*-elimination of the same fluorine atom regardless of the geometry of the alkene. As such, it is expected that **3ib** was produced with opposite configuration through these inverse combination reactions.

While allenes with incorporated fluorine itself can be an interesting compound that has direct synthetic value, other transformation of the fluoroallenes is also applicable. For instance, the tosylate functionality in the product **3ee** was displaced by iodide, affording the corresponding product **3ke** in excellent yield with retention of the stereochemistry (**Scheme 3.25**). The formation of such versatile and reactive alkyl iodide may prove to be a useful synthon for further transformation, such as those of the formation of Wittig reagent.

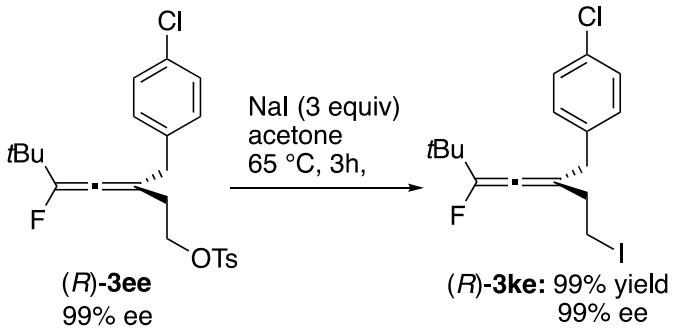

(*R*)-**3ee**
99% ee

(*R*)-**3ke:** 99% yield
99% ee

Scheme 3.25 Transformation of **3ee** to **3ke**

3.3. Conclusion

In conclusion, we have demonstrated the first asymmetric rhodium-catalyzed alkylation/β-fluoride elimination reaction to generate axially chiral fluoroallene in good yield and enantioselectivity of up to 99% ee. Axially chiral fluoroallenes with multiple substitutions of both alkyl and aryl groups have been made accessible, which has been impossible with previously reported methods. The reaction most likely involves a *syn* beta-fluoride elimination of alkenylrhodium intermediate as the critical enantioselectivity-determining step, and present work would hold promise for further development of novel synthetic methods involving this elementary step.

3.4. Experimental

3.4.1. General method

All anaerobic and moisture-sensitive manipulations were carried out with standard Schlenk techniques under inert gas. NMR spectra were recorded on a AV 300, BBO probe (300 MHz for ^{1}H, 75 MHz for ^{13}C, 282 MHz for ^{19}F), or Bruker AV 400, QNP probe (400 MHz for ^{1}H, 100 MHz for ^{13}C, 376 MHz for ^{19}F), or Bruker AVIII 400 MHz NMR, BBFO Probe (400 MHz for ^{1}H, 100 MHz for ^{13}C, 376 MHz for ^{19}F), or Bruker AV 500, BBI probe (500 MHz for ^{1}H, 125 MHz for ^{13}C, 470 MHz for ^{19}F). Chemical shifts are reported in δ (ppm) referenced to the residual peaks of $CDCl_3$ (δ 7.26) for ^{1}H NMR and $CDCl_3$ (δ 77.00) for ^{13}C NMR. The following abbreviations are used; s: singlet, d: doublet, t: triplet, q: quartet, quint: quintet, sext: sextet, sep: septet, m: multiplet. High resolution mass spectra (HRMS) were obtained on a Waters Q-Tof Premier mass spectrometer. For thin layer chromatography (TLC), Merck pre-coated TLC plates (Merck 60 F254) were used, and compounds were visualized with a UV light at 254 nm. Further visualization was achieved by basic aqueous $KMnO_4$ solution stain. Flash column chromatography was performed with Silica gel 60 (Merck). Optical rotations were recorded on an Anton Paar MCP 150 machine. Enantiomeric excesses (ee) were determined by HPLC analysis on Shimadzu HPLC with Daicel chiral columns. Separation of enantiomers was performed with a JAI recycling preparative HPLC.

3.4.2. Materials

All commercially available reagents listed below were used as received for the reactions without further purification: 1-octyne (Sigma Aldrich), 4-phenyl-1-butyne (Sigma Aldrich), methyl propargyl ether (Sigma Aldrich), 3-cyclohexyl-1-propyne (Fluorochem), 3-butyn-1-ol (Alfa Aesar), 1-ethynyl-3,5-difluorobenzene (Sigma Aldrich), magnesium turnings (Sigma Aldrich), 1-bromo-3,5-difluorobenzene (Sigma Aldrich), 1-bromo-3,5-dimethoxybenzene (Sigma Aldrich), 3-methoxybenzyl bromide (Sigma Aldrich), benzyl chloride (Sigma Aldrich), 3-methylbenzyl chloride (Sigma Aldrich), 4-methoxybenzyl chloride (Sigma Aldrich), 4-chlorobenzyl chloride (Sigma Aldrich), 4-methylbenzyl chloride (Sigma Aldrich), 4-isopropylbenzyl chloride (Sigma Aldrich), neopentyl bromide (Alfa Aesar), *n*-butyllithium (Kanto Chemical), isopropylmagnesium bromide (Sigma Aldrich), diethylaminosulfur trifluoride (DAST) (Fluorochem), sodium iodide (Sigma Aldrich), zinc chloride (Sigma Aldrich), zinc fluoride (Sigma Aldrich), zinc bromide (Sigma Aldrich), zinc fluoride (Sigma Aldrich), lithium chloride (Sino), (*S*)-BINAP (Kanto Chemical), (*R*)-BINAP (Kanto Chemical), (*R*)-SEGPHOS (TCI), acetone (VWR), anhydrous acetonitrile (Sigma Aldrich), eriochrome black T (Sigma Aldrich), ethylenediaminetetraacetic acid (Sigma Aldrich), iodine (Tokyo Chemical Industry). Dry tetrahydrofuran was obtained via a solvent purification system (PS-400-5, innovative technology Inc.). 3-MeO(C_6H_4)CH_2SnBu_3 was synthesized according to reported procedures.[21]

L1*,[22] L2*,[23], L3*,[24] [RhCl(cod)]$_2$,[25] [RhCl(coe)$_2$]$_2$,[26] [RhCl((*R*,*R*)-Fc-tfb]$_2$,[27] [RhCl(diene*-N*t*Bu)]$_2$,[28-29] and [RhCl((*R*,*R*)-Ph-bod]$_2$[30] were prepared accordingly to the reported procedures.

3.4.3. Preparation of Weinreb amide

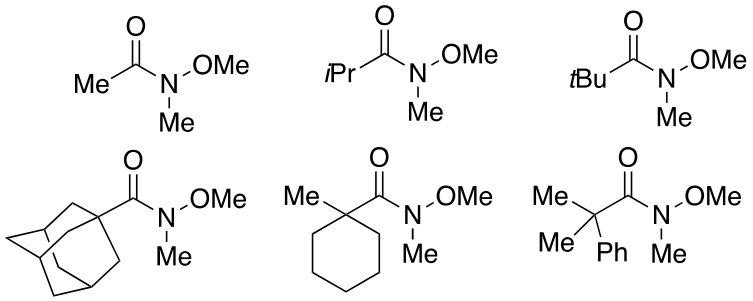

N-methoxy-*N*-methylacetamide, *N*-methoxy-*N*-methylisobutyramide, *N*-methoxy-*N*-methylpivalamide, *N*-methoxy-*N*-methyladmantane-1-carboxamide, *N*-methoxy-*N*,1-dimethylcyclohexane-1-carboxamide, and *N*-methoxy-*N*,2-dimethyl-2-phenylpropanamide were prepared according to previously reported procedures.[31]

3.4.4. Preparation of ketones and difluoroalkynes

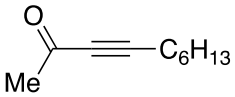

It was prepared according to reported procedure.[32]

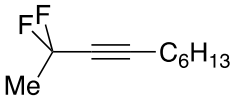

A 2-neck vessel was charged with dec-3-yn-2-one (0.298 g, 1.80 mmol) under N_2 gas. Three vacuum/refill cycles were performed, and 5 drops of EtOH were added. The solution was cooled to 0 °C, followed by the addition of DAST (0.723 g, 0.600 mL, 4.50 mmol) in portion. The mixture was kept stirring for 0.5 h before warming to room temperature and heated at 50 °C for 6 h. The mixture was cooled to 0 °C before being diluted with dichloromethane (20 mL). Saturated NH_4Cl (20 mL) was added dropwise at 0 °C. The mixture was warmed to room temperature, followed by extraction with dichloromethane (10 mL x 2). The combined organic layer was dried over Na_2SO_4, and

filtered. Removal of solvent on a rotary evaporator and silica gel chromatography of the residue with hexane gives 2,2-difluorodec-3-yne (30.0 mg, 10% yield).

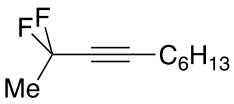

(pale yellow liquid). ^{1}H NMR (300 MHz, $CDCl_3$) δ 0.89 (t, J = 6.4 Hz, 3H), 1.23–1.35 (m, 4H), 1.54 (quint, J = 6.7 Hz, 2H), 1.48–1.60 (m, 2H), 1.84 (t, J = 17.1 Hz, 3H), 2.25 (tt, J = 6.9 Hz, 5.1 Hz, 2H).^{19}F{^{1}H} NMR ($CDCl_3$) δ –75.3. ^{13}C NMR (100 MHz, $CDCl_3$) δ 14.0, 18.3 (t, J_{CF} = 2.3 Hz), 22.5, 27.1, (t, J_{CF} = 29.3 Hz), 27.7 (t, J_{CF} = 1.9 Hz), 28.4, 31.2, 74.7 (t, J_{CF} = 40.0 Hz), 87.9 (t, J_{CF} = 6.5 Hz), 112.9 (t, J_{CF} = 227.2 Hz). HRMS (ESI) calcd for $C_{10}H_{17}F_2$ $[M+H]^+$ 175.1298, found 175.1298.

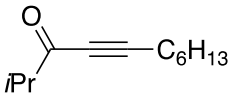

A 2-neck vessel was charged with 1-octyne (1.10 g, 10.0 mmol) under N_2 gas. THF (10 mL) was added and the solution was cooled to –78 °C for 10 min. To the solution was added dropwise 1.57 M *n*-BuLi (7.0 mL, 11.0 mmol), followed by stirring for 1h. *N*-methoxy-*N*-methylisobutyramide (1.44 g, 11.0 mmol) was added to the mixture and stirred for 5 min at –78 °C. The mixture was warmed to room temperature and kept stirring for 6 h. H_2O (20 mL) was added and the mixture was extracted with dichloromethane (20 mL x 2). The combined layer was dried over $NaSO_4$, and filtered. Removal of solvent on a rotary evaporator and silica gel chromatography of the residue with hexane/ether (10/1) give a pale-yellow liquid (0.614 g, 34% yield). The NMR spectra obtained is in agreement with those as reported.[33]

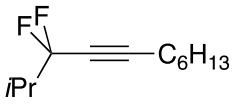

A 2-neck vessel was charged with 2-methylundec-4-yn-3-one (0.510 g, 2.83 mmol) under N_2 gas. Three vacuum/refill cycles were performed, and 5 drops of EtOH were added. The solution was cooled to 0 °C, followed by the addition of DAST (1.14 g, 0.900 mL, 7.08 mmol) in portion. The mixture was kept stirring for 0.5 h before warming to room temperature and heated at 50 °C for 14 h. The mixture was cooled to 0 °C before being diluted with dichloromethane (20 mL). Saturated NH_4Cl (20 mL) was added dropwise at 0 °C. The mixture was warmed to room temperature, followed by extraction with dichloromethane (10 mL x 2). The combined organic layer was dried over $NaSO_4$, and filtered. Removal of solvent on a rotary evaporator and silica gel chromatography of the residue with hexane gives 3,3-difluoro-2-methylundec-4-yne (0.170 g, 30% yield).

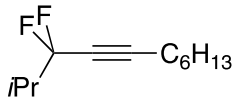

(pale yellow liquid). ^{1}H NMR (300 MHz, $CDCl_3$) δ 0.89 (t, J = 6.8 Hz, 3H), 1.07 (d, J = 6.8 Hz, 6H), 1.22–1.35 (m, 4H), 1.35–1.47 (m, 2H), 1.56 (quint, J = 6.8 Hz, 2H), 2.09–2.23 (m, 1H), 2.23–2.33 (m, 2H), .^{19}F{^{1}H} NMR ($CDCl_3$) δ –88.5. ^{13}C NMR (100 MHZ, $CDCl_3$) δ 14.0, 16.1 (t, J_{CF} = 3.7 Hz), 18.3 (t, J_{CF} = 2.3 Hz), 22.5, 27.8 (t, J_{CF} = 2.0 Hz), 28.4, 31.2, 37.0 (t, J_{CF} = 25.6Hz), 72.8 (t, J_{CF} = 40.1 Hz), 89.1 (t, J_{CF} = 6.6 Hz), 117.7 (t, J_{CF} = 231.7 Hz).HRMS (ESI) calcd for $C_{12}H_{21}F_2$ $[M+H]^+$ 203.1611, found 203.1611.

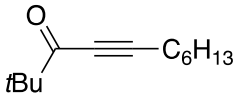

A 2-neck vessel was charged with 1-octyne (1.65 g, 15.0 mmol) under N_2 gas. THF (10 mL) was added and the solution was cooled to –78 °C for 10 min. To the solution was added dropwise 1.57 M *n*-BuLi (10.5 mL, 16.5 mmol), followed by stirring for 1h. *N*-methoxy-*N*-methylpivalamide (2.61 g, 18.0 mmol) was added to the mixture and stirred for 5 min at –78 °C. The mixture was warmed to room temperature and kept stirring for 5 h. H_2O (20 mL) was added and the mixture was extracted with dichloromethane (20 mL x 2). The combined layer was dried over $NaSO_4$, and filtered. Removal of solvent on a rotary evaporator and silica gel chromatography of the residue with hexane/ether (10/1) give a pale-yellow liquid (1.31 g, 45% yield). The NMR spectra obtained is in agreement with those as reported.[34]

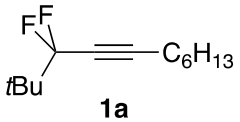

1a

A 2-neck vessel was charged with 2,2-dimethylundec-4-yn-3-one (1.08 g, 5.55 mmol) under N_2 gas. Three vacuum/refill cycles were performed, and 5 drops of EtOH were added. The solution was cooled to 0 °C, followed by the addition of DAST (2.24 g, 1.80 mL, 13.9 mmol) in portion. The mixture was kept stirring for 0.5 h before warming to room temperature and heated at 50 °C for 14 h. The mixture was cooled to 0 °C before being diluted with dichloromethane (20 mL). Saturated NH_4Cl (20 mL) was added dropwise at 0 °C. The mixture was warmed to room temperature, followed by extraction with dichloromethane (10 mL x 2). The combined organic layer was dried over $NaSO_4$, and filtered. Removal of solvent on a rotary evaporator and silica gel chromatography of the residue with hexane gives 3,3-difluoro-2,2-dimethylundec-4-yne (0.404 g, 34% yield).

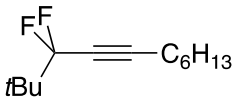

Compound 1a (pale yellow liquid). ^{1}H NMR (300 MHz, $CDCl_3$) δ 0.89 (t, J = 6.8 Hz, 3H), 1.09 (s, 9H), 1.28–1.31 (m, 4H), 1.35–1.45(m, 2H), 1.56 (quint, J = 6.8 Hz, 2H), 2.28 (tt, J = 6.9 Hz, 5.2 Hz, 2H). ^{19}F{^{1}H} NMR ($CDCl_3$) δ –94.4. ^{13}C NMR (100 MHz, $CDCl_3$) δ 13.9, 18.3 (t, J_{CF} = 2.4 Hz), 22.5, 23.6 (t, J_{CF} = 2.9 Hz), 27.9 (t, J_{CF} = 2.0 Hz), 28.4, 31.2, 39.2 (t, J_{CF} = 23.8 Hz), 72.9 (t, J_{CF} = 40.2 Hz), 88.9 (t, J_{CF} = 6.4 Hz), 118.9 (t, J_{CF} = 234.9 Hz). HRMS (ESI) calcd for $C_{13}H_{23}F_2$ $[M+H]^+$ 217.1768, found 217.1768.

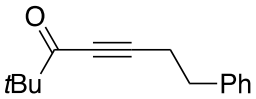

A 2-neck vessel was charged with 4-phenyl-1-butyne (1.95g, 15.0 mmol) under N_2 gas. THF (10 mL) was added and the solution was cooled to –78 °C for 10 min. To the solution was added dropwise 1.57 M *n*-BuLi (10.5 mL, 16.5 mmol), followed by stirring for 1h. *N*-methoxy-*N*-methylpivalamide (2.61 g, 18.0 mmol) was added to the mixture and stirred for 5 min at –78 °C. The mixture was warmed to room temperature and kept stirring for 5 h. H_2O (20 mL) was added and the mixture was extracted with dichloromethane (20 mL x 2). The combined layer was dried over $NaSO_4$, and filtered. Removal of solvent on a rotary evaporator and silica gel chromatography of the residue with hexane/ether (10/1) give a pale-yellow liquid (1.41 g, 44% yield). The NMR spectra obtained is in agreement with those as reported.[35]

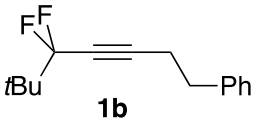

1b

A 2-neck vessel was charged with 2,2-dimethyl-7-phenylhept-4-yn-3-one (1.18 g, 5.50 mmol) under N_2 gas. Three vacuum/refill cycles were performed, and 5 drops of EtOH were added. The solution was cooled to 0 °C, followed by the addition of

DAST (2.22 g, 1.80 mL, 13.8 mmol) in portion. The mixture was kept stirring for 0.5 h before warming to room temperature and heated at 50 °C for 14 h. The mixture was cooled to 0 °C before being diluted with dichloromethane (20 mL). Saturated NH_4Cl (20 mL) was added dropwise at 0 °C. The mixture was warmed to room temperature, followed by extraction with dichloromethane (20 mL x 2). The combined organic layer was dried over $NaSO_4$, and filtered. Removal of solvent on a rotary evaporator and silica gel chromatography of the residue with hexane gives (5,5-difluoro-6,6-dimethylhept-3-yn-1-yl)benzene (0.583 g, 45% yield).

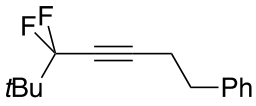

Compound 1b (pale yellow liquid). ^{1}H NMR (300 MHz, CDCl3) δ 1.02 (s, 9H), 2.58 (tt, J = 7.3 Hz, 5.0 Hz, 2H), 2.87 (t, J = 7.4 Hz, 2H), 7.17–7.25 (m, 3H), 7.25–7.33 (m, 2H). ^{19}F{^{1}H} NMR ($CDCl_3$) δ –94.5. ^{13}C NMR (100 MHz, $CDCl_3$) δ 20.5 (t, J_{CF} = 2.3 Hz), 23.5 (t, J_{CF} = 3.0 Hz), 34.1 (t, J_{CF} = 2.2 Hz), 39.1 (t, J_{CF} = 23.7 Hz), 73.7 (t, J_{CF} = 2.9 Hz), 87.9 (t, J_{CF} = 40.0 Hz), 118.8 (t, J_{CF} = 235.2 Hz), 126.5, 128.4, 128.5, 139.8. HRMS (ESI) calcd for $C_{15}H_{19}F_2$ $[M+H]^+$ 237.1455, found 237.1457.

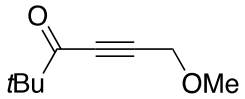

A 2-neck vessel was charged with methyl propargyl ether (0.700 g, 10.0 mmol) under N_2 gas. THF (10 mL) was added and the solution was cooled to –78 °C for 10 min. To the solution was added dropwise 1.57 M *n*-BuLi (7.0 mL, 11.0 mmol), followed by stirring for 1h. *N*-methoxy-*N*-methylpivalamide (1.74 g, 12.0 mmol) was added to the mixture and stirred for 5 min at –78 °C. The mixture was warmed to room temperature and kept stirring for 12 h. H_2O (20 mL) was added and the mixture was extracted with diethyl ether (20 mL x 2). The combined layer was dried over $NaSO_4$,

and filtered. Removal of solvent on a rotary evaporator and silica gel chromatography of the residue with hexane/ether (10/1) give 6-methoxy-2,2-dimethylhex-4-yn-3-one (0.888 g, 58% yield). The NMR spectra obtained is in agreement with those as reported.[36]

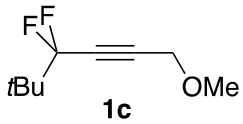

1c

A 2-neck vessel was charged with 6-methoxy-2,2-dimethylhex-4-yn-3-one (0.888 g, 5.76 mmol) under N_2 gas. Three vacuum/refill cycles were performed, and 5 drops of EtOH were added. The solution was cooled to 0 °C, followed by the addition of DAST (2.32 g, 1.90 mL, 14.4 mmol) in portion. The mixture was kept stirring for 0.5 h before warming to room temperature and heated at 50 °C for 14 h. The mixture was cooled to 0 °C before being diluted with dichloromethane (20 mL). Saturated NH_4Cl (20 mL) was added dropwise at 0 °C. The mixture was warmed to room temperature, followed by extraction with dichloromethane (20 mL x 2). The combined organic layer was dried over $NaSO_4$, and filtered. Removal of solvent on a rotary evaporator and silica gel chromatography of the residue with hexane gives 4,4-difluoro-1-methoxy-5,5-dimethylhex-2-yne (0.125 g, 12% yield).

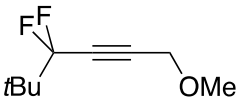

Compound 1c (pale yellow liquid). ^{1}H NMR (300 MHz, $CDCl_3$) δ 1.11 (s, 9H), 3.41 (s, 3H). 4.20 (t, J = 4.3Hz, 1H). ^{19}F{^{1}H} NMR ($CDCl_3$) δ –95.8. ^{13}C NMR (100 MHz, $CDCl_3$) δ 23.5 (t, J_{CF} = 3.0 Hz), 39.1 (t, J_{CF} = 23.4 Hz), 57.8, 59.2, 78.5 (t, J_{CF} = 40.9 Hz), 83.4 (t, J_{CF} = 6.5 Hz), 118.5 (t, J_{CF} = 236.2 Hz). HRMS (ESI) calcd for $C_9H_{15}F_2O$ $[M+H]^+$ 177.1091, found 177.1091.

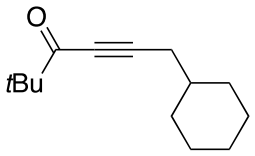

A 2-neck vessel was charged with 3-cyclohexyl-1-propyne (1.83 g, 15.0 mmol) under N_2 gas. THF (10 mL) was added and the solution was cooled to –78 °C for 10 min. To the solution was added dropwise 1.57 M *n*-BuLi (10.5 mL, 16.5 mmol), followed by stirring for 1h. *N*-methoxy-*N*-methylpivalamide (2.40 g, 16.5 mmol) was added to the mixture and stirred for 5 min at –78 °C. The mixture was warmed to room temperature and kept stirring for 12 h. H_2O (20 mL) was added and the mixture was extracted with dichloromethane (20 mL x 2). The combined layer was dried over $NaSO_4$, and filtered. Removal of solvent on a rotary evaporator and silica gel chromatography of the residue with hexane/ether (10/1) give 6-cyclohexyl-2,2-dimethylhex-4-yn-3-one (1.97 g, 64% yield). The NMR spectra obtained is in agreement with those as reported.[37]

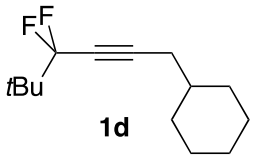

1d

A 2-neck vessel was charged with 6-cyclohexyl-2,2-dimethylhex-4-yn-3-one (1.44 g, 7.00 mmol) under N_2 gas. Three vacuum/refill cycles were performed, and 5 drops of EtOH were added. The solution was cooled to 0 °C, followed by the addition of DAST (2.82 g, 2.30 mL, 17.5 mmol) in portion. The mixture was kept stirring for 0.5 h before warming to room temperature and heated at 50 °C for 14 h. The mixture was cooled to 0 °C before being diluted with dichloromethane (20 mL). Saturated NH_4Cl (20 mL) was added dropwise at 0 °C. The mixture was warmed to room temperature, followed by extraction with dichloromethane (20 mL x 2). The combined organic layer was dried over $NaSO_4$, and filtered. Removal of solvent on a rotary

evaporator and silica gel chromatography of the residue with hexane give (4,4-difluoro-5,5-dimethylhex-2-yn-1-yl)cyclohexane (0.672 g, 42% yield).

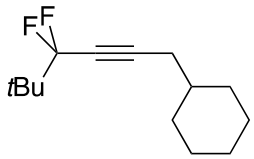

Compound 1d (pale yellow liquid). ^{1}H NMR (300 MHz, $CDCl_3$) δ 0.91–1.04 (m, 2H), 1.07 (s, 9H), 1.12–1.33 (m, 3H). 1.44–1.59 (m, 1H), 1.59–1.84 (m, 5H), 2.12–2.21 (m, 2H). ^{19}F{^{1}H} NMR ($CDCl_3$) δ –94.2. ^{13}C NMR (100 MHz, $CDCl_3$) δ 23.7 (t, J_{CF} = 2.9 Hz), 26.0, 26.11 (t, J_{CF} = 2.4 Hz), 26.12, 32.6, 36.8 (t, J_{CF} = 1.7 Hz), 39.2 (t, J_{CF} = 23.9 Hz), 73.8 (t, J_{CF} = 39.9 Hz), 87.8 (t, J_{CF} = 6.5 Hz), 118.9 (t, J_{CF} = 234.9 Hz). HRMS (ESI) calcd for $C_{14}H_{23}F_2$ $[M+H]^+$ 229.1768, found 229.1771.

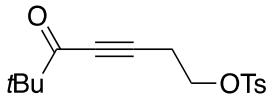

A 2-neck vessel was charged with but-3-yn-1-yl 4-methylbenzenesulfonate (4.48 g, 20.0 mmol) under N_2 gas.[38] THF (40 mL) was added and the solution was cooled to 0 °C for 10 min. To the solution was added dropwise 2 M *i*PrMgBr in THF (10.0 mL, 20.0 mmol), followed by stirring for 1h. *N*-methoxy-*N*-methylpivalamide (3.19 g, 22.0 mmol) was added to the mixture and stirred for 5 min at 0 °C. The mixture was warmed to room temperature and kept stirring for 2 h. Saturated NH_4Cl (20 mL) was added and the mixture was extracted with dichloromethane (20 mL x 2). The combined layer was dried over $NaSO_4$, and filtered. Removal of solvent on a rotary evaporator and silica gel chromatography of the residue with hexane/ether (1/1) give 6,6-dimethyl-5-oxohept-3-yn-1-yl 4-methylbenzenesulfonate (2.65 g, 43% yield).

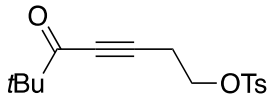

(colorless liquid). ^{1}H NMR (300 MHz, $CDCl_3$) δ 1.16 (s, 9H), 2.46 (s, 3H), 2.77 (t, *J* = 6.8 Hz, 2H), 4.15 (t, *J* = 6.8 Hz, 2H),

7.36 (d, J = 8.0 Hz, 2H), 7.80 (d, J = 8.3 Hz, 2H). ^{13}C NMR (100 MHz, $CDCl_3$) δ 20.0, 21.6, 25.9, 44.6, 66.4, 80.1, 88.4, 127.9, 130.0, 132.6, 145.2, 193.7. HRMS (ESI) calcd for $C_{16}H_{21}O_4S$ $[M+H]^+$ 309.1161, found 309.1161.

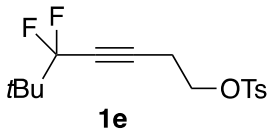

1e

A 2-neck vessel was charged with 6,6-dimethyl-5-oxohept-3-yn-1-yl 4-methylbenzenesulfonate (1.01g, 3.29 mmol) under N_2 gas. Three vacuum/refill cycles were performed, and 5 drops of EtOH were added. The solution was cooled to 0 °C, followed by the addition of DAST (1.33 g, 1.10 mL, 8.22 mmol) in portion. The mixture was warmed to room temperature and kept stirring for 0.5 h, followed by heating at 50 °C for 14 h. The mixture was cooled to 0 °C before being diluted with dichloromethane (20 mL). Saturated NH_4Cl (20 mL) was added dropwise at 0 °C. The mixture was warmed to room temperature, followed by extraction with dichloromethane (20 mL x 2). The combined organic layer was dried over $NaSO_4$, and filtered. Removal of solvent on a rotary evaporator and silica gel chromatography of the residue with hexane/ether (3/1) gives 5,5-difluoro-6,6-dimethylhept-3-yn-1-yl 4-methylbenzenesulfonate (0.583 g, 54% yield).

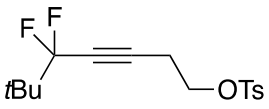

Compound 1e (pale yellow solid). ^{1}H NMR (300 MHz, $CDCl_3$) δ 1.05 (s, 9H), 2.45 (s, 3H), 2.67 (tt, J = 6.8 Hz, 4.7 Hz, 2H), 4.12 (t, J = 6.8 Hz, 2H), 7.35 (d, J = 8.0 Hz, 2H), 7.80 (d, J = 8.3 Hz, 2H).^{19}F{^{1}H} NMR ($CDCl_3$) δ –95.4. ^{13}C NMR (100 MHz, $CDCl_3$) δ 19.4 (t, J_{CF} = 2.3 Hz), 21.6, 23.5 (t, J_{CF} = 3.0 Hz), 39.1 (t, J_{CF} = 23.5 Hz), 66.6 (t, J_{CF} = 2.4 Hz), 75.1 (t, J_{CF} = 40.8 Hz), 82.7 (t, J_{CF} = 6.5 Hz), 118.5 (t, J_{CF} = 235.8 Hz), 127.9, 130.0, 132.6, 145.1. HRMS (ESI) calcd for $C_{16}H_{21}O_3F_2S$ $[M+H]^+$ 331.1179, found 331.1181.

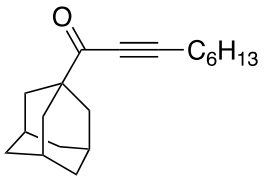

A 2-neck vessel was charged with 1-octyne (1.10 g, 10.0 mmol) under N_2 gas. THF (10 mL) was added and the solution was cooled to –78 °C for 10 min. To the solution was added dropwise 1.57 M *n*-BuLi (7.0 mL, 11.0 mmol), followed by stirring for 1h. *N*-methoxy-*N*-methyladamantane-1-carboxamide (2.46 g, 11.0 mmol) was added to the mixture and stirred for 5 min at –78 °C. The mixture was warmed to room temperature and kept stirring for 5 h. H_2O (20 mL) was added and the mixture was extracted with dichloromethane (20 mL x 2). The combined layer was dried over $NaSO_4$, and filtered. Removal of solvent on a rotary evaporator and silica gel chromatography of the residue with hexane and hexane/ether (30/1) give 1-(adamantan-1-yl)non-2-yn-1-one (1.69 g, 62% yield). The NMR spectra obtained is in agreement with those as reported.[39]

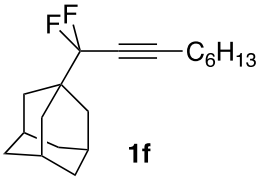

1f

A 2-neck vessel was charged with 1-(adamantan-1-yl)non-2-yn-1-one (1.37 g, 5.04 mmol) under N_2 gas. Three vacuum/refill cycles were performed, and 5 drops of EtOH were added. The solution was cooled to 0 °C, followed by the addition of DAST (2.03 g, 1.70 mL, 12.6 mmol) in portion. The mixture was kept stirring for 0.5 h before warming to room temperature and heated at 50 °C for 14 h. The mixture was cooled to 0 °C before being diluted with dichloromethane (20 mL). Saturated NH_4Cl (20 mL) was added dropwise at 0 °C. The mixture was warmed to room temperature, followed by extraction with dichloromethane (20 mL x 2). The combined organic layer was dried

over $NaSO_4$, and filtered. Removal of solvent on a rotary evaporator and silica gel chromatography of the residue with hexane give 1-(1,1-difluorononon-2-yn-1-yl)adamantane (0.318 g, 21% yield).

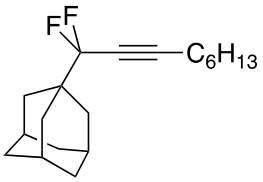

Compound 1f (pale yellow liquid). ^{1}H NMR (300 MHz, $CDCl_3$) δ 0.90 (t, J = 6.8 Hz, 3H), 1.22–1.36 (m, 4H), 1.36–1.48 (m, 2H), 1.54–1.62 (m, 2H), 1.62–1.79 (m, 12H), 2.04 (brs, 3H), 2.29 (tt, J = 6.9 Hz, 5.3 Hz, 2H). $^{19}F\{^{1}H\}$ NMR ($CDCl_3$) δ –98.3. ^{13}C NMR (100 MHz, $CDCl_3$) δ. 13.9, 18.4 (t, J_{CF} = 2.3 Hz), 22.5, 27.7, 27.9 (t, J_{CF} = 2.0 Hz), 28.4, 31.2, 35.2 (t, J_{CF} = 2.4 Hz), 36.6, 40.5 (t, J_{CF} = 23.7 Hz), 72.6 (t, J_{CF} = 40.1 Hz), 89.2 (t, J_{CF} = 6.5 Hz), 118.3 (t, J_{CF} = 233.6 Hz), HRMS (ESI) calcd for $C_{19}H_{29}F_2$ $[M+H]^+$ 295.2237, found 295.2234.

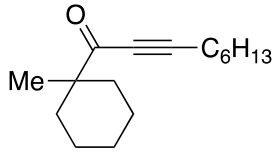

A 2-neck vessel was charged with 1-octyne (1.10 g, 10.0 mmol) under N_2 gas. THF (10 mL) was added and the solution was cooled to –78 °C for 10 min. To the solution was added dropwise 1.57 M *n*-BuLi (7.0 mL, 11.0 mmol), followed by stirring for 1h. *N*-methoxy-*N*,1-dimethylcyclohexane-1-carboxamide (2.04 g, 11.0 mmol) was added to the mixture and stirred for 5 min at –78 °C. The mixture was warmed to room temperature and kept stirring for 5 h. H_2O (20 mL) was added and the mixture was extracted with dichloromethane (20 mL x 2). The combined layer was dried over $NaSO_4$. Removal of solvent on a rotary evaporator and silica gel chromatography of the residue with hexane and hexane/ether (30/1) give 1-(1-methylcyclohexyl)non-2-yn-1-one (1.40 g, 60% yield).

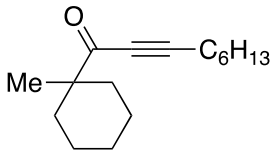

(pale yellow liquid). ^{1}H NMR (300 MHz, $CDCl_3$) δ 0.89 (t, *J* = 6.7 Hz, 3H), 1.12 (s, 3H), 1.24–1.36 (m, 8H), 1.36–1.48 (m, 4H), 1.51–1.64 (m, 4H), 2.00–2.11 (m, 2H), 2.37 (t, *J* = 6.9 Hz, 2H). ^{13}C NMR (100 MHz, $CDCl_3$) δ 13.9, 18.9, 22.4, 22.7, 24.9, 25.7, 27.7, 28.4, 31.1, 34.4, 48.4, 79.0, 94.6, 194.4. HRMS (ESI) calcd for $C_{16}H_{27}O$ $[M+H]^+$ 235.2062, found 235.2056.

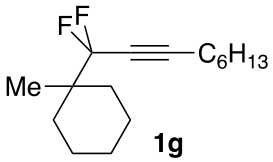

1g

A 2-neck vessel was charged with 1-(1-methylcyclohexyl)non-2-yn-1-one (1.17 g, 5.00 mmol) under N_2 gas. Three vacuum/refill cycles were performed, and 5 drops of EtOH were added. The solution was cooled to 0 °C, followed by the addition of DAST (2.02 g, 1.70 mL, 12.5 mmol) in portion. The mixture was kept stirring for 0.5 h before warming to room temperature and heated at 50 °C for 14 h. The mixture was cooled to 0 °C before being diluted with dichloromethane (20 mL). Saturated NH_4Cl (20 mL) was added dropwise at 0 °C. The mixture was warmed to room temperature, followed by extraction with dichloromethane (20 mL x 2). The combined organic layer was dried over $NaSO_4$, and filtered. Removal of solvent on a rotary evaporator and silica gel chromatography of the residue with hexane give 1-(1,1-difluoronon-2-yn-1-yl)-1-methylcyclohexane (0.122 g, 10% yield).

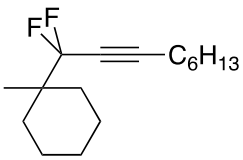

Compound 1g (pale yellow liquid). ^{1}H NMR (300 MHz, $CDCl_3$) δ 0.89 (t, *J* = 6.7 Hz, 3H), 1.10 (s, 3H), 1.11–1.21 (m, 1H), 1.22–1.35 (m, 4H), 1.35–1.48 (m, 4H), 1.48–1.53 (m, 3H), 1.54–1.72 (m, 6H), 2.28 (tt, *J* = 6.9 Hz, 5.3 Hz, 2H).^{19}F{^{1}H} NMR ($CDCl_3$) δ –95.7. ^{13}C NMR (100 MHz, $CDCl_3$) δ 14.0, 16.8 (t, J_{CF} = 2.9 Hz), 18.4 (t, J_{CF} = 2.3 Hz), 21.2, 22.5, 25.9, 27.9

(t, J_{CF} = 2.0 Hz), 28.4, 30.1 (t, J_{CF} = 2.6 Hz), 31.2, 42.0 (t, J_{CF} = 22.4 Hz), 73.0 (t, J_{CF} = 40.0 Hz), 89.1 (t, J_{CF} = 6.5 Hz), 119.4 (t, J_{CF} = 235.1 Hz). HRMS (ESI) calcd for $C_{16}H_{27}F_2$ $[M+H]^+$ 257.2081, found 257.2074.

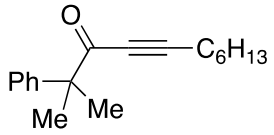

A 2-neck vessel was charged with 1-octyne (1.10 g, 10.0 mmol) under N_2 gas. THF (10 mL) was added and the solution was cooled to –78 °C for 10 min. To the solution was added dropwise 1.57 M *n*-BuLi (7.0 mL, 11.0 mmol), followed by stirring for 1h. *N*-methoxy-*N*,2-dimethyl-2-phenylpropanamide (2.28 g, 11.0 mmol) was added to the mixture and stirred for 5 min at –78 °C. The mixture was warmed to room temperature and kept stirring for 5 h. H_2O (20 mL) was added and the mixture was extracted with dichloromethane (20 mL x 2). The combined layer was dried over $NaSO_4$, and filtered. Removal of solvent on a rotary evaporator and silica gel chromatography of the residue with hexane and hexane/ether (30/1) give 2-methyl-2-phenylundec-4-yn-3-one (1.57 g, 61% yield).

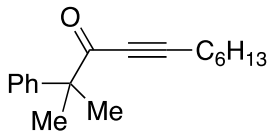

(pale yellow liquid). ^{1}H NMR (300 MHz, $CDCl_3$) δ 0.87 (t, *J* = 6.7 Hz, 3H), 1.12–1.31 (m, 6H), 1.32–1.48 (m, 2H), 1.56 (s, 6H), 2.21 (t, *J* = 6.9 Hz, 2H), 7.21–7.39 (m, 5H). ^{13}C NMR (100 MHz, $CDCl_3$) δ 13.9, 18.8, 22.3, 24.9, 27.4, 28.2, 31.1, 52.4, 79.3, 96.8, 126.4, 126.8, 128.4, 143.2, 191.0. HRMS (ESI) calcd for $C_{18}H_{25}O$ $[M+H]^+$ 257.1905, found 257.1903.

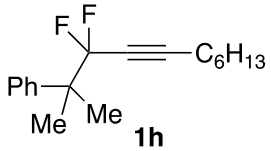

1h

A 2-neck vessel was charged with 2-methyl-2-phenylundec-4-yn-3-one (1.28 g, 5.00 mmol) under N_2 atmosphere. Three vacuum/refill cycles were performed, and 5 drops of EtOH were added. The solution was cooled to 0 °C, followed by the addition of DAST (2.02 g, 1.70 mL, 12.5 mmol) in portion. The mixture was kept stirring for 0.5 h before warming to room temperature and heated at 50 °C for 14 h. The mixture was cooled to 0 °C before being diluted with dichloromethane (20 mL). Saturated NH_4Cl (20 mL) was added dropwise at 0 °C. The mixture was warmed to room temperature, followed by extraction with dichloromethane (20 mL x 2). The combined organic layer was dried over $NaSO_4$, and filtered. Removal of solvent on a rotary evaporator and silica gel chromatography of the residue with hexane give (3,3-difluoro-2-methylundec-4-yn-2-yl)benzene (0.120 g, 9% yield).

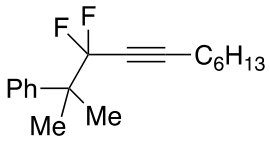

Compound 1h (pale yellow liquid). ^{1}H NMR (300 MHz, $CDCl_3$) δ 0.89 (t, J = 7.1 Hz, 3H), 1.17–1.37 (m, 6H), 1.39–1.51 (m, 2H), 1.55 (s, 6H), 2.19 (tt, J = 6.9 Hz, 5.2 Hz, 2H), 7.22–7.37 (m, 3H), 7.46–7.55 (d, J = 7.2 Hz, 2H) .^{19}F{^{1}H} NMR ($CDCl_3$) δ –90.3. ^{13}C NMR (100 MHz, $CDCl_3$) δ 14.0, 18.3 (t, J_{CF} = 2.4 Hz), 22.5, 23.0 (t, J_{CF} = 3.0 Hz), 27.7 (t, J_{CF} = 1.9 Hz), 28.4, 31.2, 46.0 (t, J_{CF} = 23.5 Hz), 73.0 (t, J_{CF} = 39.4 Hz), 89.9 (t, J_{CF} = 6.4 Hz), 117.5 (t, J_{CF} = 237.0 Hz), 127.0, 127.7, 128.0 (t, J_{CF} = 1.7 Hz), 141.7. HRMS (ESI) calcd for $C_{18}H_{25}F_2$ $[M+H]^+$ 279.1924, found. 279.1920

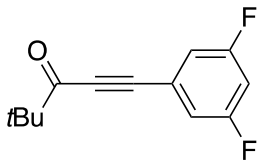

A 2-neck vessel was charged with 1-ethynyl-3,5-difluorobenzene (1.318 g, 10 mmol) under N_2 gas. THF (10 mL) was added and the solution was cooled to –78 °C for 10 min. To the solution was added dropwise 1.57 M *n*-BuLi (6.4 mL, 10 mmol), followed by stirring for 1h. *N*-methoxy-*N*-methylpivalamide (1.43 g, 10 mmol) was added to the mixture and stirred for 5 min at –78 °C. The mixture was warmed to room temperature and kept stirring for 15 h. H_2O (20 mL) was added and the mixture was extracted with dichloromethane (20 mL x 2). The combined layer was dried over $NaSO_4$, and filtered. Removal of solvent on a rotary evaporator and silica gel chromatography of the residue with hexane/ether (30/1) give 1-(3,5-difluorophenyl)-4,4-dimethylpent-1-yn-3-one (1.0304 g, 46% yield).

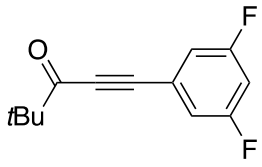

(pale yellow liquid). ^{1}H NMR (400 MHz, $CDCl_3$) δ 1.27 (s, 9H), 6.92 (tt, J = 8.8 Hz, 2.2 Hz, 1H), 7.08 (m, 2H). ^{19}F{^{1}H} NMR ($CDCl_3$) δ –108.3. ^{13}C NMR (100 MHz, $CDCl_3$) δ 25.8, 44.8, 86.6, 88.4 (t, J_{CF} = 4.0 Hz), 106.6 (t, J_{CF} = 25.1 Hz), 115.6 (dd, J_{CF} = 19.4 Hz, 7.9 Hz), 122.8 (t, J_{CF} = 11.4 Hz), 162.6 (dd, J_{CF} = 249.1 Hz, 12.9 Hz), 193.4. HRMS (ESI) calcd for $C_{13}H_{13}F_2O$ $[M+H]^+$ 223.0934, found 223.0928.

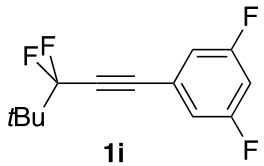

1i

A 2-neck vessel was charged with 1-(3,5-difluorophenyl)-4,4-dimethylpent-1-yn-3-one (0.20 g, 0.90 mmol) under N_2 gas. Three vacuum/refill cycles were performed, and 5 drops of EtOH were added. The solution was cooled to 0 °C, followed by the

addition of DAST (0.364 g, 0.300 mL, 2.25 mmol) in portion. The mixture was kept stirring for 0.5 h before warming to room temperature and heated at 50 °C for 8 h. The mixture was cooled to 0 °C before being diluted with dichloromethane (20 mL). Saturated NH_4Cl (20 mL) was added dropwise at 0 °C. The mixture was warmed to room temperature, followed by extraction with dichloromethane (20 mL x 2). The combined organic layer was dried over $NaSO_4$, and filtered. Removal of solvent on a rotary evaporator and silica gel chromatography of the residue with hexane give 1-(3,3-difluoro-4,4-dimethylpent-1-yn-1-yl)-3,5-difluorobenzene (0.0523 g, 24% yield).

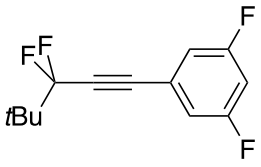

Compound 1i (pale yellow liquid). ^{1}H NMR (400 MHz, $CDCl_3$) δ 1.16 (s, 9H), 6.88 (tt, J = 2.2 Hz, 0.6 Hz, 1H), 7.03 (m, 2H). ^{19}F{^{1}H} NMR ($CDCl_3$) δ –109.3 (2F), –96.8 (2F). ^{13}C NMR (100 MHz, $CDCl_3$) δ 23.6 (t, J_{CF} = 3.0 Hz), 39.4 (t, J_{CF} = 23.3 Hz), 82.7 (t, J_{CF} = 41.3 Hz), 84.4 (tt, J_{CF} = 6.5 Hz, 3.9 Hz), 106.0 (t, J_{CF} = 25.1 Hz), 115.2 (ddt, J_{CF} = 19.3 Hz, 7.8 Hz, 2.3 Hz), 118.9 (t, J_{CF} = 236.9 Hz), 123.1 (tt, J_{CF} = 11.6 Hz. 2.6. Hz), 162.7 (dd, 248.6 Hz, 12.9 Hz). HRMS (ESI) calcd for $C_{13}H_{13}F_4$ $[M+H]^+$ 245.0953, found 245.0957.

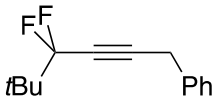

1j

A 2-neck vessel was charged with 3-phenyl-1-propyne (1.16 g, 10.0 mmol) under N_2 gas. THF (10 mL) was added and the solution was cooled to –78 °C for 10 min. To the solution was added dropwise 1.57 M n-BuLi (6.4 mL, 10.0 mmol), followed by stirring for 1h. *N*-methoxy-*N*-methylpivalamide (1.45 g, 10.0 mmol) was added to the mixture and stirred for 1 h at –78 °C. The mixture was warmed to room temperature and kept stirring for 2 h. H_2O (20 mL) was added and the mixture was extracted with

dichloromethane (20 mL x 2). The combined layer was dried over $NaSO_4$. Removal of solvent on a rotary evaporator and silica gel chromatography of the residue with hexane/ether (30/1) give 2,2-dimethyl-6-phenylhex-4-yn-3-one with impurity (0.82 g, 41% yield).

A 2-neck vessel was charged with this crude under N_2 gas. Three vacuum/refill cycles were performed, and 5 drops of EtOH were added. The solution was cooled to 0 °C, followed by the addition of DAST (1.63 g, 1.50 mL, 10.3 mmol) in portion. The mixture was kept stirring for 0.5 h before warming to room temperature and heated at 50 °C for 7 h. The mixture was cooled to 0 °C before being diluted with dichloromethane (20 mL). Saturated NH_4Cl (20 mL) was added dropwise at 0 °C. The mixture was warmed to room temperature, followed by extraction with dichloromethane (20 mL x 2). The combined organic layer was dried over $NaSO_4$, filtered. Removal of solvent on a rotary evaporator and silica gel chromatography of the residue with hexane give (4,4-difluoro-5,5-dimethylhex-2-yn-1-yl)benzene (0.239 g, 11% yield).

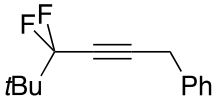

Compound 1j (pale yellow liquid). ^1H NMR (400 MHz, $CDCl_3$) δ 1.11 (s, 9H), 3.72 (t, J = 5.0, 2H), 7.23–7.29 (m, 1H), 7.30–7.37 (m, 4H).$^{19}F\{^1H\}$ NMR ($CDCl_3$) δ –94.6. ^{13}C NMR (100 MHz, $CDCl_3$) δ 23.6 (t, J_{CF} = 3.0 Hz), 24.6 (t, J_{CF} = 2.4 Hz), 39.3, (t, J_{CF} = 23.7 Hz), 75.0 (t, J_{CF} = 40.4 Hz), 86.2 (t, J_{CF} = 6.5 Hz), 118.8 (t, J_{CF} = 235.5 Hz), 127.0, 127.8, 128.7, 134.9 (t, J_{CF} = 2.0 Hz). HRMS (ESI) calcd for $C_{14}H_{17}F_2$ $[M+H]^+$ 223.1298, found 223.1296.

3.4.5. Preparation of zinc chloride or zinc bromide solution

Anhydrous $ZnCl_2$/$ZnBr_2$ was heated under vacuum at 150 °C for 9 h. A 1.5 M stock solution of $ZnCl_2$/$ZnBr_2$ in THF was prepared. Titration of $ZnCl_2$/$ZnBr_2$ was performed by the following: quenching zinc halide solution (0.3 mL) by pH 10 buffer (2.0 mL). 3 drops of eriochrome black T was added and a purplish pink solution was observed. 0.01 M ethylenediaminetetraacetic (EDTA) solution was added via a pipette until tin blue color was observed.

3.4.6. Titration of Grignard & zinc reagent

A 2-neck vessel was charged with I_2 (76.2 mg, 0.300 mmol) under N_2 gas. To the vessel was added 0.5M LiCl THF solution (1.5 mL).[40] The solution was cooled to 0 °C, followed by dropwise addition of RMgX/RZnCl until discoloration of the solution was observed.

3.4.7. Preparation of arylzinc chloride

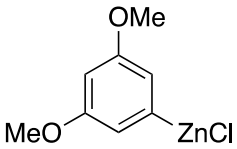

A 0.75M 3,5-$(MeO)_2(C_6H_3)$MgBr solution was prepared from magnesium turnings (0.158 g, 6.60 mmol) and 1-bromo-3,5-dimethoxybenzene (1.30 g, 6.00 mmol) in THF (6.0 mL) at 40 °C for 2 h. A 2-neck round bottom flask (rbf) was charged with 0.75M 3,5-$(MeO)_2(C_6H_3)$MgBr solution (6.00 mL, 4.50 mmol) under N_2 gas. To this solution was added 1.5M $ZnCl_2$ THF solution (6.00 mL, 9.00 mmol) at 25 °C, followed by THF (10.5 mL). The mixture was stirred for 1 h to afford 0.2 M 3,5-

$(MeO)_2(C_6H_3)ZnCl$. The mixture was allowed to settle before the supernatant was used for catalysis.

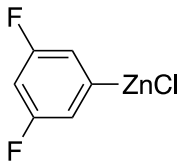

2i

A 0.46 M 3,5-$F_2(C_6H_3)MgBr$ solution was prepared from magnesium turnings (0.360 g, 15.0 mmol) and 1-bromo-3,5-difluorobenzene (1.93 g, 10.0 mmol) in THF (10.0 mL) at 25 °C for 2 h. A 2-neck rbf was charged with 0.46 M 3,5-$F_2(C_6H_3)MgBr$ solution (9.00 mL, 4.14 mmol) under N_2 gas. To this solution was added 1.5M $ZnCl_2$ THF solution (6.00 mL, 9.00 mmol) at 25 °C, followed by THF (5.7 mL). The mixture was stirred for 15 min to afford 0.2 M 3,5-$F_2(C_6H_3)ZnCl$. The mixture was allowed to settle before the supernatant was used for catalysis.

3.4.8. Preparation of alkylzinc chloride

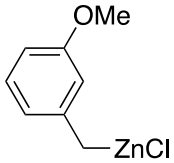

2a

A 0.46 M 3-$MeO(C_6H_4)CH_2MgBr$ solution was prepared from magnesium turnings (0.360 g, 15.0 mmol) and 3-methoxybenzyl bromide (2.01 g, 1.40 mL, 10.0 mmol) in THF (10.0 mL) at 0 °C. A 2-neck rbf was charged with 0.46 M 3-$MeO(C_6H_4)CH_2MgBr$ solution (5.00 mL, 2.30 mmol) under N_2 gas. To this solution was added 1.5M $ZnCl_2$ THF solution (3.40 mL, 5.06 mmol) at 25 °C, followed by THF (3.1 mL). The mixture was stirred for 1.5 h to afford 0.2 M 3-$MeO(C_6H_4)CH_2ZnCl$. The mixture was allowed to settle before the supernatant was used for catalysis.

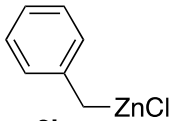

2b

A 0.50 M $(C_6H_5)CH_2MgCl$ solution was prepared from magnesium turnings (0.360 g, 15.0 mmol) and benzyl chloride (1.26 g, 1.20 mL, 10.0 mmol) in THF (10.0 mL) at 0 °C. A 2-neck rbf was charged with 0.50 M $(C_6H_5)CH_2MgCl$ solution (5.00 mL, 2.50 mmol) under N_2 gas. To this solution was added 1.5M $ZnCl_2$ THF solution (3.70 mL, 5.50 mmol) at 25 ℃, followed by THF (3.8 mL). The mixture was stirred for 1.5 h to afford 0.2 M $(C_6H_5)CH_2ZnCl$. The mixture was allowed to settle before the supernatant was used for catalysis.

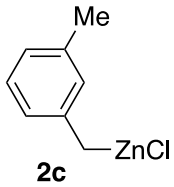

2c

A 0.42 M 3-Me$(C_6H_4)CH_2MgCl$ solution was prepared from Rieke magnesium suspension (2.50 g in 100 mL THF) (6.00 mL, 6.00 mmol) and 3-Me$(C_6H_4)CH_2Cl$ (0.562 g, 0.530 mL, 4.00 mmol) in THF (1.0 mL) at –78 °C for 2 h. A 2-neck rbf was charged with 0.42 M 3-Me$(C_6H_4)CH_2MgCl$ solution (5.80 mL, 2.44 mmol) under N_2 gas. To this solution was added 1.5M $ZnCl_2$ THF solution (3.60 mL, 5.36 mmol) at 25 °C, followed by THF (2.8 mL). The mixture was stirred for 1 h to afford 0.2 M 3-Me$(C_6H_4)CH_2ZnCl$. The mixture was allowed to settle before the supernatant was used for catalysis.

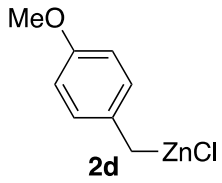

2d

A 0.31 M 4-MeO(C_6H_4)CH_2MgCl solution was prepared from Rieke magnesium suspension (2.50 g in 100 mL THF) (6.00 mL, 6.00 mmol) and 4-MeO(C_6H_4)CH_2Cl (0.626 g, 0.500 mL, 4.00 mmol) in THF (1.0 mL) at –78 °C for 1 h. A 2-neck rbf was charged with 0.31 M 4-MeO(C_6H_4)CH_2MgCl THF solution (5.00 mL, 1.55 mmol) under N_2 gas. To this solution was added 1.25M $ZnCl_2$ THF solution (2.70 mL, 3.40 mmol) at 25 °C. The mixture was stirred for 1 h to afford 0.2 M 4-MeO(C_6H_4)CH_2ZnCl. The mixture was allowed to settle before the supernatant was used for catalysis.

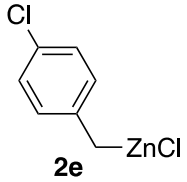

2e

A 0.375 M 4-Cl(C_6H_4)CH_2MgCl solution was prepared from Rieke magnesium suspension (2.50 g in 100 mL THF) (6.00 mL, 6.00 mmol) and 4-Cl(C_6H_4)CH_2Cl (0.644 g, 4.00 mmol) in THF (1.0 mL) at –78 °C for 2 h. A 2-neck rbf was charged with 0.375 M 4-Cl(C_6H_4)CH_2MgCl THF solution (5.00 mL, 1.88 mmol) under N_2 gas at –78 °C. To this solution was added 1.25M $ZnCl_2$ THF solution (3.30 mL, 4.10 mmol), followed by THF (1.1 mL). The mixture was warmed to room temperature and kept stirring for 1 h to afford 0.2 M 4-Cl(C_6H_4)CH_2ZnCl. The mixture was allowed to settle before the supernatant was used for catalysis.

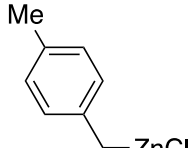

2f

A 0.50 M 4-Me(C_6H_4)CH_2MgCl solution was prepared from magnesium turnings (0.360 g, 15.0 mmol) and 4-methylbenzyl chloride (1.41 g, 1.30 mL, 10.0 mmol) in THF (10.0 mL) at 0 °C for 1h. A 2-neck rbf was charged with 0.50 M 4-Me(C_6H_4)CH_2MgCl solution (5.00 mL, 2.50 mmol) under N_2 gas. To this solution was added 1.25M $ZnCl_2$ THF solution (4.40 mL, 5.50 mmol) at 25 °C, followed by THF (3.1 mL). The mixture was stirred for 1.5 h to afford 0.2 M 4-Me(C_6H_4)CH_2ZnCl. The mixture was allowed to settle before the supernatant was used for catalysis.

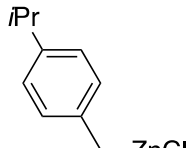

2g

A 0.375 M 4-*i*Pr(C_6H_4)CH_2MgCl solution was prepared from Rieke magnesium suspension (2.50 g in 100 mL THF) (6.00 mL, 6.00 mmol) and 4-*i*Pr(C_6H_4)CH_2Cl (0.675 g, 4.00 mmol) in THF (1.0 mL) at –78 °C for 1 h. A 2-neck rbf was charged with 0.375 M 4-*i*Pr(C_6H_4)CH_2MgCl THF solution (5.00 mL, 1.88 mmol) under N_2 gas at –78 °C. To this solution was added 1.5M $ZnCl_2$ THF solution (2.80 mL, 4.10 mmol), followed by THF (1.6 mL). The mixture was warmed to room temperature and kept stirring for 1 h to afford 0.2 M 4-*i*Pr(C_6H_4)CH_2ZnCl. The mixture was allowed to settle before the supernatant was used for catalysis.

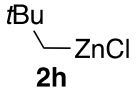

2h

A 0.50M $(CH_3)_3CCH_2MgBr$ solution was prepared from magnesium turnings (0.360 g, 15.0 mmol) and neopentyl bromide (1.51 g, 1.30 mL, 10.0 mmol) in THF (10.0 mL) at 0 °C for 2 h. A 2-neck rbf was charged with 0.50M $(CH_3)_3CCH_2MgBr$ THF solution (5.00 mL, 2.50 mmol) under N_2 gas. To this solution was added 1.5M $ZnCl_2$ THF solution (3.30 mL, 5.00 mmol) at 25 °C, followed by THF (4.2 mL). The mixture was stirred for 1.5 h to afford 0.2 M $(CH_3)_3CH_2ZnCl$. The solution was allowed to settle before the supernatant was used for catalysis.

3.4.9. Procedures for rhodium-catalyzed alkylation/elimination

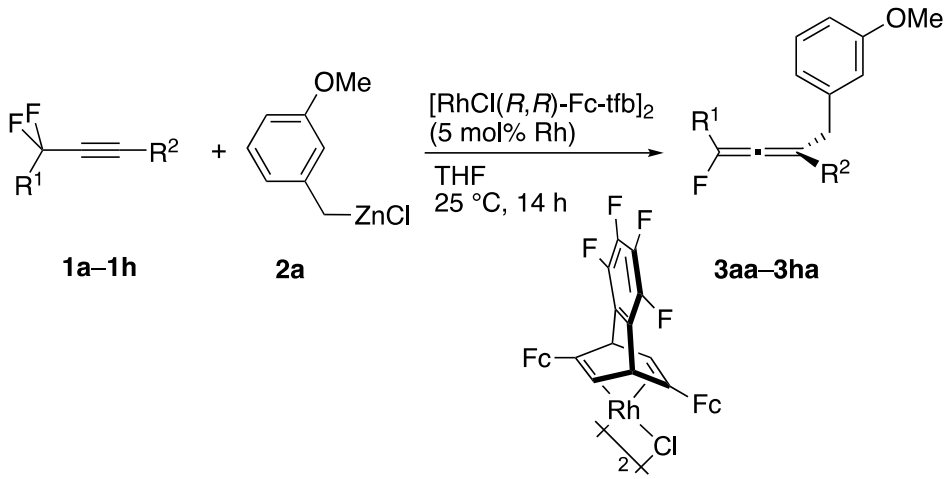

A Schlenk tube was first charged with difluoroalkyne **1a**–**1h** (0.15 mmol), [RhCl(*R*,*R*)-Fc-tfb]$_2$ (5 mol% Rh, 5.49 mg) under N_2 atmosphere. To the tube was added THF (0.8 mL) and 0.2 M 3-MeO(C_6H_4)CH_2ZnCl **2a** (0.30 mmol, 1.5 mL). The mixture was kept stirring at 25 °C for 14 h, before H_2O (0.2 mL) was added. Dilution with diethyl ether and passing through a short silica pad was followed by crude NMR analysis. Silica gel column chromatography with hexane afforded the fluoroallene **3**.

3.4.10. Characterization of fluoroallene 3aa–3ha

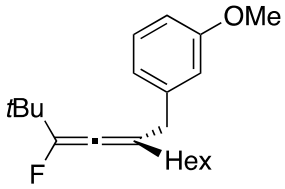

Compound 3aa (pale yellow liquid, 75% yield, 98% ee). The ee was measured by HPLC (Chiralpak IC column, 1.0 mL/min, 100% hexane, 220 nm, t_{minor} = 7.9 min (*R*), t_{major} = 8.5 min (*S*)); $[\alpha]^{25}_D$ –8.3 (*c* 1.418, $CHCl_3$) for 98% ee. ^1H NMR (300 MHz, $CDCl_3$) δ 0.87 (t, *J* = 7.0 Hz, 3H), 0.99 (s, 9H), 1.19–1.37 (m, 6H), 1.38–1.51 (m, 2H), 1.96–2.18 (m, 2H), 3.32 (dd, *J* = 15.1 Hz, 7.8 Hz, 1H), 3.42 (dd, *J* = 15.1 Hz, 8.0 Hz, 1H), 3.79 (s, 3H), 6.72–6.80 (m, 3H), 7.19 (t, *J* = 7.7 Hz, 1H). $^{19}F\{^1H\}$ NMR ($CDCl_3$) δ –142.1. ^{13}C NMR (100 MHz, $CDCl_3$) δ 14.0, 22.6, 27.36, 27.41 (d, J_{CF} = 2.4 Hz), 28.9, 31.7, 33.95 (d, J_{CF} = 29.8 Hz), 33.96, 42.0, 55.1, 112.0, 114.6, 121.6, 122.7 (d, J_{CF} = 12.6 Hz), 129.1, 140.2 (d, J_{CF} = 3.4 Hz), 148.7 (d, J_{CF} = 241 Hz), 159.5, 184.2 (d, J_{CF} = 24.4 Hz). HRMS (ESI) calcd for $C_{21}H_{32}OF$ $[M+H]^+$ 319.2437, found 319.2444.

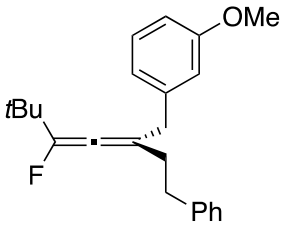

Compound 3ba (colorless liquid, 85% yield, 96% ee). The ee was measured by HPLC (Chiralpak IC column, 1.0 mL/min, hexane/DCM = 99/1, 220 nm, t_{minor} = 19.0 (*R*), t_{major} = 19.9 (*S*)); $[\alpha]^{25}_D$ +2.1 (*c* 0.574, $CHCl_3$) for 96% ee. ^1H NMR (300 MHz, $CDCl_3$) δ 1.00 (s, 9H), 2.34–2.48 (m, 2H), 2.66–2.86 (m, 2H), 3.35 (dd, *J* = 15.1 Hz, 7.7 Hz, 1H), 3.45 (dd, *J* = 15.2 Hz, 7.8 Hz, 1H), 3.79 (s, 3H), 6.70–6.82 (m, 3H), 7.13–7.32 (m, 6H). $^{19}F\{^1H\}$ NMR ($CDCl_3$) δ –141.2. ^{13}C NMR (100 MHz, $CDCl_3$) δ 27.3, 33.9 (d, J_{CF} = 2.0 Hz), 34.1, 35.5, 42.1, 55.1, 112.1, 114.6, 121.6, 122.1 (d, J_{CF} = 12.4 Hz), 125.9, 128.3, 129.2, 139.9 (d, J_{CF} = 3.3 Hz), 141.6, 149.1 (d, J_{CF} = 242.1 Hz), 159.6, 184.5 (d, J_{CF} = 24.7 Hz). HRMS (ESI) calcd for $C_{23}H_{28}OF$ $[M+H]^+$ 339.2124, found 339.2121.

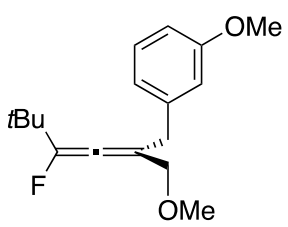

Compound 3ca (pale yellow liquid, 60% yield, 86% ee). The ee was measured by HPLC (Chiralpak IF column, 1.0 mL/min, hexane, 280 nm, t_{major} = 26.8 min (*R*), t_{minor} = 34.4 min (*S*)); $[\alpha]^{25}_{D}$ –33.7 (*c* 0.525, $CHCl_3$) for 86% ee. ^{1}H NMR (500 MHz, $CDCl_3$) δ 0.98 (s, 9H), 3.34 (s, 3H), 3.40 (dd, *J* = 15.5 Hz, 7.7 Hz, 1H), 3.45 (dd, *J* = 15.3 Hz, 8.2 Hz, 1H), 3.79 (s, 3H), 3.94 (dd, *J* = 10.7 Hz, 4.3 Hz, 1H), 3.96 (dd, *J* = 10.6 Hz, 4.9 Hz, 1H), 6.72–6.82 (m, 3H), 7.20 (m, 1H). ^{19}F{^{1}H} NMR ($CDCl_3$) δ –142.4. ^{13}C NMR (100 MHz, $CDCl_3$) δ 27.2, 33.9 (d, J_{CF} = 28.7 Hz), 38.0, 55.1, 57.9, 73.2, 112.1, 114.7, 118.9 (d, J_{CF} = 12.0 Hz), 121.7, 129.2, 139.7, 149.1 (d, J_{CF} = 243.0 Hz), 159.6, 186.7 (d, J_{CF} = 26.2 Hz). HRMS (ESI) calcd for $C_{17}H_{24}O_2F$ $[M+H]^+$ 279.1760, found 279.1761.

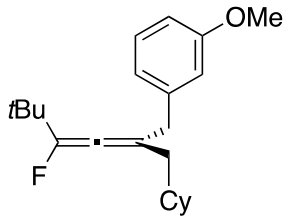

Compound 3da (pale yellow liquid, 72% yield, 98% ee). The ee was measured by HPLC (Chiralpak IC column, 1.0 mL/min, 100% hexane, 280 nm, t_{minor} = 9.3 min (*R*), t_{major} = 9.8 min (*S*)); $[\alpha]^{25}_{D}$ –14.5 (*c* 1.204, $CHCl_3$) for 98% ee. ^{1}H NMR (300 MHz, $CDCl_3$) δ 0.81–0.94 (m, 2H), 0.98 (s, 9H), 1.09–1.31 (m, 3H), 1.43–1.53 (m, 1H), 1.58–1.81 (m, 5H), 1.88–2.07 (m, 2H), 3.30 (dd, *J* = 15.3 Hz, 8.1 Hz, 1H), 3.39 (dd, *J* = 15.2 Hz, 8.5 Hz, 1H), 3.79 (s, 3H), 6.69–6.80 (m, 3H), 7.19 (t, *J* = 7.7 Hz, 1H).^{19}F{^{1}H} NMR ($CDCl_3$) δ –142.5. ^{13}C NMR (100 MHz, $CDCl_3$) δ 26.2, 26.3, 26.5, 27.3, 33.3, 33.4, 34.0 (d, J_{CF} = 29.7 Hz), 36.2 (d, J_{CF} = 2.8 Hz), 41.98, 42.00, 55.1, 112.0, 114.7, 121.1 (d, J_{CF} = 12.9 Hz), 121.6, 129.1, 140.2 (d, J_{CF} = 3.3 Hz), 148.3 (d, J_{CF} = 241 Hz), 159.5, 185.0 (d, J_{CF} = 23.9 Hz). HRMS (ESI) calcd for $C_{22}H_{32}OF$ $[M+H]^+$ 331.2437, found 331.2434.

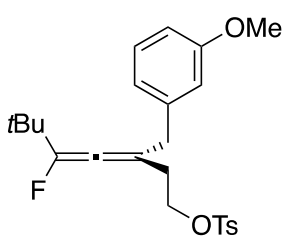

Compound 3ea (pale yellow liquid, 71%, 94% ee). The ee was measured by HPLC (Chiralpak IC column, 1.0 mL/min, hexane/2-propanol/DCM = 95/1/4, 280 nm, t_{major} = 39.3 min (*R*), t_{minor} = 42.0 min (*S*)); $[\alpha]^{25}_{D}$ –2.6 (*c* 1.155, $CHCl_3$) for 94% ee. ^1H NMR (300 MHz, $CDCl_3$) δ 0.96 (s, 9H), 2.36–2.50 (m, 2H), 2.44 (s, 3H), 3.30 (dd, *J* = 15.2 Hz, 7.7 Hz, 1H), 3.38 (dd, *J* = 15.2 Hz, 7.9 Hz, 1H), 3.77 (s, 3H), 4.10 (t, *J* = 7.00 Hz, 2H), 6.68 (d, *J* = 2.0 Hz, 1H), 6.70 (d, *J* = 7.5 Hz, 1H), 6.76 (dd, *J* = 8.3 Hz, 2.5 Hz, 1H), 7.18 (t, *J* = 7.8 Hz, 1H), 7.33 (d, *J* = 8.0 Hz, 2H), 7.76 (d, *J* = 8.3 Hz, 2H). $^{19}F\{^1H\}$ NMR ($CDCl_3$) δ –140.2. ^{13}C NMR (100 MHz, $CDCl_3$) δ 21.6, 27.1, 32.9, 34.0 (d, J_{CF} = 28.7 Hz), 41.9, 55.1, 67.9 (d, J_{CF} = 2.7 Hz), 112.3, 114.6, 117.1 (d, J_{CF} = 12.0 Hz), 121.5, 127.9, 129.3, 129.8, 133.1, 139.1 (d, J_{CF} = 3.2 Hz), 144.8, 149.7 (d, J_{CF} = 244.8 Hz), 159.7, 185.2 (d, J_{CF} = 25.6 Hz). HRMS (ESI) calcd for $C_{24}H_{30}O_4FS$ $[M+H]^+$ 433.1849, found 433.1848.

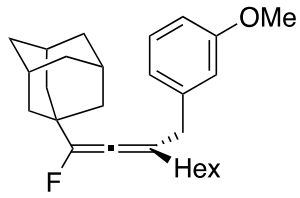

Compound 3fa (pale yellow liquid, 73% yield, 99% ee). The ee was measured by HPLC (Chiralpak IC column, 1.0 mL/min, 100% hexane, 220 nm, t_{minor} = 15.2 min (*R*), t_{major} = 15.5 min (*S*); $[\alpha]^{25}_{D}$ –19.9 (*c* 1.50, $CHCl_3$) for 99% ee. ^1H NMR (300 MHz, $CDCl_3$) δ 0.88 (t, *J* = 6.8 Hz, 3H), 1.26–1.37 (m, 6H), 1.38–1.51 (m, 2H), 1.56–1.76 (m, 12H), 1.89–2.00 (brs, 3H), 2.07 (m, 2H), 3.33 (dd, *J* =14.9 Hz, 7.9 Hz, 1H), 3.42 (dd, *J* = 15.0 Hz, 8.0 Hz), 3.79 (s, 3H), 6.69–6.82 (m, 3H), 7.15–7.23 (m, 1H). $^{19}F\{^1H\}$ NMR ($CDCl_3$) δ –147.8. ^{13}C NMR (100 MHz, $CDCl_3$) δ 14.1, 22.6, 27.5 (d, J_{CF} = 2.3 Hz), 28.1, 28.9, 31.7, 34.0, 35.7 (d, J_{CF} = 29.6 Hz), 36.7, 39.4, 42.1, 55.1, 112.0, 114.6, 121.7, 123.0 (d, J_{CF} = 12.8 Hz), 129.1, 140.3 (d, J_{CF} = 3.4 Hz), 148.8 (d, J_{CF} = 239.9 Hz), 159.5, 184.6 (d, J_{CF} = 24.5 Hz). HRMS (ESI) calcd for $C_{27}H_{38}OF$ $[M+H]^+$ 397.2907, found 397.2906.

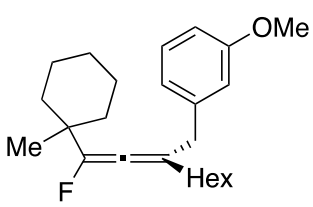

Compound 3ga (pale yellow liquid, 90% yield, 99% ee). The ee was measured by HPLC (Chiralpak IC column, 1.0 mL/min, 100% hexane, 280 nm, t_{minor} = 10.4 min (*R*), t_{major} = 11.0 min (*S*)); $[\alpha]^{25}_{D}$ –16.8 (*c* 0.434, $CHCl_3$) for 99% ee. ^1H NMR (300 MHz, $CDCl_3$) δ 0.87 (t, *J* = 6.5 Hz, 3H), 1.01 (s, 3H), 1.13–1.52 (m, 18H), 2.08 (m, 2H), 3.36 (dd, *J* = 15.3 Hz, 8.1 Hz, 1H), 3.43 (dd, *J* = 15.3 Hz, 8.2 Hz, 1H), 3.79 (s 3H), 6.72–6.82 (m, 3H), 7.15–7.23 (m, 1H).$^{19}F\{^1H\}$ NMR ($CDCl_3$) δ –144.6. ^{13}C NMR ($CDCl_3$) δ 14.0, 22.2, 22.3, 22.6, 25.5, 26.1, 27.5 (d, J_{CF} = 2.5 Hz), 28.9, 31.7, 34.0, 34.99, 35.06, 37.5 (d, J_{CF} = 28.0 Hz), 41.9, 55.1, 112.1, 114.7, 121.7, 122.5 (d, J_{CF} = 13.3 Hz), 129.1, 140.2 (d, J_{CF} = 3.5 Hz), 147.7 (d, J_{CF} = 240.2 Hz), 159.6, 186.0 (d, J_{CF} = 23.8 Hz). HRMS (ESI) calcd for $C_{24}H_{36}OF$ $[M+H]^+$ 359.2750, found 359.2749.

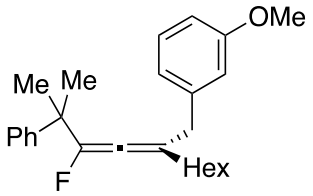

Compound 3ha (pale yellow liquid, 80% yield, 98% ee). The ee was measured by HPLC (Chiralpak IC column, 1.0 mL/min, hexane/DCM = 98/2, 220 nm, t_{minor} = 17.4 min (*R*), t_{major} = 18.0 min *S*)); $[\alpha]^{25}_{D}$ +7.2 (*c* 1.756, $CHCl_3$) for 98% ee. ^1H NMR (300 MHz, $CDCl_3$) δ 0.89 (t, *J* = 6.9 Hz, 3H), 1.25 (s, 3H), 1.27–1.38 (m, 6H), 1.39 (s, 3H), 1.46–1.57 (m, 2H), 2.05–2.25 (m, 2H), 3.38 (dd, *J* = 15.7 Hz, 8.1 Hz, 1H), 3.48 (dd, *J* = 15.5 Hz, 8.6 Hz, 1H), 3.76 (s, 3H), 6.73–6.86 (m, 3H), 7.14–7.29 (m, 6H). $^{19}F\{^1H\}$ NMR ($CDCl_3$) δ –136.3. ^{13}C NMR (100 MHz, $CDCl_3$) δ 14.1, 22.6, 27.0, 27.5, 27.6, 28.9, 31.7, 34.4, 41.8, 41.9 (d, J_{CF} = 29.9 Hz), 55.1, 112.2, 114.8, 121.7, 124.0 (d, J_{CF} = 12.1 Hz), 126.0, 126.1, 128.1, 129.3, 140.0 (d, J_{CF} = 2.7 Hz), 145.9 (d, J_{CF} = 1.8 Hz), 147.1 (d, J_{CF} = 240.9 Hz), 159.7, 185.4 (d, J_{CF} = 23.5 Hz). HRMS (ESI) calcd for $C_{26}H_{34}OF$ $[M+H]^+$ 381.2594, found 381.2590.

3.4.11. Procedures for the preparation of fluoroallenes 3ea–3eh

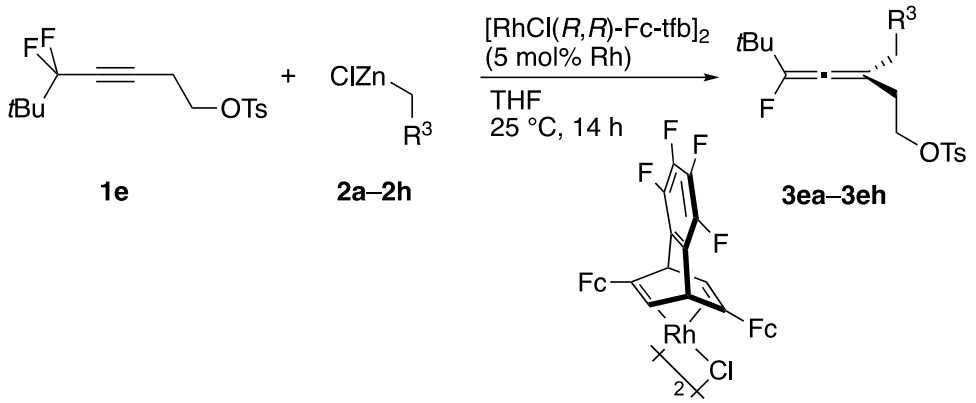

A Schlenk tube was first charged with **1e** (0.15 mmol, 49.5 mg), [RhCl(*R*,*R*)-Fc-tfb]$_2$ (5 mol% Rh, 5.49 mg) under N_2 atmosphere. To the tube was added THF (0.8 mL) and 0.2 M **2a**–**2h** (0.30 mmol, 1.5 mL). The mixture was kept stirring at 25 °C for 14 h, before H_2O (0.2 mL) was added. Dilution with diethyl ether and by passing through a short silica pad was followed by crude NMR analysis. Silica gel column chromatography with hexane afforded the fluoroallene **3ea**–**3eh**.

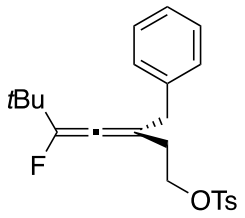

Compound 3eb (pale yellow liquid, 47% yield, 96% ee). The ee was measured by HPLC (Chiralpak IC column, 1.0 mL/min, hexane/2-propanol = 99/1, 220 nm, t_{major} = 38.0 (*R*), t_{minor} = 41.7 min (*S*)); $[\alpha]^{25}_D$ +1.2 (*c* 1.430, $CHCl_3$) for 96% ee. ^{1}H NMR (400 MHz, $CDCl_3$) δ 0.93 (s, 9H), 2.36–2.50 (m, 2H), 2.45 (s, 3H), 3.32 (dd, *J* = 15.4 Hz, 7.6 Hz, 1H), 3.40 (dd, *J* = 15.3 Hz, 8.2 Hz, 1H), 4.11 (t, *J* = 7.0 Hz, 2H), 7.11 (d, *J* = 7.5 Hz, 2H), 7.17–7.31 (m, 3H), 7.33 (d, *J* = 8.1 Hz, 2H), 7.77 (d, *J* = 8.3 Hz, 2H). ^{19}F{^{1}H} NMR ($CDCl_3$) δ –140.3. ^{13}C NMR (100 MHz, $CDCl_3$) δ 21.6, 27.1, 33.0, 33.9 (d, J_{CF} = 28.8 Hz), 41.9, 67.9 (d, J_{CF} = 2.7 Hz), 117.4 (d, J_{CF} = 11.9 Hz), 126.6, 127.9, 128.3, 129.1, 129.8, 133.0, 137.6, 144.8, 149.7 (d, J_{CF} = 244.7 Hz), 185.1 (d, J_{CF} = 25.6 Hz). HRMS (ESI) calcd for $C_{23}H_{28}O_3FS$ $[M+H]^+$ 403.1743, found 403.1738.

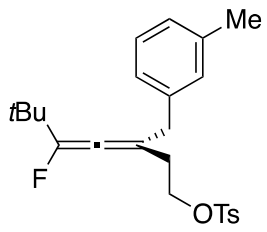

Compound 3ec (pale yellow liquid, 51% yield, 93% ee). The ee was measured by HPLC (Chiralpak IG column, 1.0 mL/min, hexane/2-propanol/DCM = 89/1/10, 220 nm, t_{major} = 10.2 min (*R*), t_{minor} = 8.3 min (*S*)); $[\alpha]^{25}_D$ –1.1 (*c* 0.941, $CHCl_3$) for 93% ee. ^1H NMR (400 MHz, $CDCl_3$) δ 0.94 (s, 9H), 2.31 (s, 3H), 2.35–2.52 (m, 2H), 2.44 (s, 3H), 3.28 (dd, *J* = 15.2 Hz, 7.3 Hz, 1H), 3.35 (dd, *J* = 15.3 Hz, 7.6 Hz, 1H), 4.10 (t, *J* = 6.8 Hz, 2H), 6.88–6.96 (m, 2H), 7.02 (d, *J* = 7.4 Hz, 1H), 7.15 (t, *J* = 7.4 Hz, 1H), 7.33 (d, *J* = 7.6 Hz, 2H), 7.76 (d, *J* = 7.8 Hz, 2H). $^{19}F\{^1H\}$ NMR ($CDCl_3$) δ –140.3. ^{13}C NMR (100 MHz, $CDCl_3$) δ 21.3, 21.6, 27.1, 32.9, 34.0 (d, J_{CF} = 28.7 Hz), 41.9, 68.0 (d, J_{CF} = 2.8 Hz), 117.4 (d, J_{CF} = 12.0 Hz), 126.1, 127.3, 127.9, 128.3, 129.8, 129.9, 133.1, 137.5 (d, J_{CF} = 3.1 Hz), 137.9, 144.7, 149.7 (d, J_{CF} = 244.4 Hz), 185.1 (d, J_{CF} = 25.7 Hz). HRMS (ESI) calcd for $C_{24}H_{30}O_3FS$ $[M+H]^+$ 417.1900, found 417.1906.

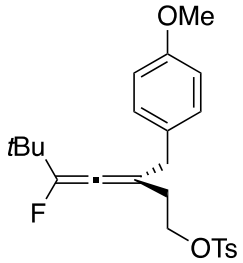

Compound 3ed (pale yellow liquid, 56% yield, 96% ee). The ee was measured by HPLC (Chiralpak IG column, 1.0 mL/min, hexane/2-propanol/dichloromethane = 94/1/5, 220 nm, t_{major} = 30.7 min (*R*), t_{minor} = 23.6 min (*S*)); $[\alpha]^{25}_D$ +2.2 (*c* 0.463, $CHCl_3$) for 96% ee. ^1H NMR (400 MHz, $CDCl_3$) δ 0.95 (s, 9H), 2.33–2.49 (m, 2H), 2.44 (s, 3H), 3.25 (dd, *J* = 15.4 Hz, 7.6 Hz, 1H), 3.33 (dd, *J* = 15.4 Hz, 8.0 Hz, 1H), 3.78 (s, 3H), 4.09 (t, *J* = 7.1 Hz, 2H), 6.81 (d, *J* = 8.6 Hz, 2H), 7.03 (d, *J* = 8.6 Hz, 2H), 7.33 (d, *J* = 8.0 Hz, 2H), 7.76 (d, *J* = 8.3 Hz, 2H). $^{19}F\{^1H\}$ NMR ($CDCl_3$) δ –140.3. ^{13}C NMR (100 MHz, $CDCl_3$) δ 21.6, 27.2, 32.8, 34.0 (d, J_{CF} = 28.8 Hz), 41.1, 55.3, 68.0 (d, J_{CF} = 2.9 Hz), 113.8, 117.7 (d, J_{CF} = 12.0 Hz), 127.9, 129.7 (d, J_{CF} = 3.1 Hz), 129.8, 130.1, 133.1, 144.8, 149.6 (d, J_{CF} = 242 Hz), 158.4, 184.9 (d, J_{CF} = 27.8 Hz). HRMS (ESI) calcd for $C_{24}H_{30}O_4FS$ $[M+H]^+$ 433.1849, found 433.1841.

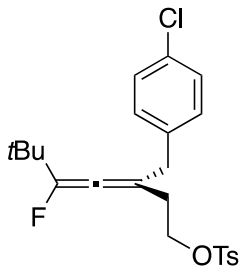

Compound 3ee (pale yellow liquid, 65% yield, 99% ee). The ee was measured by HPLC (Chiralpak IG column, 1.0 mL/min, hexane/2-propanol = 99/1, 220 nm, t_{major} = 40.5 min (*R*), t_{minor} = 25.3 min (*S*)); $[\alpha]^{25}_D$ –7.7 (*c* 0.984, $CHCl_3$) for 99% ee. ^1H NMR (400 MHz, $CDCl_3$) δ 0.92 (s, 9H), 2.34–2.51 (m, 2H), 2.45 (s, 3H), 3.29 (dd, *J* = 15.6 Hz, 7.6 Hz, 1H), 3.36 (dd, *J* = 15.5 Hz, 8.4 Hz, 1H), 4.11 (t, *J* = 6.8 Hz, 2H), 7.04 (d, *J* = 8.4 Hz. 2H), 7.24 (d, *J* = 8.4 Hz, 2H), 7.33 (d, *J* = 8.0 Hz, 2H), 7.76 (d, *J* = 8.3 Hz, 2H). $^{19}F\{^1H\}$ NMR ($CDCl_3$) δ –140.0. ^{13}C NMR (100 MHz, $CDCl_3$) δ 21.6, 27.1, 33.1, 34.0 (d, J_{CF} = 28.6 Hz), 41.2, 67.8 (d, J_{CF} = 2.7 Hz), 117.1 (d, J_{CF} = 11.9 Hz), 127.9, 128.5, 129.8, 130.5, 132.5, 133.1, 136.1 (d, J_{CF} = 3.0 Hz), 144.8, 150.2 (d, J_{CF} = 245.4), 185.4 (d, J_{CF} = 25.9 Hz). HRMS (ESI) calcd for $C_{23}H_{27}O_3FSCl$ $[M+H]^+$ 437.1353, found 437.1348.

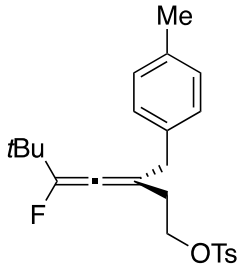

Compound 3ef (pale yellow liquid, 53% yield, 79% ee). The ee was measured by HPLC (Chiralpak IG column, 1.0 mL/min, hexane/2-propanol = 98/2, 220 nm, t_{major} = 25.3 min (*R*), t_{minor} = 15.7 min (*S*)); $[\alpha]^{25}_D$ +3.8 (*c* 0.913, $CHCl_3$) for 79% ee. ^1H NMR (400 MHz, $CDCl_3$) δ 0.95 (s, 9H), 2.31 (s, 3H), 2.33–2.49 (m, 2H), 2.44 (s, 3H), 3.28 (dd, *J* = 15.2 Hz, 7.5 Hz, 1H), 3.35 (dd, *J* = 15.2 Hz, 7.8 Hz, 1H), 4.09 (t, *J* = 6.9 Hz, 2H), 7.00 (d, *J* = 7.9 Hz, 2H), 7.08 (d, *J* = 7.8 Hz, 2H), 7.33 (d, *J* = 8.0 Hz, 2H), 7.76 (d, *J* = 8.2 Hz, 2H). $^{19}F\{^1H\}$ NMR ($CDCl_3$) δ –140.3. ^{13}C NMR (100 MHz, $CDCl_3$) δ 21.0, 21.6, 27.2, 32.8, 34.0 (d, J_{CF} = 28.7 Hz), 41.6, 68.0 (d, J_{CF} = 2.7 Hz), 117.5 (d, J_{CF} = 12.0 Hz), 127.9, 128.98, 129.03, 129.8, 133.1, 134.5 (d, J_{CF} = 3.2 Hz), 136.1, 144.7, 149.6 (d, J_{CF} = 243.3 Hz), 185.0 (d, J_{CF} = 26.0 Hz). HRMS (ESI) calcd for $C_{24}H_{30}O_3FS$ $[M+H]^+$ 417.1900, found 417.1904.

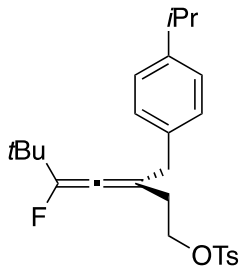

Compound 3eg (colorless liquid, 53% yield, 94% ee). The ee was measured by HPLC (Chiralpak IG column, 1.0 mL/min, hexane/2-propanol = 98/2, 220 nm, t_{major} = 18.2 min (*R*), t_{minor} = 12.8 min (*S*)); $[\alpha]^{25}_{D}$ +5.5 (*c* 0.779, $CHCl_3$) for 94% ee. ^1H NMR (400 MHz, $CDCl_3$) δ 0.91 (s, 9H), 1.22 (d, *J* = 6.9 Hz, 6H), 2.36–2.52 (m, 2H), 2.45 (s, 3H), 2.87 (sep, *J* = 7.0 Hz, 1H), 3.27 (dd, *J* = 15.4 Hz, 7.6 Hz, 1H), 3.37 (dd, *J* = 15.4, 8.3 Hz, 1H), 4.11 (td, *J* = 7.0 Hz, 1.0 Hz, 2H), 7.03 (d, *J* = 8.0 Hz, 2H), 7.13 (d, *J* = 8.0 Hz, 2H), 7.33 (d, *J* = 8.0 Hz, 2H), 7.77 (d, *J* = 8.3 Hz). $^{19}F\{^1H\}$ NMR ($CDCl_3$) δ –140.5. ^{13}C NMR (100 MHz, $CDCl_3$) δ 21.6, 23.99, 24.00, 27.1, 32.9, 33.8, 33.9 (d, J_{CF} = 28.8 Hz), 41.5, 68.0 (d, J_{CF} = 2.7 Hz), 117.7 (d, J_{CF} = 12.0 Hz), 126.4, 127.9, 129.1, 129.8, 133.1, 134.9 (d, J_{CF} = 3.0 Hz), 144.7, 147.2, 149.8 (d, J_{CF} = 244.4), 185.0 (d, J_{CF} = 25.6 Hz). HRMS (ESI) calcd for $C_{26}H_{34}O_3FS$ $[M+H]^+$ 445.2213, found 445.2212.

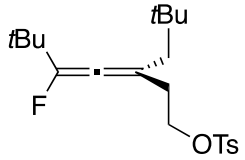

Compound 3eh (pale yellow liquid, 69% yield, 92% ee). The ee was measured by HPLC (Chiralpak IG column, 1.0 mL/min, hexane/2-propanol = 99/1, 220 nm, t_{major} = 12.7 min (*R*), t_{minor} = 11.3 min (*S*)); $[\alpha]^{25}_{D}$ –17.5 (*c* 1.283, $CHCl_3$) for 92% ee. ^1H NMR (300 MHz, $CDCl_3$) δ 0.92 (s, 9H), 1.06 (s, 9H), 1.88 (dd, *J* = 14.2 Hz, 5.0 Hz, 1H), 1.99 (dd, *J* = 13.9 Hz, 7.8 Hz, 1H), 2.32–2.55 (m, 2H), 2.44 (s, 3H), 4.09 (t, *J* = 6.6 Hz, 2H), 7.34 (d, *J* = 7.5 Hz, 2H), 7.78 (d, *J* = 7.2 Hz, 2H). $^{19}F\{^1H\}$ NMR ($CDCl_3$) δ –140.4. ^{13}C NMR (100 MHz, $CDCl_3$) δ 21.6, 27.2, 29.5, 31.6 (d, J_{CF} = 4.4 Hz), 34.1 (d, J_{CF} = 29.1 Hz), 35.6, 48.9, 68.1 (d, J_{CF} = 2.9 Hz), 115.4 (d, J_{CF} = 12.5 Hz), 127.9, 129.8, 133.1, 144.7, 148.5 (d, J_{CF} = 243.2 Hz), 185.5 (d, J_{CF} = 23.9 Hz). HRMS (ESI) calcd for $C_{21}H_{32}O_3FS$ $[M+H]^+$ 383.2056, found 383.2060.

3.4.12. Procedures for the preparation of fluoroallenes 3ie

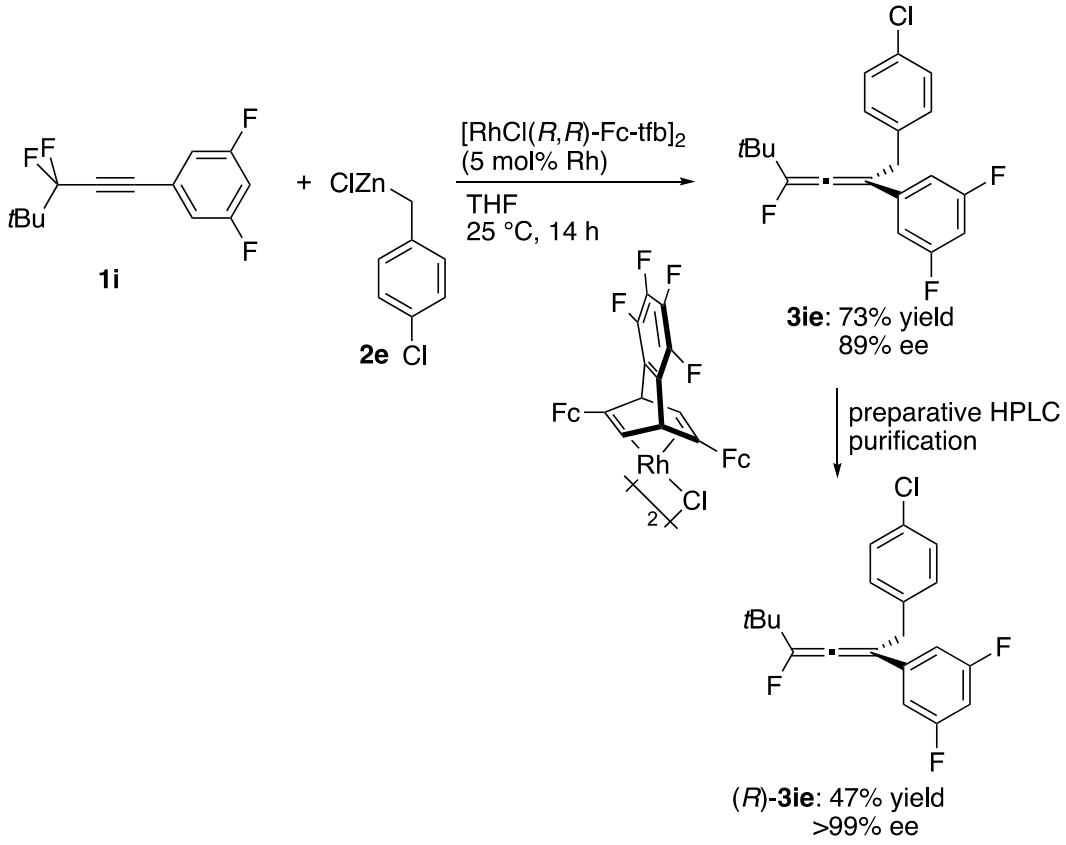

A Schlenk tube was first charged with **1i** (0.15 mmol, 37.5 mg), [RhCl(*R*,*R*)-Fc-tfb]$_2$ (5 mol% Rh, 5.63 mg) under N_2 atmosphere. To the tube was added THF (0.8 mL) and 0.2 M **2e** (0.30 mmol, 1.5mL). The mixture was kept stirring at 25 °C for 14 h, before H_2O (0.2 mL) was added. Dilution with diethyl ether and passing through a short silica pad, was followed by crude NMR analysis. Silica gel column chromatography with hexane afforded the fluoroallene **3ie** (73% yield, 89% ee). Enantiopure (*R*)-**3ie** was obtained by preparative HPLC separation of 89% ee-**3ie** (Chiralpak semi-preparative IB column, 8.0 mL/min, pure hexane, 254 nm, t_1 = 103 min, t_2 = 113 min). 89% ee-**3ie** (39.2 mg) was dissolved in 8 mL of hexane and injected into the recycling HPLC. After recycling for 6 rounds, a baseline separation of the enantiomers was obtained to give (*R*)-**3ie** (25.3 mg, 47% yield).

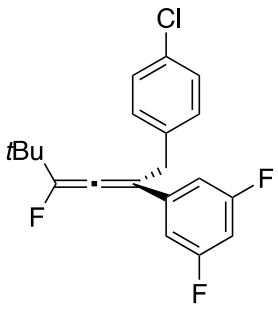

Compound 3ie (colorless crystalline, 47% yield, >99% ee). The ee was measured by HPLC (Chiralpak column ID, 1.0 mL/min, pure hexane, 254 nm, t_{major} = 5.0 min (*R*), t_{minor} = 5.6 min (*S*)); $[\alpha]^{25}_D$ +3.3 (*c* 1.26, $CHCl_3$) for >99% ee. ^{1}H NMR (400 MHz, $CDCl_3$) δ 0.99 (s, 9H), 3.75 (dd, *J* = 16.1 Hz, 7.9 Hz, 1H), 3.84 (dd, *J* = 16.1 Hz, 9.1 Hz, 1H), 6.73 (t, *J* = 8.6 Hz, 1H), 6.98 (d, *J* = 6.6 Hz, 2H), 7.15 (d, *J* = 8.3 Hz, 2H), 7.28 (d, *J* = 8.3 Hz, 2H). ^{19}F{^{1}H} NMR ($CDCl_3$) δ –140.0 (s, 1F), –109.55 (s, 2F). ^{13}C NMR (100 MHz, $CDCl_3$) δ 27.0, 34.5 (d, J_{CF} = 28.2 Hz), 37.9, 103.5 (td, J_{CF} = 25.2 Hz, 1.3 Hz), 109.5 (ddd, J_{CF} = 25.6 Hz, 7.2 Hz, 2.6 Hz), 119.3 (dt, J_{CF} = 12.1 Hz, 2.9 Hz), 128.5, 130.5, 132.6, 136.1 (d, J_{CF} = 2.5 Hz), 139.5 (td, J_{CF} = 9.2 Hz, 2.0 Hz), 151.4 (d, J_{CF} = 247.6 Hz), 163.1 (dd, J_{CF} = 245.2 Hz, 12.8 Hz), 190.7 (d, J_{CF} = 26.9 Hz). HRMS (ESI) calcd for $C_{20}H_{19}ClF_3$ $[M+H]^+$ 351.1127, found 351.1131.

3.4.13. Procedures for rhodium-catalyzed benzylation/arylation & elimination for inversed combination reactions

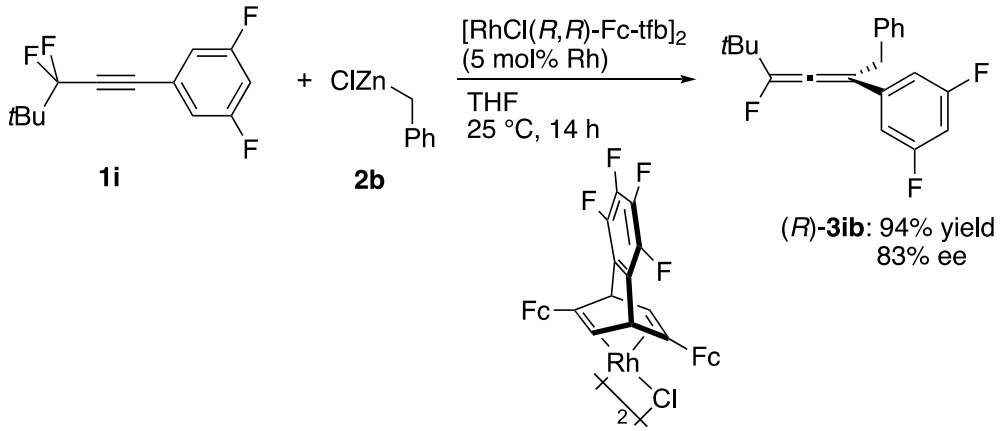

A Schlenk tube was first charged with **1i** (0.10 mmol, 21.0 mg), [RhCl(*R*,*R*)-Fc-tfb]$_2$ (5 mol% Rh, 3.15 mg) under N_2 atmosphere. To the tube was added THF (0.5 mL) and 0.2 M **2b** (0.20 mmol, 0.9 mL). The mixture was kept stirring at 25 °C for 14 h, before H_2O (0.2 mL) was added. To the crude was added diethyl ether, followed by

passing through a short silica pad for crude NMR analysis. Silica gel column chromatography with hexane afforded the fluoroallene (*R*)-**3ib**.

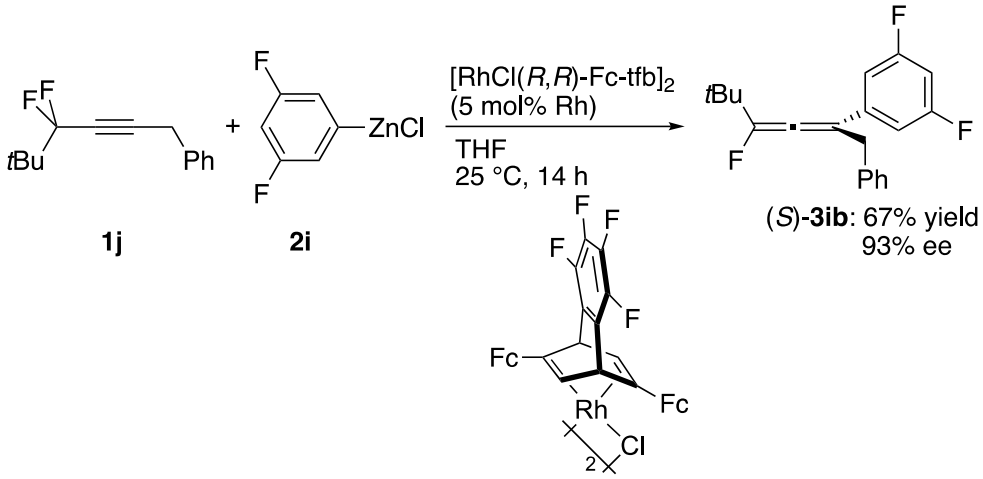

A Schlenk tube was first charged with **1j** (0.10 mmol, 22.2 mg), [RhCl(*R*,*R*)-Fc-tfb]$_2$ (5 mol% Rh, 3.66 mg) under N_2 atmosphere. To the tube was added THF (0.5 mL) and 0.2 M **2i** (0.20 mmol, 1.0 mL). The mixture was kept stirring at 25 °C for 14 h, before H_2O (0.2 mL) was added. To the crude was added diethyl ether, followed by passing through a short silica pad for crude NMR analysis. Silica gel column chromatography with hexane afforded the fluoroallene (*S*)-**3ib**.

3.4.14. Characterization of fluoroallene 3ib

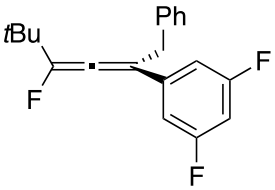

Compound (*R*)-3ib (colorless crystalline, 94% yield, 83% ee). The ee was measured by HPLC (Chiralpak ID column, 1.0 mL/min, pure hexane, 254 nm, t_{major} = 4.7 min (*R*), t_{minor} = 5.2 min (*S*)); $[\alpha]^{25}_D$ +6.4 (*c* 1.364, $CHCl_3$) for 83% ee.

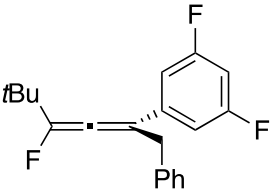

Compound (*S*)-3ib (colorless crystalline, 67% yield, 93% ee). The ee was measured by HPLC (Chiralpak ID column, 1.0 mL/min, pure hexane, 254 nm, t_{minor} = 4.7 min (*R*), t_{major} = 5.1 min (*S*)); $[\alpha^{25}_D$ –9.4 (*c* 0.373, $CHCl_3$) for 93% ee. ^{1}H NMR (400 MHz, $CDCl_3$) δ 0.97 (s,

9H), 3.78 (dd, *J* = 16.0 Hz, 7.9 Hz, 1H), 3.88 (dd, *J* = 16.0 Hz, 9.1 Hz, 1H), 6.72 (t, *J* = 8.7 Hz, 1H), 6.97–7.05 (m, 2H), 7.19–7.25 (m, 3H), 7.28–7.33 (m, 2H). $^{19}F\{^{1}H\}$ NMR ($CDCl_3$) δ –140.5 (s, 1F), –109.8 (s, 2F). ^{13}C NMR (100 MHz, $CDCl_3$) δ 27.0, 34.4 (d, J_{CF} = 28.2 Hz), 38.6, 103.3 (td, J_{CF} = 25.6 Hz, 1.6 Hz), 109.5 (ddd, J_{CF} = 18.9 Hz, 7.2 Hz, 2.6 Hz), 119.7 (dt, J_{CF} = 12.3 Hz, 3.0 Hz), 126.7, 128.4, 129.2, 137.6 (d, J_{CF} = 2.5 Hz), 139.8 (td, J_{CF} = 9.1 Hz, 2.2 Hz), 151.2 (d, J_{CF} = 246.8 Hz), 163.1 (ddd, J_{CF} = 246.4 Hz, 12.7 Hz, 1.5 Hz), 190.7 (d, J_{CF} = 26.6 Hz). HRMS (ESI) calcd for $C_{20}H_{20}F_3$ $[M+H]^+$ 317.1517, found 317.1526.

3.4.15. Procedures for transformation of 3ee to give 3ke

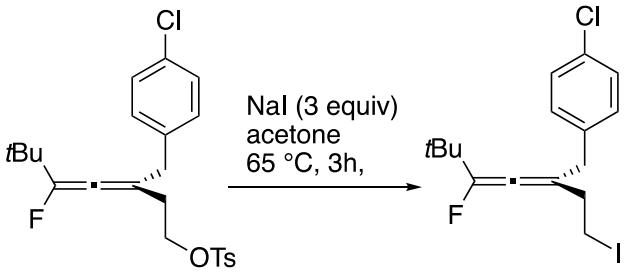

3ke was synthesized with a modified reported procedure.[41] A 2-neck rbf was charged with **3ee** (42.2 mg, 0.10 mmol,), sodium iodide (36.5 mg, 0.30 mmol) under N_2 atmosphere. To the tube was added acetone (3.0 mL). The mixture was kept stirring at 65 °C for 3 h. Removal of solvent on a rotary evaporator was followed by the addition of H_2O (10 mL) and extraction with dichloromethane (10 mL x 2). The combined layer was dried over Na_2SO_4, and filtered. Removal of solvent on a rotary evaporator gives a yellow liquid (*R*)-**3ke** (37.6 mg, 99% yield).

3.4.16. Characterization of 3ke

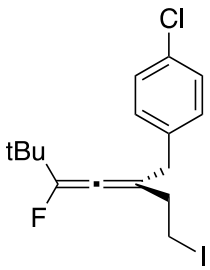

Compound 3ke (yellow liquid, 99% yield, 99% ee). The ee was measured by HPLC (Chiralpak IA column, 1.0 mL/min, pure hexane, 220 nm, t_{major} = 5.9 min (*R*), t_{minor} = 6.3 min (*S*)); $[\alpha]^{25}_{D}$ –15.1 (*c* 1.88, $CHCl_3$) for 99% ee. ^{1}H NMR (400 MHz, $CDCl_3$) δ 0.99 (s, 9H), 2.65 (m, 2H), 3.19 (m, 2H), 3.33 (dd, *J* = 15.5 Hz, 7.6 Hz, 1H), 3.42 (dd, *J* = 15.5 Hz, 8.3 Hz, 1H), 7.10 (d, *J* = 8.3 Hz, 2H), 7.27 (d, *J* = 7.8 Hz, 2H). ^{19}F{^{1}H} NMR ($CDCl_3$) δ –139.9. ^{13}C NMR (100 MHz, $CDCl_3$) δ 0.7 (d, J_{CF} = 2.8 Hz), 27.3, 34.1 (d, J_{CF} = 28.8 Hz), 37.9, 41.0, 121.4 (d, J_{CF} = 12.0 Hz), 128.5, 130.5, 132.4, 136.3 (d, J_{CF} = 2.9 Hz), 150.6 (d, J_{CF} = 245.2 Hz), 185.2 (d, J_{CF} = 25.5 Hz). HRMS (ESI) calcd for $C_{16}H_{20}ClFI$ $[M+H]^+$ 393.0282, found 393.0282.

3.4.17. Data for X–ray crystal structures

Crystals of **3ie** suitable for X-ray crystallographic analysis were obtained by recrystallization from methanol. The ORTEP drawing of **3ie** is shown in Figure S1. The absolute configuration of **3ie** was determined to be (*R*).

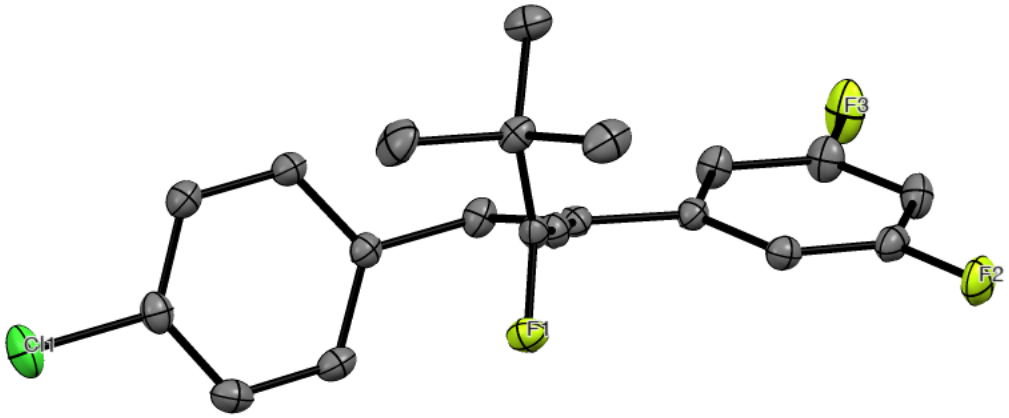

Figure S1. ORTEP illustration of compound (*R*)-**3ie**.

Table S1. Sample and crystal data for (*R*)-**3ie**

Chemical formula	$C_{20}H_{18}ClF_3$

Formula weight	350.79 g/mol	
Temperature	100(2) K	
Wavelength	0.71073 Å	
Crystal size	0.020 x 0.040 x 0.220 mm	
Crystal habit	colorless needle	
Crystal system	orthorhombic	
Space group	P 21 21 21	
Unit cell dimensions	a = 5.7612(2) Å	α = 90°
	b = 10.0055(3) Å	β = 90°
	c = 30.2835(9) Å	γ = 90°
Volume	1745.65(10) $Å^3$	
Z	4	
Density (calculated)	1.335 g/cm^3	
Absorption coefficient	0.246 mm^{-1}	
F(000)	728	

Table S2. Data collection and structure refinement for (*R*)-**3ie**

Theta range for data collection	2.44 to 32.58°	
Index ranges	-8<=h<=7, -15<=k<=15, -45<=l<=45	
Reflections collected	20471	
Independent reflections	6312 [R(int) = 0.0693]	
Coverage of independent reflections	99.6%	
Absorption correction	Multi-Scan	
Max. and min. transmission	0.9950 and 0.9480	
Structure solution technique	direct methods	
Structure solution program	XT, VERSION 2014/5	
Refinement method	Full-matrix least-squares on F^2	
Refinement program	SHELXL-2018/3 (Sheldrick, 2018)	
Function minimized	$\Sigma\, w(F_o^2 - F_c^2)^2$	
Data / restraints / parameters	6312 / 0 / 220	
Goodness-of-fit on F^2	1.032	
Δ/σ_{max}	0.002	
Final R indices	5304 data; I>2σ(I)	R1 = 0.0465, wR2 = 0.0987
	all data	R1 = 0.0605, wR2 = 0.1091
Weighting scheme	$w=1/[\sigma^2(F_o^2)+(0.0377P)^2+0.2160P]$ where $P=(F_o^2+2F_c^2)/3$	

Absolute structure parameter	0.07(4)
Largest diff. peak and hole	0.296 and -0.337 eÅ^{-3}
R.M.S. deviation from mean	0.056 eÅ^{-3}

3.5. References

1. Wang, J.; Sánchez-Roselló, M.; Aceña, J. L.; del Pozo, C.; Sorochinsky, A. E.; Fustero, S.; Soloshonok, V. A.; Liu, H. *Chem. Rev.* **2014**, *114*, 2432–2506.
2. Jeschke, P. *Chembiochem* **2004**, *5*, 570–589.
3. Fujiwara, T.; O'Hagan, D. *J. Fluor. Chem.* **2014**, *167*, 16–29.
4. Berger, R.; Resnati, G.; Metrangolo, P.; Weber, E.; Hulliger, J. *Chem. Soc. Rev.* **2011**, *40*, 3496–3508.
5. Champagne, P. A.; Desroches, J.; Hamel, J.-D.; Vandamme, M.; Paquin, J.-F. *Chem. Rev.* **2015**, *115*, 9073–9174.
6. Williamson, J. F. *Phys. Med. Biol.* **2006**, *51*, 303–325.
7. Hollingworth, C.; Gouverneur, V. *Chem. Commun.* **2012**, *48*, 2929–2942.
8. Wu, J. *Tetrahedron Lett.* **2014**, *55*, 4289–4294.
9. Taylor, S. D.; Kotoris, C. C.; Hum, G. *Tetrahedron* **1999**, *55*, 12431–12477.
10. Dolbier, W. R.; Burkholder, C. R.; Piedrahita, C. A. *J. Fluor. Chem.* **1982**, *20*, 637–647.
11. Castelhano, A. L.; Krantz, A. *J. Am. Chem. Soc.* **1987**, *109*, 3491–3493.
12. Shi, G.; Xu, Y. *J. Fluor. Chem.* **1989**, *44*, 161–166.
13. Wang, Z.; Hammond, G. B. *J. Org. Chem.* **2000**, *65*, 6547–6552.
14. Mae, M.; Hong, J. A.; Xu, B.; Hammond, G. B. *Org. Lett.* **2006**, *8*, 479–482.
15. Wang, X.; Wu, Z.; Wang, J. *Org. Lett.* **2016**, *18*, 576–579.
16. Li, T.; Zhou, C.; Yan, X.; Wang, J. *Angew. Chem. Int. Ed.* **2018**, *57*, 4048–4052.
17. Huang, Y.; Hayashi, T. *J. Am. Chem. Soc.* **2016**, *138*, 12340–12343.
18. Kim, J. G.; Walsh, P. J. *Angew. Chem. Int. Ed.* **2006**, *45*, 4175–4178.
19. Armstrong, D. R.; Clegg, W.; García-Álvarez, P.; Kennedy, A. R.; McCall, M. D.; Russo, L.; Hevia, E. *Chem. Eur. J.* **2011**, *17*, 8333–8341.
20. Gourdet, B.; Lam, H. W. *J. Am. Chem. Soc.* **2009**, *131*, 3802–3803.
21. Azizian, H.; Eaborn, C.; Pidcock, A. *J. Organomet. Chem.* **1981**, *215*, 49–58.
22. Shintani, R.; Tsutsumi, Y.; Nagaosa, M.; Nishimura, T.; Hayashi, T. *J. Am. Chem. Soc.* **2009**, *131*, 13588–13589.
23. Shintani, R.; Soh, Y.-T.; Hayashi, T. *Org. Lett.* **2010**, *12*, 4106–4109.

24. Nishimura, T.; Noishiki, A.; Chit Tsui, G.; Hayashi, T. *J. Am. Chem. Soc.* **2012**, *134*, 5056–5059.
25. Di-μ-Chloro-Bis(η4-1,5-Cyclooctadiene)-Dirhodium(I). In *Inorg. Synth.*, pp 88–90.
26. Chlorobis(Cyclooctene)Rhodium(I) and–Iridium(I) Complexes. In *Inorg. Synth.*, pp 90–92.
27. Nishimura, T.; Kumamoto, H.; Nagaosa, M.; Hayashi, T. *Chem. Commun.* **2009**, 5713–5715.
28. Miyamura, H.; Nishino, K.; Yasukawa, T.; Kobayashi, S. *Chem. Sci.* **2017**, *8*, 8362–8372.
29. Hatano, M.; Nishimura, T. *Angew. Chem. Int. Ed.* **2015**, *54*, 10949–10952.
30. Otomaru, Y.; Kina, A.; Shintani, R.; Hayashi, T. *Tetrahedron: Asymmetry.* **2005**, *16*, 1673–1679.
31. Kerr, W. J.; Morrison, A. J.; Pazicky, M.; Weber, T. *Org. Lett.* **2012**, *14*, 2250–2253.
32. Leung, L. T.; Leung, S. K.; Chiu, P. *Org. Lett.* **2005**, *7*, 5249–5252.
33. Rotsides, C. Z.; Hu, C.; Woerpel, K. A. *Angew. Chem. Int. Ed.* **2013**, *52*, 13033–13036.
34. Atobe, S.; Masuno, H.; Sonoda, M.; Suzuki, Y.; Shinohara, H.; Shibata, S.; Ogawa, A. *Tetrahedron Lett.* **2012**, *53*, 1764–1767.
35. Picher, M.-I.; Plietker, B. *Org. Lett.* **2020**, *22*, 340–344.
36. Van den Hoven, B. G.; Ali, B. E.; Alper, H. *J. Org. Chem.* **2000**, *65*, 4131–4137.
37. Cheng, X.; Wang, Z.; Quintanilla, C. D.; Zhang, L. *J. Am. Chem. Soc.* **2019**, *141*, 3787–3791.
38. Falck, J. R.; He, A.; Fukui, H.; Tsutsui, H.; Radha, A. *Angew. Chem. Int. Ed.* **2007**, *46*, 4527–4529.
39. Santra, S.; Ranjan, P.; Bera, P.; Ghosh, P.; Mandal, S. K. *RSC Advances* **2012**, *2*, 7523–7533.
40. Knochel, P.; Krasovskiy, A. *Synthesis* **2006**, *2006*, 890–891.
41. Mohapatra, D. K.; Das, P. P.; Pattanayak, M. R.; Gayatri, G.; Sastry, G. N.; Yadav, J. S. *Eur. J. Org. Chem.* **2010**, *2010*, 4775–4784.